

HORMONAL REGULATION OF BONE HEALTH: NOVEL UNDERSTANDINGS
OF XENOESTROGENS AND ESTROGEN RECEPTOR- α

A Dissertation
presented to
The Faculty of the Graduate School
University of Missouri, Columbia

In Partial Fulfillment
of the Requirements for the Degree:
Doctor of Philosophy

By
REBECCA DIRKES
Dr. Pamela Bruzina, Dissertation Supervisor
December 2020

The undersigned, appointed by the Dean of the Graduate School, have examined the dissertation titled:

HORMONAL REGULATION OF BONE HEALTH: NOVEL UNDERSTANDINGS
OF XENOESTROGENS AND ESTROGEN RECEPTOR- α

Presented by Rebecca Dirkes,

a candidate for the degree of Doctor of Philosophy,

and hereby certify that, in their opinion, it is worth of acceptance.

Dr. Pamela Bruzina

Dr. R. Scott Rector

Dr. Jaume Padilla

Dr. Catherine Peterson

Dr. Kevin Middleton

ACKNOWLEDGEMENTS

I would like to take this opportunity to thank any and all that helped me throughout my time as a graduate student at the University of Missouri. First, I would like to thank Dr. Pamela Bruzina for all of her support and guidance as my mentor through this process. She has showed several times throughout this process that she cared just as much about me as a person as she did about me as a researcher, and I cannot thank her enough for being there through the thick and thin. I would also like to thank the rest of my committee members for their help and guidance along the way – Dr. Scott Rector, for allowing me to use laboratory space and equipment; Dr. Jaume Padilla for providing some of the animals in my studies; Dr. Catherine Peterson for her help with both research and teaching, and being a great professor to TA for; and finally, Dr. Kevin Middleton for sharing methods and supplies, as well as allowing me to use laboratory space and equipment. I would also like to thank the laboratory staff and managers that have helped me optimize methods and train on basic laboratory skills, Grace Meers and Becky Welly, as well as the core programs that helped with imaging and scans, particularly the MU X-Ray Microanalysis Core (MizzoμX) and the Molecular Cytology Core. Finally, I would like to thank the NEP department and office staff for their continued support throughout my time here.

TABLE OF CONTENTS

ACKNOWLEDGEMENTS	ii
LIST OF FIGURES	iv
LIST OF TABLES	vi
ABSTRACT	vii
CHAPTER 1 – <i>Introduction</i>	1
CHAPTER 2 – <i>Extended Literature Review</i>	10
CHAPTER 3 – <i>Global estrogen receptor-α knockout has differential effects on cortical and cancellous bone in aged male mice</i>	77
CHAPTER 4 – <i>Voluntary wheel running partially compensates for the effects of global estrogen receptor-α knockout on cortical Bone in young male mice</i>	106
CHAPTER 5 – <i>Gestational exposure to BPA, but not BPS, significantly impairs trabecular microarchitecture and cortical geometry in male adult offspring</i>	129
CHAPTER 6 – <i>Gestational exposure to BPA or BPS has minimal effects on skeletal outcomes in adult, female mice</i>	152
CHAPTER 7 – <i>Discussion</i>	166
REFERENCES	179
APPENDIX A – <i>Detailed Methods and Protocols</i>	207
VITA	232

LIST OF FIGURES

CHAPTER 1

Figure 1.1 Overview of study aims	9
--	---

CHAPTER 2

Figure 2.1 Load-displacement and stress-strain curves	22
Figure 2.2 Overview of bone remodeling	30
Figure 2.3 Overview of endochondral ossification	35
Figure 2.4 Bone mass across the lifespan	46
Figure 2.5 Overview of Wnt signaling	51
Figure 2.6 Chemical structures of the bisphenol analogs	70
Figure 2.7 Overview of the actions of BPA and other bisphenol analogs on bone cells	76

CHAPTER 3

Figure 3.1 Cortical Geometry of the Femur	87
Figure 3.2 Trabecular Microarchitecture of the Distal Femur	89
Figure 3.3 Trabecular Microarchitecture of the Lumbar Vertebrae	91
Figure 3.4 3D Reconstructions of Regions of Interest in Cortical and Cancellous Bone	92
Figure 3.5 Femoral Cortical Collagen and Advanced Glycated End-product Concentrations.....	93
Figure 3.6 Femoral Mineral Content	94
Figure 3.7 Osteocyte Sclerostin Expression and Empty Lacunae in Cortical and Cancellous Bone	96
Figure 3.8 Representative Photos of Sclerostin Staining in Cortical and Cancellous Bone	97

CHAPTER 4

Figure 4.1 Average weekly running distances	116
Figure 4.2 Cortical Geometry of the Tibia	118
Figure 4.3 Biomechanical Strength of the Tibia	120
Figure 4.4 Trabecular Microarchitecture of the Tibia	122
Figure 4.5 Sclerostin Expression in Femoral Cortical and Cancellous Bone ..	123

CHAPTER 5

Figure 5.1 Animal Characteristics	139
Figure 5.2 Cortical Geometry of the Femur	141
Figure 5.3 Biomechanical Strength of the Femur	143
Figure 5.4 Trabecular Microarchitecture of the Femur	145
Figure 5.5 Sclerostin Expression of the Tibia	146
Figure 5.6 Mineral Apposition Rate of the Femur	147

CHAPTER 6

Figure 6.1 Animal Characteristics	155
Figure 6.2 Cortical Geometry of the Femur	157
Figure 6.3 Biomechanical Strength of the Femur	158
Figure 6.4 Trabecular Microarchitecture of the Femur	160
Figure 6.5 Sclerostin Expression of the Tibia	161
Figure 6.6 Mineral Apposition Rate of the Femur	162

CHAPTER 7

Figure 7.1 Overview of Findings	167
Figure 7.2 Sexual dimorphism in gestational BPA and BPS exposure	173
Figure 7.3 Chemical structures of estradiol and bisphenol analogs	174

LIST OF TABLES

CHAPTER 3

Table 3.1 Metabolic Characteristics	85
--	----

CHAPTER 4

Table 4.1 Metabolic characteristics	115
--	-----

ABSTRACT

Estrogen is one of the most influential hormones on bone growth and maintenance throughout the life cycle in both men and women, but there are still unknown roles of estrogen and the estrogen receptors in males. In addition, exposure to xenoestrogens, or environmental compounds that have anti-estrogenic qualities, is increasing in industrial countries, but the impact of these compounds on skeletal health in males and females remains unknown. In this dissertation, we used animal models to explore a, the importance of estrogen receptor- α (ER α) in male mice at different points in the life cycle and b, the long-term impact of gestational exposure to xenoestrogens, specifically bisphenol-A (BPA) and bisphenol-S (BPS), on male and female offspring. We found that both young and aged male ER α knockout (ERKO) animals had impaired measures of cortical geometry, but improved measures of trabecular microarchitecture, implying differential roles for ER α in different bone compartments. We also found that ERKO could lead to increased expression of sclerostin, a bone growth inhibitor, in aged, male mice. In younger, male ERKO mice we found that ER α is not required for an osteogenic response to exercise, which is in direct contrast with females. Finally, we found that gestational and lactational exposure to BPA, but not BPS, had significant negative impacts on the skeleton of adult male, but not female, mice. Male offspring exposed to BPA had significantly lower measures of both cortical geometry and trabecular microarchitecture, indicating long-term effects of interrupted estrogen signaling during uterine and early childhood on skeletal development. These findings further our understandings of the importance of estrogen on skeletal health across the lifespan and could have significant public health impacts if they are translatable to humans.

CHAPTER 1

Introduction

Estrogen is one of the most influential hormones in growth and maintenance of the skeleton in both males and females across the entire lifespan [1–3]. However, unanswered questions remain about the specific mechanistic role of estrogen and the estrogen receptors in bone cells, as well as the potential impact of environmental endocrine disruptors on normal estrogenic signaling in bone. In this dissertation, I will be exploring the specific role of ER α in the osteogenic response to exercise in the osteocyte, as well as the possible impact that gestational exposure to known endocrine disruptors bisphenol-A and bisphenol-S will have on skeletal outcomes in progeny of exposed dams **(Figure 1.1)**.

Estrogen actions in bone

Estrogen has significant, cell-specific actions in the development and maintenance of bone mass (reviewed in [3,4]). In cells of the osteoblast lineage, estrogen protects against apoptosis [5,6], and induces differentiation [7]. Estrogen also induces osteoclast apoptosis [8], and reduces osteoclast differentiation both through direct suppression of receptor activator of NF κ B ligand (RANKL) expression [3,9], and by increasing expression of osteoprotegerin (OPG), a decoy receptor for RANKL [10,11]. The OPG/RANKL ratio is considered a major predictor of bone mass [12], so the actions of estrogen on OPG and RANKL expression are especially significant. Finally, estrogen can modulate the osteogenic response to exercise on a cellular level [13,14].

Estrogen actions are mediated primarily by estrogen binding with the nuclear estrogen receptor (ER), which is found in two isoforms, ER α and ER β . Both ER α and ER β are found in bone; however, ER α tends to be more prevalent in cortical bone, whereas ER β is more widely distributed in cancellous bone [15]. Animal models indicate that ER α and ER β have sex- and bone compartment-dependent actions. Previous studies using global ER α knock out (ERKO) mice have shown that loss of ER α signaling decreased longitudinal bone growth in both male and female mice [16–18]. Female ERKO mice also have decreased cortical BMD compared to WT [16,19,20], as well as decreases in cortical thickness [20]. Similarly, male ERKO mice had reduced cortical bone area and cortical thickness [18,21], as well as decreased biomechanical bending strength compared to WT [18]. In cancellous bone, both male and female ERKO animals have increased BMD and trabecular bone volume [16,20]. Male ERKO mice also had an increase in trabecular number [21,22]. These differential responses to the loss of ER α in cortical versus cancellous bone are most likely due to the variable distribution of the estrogen receptors [15]. They could also be partially due to increased signaling through ER β , as ERKO models can have a significant increase in circulating concentrations of estrogen due to an interruption of feedback signaling in the brain [23].

ER α also has a significant role in modulating the osteogenic response to exercise, especially in females. Cell culture models show that ER α is upregulated and activated in osteoblasts after application of mechanical strain [24–26]. Osteoblast cultures taken from male and female ERKO mice do not proliferate and respond to strain like osteoblast cultures from WT controls [7], and female global ERKO mice have a significantly smaller osteogenic response to loading in cortical bone [27,28]. However, male ERKO

mice had an increased osteogenic response to mechanical loading compared to WT [28]. In addition, male mice that had no ER α in mature osteoblasts and osteocytes had no differences in the osteogenic response to loading when compared to littermate controls [29]. This implies some type of secondary mechanism allowing an osteogenic response to mechanical loading in ERKO males, possibly through ER β or the androgen receptors in bone [30].

One recently discovered action of estrogen related the skeletal response to mechanical loading is the downregulation of sclerostin. Sclerostin is a protein expressed in osteocytes, which acts as a competitive inhibitor of the canonical Wnt signaling pathway. Canonical Wnt signaling upregulates transcription of multiple osteogenic genes (reviewed in [31,32]) and ultimately increases bone mass. Inhibition of the Wnt signaling pathway via sclerostin blocks bone growth, whereas downregulation of sclerostin is associated with increases in bone [33]. Animal and cell culture models show that sclerostin expression in osteocytes can be regulated by several external factors, such as insulin-like growth factor-I, parathyroid hormone, androgens and estrogens, and especially the stimulation of mechanical loading [33].

There appears to be an inverse relationship between estrogen and sclerostin expression. Estrogen treatment decreased circulating sclerostin [34] and sclerostin expression in the posterior iliac crest [35] in older women. Estrogen treatment, but not testosterone treatment, lowered circulating levels of sclerostin in older men [34]. However, circulating levels may not reflect bone sclerostin expression [36], and thus further study in males is needed. In female mice and rats, ovariectomy increased sclerostin expression, and treatment with estrogen reversed this change [37,38]. In

osteoblastic cells derived from female mice, sclerostin expression was downregulated after the application of endogenous estrogen, although ER β appeared to play a greater role in the regulation of sclerostin levels than ER α [24]. However, the specific role of estrogen receptors in the control of sclerostin expression, and the effects this could have on the skeletal response to mechanical loading are still unknown.

Xenoestrogens and human health

Humans are exposed to xenoestrogens through the environment on a daily basis, and the impact they have on our overall health is still unclear. Xenoestrogens are synthetic or natural compounds that mimic or interrupt normal estrogen signaling in the body and can have positive or negative effects. Common examples of xenoestrogens are phytoestrogens, such as those found in soy which are considered beneficial, and bisphenol molecules, which are a component of certain plastics and are considered harmful. Bisphenol-A (BPA) and its analogs Bisphenol-S (BPS) and Bisphenol-F (BPF) are known endocrine disruptors that can have significant negative impacts on human health [39,40].

BPA and BPS are selective estrogen receptor modulators (SERM), meaning that binding to these molecules to the estrogen receptors leads to a modification of gene expression, but a different pattern of gene expression than classic estrogen binding [41–43]. BPA has been shown to bind to both ER α and ER β , but it has a higher affinity for ER β [41], whereas BPS binds only to ER α [44]. In addition to directly binding to the estrogen receptors, BPA can indirectly impact normal endocrine signaling by altering epigenetic programming. Animal models have shown that gestational BPA exposure can

affect methylation of both DNA and histone proteins [45–48]. Interestingly, studies have shown that these epigenetic effects of BPA exposure are not seen in adult exposure models [49], implying that BPA only effects the epigenome during critical periods of development, primarily uterine development.

Human studies have associated BPA exposure with several endocrine issues, from low circulating sex hormones and decreased birth weight to metabolic diseases, such as obesity and cardiovascular disease [39]. BPA exposure is essentially ubiquitous in humans, with BPA being detectable in almost 100% of the blood or urine samples tested [39]. In addition, BPA has been detected in samples of breast milk, cord blood, and fetal tissue [39], implying that humans are exposed to BPA at varying levels at all ages and stages of life. The presence of BPA in cord blood and fetal tissue implies direct transfer across the placenta, and this has been confirmed in human studies of placental explants [50–52]. All three studies showed that the ratio between fetal and maternal serum levels of BPA was 1, implying that the exposure of the fetus is equal to that of the mother. The most common route of exposure in humans is food contamination, usually from BPA found in epoxy resins, which are used to line metal cans to stop food from being exposed to the metal [53]. While less impactful to human exposure, BPA and its analogues can also be found in thermal paper, dust, and certain dental and medical equipment [53]. Many industrialized countries, such as the United States, China, Germany, and Australia have high exposure rates, often times above the current tolerable daily intake (TDI) [54]. In addition, the majority of epidemiological studies show that BPA exposure is associated with adverse effects on human health even at intakes below the current TDI [39]. Considering the possible effects that even low levels of exposure could have on human

health, more information is needed to understand the consequences of exposure to BPA and its analogues.

BPA and Bone

In spite of the known anti-estrogenic effects of BPA and BPS, few studies have looked at the impact that BPA exposure might have on bone health, and no studies have looked at BPS exposure outside of cell culture. In humans, only four studies have looked at possible relationships between BPA exposure and skeletal health. In adult women, there have been no correlations between serum or urine BPA levels and BMD [55–57]. In a study in school-aged children, there was no correlation between urinary BPA levels and height in girls however, there was a significant negative correlation between urinary BPA levels and height in boys, which remained even when adjusted for pubertal status and at follow up 19 months later [58]. No studies have looked at BPA exposure and fracture incidence, and no studies in adults looked at possible changes in BMD over time.

Few studies have looked at BPA exposure and skeletal health in animal models as well, and they often have conflicting results. In female ovariectomized (OVX) rats, BPA exposure decreased cancellous BMD more than just OVX alone [59]; however, BPA exposure increased femoral BMD in female aromatase knockout mice in a dose-dependent manner [60]. When given during gestation, BPA appears to have sex- and dose-dependent results. Almost no studies showed any differences in female offspring of BPA-exposed dams compared to control offspring [61–64]. In rats, male offspring had increased cortical thickness at the 25 μg dose compared to control, but decreased cortical thickness at the 250 μg dose [61]. In another study in rats, male offspring in all groups

had shorter femoral length, but only male offspring in the 0.5 $\mu\text{g}/\text{kg}$ BW dose group had lower trabecular bone volume and cortical area [62]. In mice, male offspring had increased femur lengths, but no differences in biomechanical strength [63]. In another study in mice, male offspring showed decreased cortical thickness and biomechanical strength regardless of dose [64]. In addition to animal models, BPA exposure blocks osteoblastic and osteoclastic differentiation and increases markers of apoptosis in a dose-dependent manner in progenitor cells [65] and human osteosarcoma cells [66]. Overall, these data suggest that BPA exposure can have significant effects on bone cell activity and gestational exposure might have significant impacts on bone mass and strength, especially in male offspring.

The essential role of estrogen in bone health throughout the life cycle has been well established in both males and females. However, questions still remain regarding the relative importance of specific estrogen receptors, especially $\text{ER}\alpha$, in the osteogenic response to exercise and expression of sclerostin in the osteocyte, considering the contrasting human and animal studies currently in the literature. In addition, there are several unexplored questions relating to the effect that xenoestrogen exposure, specifically BPA and BPS, could have on the vital activities of estrogen in bone, especially related to bone remodeling and cellular activity of osteoblasts. Considering that the current exposure levels BPA and BPS in industrialized countries is often higher than the tolerable daily intake level, understanding more about how this could affect skeletal health has significant public health importance. With this in mind, my dissertation project includes three studies to determine: 1) if the loss of estrogen signaling through $\text{ER}\alpha$ in aged, male mice is associated with an increase in sclerostin expression in

the osteocyte; 2) if the loss of estrogen signaling through ER α affects the osteogenic response to exercise in young, male mice, and if possible differences are associated with differential expression of sclerostin in the osteocyte; and 3) the extent to which BPA or BPS exposure during gestation and lactation affects bone outcomes in the offspring, especially related to bone remodeling via osteoblast and osteoclast activity. (**Figure 1.1**)

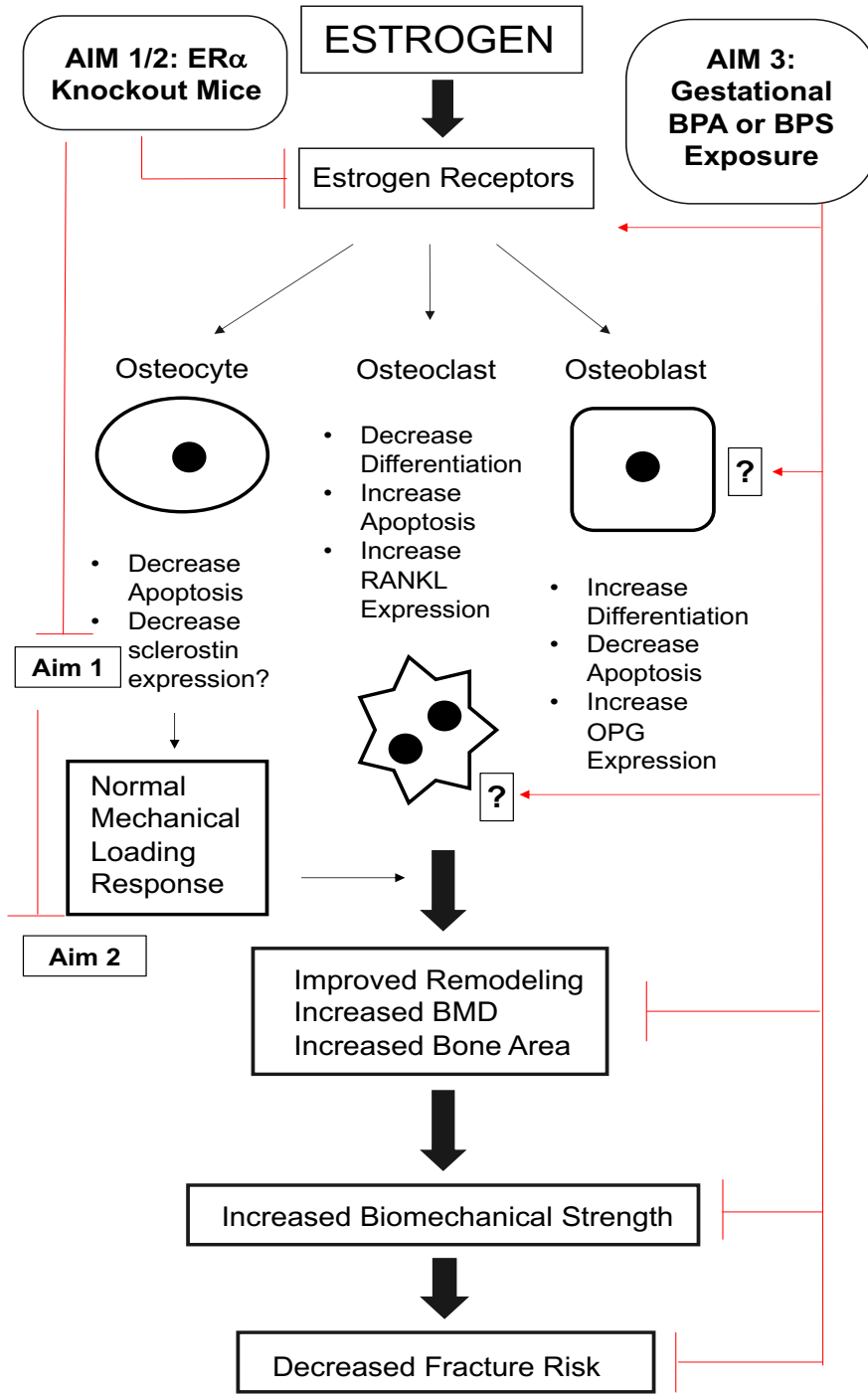


Figure 1.1. Overview of study aims

CHAPTER 2

Extended Literature Review

Bone as an Organ

Bone is a dynamic tissue with several important roles in the body, from locomotion to calcium availability to energy balance. The adult human skeleton is made up of over 200 bones, from the top of the cranium to the tip of the phalanges. While not every bone is the same in shape or function, all bones in the body are made of the same primary material, a mineralized collagen matrix, and constantly undergoing modeling and remodeling processes to help them adapt to external forces and maintain healthy bone tissue. The four general categories of bone are long bones, short bones, flat bones, and irregular bones [67]. Because of differences in development and function between types, this dissertation will primarily be focusing on long bones, such as the humerus, tibia, and femur.

The skeleton serves a variety of functions in the human body. Bones provide support and protection for other vital tissues of the body, as well as allowing for movement and locomotion by acting as levers for muscles. Bones also play a significant role in both mineral homeostasis and acid-base balance by acting as a reservoir for mineral material. In addition, long bones provide the environment for hematopoiesis within the marrow spaces. Finally, through the production of cytokines and other factors, bones can play a role in overall energy homeostasis. [67].

Bone 101 – terms you should know

Bone Material

Bone as a tissue is composed of two phases – organic and inorganic. By weight, bone tissue is about 60% inorganic material, 10% water, and 30% organic material [68]. On average, the organic phase is comprised of 90% type I collagen, 8% non-collagen proteins, and 2% cells [68,69]. Type I collagen consists of two $\alpha 1$ and one $\alpha 2$ polypeptide chains assembled in a triple helix [69], and these helices are further assembled into fibrils. This triple helical structure allows for the molecules to elongate and slide in response to tension, which is a vital attribute of bone material that will be discussed in a later section. Non-collagenous proteins make up 8% of the organic phase and play several different roles in bone tissue. Some, such as osteopontin, work as a “glue” to help hold the collagen fibrils together and absorb the energy of elongation, which allows for deformation of the bone material without fracture [69]. Others, such as osteocalcin and matrix Gla protein (MGP) regulate the mineralization of the extracellular matrix [68,69]. Finally, growth factors such as insulin-like growth factor (IGF) and bone morphogenic proteins make up a small percentage of the organic material. The inorganic material of bone is primarily comprised of hydroxyapatite ($\text{Ca}_{10}(\text{PO}_4)_6(\text{OH})_2$), a naturally occurring calcium phosphate. However, some impurities can be found, and 4-6% of the hydroxyapatite is actually tainted with other minerals, often carbonate in place of the phosphate group, potassium or magnesium in place of the calcium ions, or chloride or fluoride in place of the hydroxyl group [68]. These impurities can affect the solubility of the mineral matrix, which in turn affects mineral homeostasis by not allowing minerals to be released from the bone when needed by the body [68].

Bone Anatomy

Long bones, such as the femur and tibia, are divided into three parts: the epiphysis, metaphysis, and diaphysis. The epiphysis is located at each end of the bone and develops from a center of ossification distinct from the rest of the bone (see *bone in utero* for more information on centers of ossification). The epiphysis is separated from the rest of the bone by a thin layer of growth cartilage known as the *physis*, until the growth cartilage fuses and longitudinal growth ends. The metaphysis is the region of transition between the wider epiphysis and the narrow, central shaft of the bone, which is known as the diaphysis [68]. Within each of these structural sections, two primary types of bone can be found: cortical, also known as dense or compact bone, and cancellous, also known as trabecular or spongy bone. On average, cortical bone comprises 80% of skeletal mass and cancellous bone comprises 20%. Cancellous bone is a porous structure comprised of a network of interconnected trabeculae, filled with bone marrow and some adipose tissue. Cortical bone is a dense, continuous structure of bone that surrounds the marrow cavity of long bones. Both the epiphyses and metaphyses of long bones are comprised of cancellous bone with a thin cortical shell, whereas the diaphyses are exclusively comprised of thicker cortical bone. Covering all of these structural sections are membranes on the outer and inner surfaces of the bone that play significant roles in bone growth and development. These membranes are known as the periosteum and endosteum, respectively, and both contain a multitude of cell types necessary for bone modeling and remodeling.

Bone Cells

There are four main types of cells found in bone: osteoclasts, osteoblasts, osteocytes, and bone-lining cells. Each of these will be covered in more detail later in the review (see **Bone Cell Types**). Osteoclasts and osteoblasts are found on the outer surfaces of bone, often in or around the periosteum and endosteum. Osteoclasts are responsible for bone resorption, or the breaking down of old or damaged bone. Osteoblasts are responsible for bone formation and laying down the new collagen matrix to be mineralized. Osteocytes are mature osteoblasts that have been buried in the mineralized matrix and are primarily responsible for sensing external signals and translating them to the osteoblasts and osteoclasts. Bone-lining cells line the surface of the bone where neither formation nor resorption is taking place. While the role of bone-lining cells is still under question, some studies indicate that they serve as a barrier between healthy bone and osteoclasts, to stop resorption from occurring [70]. Bone formation and resorption happen under the control of two distinct processes, bone modeling and remodeling.

Bone modeling is the process in which bone is grown and shaped by independent actions of osteoblasts and osteoclasts, often in separate anatomical locations. Bone modeling primarily occurs during skeletal growth and development; however, bone modeling can occur in the adult skeleton, particularly in response to lifestyle changes or injuries that would lead to the reshaping of bone. Bone remodeling, on the other hand, is the process in which bone is renewed by the coupled actions of osteoclasts and osteoblasts in the same anatomical location in order to repair areas of damaged bone. Bone remodeling persists through life, and it is estimated that the entire adult skeleton is remodeled every 10 years. Remodeling occurs in distinct areas known as bone

remodeling units (BRUs, also sometimes called basic multicellular units, or BMUs), and it is estimated that around 1 million BRUs are actively remodeling bone at any one time. Remodeling involves four distinct phases: the activation phase, where osteoclasts are recruited, the resorption phase, in which osteoclasts resorb bone, the reversal phase, where osteoclasts undergo apoptosis, or cellular death, and osteoblasts are recruited, and the formation phase, in which osteoblasts lay down new bone matrix which is then mineralized. In order to maintain bone mass, bone remodeling needs to be balanced with equal amounts of bone resorbed and reformed. [71] See **Bone remodeling** for more information.

Bone Blood Flow

Like all other tissues, bone is served by an extensive vascular network that delivers oxygen and nutrients and removes waste products. Bone blood vessels also deliver systemic hormones and growth factors, participate in hematopoiesis by delivering blood and immune factors to and from the bone marrow, and are a key component of each individual BRU [72]. Bone development and maintenance are dependent on a healthy blood supply, and the skeleton is considered a highly vascularized organ. In fact, the bone vascular network is so vast that the adult skeleton accounts for 10-15% of resting cardiac output [73]. Originally, blood flow in the bone was thought to occur in a centrifugal pattern – blood entered the bone through arteries into the marrow cavity and then was returned via periosteal veins [73]. However, recent studies have shown that blood flow through the bone can vary depending on skeletal site, and often the epiphyses and diaphysis of long bones have functionally separate blood supplies. In addition, some

areas of the bone, such as the femoral neck, have both medial and lateral arteries, concluding that not all bones rely on centrifugal blood flow [73].

Bone metabolism

Bone's role in mineral balance.

Bone is a dynamic, metabolically active tissue, most well-known for its role in mineral homeostasis. Bone acts as a reservoir for minerals in the body, primarily calcium and phosphorus, but also some magnesium and potassium. These minerals are released when needed and deposited when in excess by the process of bone remodeling. Mineral homeostasis is a highly regulated process that involves the coordination of several different organ systems. For example, blood calcium concentrations need to be 1.0-1.3 mM for normal functioning of neuromuscular signaling and other physiological processes [74], which is a very narrow window for the body to maintain. When blood calcium is low, parathyroid hormone (PTH) is released from the parathyroid gland and acts on the kidney and bones to increase calcium concentrations. In the bone, PTH increases osteoclast activity leading to bone resorption, which releases calcium into the blood. In the kidney, PTH leads to the conservation of calcium through reabsorption in the renal tubules and increases the hydroxylation of vitamin D into its active form, 1,25(OH)₂-D₃. Activated vitamin D acts in the intestines to increase calcium absorption from food and supplements. When calcium levels return to normal, secretion of PTH is decreased and actions of PTH are stopped or reversed [74]. When calcium levels are high, calcitonin is released from the thyroid gland. Calcitonin acts directly on bone cells to inhibit

resorption in osteoclasts [75] and inhibit apoptosis in osteoblasts [76], which allows excess calcium to be deposited.

Bone's role in energy balance

In addition to mineral balance, bones play a significant role in overall energy homeostasis, which has been underappreciated until recent decades. For one, calcium is required for intracellular signaling that allows for the release of certain hormones involved in energy homeostasis, such as insulin [77]. Although intracellular calcium does not come directly from bones, excess calcium is stored in the bones until needed as previously discussed. More directly, there is a positive association between bone mineral density (BMD), a measure of bone mass, and resting energy expenditure, particularly in women [78,79]. This increase in energy usage is primarily due to the high energy requirements of osteoblasts and osteoclasts during remodeling [80]. Finally, recent studies have shown that bone releases proteins that have metabolic actions. For example, some non-collagenous proteins produced by the bone, particularly osteocalcin, can act as cytokines to influence systemic glucose homeostasis by increasing insulin secretion in the pancreas and sensitizing other tissues to the actions of insulin [81].

Mechanical and material properties of bone

Bone is unique compared to other organ systems, in that its mechanical and material properties are just as important as its metabolic properties and are essential to its structural function. Bone acts as a scaffolding for ligaments, tendons, and muscles that allows individuals to perform daily tasks of living, from standing and walking to chewing

food and playing an instrument. In order to accomplish this, bones must be strong enough to withstand both internal (muscular) and external (gravitational) forces that are applied to the bone on a daily basis. Bone strength is defined as the maximal amount of load (force) tolerated before fracture occurs [82]. Ultimate bone strength is dependent on several factors, including the mass, size, shape, and material of the bone.

Determinants of bone strength

Bone mineral density (BMD) is measured by dual-energy x-ray absorptiometry (DXA) and is considered the gold standard measurement of bone mass in humans. A DXA scan is an easy, noninvasive procedure, and BMD is used clinically as a diagnostic tool for bone diseases, particularly diseases of low bone mass such as osteopenia and osteoporosis, and fracture risk assessment [82]. Experimentally, changes in BMD are often used as an outcome to evaluate the efficacy of a treatment on improving bone mineral density, as a proxy measure of bone strength in humans. However, BMD only predicts 60-70% of the variations in bone strength in *ex vivo* testing of human bone material [83], and some studies have shown increased strength without corresponding increases in BMD [82]. This highlights the importance of the other determinants of bone strength.

Both size and shape of the bone can also impact strength, but cortical and cancellous bone have different measures of size and shape. The size and shape of cortical bone is called cortical geometry and includes measures of amount of bone (cortical thickness), size of bone (cortical diameter) and shape of bone (if the diaphysis is round or oval). Increases in cortical thickness correlate with increases in bone strength due to

higher bone mass, but increases in cortical diameter are a stronger influencer of bone strength due to the exponential relationship between diameter and strength in hollow cylinders [82,83]. In fact, outer diameter of long bones can predict up to 50% of variations in bone strength [83]. Trabecular microarchitecture refers to the amount and structure of cancellous bone. Measures of trabecular microarchitecture include the amount of bone (trabecular bone volume), as well as 3-D morphologic measures such as the number, thickness, and spacing of individual trabeculae and the degree of anisotropy (uniformity in direction) between the trabeculae. Trabecular bone volume and degree of anisotropy are two of the strongest predictors of trabecular bone strength, but the thickness, spacing, and number of individual trabeculae often correlate with trabecular bone volume [83]. Evaluation of cortical geometry and trabecular microarchitecture in humans has just recently been accomplished with the use of high-resolution peripheral quantitative computed tomography (HR-pQCT) [84], but has long been done in animal models using micro-computed tomography (μ CT) [85].

Mechanical properties of bone

Mechanical properties of the bone can be split into two categories: whole-bone or tissue-level mechanics, i.e. mechanical properties of the femoral diaphysis as a whole, and tissue- or material-level mechanics, i.e. mechanical properties of cortical bone tissue that makes up the femoral diaphysis [86]. Whole-bone mechanical properties include strength, stiffness, and work-to-fracture or energy-to-fracture. Tissue-level mechanical properties include ultimate stress, Young's modulus of elasticity, or elastic modulus, and toughness [86,87]. Strength, also referred to as maximal load, is the amount of force that

the bone can withstand before failing, or fracturing. Stiffness and elasticity are both measures of the hardness of the bone, or the ability of the bone to resist deformation as load is applied [86,87]. The difference is that stiffness measures deformation of the bone as a whole, whereas the elastic modulus measures deformation of the material. A hard material, like glass, will resist deformation until failure, meaning it will not change shape at all until it actually breaks. A soft material, like a sponge, will not resist deformation, but will resist failure, meaning it will change shape very quickly, but then often not break at all. Bones need to be somewhere in the middle - both too hard and too soft can be detrimental to the mechanical properties of bone and its ability to withstand internal and external forces [87]. Work-to-fracture and toughness are measures of the ability of the whole bone or the bone material, respectively, to absorb energy before deformation or failure [88]. Similar to stiffness and elasticity, there is an ideal middle level – both too tough and too weak can be detrimental to the overall ability of the whole bone to resist fracture. Elasticity and toughness of bone are determined by different material properties but work together to define the overall strength and stiffness of the bone. Strength, stiffness, elasticity, and toughness are all interrelated, and often a material change that increases one can decrease another [88].

Material properties of bone

Material properties of bone are determined by the organic and inorganic phases of bone material, as well as the interactions between the two. These can include collagen crosslinking, protein-mineral interfaces, and many more. There are two types of crosslinks between collagen fibrils, enzymatic and non-enzymatic. Enzymatic crosslinks

stabilize the collagen fibrils and are associated with improved mechanical properties, whereas non-enzymatic are associated with impaired mechanical properties [69]. Advanced glycation end products (AGEs) are non-enzymatic crosslinks formed when free glucose molecules react with free amino groups in the collagen fibrils. This introduction of a sugar molecule in the collagen can block the remodeling process, which stops the repair of damaged areas and leads to impaired mechanical properties as well [89]. Non-collagenous proteins also interact with both collagen and mineral material to form collagen-mineral and collagen-collagen interfaces that impact mechanical properties. For example, osteopontin connects two osteocalcin molecules with calcium ions to form a complex that can fold and unfold in response to forces, which allows for lengthening of the material without damage [69]. This improves the mechanical properties of bone, and in fact osteopontin-deficient mice have been shown to decrease bone toughness by 30%, without any losses in total bone mass [90]. Other material properties include the levels of crystallinity, which impacts the elasticity of bone material, and total water content, which can impact the toughness of bone material [69].

The stress-strain curve – evaluating bone's material and mechanical properties

Strength, stiffness, elasticity, and toughness of long bones in rodent models can be evaluated using a variety of *ex vivo* experimental techniques, the most common of which are three- and four-point bending. In each of these techniques, the whole bone is placed in a bending apparatus with either three or four points evenly spaced out along the diaphysis of the bone, and a uniform force (N) is applied at a steady rate (mm/s) to the middle one or two points until the bone fails, or fractures [91]. The software of the

bending apparatus will then produce a load-displacement (N vs mm) curve which presents the absolute force applied to the bone and the distance the points moved, which is a measure of deformation of the bone. A load-displacement curve is used to measure whole-bone mechanical properties, such as absolute strength, stiffness, and work-to-fracture. Strength, or maximum load, is simply the maximum load achieved before failure, or fracture of the bone. Stiffness is defined by the slope of the linear portion of a load-displacement curve, and work-to-fracture is the area under the curve of a load-displacement curve [86]. **(Figure 2.1)**

To measure tissue-level properties such as elasticity and toughness, absolute load and deformation need to be converted to stress and strain. Stress and strain are measures of load and deformation that are dependent on measures of size and shape, such as the moment of inertia and the diameter of the bone (See Appendix A for equations). A stress-strain curve is analogous to a load-displacement curve but allows for comparison of mechanical and material properties across materials or experimental groups, because they have been normalized for size and shape [87]. A stress-strain curve is used to calculate the elasticity and toughness of a material. Similar to their whole-bone counterparts, the elasticity of the material is defined by the linear slope of the stress-strain curve, and toughness is defined by the area under the curve of a stress-strain curve [87,91]. Many researchers also report ultimate stress, or tissue-level strength. Similar to strength, ultimate stress is also defined as the highest load achieved before fracture, but measured on the stress-strain curve rather than the load-displacement curve [86]. **(Figure 2.1)**

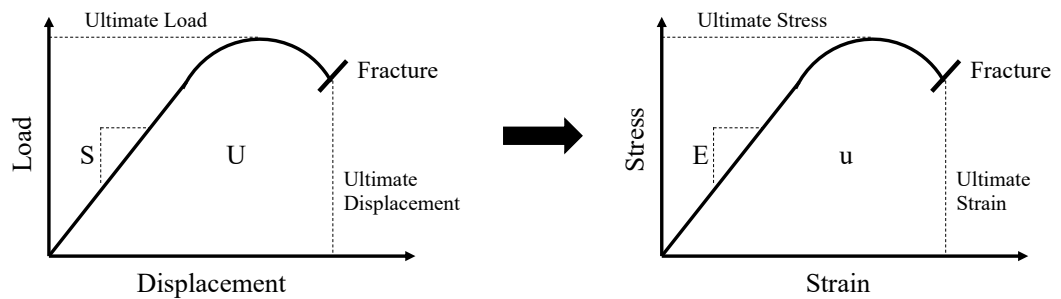


Figure 2.1 Load-displacement and stress-strain curves. S, stiffness. U, work-to-fracture. E, Young's modulus of elasticity. u, modulus of toughness.

Bones are exposed to internal and external forces on a daily basis, and how the bone responds to these forces is the major determinant of the size, shape, material properties, and subsequent strength of the bone. Low magnitude forces cause little to no damage to the bone, whereas medium magnitude forces can cause deformation of the bone material while the force is being applied. Repetitive medium magnitude forces can change the shape of a bone over time, as remodeling occurs to repair the damaged areas of the bone. Large magnitude forces can cause significant deformation of the material, which often leads to failure of the bone, or fracture. Ultimately, it is the magnitude, direction, and rate of application of the force, combined with the material properties, size, and shape of the bone that determines the amount of deformation [92]. Deformation caused by low or medium magnitude of forces can be difficult to measure, so often fracture is used as an endpoint to evaluate overall bone strength.

Bone Cell Types

Osteoclasts

Osteoclasts are cells of hematopoietic origin, meaning they differentiate from hematopoietic stem cells (HCS's) [93]. They are multi-nucleated cells uniquely adapted to degrade mineralized matrices, particularly bone and cartilage, through acid secretion and proteolysis [94]. The differentiation and activity of osteoclasts is under the control of several different factors, from estrogen and growth hormone to cytokines locally produced in the bone. Interestingly, there is evidence that there are several different subtypes of osteoclast at work in the body, from osteoclasts found on long bones and flat bones that are functionally different to chondroclasts, or osteoclasts that specifically degrade collagen [94]. However, these subtypes are outside of the scope of this review and thus only classical osteoclast signaling and activity will be discussed here.

The differentiation of HCS's into osteoclasts is dependent on two essential factors: macrophage colony stimulating factor (M-CSF) and receptor activator of nuclear factor- κ B (RANK) ligand (RANKL). M-CSF promotes the proliferation of osteoclast precursors from HCS's, and RANKL promotes the differentiation of precursors into active osteoclasts [93]. M-CSF is expressed by a variety of different tissues and cells, but the two primary sources of M-CSF in the bone microenvironment are bone marrow stromal cells and osteoblasts [93]. RANKL is also expressed by a variety of different tissues and cells, but the primary sources for RANKL in the bone microenvironment are bone marrow stromal cells, osteoblasts, and osteocytes. However, there is some evidence that RANKL produced by B- and T-cells systemically could contribute to bone loss with age [93]. *In vitro* experiments have shown that binding of M-CSF and RANKL with their

receptors, c-Fms and RANK, respectively is enough to stimulate osteoclastogenesis from HCS's [93]. The primary inhibitory molecule of osteoclastogenesis is osteoprotegerin (OPG), produced by osteoblasts and osteocytes, which serves as a decoy receptor for RANKL and decreases the binding of RANKL to RANK (see **Bone remodeling** for more information). Fully differentiated osteoclasts bind to bone through the actions of integrins, which create a seal between the osteoclast and the bone matrix. This sealed region is known as the ruffled border, and it is where resorption takes place through the secretion of hydrochloric acid and proteases, such as cathepsin K [93,95]. Once a resorption cycle is complete, osteoclasts detach from the bone and either migrate to a new site and activate a new resorption cycle, or they undergo apoptosis [94,95].

Osteoblasts

Osteoblasts differentiate from mesenchymal stem cells (MSCs), which means they are from a different cell line than osteoclasts. They are mononucleated cells that are responsible for creating and maintaining bone tissue through the production of extracellular matrix proteins and regulators of matrix mineralization [96]. In addition, osteoblasts regulate osteoclast differentiation through the production of cytokines, such as RANKL [96,97]. Osteoblast differentiation, proliferation, and activation is regulated by several factors, from systemic hormones such as growth hormone and estrogen to local cytokines produced by other bone cells and direct cell-to-cell interactions [96,98].

MSCs can differentiate into a multitude of different cell types other than osteoblasts, such as myocytes, chondrocytes, and adipocytes. The differentiation of MSCs into osteoblast precursors is stimulated by growth factors such as the Wnt family

of proteins, bone morphogenic proteins (BMPs), hedgehog proteins, fibroblast growth factors, and transforming growth factor- β 1. Differentiation into osteoblasts is inhibited by several growth factors, but one of the most influential is peroxisome proliferator-activated receptor (PPAR)- γ , which stimulates adipogenesis [97,98]. Signaling by stimulatory growth factors leads to the production of transcription factors, such as β -catenin, Runx2, and osterix, which all work together to confirm the MSC to the osteoblast lineage and stimulate the differentiation and proliferation of osteoblast precursors [98]. The differentiation and activation of osteoblast precursors into mature, matrix-producing osteoblasts is under the control of systemic factors, such as parathyroid hormone, estrogen, and vitamin D, as well as paracrine factors, such as insulin-like growth factor-1, and direct cell-to-cell interactions between preosteoblasts and active osteoblasts or preosteoblasts and osteocytes [98]. Active osteoblasts are indicated by a cuboidal shape and a large rough endoplasmic reticulum and Golgi apparatus, which are characteristics of secretory cells [98]. Active osteoblasts synthesize and secrete type I collagen and other non-collagenous proteins, such as osteocalcin, osteopontin, and bone sialoprotein, as well as matrix vesicles [96]. The matrix vesicles contain enzymes, such as alkaline phosphatase, as well as growth factors, such as IGF-1, that interact with non-collagenous proteins to stimulate the mineralization of the collagen matrix [98]. At the end of each bone formation cycle, 50-70% of osteoblasts undergo apoptosis, whereas the rest further differentiate into either bone-lining cells or osteocytes [96,98].

Osteocytes

Osteocytes are the most abundant bone cell type, composing 90-95% of all bone cells [99]. They are part of the osteoblast lineage, the result of osteoblasts that have been further differentiated and then fully surrounded by mineralized matrix. While originally this was considered a passive process, studies have shown that osteocytogenesis is an active process requiring the breakdown of collagen and the growth of dendritic processes from the cell itself [100]. These dendritic processes branch out from the cell in all directions through canaliculi, which allow osteocytes to connect to both each other and cells on the bone surface [99]. This results in a massive network of interconnected cells which give osteocytes the ability to serve as bone “communicators” and play a sensory or regulatory role in many bone processes. Osteocytes have a regulatory role in calcium and phosphate homeostasis and bone remodeling, as well as being the main mechanosensory cells in bone, which give it the ability to respond to external forces [99].

Because of their primary role in regulation, osteocytes produce a number of signaling molecules in response to certain stimuli. Signals that regulate bone formation through the activation of osteoblasts include stimulatory molecules, such as nitric oxide (NO) and prostaglandins, and inhibitory molecules, such as Dickkopf 1 (Dkk1) and sclerostin, which both inhibit Wnt signaling. Signals that regulate bone resorption through actions on the osteoclasts include RANKL and OPG. In addition, osteocytes can “signal” for bone resorption through their death. Osteocyte apoptosis can occur in response to several different factors, such as microdamage, aging, loss of estrogen, or hypoxia, but it ultimately leads to the activation and osteoclasts and bone resorption. [99]

Bone-lining Cells

Bone-lining cells are flat cells derived from the osteoblast lineage that line the surface of the bone. The exact signals that cause osteoblasts to differentiate into bone-lining cells are unknown, and the functions of bone-lining cells are not fully understood [98]. Several functions have been proposed, such as operating as a barrier between healthy bone and osteoclasts to block unnecessary resorption [70], contributing to mineral homeostasis through the regulation of calcium and phosphate flux [98], or helping maintain the marrow stem cell niche [98]. Bone-lining cells are also in direct communication with osteocytes through dendritic processes, and thus could work with the osteocyte to respond to mechanical loads and regulate bone remodeling [98]. Finally, bone-lining cells retain the ability to re-differentiate back into osteoblasts in response to certain stimuli such as mechanical loads and systemic hormones [96], and some mouse studies have shown that they can serve as a source of osteoblasts in the adult skeleton, when the MSC pool for differentiation of new osteoblasts is limited [101]. More research is necessary to fully elucidate the role of bone-lining cells to overall skeletal homeostasis.

Bone Remodeling

Bone remodeling is a continual cycle of sequential bone resorption and formation through the coupled actions of osteoclasts and osteoblasts that is necessary to maintain integrity of the skeletal system by repairing areas of microdamage [102]. Bone remodeling also plays a role in mineral and acid/base homeostasis by releasing or sequestering minerals such as calcium and phosphorus, and the release of growth factors embedded in the bone matrix [71]. Finally, bone remodeling is the only process by which dead or dying osteocytes can be replaced with healthy cells [71]. Bone remodeling primarily takes place on the surface of the bone in distinct areas known as bone remodeling units (BRUs). Because of its high surface area to volume ratio, cancellous bone is more actively remodeled than cortical bone, with around 80% of remodeling activity taking place on the trabecular surface [71,102].

Systemic and local control of bone remodeling

The process of bone remodeling is under the control of many local and systemic factors. Systemically, remodeling is primarily controlled by hormones involved in mineral homeostasis, such as PTH and vitamin D, or those that regulate growth, such as growth hormone, estrogens, and androgens [102,103]. Estrogen is considered one of the most important controllers of bone remodeling in adults, due to its direct actions on all bone cell types (see *Estrogen Actions* for more information) [103]. Locally, bone remodeling is under the control of factors that regulate the differentiation and activity of osteoclasts and osteoblasts, such as M-CSF, OPG, prostaglandins, and nitric oxide [102,103]. Importantly, most local factors that regulate osteoblast and osteoclast activity

come from other bone cells, which allows for the coupling of the resorptive and formative activities. Without the coupled actions of osteoblasts and osteoclasts, bone resorption could be happening without subsequent bone formation, or vice versa, which could significantly alter the shape and material of the whole bone, which would in turn significantly impact the strength of the bone.

Phases of bone remodeling

Bone remodeling occurs in four distinct and sequential phases. Phase one is the activation phase, in which osteoclasts are recruited [71]. Osteoclast precursors from the bone marrow are recruited into the BRU, where they begin to differentiate fully into active osteoclasts through the binding of RANKL. This RANKL is produced by bone marrow stromal cells or osteocytes, which shows how bone cells, particularly osteocytes, regulate each other to maintain bone mass [93]. The second phase is the resorption phase, during which fully differentiated osteoclasts bind to the bone and actively begin to resorb the damaged bone area. The third phase is the reversal phase, in which osteocytes either move to a new BRU or undergo apoptosis and osteoblasts are recruited [71]. Osteoblast precursors are recruited into the BRU and differentiated into mature osteoblasts by local factors, such as nitric oxide and prostaglandins produced by the osteocytes, or systemic factors such as PTH and estrogen [104]. The final stage is formation, where activated osteoblasts lay down new organic matrix which is then mineralized [71]. In adults, remodeling is balanced, with equal amounts of bone resorbed and formed to maintain total bone mass. However, with aging and with the loss or disruption of systemic hormones, particularly estrogen, bone remodeling becomes unbalanced, with increases in

resorptive activity and decreases in formation [71]. This ultimately leads to loss of bone mass and diseases of low bone mass, such as osteoporosis.

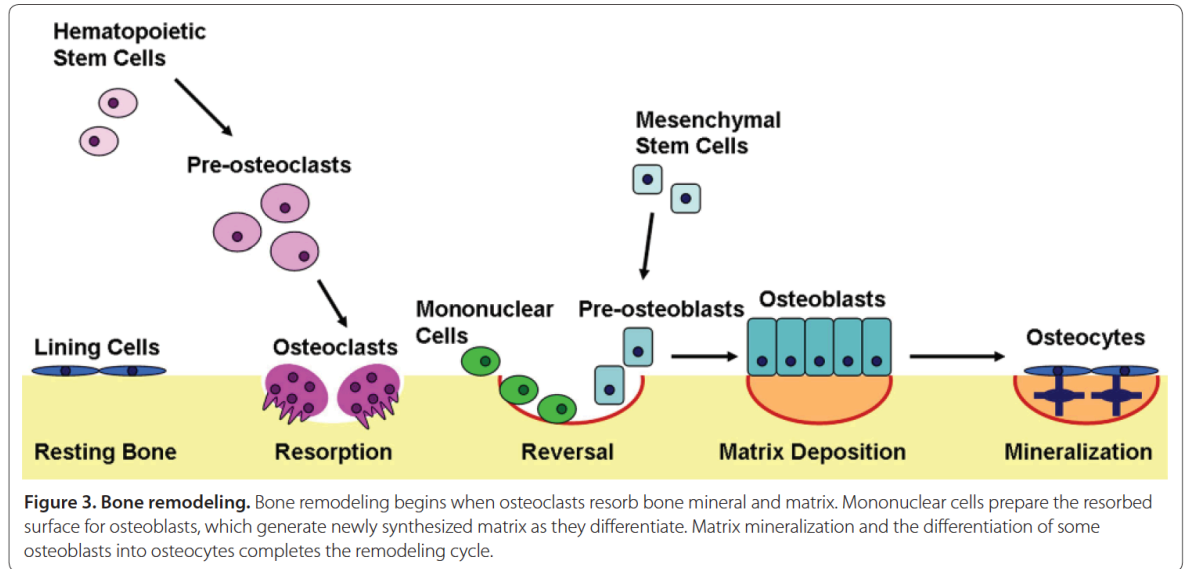


Figure 2.2 Overview of Bone Remodeling [273]

Osteoblast-osteoclast interactions – the RANK/RANKL/OPG axis

Many of the regulatory signals controlling bone remodeling come from osteocytes, but osteoblasts and osteoclasts communicate with either other, through direct cell-to-cell contact or the production of various cytokines and other proteins [105]. For example, osteoblasts can produce both M-CSF, which stimulates the differentiation of HSCs into osteoclast precursors, and Factor associated suicide ligand (FasL), which initiates osteoclast apoptosis [105]. Osteoclasts produce cytokines, such as complement component 3, and microRNAs, which stimulate osteoblast differentiation or activity [105]. However, one of the most important pathways of osteoblast-osteoclast interaction is the RANK/RANKL/OPG axis, which regulates osteoclastogenesis and bone turnover.

RANK is a receptor expressed on the membranes of osteoclast precursors and mature osteoclasts [105]. The binding of RANK with its ligand, RANKL, activates downstream signaling pathways, which induce differentiation and activation of osteoclasts and thus begin bone resorption. RANKL is highly expressed in osteoblast progenitor cells and mature osteoblasts, as well as other cell types such as activated T cells and osteocytes. A variety of systemic hormones regulate RANKL expression, such as PTH and estrogen. OPG is also a cell-membrane receptor, though it is primarily expressed on osteoblasts and B-cells in the bone marrow [105]. OPG acts as a decoy receptor for RANKL, which inhibits its binding activity with RANK. This decreases osteoclast activation and subsequently lowers bone resorption activity. OPG expression is also regulated by several systemic hormones, such as estrogen and vitamin D. The OPG/RANKL ratio is one of the strongest influencers of osteoclast formation and activity, and thus plays a significant role in the maintenance of bone mass through regulation of bone remodeling [105]. In fact, one of the primary mechanisms behind age-related bone loss is a loss of estrogen leading to an increase in RANKL and decrease in OPG expression. This imbalance of the OPG/RANKL ratio leads to increased bone resorption and a subsequent imbalance in bone remodeling [71].

Assessment of Bone Turnover

Bone turnover refers to a complete remodeling cycle, or bone resorption followed by bone formation. Clinically, both the bone turnover balance and rate are important, as abnormalities in either can lead to bone loss [106]. Measurement of bone turnover thus depends on measurement of both bone resorption and formation. In humans and animals,

bone turnover can be measured either directly in the bone, or indirectly in serum or urine. In humans, biochemical markers related to the production or degradation of collagen, bone-cell specific enzymes, or other non-collagenous constituents of the bone matrix that are released during remodeling [106] are measured in urine or serum. Although rarely done, biochemical markers of bone formation or resorption can also be measured in bone through a bone biopsy [107]. In animal models, biochemical markers of bone turnover can be measured in urine or serum or in bone. An advantage of animal models is that bone formation and resorption rates can be measured directly through histology or immunochemistry [108].

Assessment of bone resorption

Osteoclast number and activity are both clinically relevant measures of bone resorption, and thus both should be evaluated. Osteoclast activity markers are those that are released from the bone matrix during bone resorption, such as pyridinoline (PYD) and deoxypyridinoline (DPD), which form crosslinks between collagen fibrils, and the N- and C-terminal cross-linked telopeptides of type I collagen (NTX or NTX-I and CTX or CTX-I, respectively), which are peptide fragments of type I collagen. Clinically and experimentally, the most common marker of osteoclast activity measured is CTX, as recommended by the International Osteoporosis Foundation (IOF) [106,107]. Markers of osteoclast number are osteoclast specific enzymes, the most common of which is tartrate resistant acid phosphatase type 5 (TRAP), although there is some evidence that serum levels of cathepsin K also correlate with osteoclast activity. However, more evidence is needed before cathepsin K can become a standard marker of resorption [106,107].

Assessment of bone formation

Bone turnover markers of bone formation include by-products of collagen synthesis, osteoblast-specific enzymes, and non-collagenous matrix proteins produced by the osteoblast. By-products of collagen synthesis are the N- and C-terminal propeptides of type I pro-collagen (P1NP and P1CP, respectively). While collagen can be made in tissues other than bone, studies have shown that the majority of circulating P1NP and P1CP are from the bone, and the IOF recommends P1NP be used as a standard marker of bone formation, usually a measure of osteoblast activity [107]. Other markers of bone formation are osteoblast-specific enzymes, such as bone-specific alkaline phosphatase (bone-specific ALP or BAP) or non-collagenous matrix proteins synthesized by the osteoblast, such as osteocalcin [106,107]. Although approximately half of the circulating ALP comes from bone, there can be some cross reactivity in assays with other forms of ALP, such as those produced in the liver, making the specificity of the test low and thus subtle changes in bone formation can be hard to detect using only BAP [106]. Because of this issue, osteocalcin and P1NP have become the most common pairing of bone formation markers in the last couple decades [106,107].

Bone throughout the life cycle

Bone development is a unique process because it involves the construction of a temporary structure, a collagen model in utero, which is then slowly replaced with a permanent structure uniquely suited for an individual body's needs [109]. In addition, this development of the permanent structure, the adult skeleton, takes place over a decades-long growth cycle, which has unique implications on the process of organogenesis.

Bone in utero

Bone development begins in utero through a process called endochondral ossification [110]. Briefly, endochondral ossification begins in utero with the migration of mesenchymal stem cells to the pre-determined sites of future bones, where they differentiate into chondrocytes and form the cartilage model. These chondrocytes proliferate and differentiate into hypertrophic chondrocytes, which then recruit osteoclasts and osteoblast progenitors, as well as endothelial and hematopoietic cell precursors through the production of various cytokines and growth factors. Osteoclasts begin to degrade the cartilage, and osteoblast progenitors differentiate into osteoblasts and begin to lay down new bone where there was cartilage previously. Endothelial cells begin to differentiate and grow into blood vessels, and hematopoietic cells begin to establish bone marrow. This combination of differentiated bone cells, bone marrow, and blood vessels is known as the primary ossification center, and it is located in what will end up being the diaphysis of the bone. As the fetus grows, the primary ossification center begins to expand as more and more of the collagen model is degraded and then replaced with bone material. [109,111]

After the primary ossification center is established at the center of the bone, secondary ossification centers begin to develop at each end of the long bone. These secondary centers often develop near the end of gestation, but in some bones they develop in the first few months of life after birth [112]. Secondary ossification centers are made up of a similar combination of osteoclast, osteoblast, and endothelial progenitor cells as primary centers, and they degrade the collagen model to develop bone in what will become the epiphysis. In between the primary and secondary ossification centers are the epiphyseal growth plates, made of cartilage, which are necessary for longitudinal growth of the bone. Post-natal, endochondral ossification continues into adolescence, until the growth cartilage becomes fully fused into the secondary ossification center and longitudinal growth ends [109,113].

48

E.J. Mackie et al. / The International Journal of Biochemistry & Cell Biology 40 (2008) 46–62

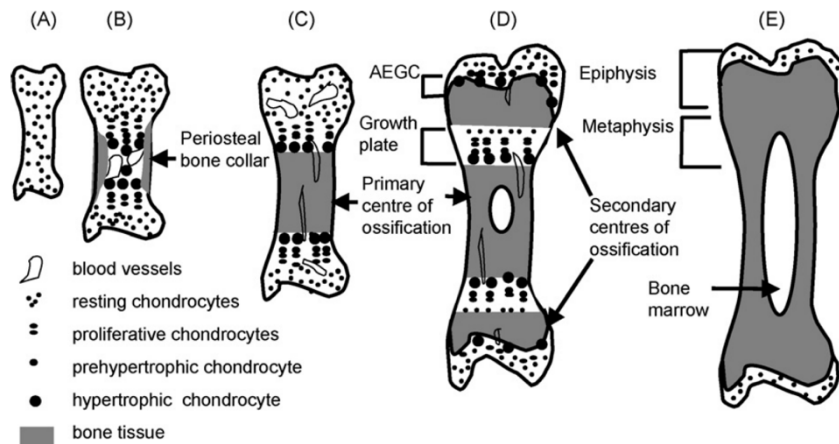


Fig. 1. Development of endochondral bones. Schematic diagram showing the events leading to replacement of an embryonic cartilage model by bone. (A) Cartilage model. (B) Initiation of formation of the primary centre of ossification in the centre of the cartilage model, with chondrocyte hypertrophy and vascular invasion. (C) Well established primary centre of ossification; blood vessels are present in cartilage canals in the remaining cartilage. (D) The secondary centres of ossification have formed and are separated from the primary centre of ossification by the growth plate, which is responsible for longitudinal growth. Articular-epiphyseal growth cartilage (AEGC) remains under the permanent articular cartilage, and is responsible for growth and shaping of the epiphysis. (E) In the adult bone, the metaphyseal and epiphyseal bone have fused to each other, leading to the disappearance of the growth plate. The AEGC has been replaced by bone, and the only remaining cartilage is the permanent articular cartilage at each end of the bone.

Figure 2.3 Overview of Endochondral Ossification [109]

Bone accrual – birth through adulthood

Longitudinal bone growth is controlled by the ossification of the epiphyseal growth plate, or growth cartilage, and the timing and rate of growth plate ossification is what determines an individual's final height [113]. Longitudinal growth ends when the growth cartilage fuses completely with the epiphysis, which is often in late puberty [114]. However, bone accrual can still occur through appositional growth, or growth of the diameter of the bone through the addition of bone on the periosteal surface, long after longitudinal growth has ended. Bone mass can continue to increase until around the age of 30, at which point most individuals reach their peak bone mass [115].

Longitudinal growth

Longitudinal bone growth is under the control of several endocrine and paracrine factors, through their actions on the epiphyseal growth plate. These factors include growth hormone (GH), insulin-like growth factor-1 (IGF-1), glucocorticoids, thyroid hormones, and estrogens and androgens [113,116]. GH is one of the most potent stimulators of bone growth in childhood, both through direct actions on the growth cartilage and indirectly by increasing production of IGF-1 in the liver [113,116]. IGF-1 increases the activity of both chondrocytes and osteoblasts, which stimulates the growth of both new collagen and new bone needed for longitudinal growth [117]. Glucocorticoids can have the opposite effect, and inhibit longitudinal growth by inhibiting the proliferation of chondrocytes [116]. Hypothyroidism can also impair longitudinal growth, because thyroid hormone is necessary for the conversion of resting

chondrocytes into hypertrophic chondrocytes. Thyroid hormone can also indirectly effect longitudinal growth through the GH/IGF-1 axis, because individuals with hypothyroidism also often have low circulating levels of GH and IGF-1 [116].

Once an individual begins puberty, estrogen becomes the most important endocrine factor controlling longitudinal growth, in both males and females. Initially, low doses of estrogen stimulate the GH/IGF-1 axis into the pubertal “growth spurt”, or time of accelerated longitudinal growth [114]. As puberty continues and estrogen levels increase, estrogen acts directly on the growth cartilage and induces growth plate senescence and fusion [114,116]. Growth plate senescence is a time in which chondrocyte proliferation and differentiation slow dramatically until they reach zero. Fusion happens when proliferation ends and the remaining chondrocytes are rapidly replaced with bone material [118]. Androgens in males can also stimulate the GH/IGF-1 axis and accelerate longitudinal growth at the beginning of puberty, but the final closure of the epiphyseal plate and subsequent end of longitudinal growth is solely dependent on estrogen [116].

Mineralization and Appositional Growth

Longitudinal growth and full mineralization of the bone material are coordinated, but do not occur at the same pace [119]. Mineralization lags behind growth, which can have unique implications on skeletal health in childhood. In general, adolescents achieve peak mineral acquisition rates about one year after they achieve peak growth rates [119]. This lag in mineralization can lead to a one year period where adolescents have lower BMD and lower bone strength, which puts them at higher risk for fracture [115]. Khosla,

et al. showed that the incidence of forearm fractures peaks during the same ages as the pubertal growth spurt in both boys and girls [120]. Mineral acquisition then continues even as longitudinal growth slows and stops – within 4 years of peak high velocity individuals have acquired 90-95% of their peak bone mass [121], but 6-10% of peak bone mass is acquired after longitudinal growth stopped [119]. Mineralization rates can vary between skeletal sites, but whole body peak bone mass is acquired by the end of the second or beginning of the third decade of life [121,122].

Bones grow in both length and width until epiphyseal plate closure, but growth in width can continue after longitudinal growth ends. Bones get wider primarily through actions of osteoblasts on the periosteal (outer) surface of the bone, a process known as periosteal apposition or periosteal expansion [123]. Periosteal expansion is under similar hormonal control as longitudinal growth, with GH, IGF-1, PTH, estrogen, and androgens being the primary players. The GH/IGF-1 axis stimulates periosteal expansion, whereas the effects of sex hormones are more complicated [117,123]. Androgens and estrogens can have differing effects on periosteal expansion in men and women, which partially explains the common sex differences seen in bone mass between men and women [124].

Sex Differences in Bone Accrual

Males

On average, males tend to hit developmental milestones at later ages than females. Males often have their pubertal growth spurt around the age of 13, and studies have shown that their peak height velocity occurs around 13.5 years of age [119], and then growth rates slowed until epiphyseal plate closure. Mineralization lags behind growth,

and on average males achieve peak mineral acquisition rates around 14 [119]. While males tend to have higher bone mass even through periods of growth, they also can have higher cortical porosity during this time, which is an indicator of weaker bones and puts them at higher risk for fracture in adolescence [125]. After puberty and adolescence, however, males end up with higher bone mass than females – on average young adult men have 25-33% higher cross-sectional bone area than young adult women. [126]. Young adult men also have higher trabecular bone volume than young adult women, which contributes to increases in bone strength [126]. These increases in bone mass and strength are maintained through the lifespan, which puts men at lower risk for fracture later in life [115,124].

Larger increases in periosteal expansion and trabecular bone volume in young men have been positively associated with circulating levels of free testosterone in some, but not all studies [124]. However, it should be noted that part of testosterone's effects on bone could be mediated by the aromatization of testosterone to estrogen locally in bone, and not directly related to testosterone levels. The importance of aromatase to bone health can be seen in a case study of a young man with aromatase deficiency, who had no signs of epiphyseal plate closure and thin bones at the time of treatment [127]. Two years of daily estrogen administration led to the closure of epiphyseal plates and a 45% increase in cross-sectional area of the radius, implying that estrogen is necessary in men for both longitudinal and transverse growth [127]. However, estrogen treatment had no effect on trabecular bone volume, implying that androgens are the primary determinants of trabecular bone development in men [127].

Females

Females tend to have lower total bone mass than males, partly because they achieve developmental milestones at earlier ages than males. Females often have their pubertal growth spurt around the age of 10 or 11, and studies have shown that their peak height velocity occurs between 11 and 11.5 years of age dependent on race [119]. African-American girls tend to achieve peak height and mineralization velocities earlier than non-African American girls [119]. On average, females achieve peak mineral acquisition rates between 12 and 12.5 years, again depending on race [119]. Females grow less total bone mass than males, which protects them from the high cortical porosity seen in males during adolescence [125], and female adolescents tend to have lower rates of fracture than males [115]. However, after adolescence and puberty, females tend to have lower measures of peak bone mass which can have significant implications on bone health later in life [128].

Similar to males, estrogen is responsible for the closure of epiphyseal plates and increases in periosteal bone mass in females. In addition, estrogen appears to be responsible for trabecular bone development in females. BMD is positively associated with free estrogen in premenopausal women [129], and women with estrogen deficiency and impaired ovulation have lower BMD than regularly ovulating women at all skeletal sites [130]. There is some evidence that high circulating levels of androgens can impact bone mass in women in certain disease states, such as polycystic ovarian syndrome, but further studies are needed to elucidate the specific role of androgens in normal bone development, and if these actions are specific to androgens or secondary to androgens being aromatized into estrogens [131].

Bone maintenance and loss – adulthood through senescence

Peak bone mass in both sexes is achieved by the age of 30 [121]. After 30 years of age, bone mass either remains stable or begins declining slowly, dependent on an individual's lifestyle [110,128]. In adults, total bone mass is directly related to bone remodeling. To maintain bone mass, bone remodeling needs to be coupled and equal amounts of bone need to be resorbed and formed. However, as individuals age, bone remodeling can become uncoupled, and more bone is resorbed by actions of osteoclasts than is subsequently formed by actions of osteoblasts, leading to decreases in bone mass [110]. After the age of 45, bone mass starts declining in both men and women, regardless of lifestyle choices. This decline can be linked to decreasing levels sex hormones in both men and women, but it is particularly noticeable in women with the onset of menopause [2]. Declining bone mass can lead to osteopenia and osteoporosis, diseases of low bone mass, which puts individuals at higher risk of fractures, particularly of certain skeletal sites such as the hip and spine [132].

Sex Differences in bone loss

Males

Male sex is one of the most protective factors against osteoporosis, with only one-third of osteoporotic fractures happening in men [124]. Studies have shown that age-related bone loss affects men and women equally, but men are still protected against fracture for the following reasons: 1) men have higher peak bone mass, which leads to higher bone mass later in life even after equivalent losses, and 2) men maintain their

levels of sex steroid hormones better than women, showing a steady decline over time rather than the abrupt drop seen at the onset of menopause [2,124]. As men age, they show a steady decline in bioavailable levels of both testosterone and estrogen, but the loss of estrogen seems to be particularly significant to the loss of bone mass [2]. Low bioavailable estrogen levels in older men are associated with an increased risk of fracture, whereas there is no association with bioavailable testosterone [133]. Older men can have higher circulating levels of estrogen than postmenopausal women [124], which could also contribute to their lower risk of osteoporotic fractures.

Females

Females are at much higher risk for osteoporotic fractures than men, for the following reasons: 1) calcium requirements and hormonal changes during pregnancy and lactation often lower BMD, although more studies are needed to determine if these changes are reversible and the impact these changes have on fracture risk with age, 2) women have lower bone mass overall compared to men, and 3) the steep drop in sex hormones, particularly estrogen, at the onset of menopause leads to a subsequent steep drop in BMD [2,134,135]. This steep drop in BMD which occurs in the first 8-10 years after menopause leads to low levels of BMD at earlier ages, which significantly impacts the length of time that women are susceptible to fractures [2,134]. Interestingly, there is still an association between lower bioavailable estrogen and increased fracture risk, even among the already low levels of postmenopausal women [2]. Hormone replacement therapy (HRT) of estrogen alone or combined with progestin was the premier treatment option for the prevention of osteoporosis in postmenopausal women for many years, until

the Women's Health Initiative concluded that the risks of HRT outweighed the benefits [2,136], and other treatment options were prioritized. However, even with high risks, the anti-fracture benefits of estrogen treatment could not be denied [136].

Lifestyle factors impacting bone accrual and loss

Each individual has the potential to achieve a genetically determined peak bone mass, and 60-80% of the variation in individual peak bone mass is genetically determined [137–139]. However, whether this genetic potential is reached is highly impacted by their lifestyle choices, particularly their nutrition and activity habits [128].

Nutrition

Considering the composition of bone material, it should be no surprise that mineral intake, primarily calcium, is strongly linked to bone mass accrual. Almost every single study involving supplementation in adolescents showed that calcium supplementation led to increases in BMD over time, ranging from 1-5% [128]. In general, individuals with lower baseline calcium intake saw higher increases in BMD than those with higher baseline intake, implying a threshold of calcium benefits. This threshold has been confirmed in balance studies, which show that calcium retention increases with calcium intake up to a certain point, at which calcium retention plateaus [128]. The calcium retention plateau can be affected by a variety of factors, such as sex and race, as well as other dietary components. Vitamin D has been shown to increase calcium absorption in the intestines, and often calcium and vitamin D are given together in one supplement. Studies showing supplementation with both calcium and vitamin D together

also show increases in BMD [128]; however studies supplementing with only vitamin D have been more controversial. The effects of vitamin D supplementation on bone accrual during childhood seem to be dependent on baseline vitamin D status, with improvements in BMD primarily seen in individuals with vitamin D insufficiency [128].

Interestingly, the link between vitamin D, calcium, and bone mass seems to be most important in children and young adults. Multiple meta-analyses of supplementation in adults over 50 have shown that there was no association between supplementation with vitamin D, calcium, or both with increases in BMD or decreased risk of fracture [140,141]. This implies that calcium and vitamin D are more important during bone growth to help achieve a higher peak bone mass than later in life to prevent bone loss.

Physical Activity and Exercise

Engaging in regular physical activity and exercise is considered one of the most important lifestyle choices that an individual can make throughout the lifespan in order to improve and maintain bone health [128]. Physical activity is considered “any body movement produced by muscle contraction resulting in energy expenditure above a resting level”, whereas exercise is defined as “planned, organized, and repetitive physical activity that is aimed at maintaining or enhancing one or more components of physical fitness or a specific health outcome” [128]. For research purposes, often exercise is used in randomized control trials, whereas physical activity levels are tracked in observational studies.

The majority of randomized control trials in children and adolescents showed increases in BMD in the exercising group compared to the control. Interestingly, the

magnitude of the differences decreased as the children got older, ranging from up to a 6% increase in prepubertal children to up to a 1.9% increase in late or post-pubertal adolescents over 6 months of intervention [128]. One study used the same exercise intervention in all female participants, but only showed improvements in prepubescent participants [142]. The majority of observational studies also report increases in BMD with increases in physical activity, particularly in children who participate in sports [128]. As an example, the University of Saskatchewan Pediatric Bone Mineral Accrual Study showed that children who were most physical active at 8-15 years of age had the highest BMC and BMD at 23-30 years, even after controlling for adult physical activity levels [143].

In adulthood and beyond, physical activity and exercise become about bone mass maintenance, or the prevention of bone loss, rather than bone accrual. Exercise intervention trials often have mixed results dependent on age of the participants and the type of exercise intervention [144–146]. For example, a meta-analysis showed that impact-based exercise interventions conveyed a benefit to BMD whereas walking interventions did not, in older men [144]. However, positive associations between levels of leisure physical activity and BMD remain in observational studies in both men and women [147–149]. Overall, regular, age-appropriate physical activity throughout the entire lifespan is one of the most important lifestyle choices an individual can make in order to prevent osteoporosis.

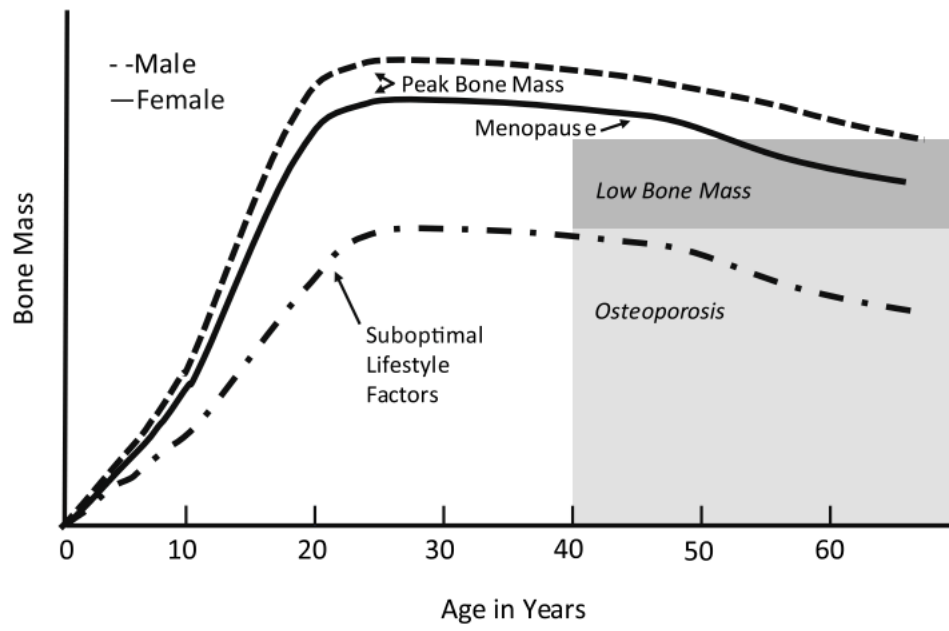


Figure 2.4 Bone Mass Across the Lifespan [128]

Mechanical Loading and Bone

It has been well established that engaging in regular, age-appropriate physical activity throughout the lifespan is one of the most influential ways to prevent age-related bone loss and fracture [128]. The benefits of physical activity are due to the mechanical forces of muscle contraction and ground-reaction forces exerted on the skeleton during exercise. Bone is a very mechanosensitive tissue, meaning it can sense external mechanical loads and then adapt to these forces [150,151]. Similar to muscle hypertrophy, bone tissue adapts in size and shape to be able to withstand new and regular forces applied to it. This idea of bone adapting to mechanical forces in order to maintain structural competence is known as the “mechanostat” theory, and it was first introduced by Harold Frost in the early 1980’s [151]. Since then, decades of research have worked to elucidate the cellular mechanisms behind bone’s mechanosensitive abilities.

Frost’s mechanostat

While Frost was not the first to notice that bone was a mechanosensitive tissue, he was the first to propose a theory regarding a regulatory mechanism through which bones sense and respond to mechanical forces, and he was the first to propose the idea of a mechanical threshold [151]. The theory of the mechanical threshold has been proven through the last decades of research – there is a low threshold of inactivity under which bone is lost, and there is a high threshold of activity over which new bone is grown. In between thresholds, bone mass is maintained [151]. As with any other homeostatic mechanism, the mechanostat is comprised of three main parts – a stimulus, a sensory

mechanism that is capable of detecting the stimulus, and effector mechanisms that can adapt to the stimulus and bring the system back to homeostasis [151].

In bone, the stimulus is ultimately strain, or amount of deformation of the bone material in response to a load applied. However, other strain-related characteristics, such as frequency of loading cycles, amount of rest between bouts of loading, and the distribution of the load within the bone structure all can affect the functional adaptation of the bone. In addition, the functional adaptation can be affected by the environment, particularly hormonal and nutritional status of the individual [151]. For example, individuals undergoing the same exercise treatment will not adapt the same if one is nutritionally or hormonally deficient [150]. Estrogen in particular seems to be a significant influencer of the mechanosensitive abilities of the bone (see *estrogen actions*) [150]. The effector cells are osteoclasts and osteoblasts, which can resorb and form bone where needed through the processes of bone modeling and remodeling [151]. The sensory mechanism, or the cell that detects the stimulus and translates it to the effector cells, is the osteocyte.

Osteocytes and the mechanostat

Osteocytes play a significant role at all three responses of the bone mechanostat – low forces leading to bone loss, normal forces leading to bone maintenance, and high forces leading to bone growth. Osteocytes are surrounded by fluid filled lacunae and canaliculi, and fluid flow shear stress resulting from loads on the bone is one of the main mechanical stimuli that leads to maintenance and increases in bone mass [151,152]. A reduction in fluid flow shear stress in the bone, such as occurs in immobilization, space

flight, and other situations of disuse, is implicated in biochemical signaling that leads to bone loss [151]. Disuse can possibly lead to lower blood flow, which inhibits the nutrient supply and impairs the removal of waste products [151]. In addition, studies in rodents have shown that diffusion in unloaded bones is not enough for large molecules, such as proteins, to reach the osteocyte where it is buried in the bone matrix [153], which means that active fluid flow stimulated by loading is required for normal protein transport and signaling. Together, this shows that disuse leads to nutrient and protein deficiencies which result in osteocyte apoptosis. Osteocyte apoptosis is a strong biochemical signal for bone resorption, as cytokines released from apoptotic osteocytes, such as RANKL, signal osteoclast differentiation and activation [151].

In the presence of loading, bone mass is either maintained or increased, depending on the magnitude of the load, as well as other confounding factors such as nutritional and hormonal status. In the presence of loading, osteocytes sense increases in fluid flow shear stress and changes in hydrostatic pressure through several cellular mechanisms, such as conformation changes in protein structures or movement of the cilia on the cell body and dendritic processes [152]. Once the mechanical signal is sensed by the osteocytes, it is translated into biological cues that both regulate gene transcription in the osteocyte itself and transduce the signal to other cell types. The main biological cues involved are intracellular calcium signaling, nitric oxide, prostaglandins, and Wnt proteins [152]. Prostaglandins can work on osteocyte in an autocrine fashion to regulate gene transcription along with intracellular calcium signaling. Nitric oxide and prostaglandins also work in a paracrine fashion to modulate osteoblast and osteoclast activities towards bone formation [152]. Wnt proteins act as signaling molecules to stimulate osteoblast

differentiation and activation [152,154]. One of the main genes downregulated in the osteocyte in response to mechanical loading is *Sost*, which codes for the protein sclerostin, a Wnt signaling inhibitor.

Wnt Signaling

Research developments in the past decades have revealed the importance of Wnt signaling in the development and maintenance of the skeleton through the discovery of certain skeletal dysplasias associated with loss- or gain-of-function alterations to genes involved in Wnt signaling pathways [155,156]. The Wnt family of proteins are secreted glycoproteins that are post-translationally modified by the addition of a lipid, usually palmitate, necessary for activity [155]. Currently there are 19 known Wnt proteins involved in three different signaling pathways – one “canonical” signaling pathway, which is the most studied and involves the transcription factor β -catenin, and two non-canonical pathways, the Wnt/Ca²⁺ pathway and the Wnt/PCP pathway [156]. The three Wnt signaling pathways are involved in a broad number of cellular processes across many organ systems. For most processes there is only one pathway involved, but there is also some evidence of overlap between the signaling pathways in certain processes [156]. In bone, canonical Wnt signaling through the Wnt/ β -catenin pathway seems to be the most important, and thus is the one that will be discussed in more detail.

Canonical signaling begins when the Wnt ligand binds with its co-receptor complex involving either lipoprotein-related receptor (LRP)-5 or -6 and the seven transmembrane-span Frizzled (FZD) receptor [155,156]. Binding of the ligand to this co-receptor complex leads to the activation of Disheveled by phosphorylation, which leads

to downstream phosphorylation of glycogen synthase kinase-3 β (GSK-3 β). GSK-3 β is a key component of a large complex of proteins responsible for the sequestration of β -catenin, a transcription factor. When not phosphorylated, GSK-3 β is marked for ubiquitination and the entire protein complex, including β -catenin, is degraded. However, when GSK-3 β is phosphorylated, the complex collapses and free β -catenin is released into the cytoplasm. β -catenin then translocates to the nucleus and interacts with other transcription factors to regulate the expression of genes related to the differentiation, proliferation, and function of various bone cells, particularly those in the osteoblast lineage [155,156]. For example, Wnt/ β -catenin signaling is required for the differentiation of MSC's to osteoblast precursors, regulates osteoprogenitor proliferation, and can increase the expression of OPG in osteoblasts [155]. In general, Wnt signaling in bone results in alterations to gene and protein expression that encourage bone formation.

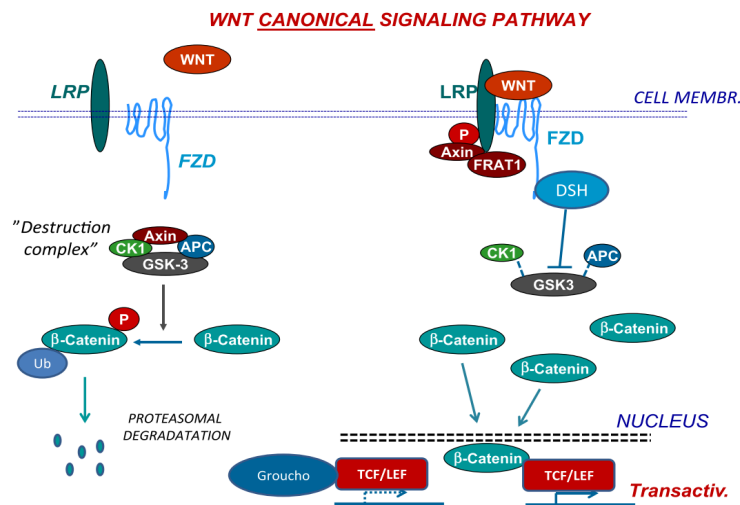


Figure 2.5 Overview of Wnt signaling [31]

Sclerostin is a Wnt inhibitor

Sclerostin was first discovered through two skeletal dysplasias resulting in higher than normal bone mass, sclerosteosis and Van Buchem's disease, which result from loss-of-function genetic mutations in or around the *Sost* gene [157]. This high-bone-mass phenotype associated with low or undetectable levels of sclerostin protein implied that sclerostin plays a role in blocking bone formation. Consistent with this hypothesis, mouse models altered to overexpress sclerostin have low bone mass, in both cortical and cancellous bone [33]. Research over the past two decades has shown that sclerostin is expressed in osteocytes, but not in other cells of the osteoblast lineage. Specifically, sclerostin is expressed only in mature osteocytes that are embedded in the mineral matrix, not recently differentiated osteocytes that are close to the active bone formation surface [33].

Sclerostin primarily inhibits bone formation by acting as a Wnt signaling inhibitor [33,157]. Sclerostin binds to LRP-5 and -6, which antagonizes canonical Wnt signaling and blocks downstream upregulation of osteogenic gene transcription. Deletion of the *Sost* gene or treatment with antibodies to sclerostin in mouse models showed higher bone mass associated with increased osteoblast number and activity [33]. Sclerostin can also indirectly increase bone resorption – overexpression of sclerostin in mice is associated with an imbalance in the OPG/RANKL ratio leading to increased osteoclast differentiation and activity [33]. Sclerostin expression is regulated by many local and systemic factors, such as mechanical loads applied to the bone and hormonal status.

Regulation of sclerostin expression

Mechanical Loading

Mechanical loading is the primary functional determinant of bone mass, and downregulation of sclerostin expression in osteocytes is one of the primary cellular mechanisms behind the functional adaptation to mechanical loading. Osteocytes sense loads through fluid shear stress and hydrostatic pressure changes, which leads to the release of paracrine and autocrine factors, such as nitric oxide and prostaglandins. Cell culture studies show that prostaglandins, specifically PGE₂, bind with EP2 and EP4 receptors on the osteocyte to trigger a cascade of signaling that ends with the downregulation of sclerostin in the osteocyte [158]. This downregulation of sclerostin allows for an increase in Wnt signaling, which leads to bone formation.

There is significant evidence that downregulation of sclerostin is required for loading-induced bone formation, and that upregulation is required for disuse-induced bone loss. In mice subjected to ulnar loading, there were significant decreases in sclerostin expression, both mRNA measured via PCR and cellular expression measured via immunohistochemistry, in the loaded ulnae compared to the unloaded ulnae [159]. This downregulation of sclerostin was associated with increased bone formation rate, and the magnitude of downregulation correlated to the magnitude of the loading strain [159]. However, in transgenic mice overexpressing sclerostin, ulnar loading did not lead to increased bone formation like it did in the wild-type counterparts [160,161]. Mice subjected to hind limb unloading or disuse via sciatic neurectomy have increased sclerostin expression associated with increased bone resorption, but sclerostin knockout mice do not [160,161]. Interestingly, the downregulation of sclerostin and subsequent increase in bone formation appears to be a localized phenomenon. Robling and Moustafa

both found in separate experiments that sclerostin downregulation was spatially distributed along the loading axis – areas of the bone that underwent the highest strains showed the largest decreases in sclerostin expression compared to areas of the bone that underwent smaller or no strain [159,162]. Overall, downregulation of sclerostin appears to be a key step in the osteogenic response to mechanical loading.

Hormonal Status

Sclerostin expression can also be influenced by systemic and local hormones, especially PTH and sex hormones, which play significant roles in the development and maintenance of bone mass. Postmenopausal women treated with intermittent PTH, one of the only approved anabolic bone treatments, had decreased circulating sclerostin levels compared to the control subjects [163]. It should be noted that sclerostin levels circulating in serum are not always reflective of sclerostin expression from a bone biopsy, and thus human data using circulating sclerostin only should be used sparingly [33,163]. However, mice treated with intermittent PTH also had decreased mRNA expression of sclerostin in the bone, providing more evidence that PTH can influence sclerostin expression.

Sex hormones are also significant regulators of sclerostin expression, especially estrogen. Postmenopausal women show higher serum sclerostin levels than premenopausal women, and there is a significant inverse relationship between bioavailable estrogen and circulating sclerostin in both older men and postmenopausal women [163]. Treatment with estrogen reduced circulating sclerostin levels in postmenopausal women, as well as in men, compared to control subjects [163].

Postmenopausal women treated with estrogen for 3 weeks also had decreased mRNA expression of sclerostin measured when assessed via RNAseq or QPCR from a bone biopsy, giving more substantial support to the influence of estrogen on sclerostin levels [164]. Many rodent models also support the influence of estrogen on sclerostin expression, but they will be discussed in a later section (see Estrogen and Sclerostin).

Estrogen and the Skeleton - Mechanisms of Action

Estrogen is one of the most influential hormones in growth and maintenance of the skeleton, and epidemiological evidence supports a strong positive correlation between bioavailable estrogen and bone mass in both women and men [1]. While the importance of estrogen was first discovered in relation to bone loss during menopause [3], estrogen plays a significant role in bone growth and maintenance across the entire lifestyle (see *Bone throughout the lifecycle*). In both adolescent girls and boys, estrogen stimulates growth spurts of the skeleton [165]. The onset of puberty in adolescent females coincides with peak mineralization velocity [166], and both adolescent boys and girls have significant increases in bone mineral density (BMD) between pre- and post-pubertal ages [167,168]. Estrogen loss associated with menopause leads to a significant loss of bone mass in older women; however, a loss of estrogen with age contributes to bone loss in men as well, albeit is at a slower rate [2]. Overall, there is significant epidemiological evidence that bioavailable estrogen is a primary influencer of total bone mass. Here, we will explore cellular mechanisms that make estrogen such a vital effector of bone health.

Mechanistic data often comes from animal or cell culture models, which allow us to manipulate and control environmental, nutritional, and genetic factors to fully explore ideas. However, there are some key differences in sex steroid hormone physiology between animals and humans that should be considered when using animal models for estrogen research. For one, rodents do not produce sex hormone binding globulin, a transport protein found in humans, which affects circulating levels of free estrogen and testosterone [124]. In addition, male rodents show a higher reliance on peripheral aromatization of testosterone to estrogen than humans. Free bioavailable estrogen in the

serum can sometimes be undetectable in male rodents, implying that their skeleton relies almost exclusively on locally produced or aromatized estrogen rather than circulating estrogen [124]. Gonadectomy is also often used as a preclinical model of menopause or osteoporosis, but findings can be confounded by the rapid loss of all gonadal hormones, not just estrogen or testosterone [124,169]. Global genetic knockout models can have indirect effects on the target tissue due to a disrupted negative feedback loop or secondary effects in another tissue – for example, global estrogen receptor knockout mice often have decreased IGF-1 production in the skeleton, but whether that is due directly to a loss of estrogen signaling in the skeleton or indirectly to a disrupted hypothalamus-pituitary axis in the brain is not clear [124]. However, recent advancements with the Cre-Lox system have allowed for cell-specific and inducible knockouts, which has lessened the influence of confounding variables seen in global knockout models. Finally, it should be noted that a single estrogen receptor knockout model does not mimic hormone deficiency exactly, given that estrogen has multiple receptors, and there appear to be ligand-independent effects of the estrogen receptors (ER), particularly estrogen receptor-alpha (ER α) [170]. Even with these physiological caveats, rodent models still provide some of the best models for hormonal research, given their lower cost and wider range of genetic manipulation compared to other models.

Estrogen receptors in bone

Estrogen actions are mediated primarily by estrogen binding with the ER, which is found in two main isoforms, ER α and ER β . ERs are part of a nuclear receptor superfamily characterized by zinc-finger-containing transcription factors that bind to

DNA sequences called hormone response elements, in this case estrogen response elements (EREs), to stimulate the transcription of target genes [169,170]. Both ER α and ER β are found in bone tissue, and in all bone cell types [4]. However, they are unevenly distributed, with higher expression of ER α in cortical bone, and higher expression of ER β in cancellous bone [15]. In addition, ER α and ER β have been found on immune cells, such as B- and T-cells, which are important in bone regulation due to their production of differentiation factors, such as RANKL [4]. The specific role of ER α and ER β in bone can be elucidated using receptor knockout models (ERKO and BERKO, respectively).

Estrogen Receptor- α

Males

Adult male ERKO mice have decreased BMD and femur length compared to WT counterparts [16,18,20,23]. They also have negative alterations in cortical bone geometry, such as decreased cortical bone area and cortical thickness, which are associated with decreases in biomechanical strength [16,18,21]. In addition, male ERKO mice have reduced bone turnover compared to WT mice, with decreased serum concentrations of both osteocalcin and CTX [18,21]. However, male ERKO mice have increased cancellous BMD and total cancellous bone, due to an increase in trabecular number and thickness, compared to WT animals [16,20–22]. They also have increased bone formation rate and decreased osteoclast number per area of bone surface in cancellous bone compared to WT [16]. These differential responses to the loss of ER α in cortical versus

cancellous bone are most likely due to the variable distribution of the estrogen receptors, since ER α is more highly expressed in cortical bone [15].

Females

Female ERKO mice usually have similar phenotypes as male ERKO mice, however the studies are not as consistent [23]. Female ERKO animals have decreased cortical BMD compared to WT animals [16,19,20], and one study showed a decrease in femoral length compared to WT [16]. In two other studies there were no differences between groups in femoral length, regardless of age of the animals [19,20]. In contrast with the male ERKO animals, one study showed increases in cortical area and bending strength in the female ERKO animals compared to their WT counterparts [16]. However, another study showed decreases in cortical thickness in the female ERKO animals, although bending strength was not tested [20]. In cancellous bone, female ERKO animals have increased BMD and total trabecular volume, similar to male ERKO animals [16,20]. They also have decreased osteoclast number and markers of bone resorption in the cancellous bone compared to WT animals [16,20]. However, measures of bone formation are more variable and seem to be dependent on age – one study showed decreases in measures of bone formation via histomorphometry at 10 and 16 weeks of age, but increases at 12 months [20]. Similar to male ERKO animals, the varied responses in cortical and cancellous bone are most likely due to the differential distribution of the ER isoforms [15]. In addition, due to the loss of the negative feedback loop in the hypothalamus, circulating concentrations of estrogen are often 10-fold higher in female ERKO animals compared to WT [4,169]. These high concentrations of estrogen could

lead to increased binding activity with ER β or signaling through non-classical pathways, such as protein-protein interactions, that could explain some of the varied results [4,23,169].

Estrogen Receptor- β

ER β is much less studied than ER α , and the role of ER β in bone is still unclear. Generally, male BERKO mice have very limited phenotypic alterations in the skeleton compared to WT counterparts [18,23,171,172]. Female BERKO mice have increased trabecular bone volume, similar to female ERKO mice [20]. However, the cortical bone impairments seen in female ERKO mice are not seen in female BERKO mice. In fact, one study in aged female BERKO mice showed that the loss of ER β protected the animals against age-induced bone loss, in both cortical and cancellous bone [171]. This was associated with an upregulation of ER α , which implies that these protective effects could partially be explained by increased estrogen binding activity [171].

While the lack of phenotypic differences in male BERKO mice implies no role for ER β in bone, the increased trabecular bone volume seen in male ERKO mice suggests otherwise. In addition, both female ERKO and BERKO animals have increased trabecular bone volume, which implies a redundancy in actions between the receptors in cancellous bone [4,23]. However, based on global knockout models, there does not appear to be a significant role for ER β in cortical bone, other than possibly regulating the expression of ER α [171]. Cell-specific knockout models would tell us more about the specific role of ER β in bone.

Cellular actions on each bone cell type

Osteoclasts

Estrogen primarily works to inhibit bone resorption in osteoclasts. Estrogen stimulates osteoclast apoptosis through the production of FasL, leading to decreased osteoclast number [3,169]. Estrogen also stimulates the production of Wnt proteins and β -catenin in osteoclasts, which would indirectly lead to increases in osteoblast activity (see *Wnt signaling*) [169]. Finally, estrogen can inhibit osteoclastogenesis both directly and indirectly. In the osteoclast itself, estrogen blocks transcription of RANKL/M-CSF activator protein and other proteins required downstream of ligand binding, which suppresses RANKL-induced osteoclastogenesis [3,169]. Indirectly, estrogen signaling in B- and T-cells in the bone marrow suppresses RANKL production and stimulates OPG expression, which decreases osteoclastogenesis. In addition, estrogen can suppress the production of other inflammatory cytokines, such as TNF- α , which stimulate bone resorption [3].

Deletion of ER α from mature osteoclasts in female mice leads to low cancellous bone mass associated with increased osteoclast number, but it had no effect on cancellous bone mass in male mice [170]. Deletion of ER α from osteoclast progenitor cells showed the same phenotype – low cancellous mass only in the female animals [173]. However, no study has shown any negative effects on cortical bone in either sex [169,170]. This implies that ER α in the osteoclast itself is protective against cancellous bone loss in females, whereas estrogen's antiresorptive actions in cortical bone and in males must occur indirectly through actions in osteoblasts or B- and T-cells and other immune cells [4].

Osteoblasts

In osteoblasts, estrogen act primarily to induce or maintain bone formation. Estrogen has been shown to protect against osteoblast apoptosis, leading to increases in osteoblast number and bone formation [3]. Estrogen modulates both the Wnt/ β -catenin and IGF-1 pathways to stimulate the differentiation, proliferation, and activation of osteoblasts [169]. Estrogen can also block the differentiation of mesenchymal stem cells to adipocyte progenitors, allowing for more differentiation into osteoblast progenitors [7,169]. Estrogen indirectly increases bone formation through decreases in oxidative stress and the production of reactive oxygen species, which have been shown to induce osteoblast apoptosis [3]. Finally, estrogen can inhibit NF- κ B activity in osteoblasts, which leads to an increase in the expression of proteins necessary for matrix formation and mineralization [3].

Deletion of ER α from osteoblast progenitors led to decreased cortical bone mass and cortical thickness in both male and female mice, associated with decreased osteoblast number, lower bone formation rate, and impaired Wnt signaling [174]. There were no differences in trabecular bone mass, again supporting the idea that direct actions of estrogen on osteoblasts are protective in cortical bone, whereas the protective actions of estrogen in cancellous bone are through the osteoclasts [169,174]. Interestingly, female mice without ER α in osteoblast progenitors do not show the expected increase in osteoclast number after ovariectomy and are protected from ovariectomy-induced cortical bone loss [170]. This supports that the antiresorptive actions of estrogen are not directly through the osteoclast but involve communication between osteoblast and osteoclast. In

addition, deletion of ER α from undifferentiated mesenchymal stem cells led to an increase in adipocyte progenitors and a decrease in osteoblast progenitors in bone marrow [174]. This shows that estrogen plays an important role in the differentiation of mesenchymal stem cells, but the exact mechanism still remains to be elucidated. However, deletion of ER α from mature osteoblast had no or little effect on the skeleton phenotype [4,169,170]. One study did show an increase in markers of osteoblast apoptosis in mature osteoblast-specific ER α knockout mice, but it was not accompanied by any skeletal differences compared to WT animals [174]. This shows that estrogen's osteogenic effects are primarily through direct actions on MSCs and osteoblast progenitors.

Osteocytes

Similar to osteoblasts, estrogen protects against apoptosis in osteocytes, which protects against bone resorption [3,169]. In addition, estrogen appears to modulate load-induced bone formation [169], although the exact role of estrogen in osteocytes during mechanical loading is still being explored. Cell culture studies show that estrogen can modulate the downregulation of sclerostin, as well as decrease RANKL production, which together would stimulate bone formation in osteoblasts [3,169].

Osteocyte-specific gene knockout models are difficult to produce, due to the limited amount of proteins produced solely by the osteocyte. However, to this date two studies on mice with ER α deleted from osteocytes have been performed with conflicting results [169]. One study showed no phenotypic differences in the female mice, but a 20% decrease in trabecular bone volume in the male mice [175]. The other study showed no

phenotypic differences in the male mice, but low bone mass associated with decreased osteoblast number in the female mice [176]. The conflicting results could be a result of animal model, as they were bred on different genetic backgrounds. The animals were similar in age at the time of the study (11 and 12 weeks, respectively), and thus age is most likely not a factor [169]. Further studies are needed to explore the role of ER α in osteocytes, particularly related to estrogen's possible role in controlling or modulating the osteogenic response to mechanical loading.

Estrogen and Mechanical Loading

Exercise is a major influencer of total bone mineral density at all stages of the lifespan, and one of the most important lifestyle choices that individuals can make to protect their bone health [128]. Understanding the key factors in this osteogenic response to exercise is important to optimize bone accrual during the lifespan. Estrogen availability has been implicated as a significant influencer of the osteogenic response to exercise, particularly in women. In adolescent female rowers, lumbar spine BMD after 18 months of training increased only in those who had regular menses and circulating estrogen levels similar to those of the non-exercising controls [177]. Rowers who had irregular menses and lower circulating estrogen levels showed no improvements in bone mineral density [177]. In postmenopausal women, the majority of studies agree that exercise is effective in preventing age-related bone loss [178,179]; however, several studies show larger improvements in BMD in response to exercise in postmenopausal women undergoing estrogen treatment compared with untreated women [180–182]. While this concept is less studied in men, one study did show that the ability to adapt to

exercise was diminished in Finnish men with a certain polymorphism in the ER α gene [183], despite no differences in circulating estrogen levels between groups. This implies that estrogen signaling, through ER α , might play a controlling role in bone's response to exercise.

Cellular actions of ERs during mechanical loading

Estrogen and the estrogen receptors in bone influence the skeletal response to mechanical loading [13,14]. Cell culture models show that ER α is directly involved in the cellular response to strain in the osteoblast [25,26,184], in that ER α is upregulated and activated after mechanical strain has been applied. Additionally, ER α appears to be required for stabilization of secondary Wnt signaling molecules, such as β -catenin [25] and for the activation of extracellular signal-related kinase (ERK) [184], both of which are required for the normal osteogenic response to mechanical loading. Cultures of osteoblasts taken from long bones normally proliferate in response to strain, but this proliferation can be blocked by the addition of ER antagonists [185]. In addition, osteoblast cultures taken from ERKO mice do not proliferate in response to strain like osteoblast cultures from WT controls [186,187]. Taken together, this implies that ER α plays a direct role in bone's response to mechanical loading.

However, the role of ER α in the osteogenic response to mechanical loading seems to be sex dependent. Cell culture models show impaired proliferation of osteoblasts without ER α in both males and females [185,186,188], but only female animal models have impaired bone growth. Female global ERKO mice have a significantly smaller osteogenic response to loading in cortical bone, whether that be at the ulna [27] or the

tibia [28], measured as the change in cortical area over the loading period. Deletion of ER α only from mature osteoblasts and osteocytes also led to an impaired osteogenic response in female mice [29]. However, male global ERKO mice have an increased osteogenic response to mechanical loading compared to WT [28]. In addition, male mice that had no ER α in mature osteoblasts and osteocytes had no differences in the osteogenic response to loading when compared to littermate controls [29]. Both groups showed a similar increase in cortical thickness after 2 weeks of loading when comparing loaded and unloaded limbs. The reason for this sex difference is unclear but implies some sort of compensatory mechanism in male mice, possibly through ER β or actions of androgens.

Few studies have looked at the role of ER β in mechanical loading, and they show conflicting results. In one study, female BERKO mice had an impaired net-osteogenic response in cortical bone to ulnar loading; however, osteoblast cell cultures from these same animals had increased proliferation when subjected to strain [27]. In another study, both male and female BERKO mice had increased net-osteogenic response to tibial loading in cortical bone [28]. Both studies measured net-osteogenic response as percent change in cortical area after the loading period. Much more research is needed to fully understand the role of ER β in mechanical loading, and how it might interact with ER α .

Estrogen and Sclerostin

The importance of estrogen and estrogen receptors in mechanical loading are clear. However, the exact cellular pathways involved are still being explored. One more recently proposed mechanism of action is the modulation of sclerostin expression by

estrogen. In women, there appears to be an inverse relationship between estrogen and sclerostin expression. Estrogen treatment decreased circulating sclerostin [34] and sclerostin expression in the posterior iliac crest [35] in older women. Treatment with aromatase inhibitors, which decrease circulating estrogen, increased circulating sclerostin in women with breast cancer [189], again supporting the inverse relationship between estrogen and sclerostin. In female mice, ovariectomy increased the percentage of sclerostin-positive osteocytes in the femur 3 weeks after ovariectomy, but treatment with endogenous estrogen reversed this change [37]. In female rats, increases in sclerostin mRNA levels were seen in lumbar vertebrae 8 weeks after ovariectomy, and this increase was reversed with estrogen treatment [38]. In cell culture experiments using osteoblastic cells derived from female mice, sclerostin expression was downregulated after the application of endogenous estrogen, although ER β appeared to play a greater role in the regulation of sclerostin levels than ER α [184]. In human males, estrogen treatment, but not testosterone treatment, lowered circulating levels of sclerostin in older men [34], implying that this inverse relationship is also present in males. However, circulating levels may not reflect bone sclerostin expression [36], so further studies looking at the effect of estrogen on bone sclerostin expression in males are warranted.

Selective Estrogen Receptor Modulators

Selective estrogen receptor modulators (SERMs) are a class of endocrine disruptors that specifically target the estrogen receptors. Endocrine disruptors are defined by the Environmental Protection Agency as “an exogenous agent that interferes with synthesis, secretion, transport, metabolism, binding action, or elimination of the natural blood-borne hormones that are present in the body and are responsible for homeostasis, reproduction, and development process” [190]. While endocrine disruptors are generally considered to be substances with negative consequences, SERMs can have both negative and positive effects.

SERMs have tissue-specific effects, meaning they can work as an agonist, or estrogen mimicker, in certain tissues while working as an antagonist, or estrogen blocker, in other tissues [191]. Recent advances in the pharmaceutical industry have produced several SERMs that are drugs, such as tamoxifen or raloxifene, often used in the treatment of certain cancers, particularly breast cancer, and osteoporosis [191]. As an example, tamoxifen can act as an antagonist in breast tissue to prevent breast cancer, while also acting as an agonist to estrogen receptors in bone, leading to increases in BMD [191]. Clinically, SERM drugs are often prescribed because they can induce some of the benefits of hormone replacement therapy (HRT) in women, although not to the same extent or magnitude, without many of the negative side effects [191]. In addition, SERMs can possibly be used to treat male osteoporosis, whereas HRT was only used in postmenopausal women [192].

SERMs can also be substances found in food or the environment. Two common examples are phytoestrogens found in plant products, i.e. isoflavones in soy protein, or

manufacturing by-products, i.e bisphenols found in plastics, which interact with estrogen receptors [193,194] Soy isoflavones and many other phytoestrogens preferentially bind with ER β over ER α , which contributes to their tissue-specific effects [195]. Individuals interested in the benefits of SERMs without a prescription might turn to increasing soy protein consumption, which has been shown to improve BMD when consumed regularly over the lifespan [196]. Other environmental SERMs, such as bisphenols, are considered substances that should be avoided, due to the growing amount of evidence that they could adversely affect human health [39].

Bisphenols

Bisphenols are endocrine disruptors and SERMs found in plastics that can have significant impacts on human health [39,40]. The most common bisphenol analog is bisphenol-A (BPA), though bisphenol-S (BPS) and bisphenol-F (BPF) can also be found in similar products (Figure 2.6). When BPA binds to the estrogen receptors, it leads to a modification of gene expression, but a different pattern of gene expression than classic estrogen binding [41–43]. This varied pattern of gene modulation is what makes BPA a SERM and contributes to its tissue-specific effects. BPA has been shown to bind to both ER α and ER β , but it has a higher affinity for ER β , which also contributes to its tissue-specific effects [41]. Less information is known about BPS and other analogs of BPA, which are often used as a substitute in “BPA-free” plastic products, but they appear to have similar endocrine disrupting activities as BPA [40].

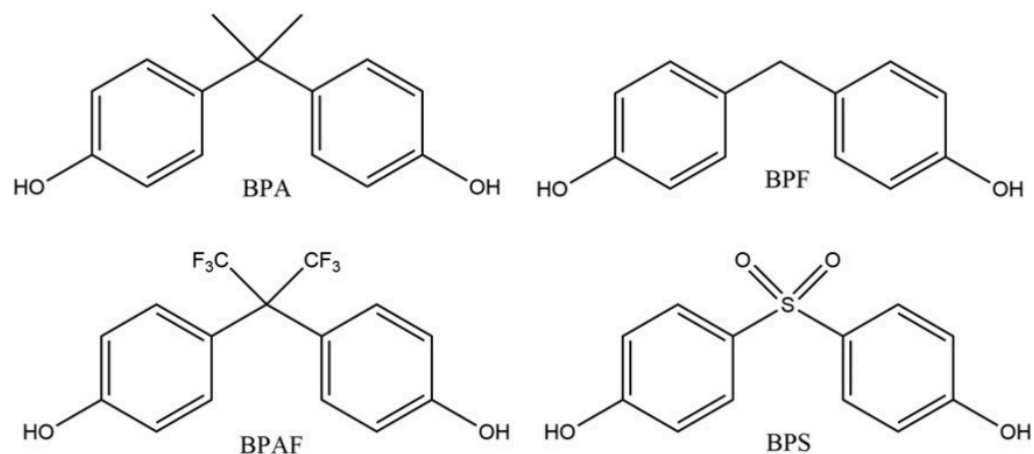


Figure 2.6 Chemical structures of the bisphenol analogs, bisphenol-A (BPA), bisphenol-F (BPF), bisphenol-AF (BPAF), and bisphenol-S (BPS) [274].

Human exposure to BPA

Human studies have associated BPA exposure with several endocrine issues, from low circulating sex hormones and decreased birth weight to metabolic diseases, such as obesity and cardiovascular disease [39]. The most common route of exposure of BPA and BPS in humans is food contamination, usually from epoxy resins used to line metal cans to stop food from being exposed to the metal [53,197]. BPA can also be released from plastic food and beverage containers, which allows the BPA to leach into the food over time [198]. This leaching process is accelerated by frequent washing of the container, storage of highly acidic or basic foods, and use of the containers at high temperatures [198]. While less impactful to human exposure, BPA and its analogues can also be found in thermal paper, dust, and certain dental and medical equipment [53,197]. BPA exposure is essentially ubiquitous in humans, with BPA being detectable in almost 100% of the blood or urine samples tested [39]. In addition, BPA has been detected in samples of

breast milk, cord blood, and fetal tissue [39], indicating that humans can be exposed to BPA at all ages and stages of life. The presence of BPA in cord blood and fetal tissue implies direct transfer across the placenta, and this has been confirmed in human studies of placental explants [50–52]. All three studies showed that the ratio between fetal and maternal serum levels of BPA was 1, implying that the exposure of the fetus is equal to that of the mother.

Before 2015, both the US Environmental Protection Agency (EPA) and the European Food Safety Authority (EFSA) recommended the tolerable daily intake (TDI) for BPA exposure be 50 µg/kg BW/day; however, in 2015, the EFSA dropped the TDI to 4 µg/kg BW/day for European countries. Most American and Asian countries still set the TDI at 50 µg/kg BW/day, although Health Canada has set the TDI at 25 µg/kg BW/day [54]. Daily exposure is difficult to assess, due to the short half-life of BPA and possible unknown exposure routes. Global estimates show that the average exposure is about 30 ng/kg BW/day in adults, but anywhere from 60-90 ng/kg BW/day in infants and children [54]. However, those are global estimates, and many individual countries, such as the United States, China, Germany, and Australia show higher daily exposure rates, often times above the current EFSA TDI of 4 µg/kg BW/day, especially in infants and children [54]. In addition, the majority of epidemiological studies show that BPA exposure is associated with adverse effects on human health, even at intakes far below the current TDI [39].

Mechanisms of Action

BPA and its analogs have structural features that allow them to bind with ERs, although BPA displays a 1000- to 2000-fold lower affinity for binding than estradiol, the most active form of estrogen [199]. Interestingly, although BPA and BPF can bind with both ER α and ER β , BPS has recently been shown to bind only with ER α in cell culture models [44]. In addition, there is some evidence that BPA can act as an agonist for ER α , but an antagonist for ER β , depending on the location of the ligand-binding domain [199]. A study using colon cancer cells showed that the presence of BPA in culture media could block the ability of estrogen to activate a pro-apoptotic signaling cascade through ER β , allowing for more growth of cancerous cells [200]. However, one of the key attributes of SERMs is that they have selective, or tissue-specific, effects on estrogen receptors, and more studies are needed to know if these mechanistic actions apply to all tissues.

In addition to actions directly on ERs, there is also evidence that BPA can affect epigenetic programming. Environmental effects on epigenetic programming primarily occur through changes in DNA methylation or histone modification [199]. Using the Agouti mouse model, which changes coat color in response to epigenetic interruptions [45], Dolinoy, et al., showed that gestational BPA exposure induced hypomethylation at the agouti locus [46]. In another study, gestational exposure led to both hypo- and hypermethylation of different genes in the forebrain of mice [47]. In addition, gestational BPA exposure increased methylation of histone 3 in female mice [48], implying that BPA can effect both DNA and histone methylation levels. Interestingly, studies have shown that these epigenetic effects of BPA exposure are not seen in adult-exposure models [49], implying that BPA only effects the epigenome during critical periods of development, primarily uterine development.

Bisphenols and Bone

Human Exposure Studies

In spite of the known estrogen-disrupting effects of BPA and BPS, few studies have looked at the impact that BPA exposure might have on bone health, and no studies have looked at BPS exposure outside of cell culture. In humans, only four studies have looked at possible relationships between BPA exposure and skeletal health. There was no correlation between serum BPA levels and BMD in a study of 51 postmenopausal women with osteoporosis [55]. However, these women were also currently undergoing treatment for osteoporosis, which could mask effects of environmental BPA exposure. In another study of 256 premenopausal women, there was no correlation between BPA exposure and BMD after adjustment for body mass index [56]. In another study of 14 women with osteoporosis and 10 age-matched healthy controls, there were no differences in urinary BPA concentrations between the two groups [57]. In a study involving 754 school-aged children, there was no correlation between urinary BPA levels and height in girls; however, there was a significant negative correlation between urinary BPA levels and height in boys, which remained when adjusted for pubertal status and at a follow-up visit 19 months later [58]. No studies have looked at BPA exposure and fracture incidence, and three of the four were cross-sectional studies involving only one study visit, which gives no information about changes in exposure leading to changes in BMD over time. More information is needed to truly understand the consequences that BPA exposure could have on skeletal health.

Animal models

Few studies have looked at BPA exposure and skeletal health in animal models as well, and those that did used either a prenatal exposure model, or a model of menopause. In female ovariectomized (OVX) rats, BPA exposure decreased cancellous BMD more than just OVX alone, although there was a slight increase in serum osteocalcin after BPA exposure [59]. However, BPA exposure increased femoral BMD in female aromatase knockout mice in a dose-dependent manner [60]. So far no studies have looked at BPA exposure in a male adult model of osteoporosis.

BPA seems to have larger effects during prenatal exposure [194], due to combination of direct hormonal actions and indirect epigenetic actions of BPA. However, few studies have looked at the effects of BPA exposure during gestation on bone, and those that exist show contrasting sex- and dose-dependent responses. In rats, dams were exposed to BPA, beginning on gestational day 7 and continuing through lactation, at varying daily doses (25, 250, 5,000, or 50,000 $\mu\text{g}/\text{kg}$ BW). At 3 months of age, female offspring had increased femoral length at 25 and 5,000 μg doses compared to control animals; male offspring had increased cortical thickness at the 25 μg dose compared to control, but decreased cortical thickness at the 250 μg dose [61]. No differences were seen in BMD or biomechanical strength in any offspring [61]. In another study in rats, dams were exposed to BPA beginning on gestational day 3, again at varying daily doses (0.5 and 50 $\mu\text{g}/\text{kg}$ BW). Male offspring in all groups had shorter femoral length, but only male offspring in the 0.5 $\mu\text{g}/\text{kg}$ BW dose group had lower trabecular bone volume and smaller cross-sectional area compared to control offspring [62]. There were no effects on female offspring. In mice, dams were exposed to BPA starting on gestational day 11 at a daily dose of 10 $\mu\text{g}/\text{kg}$ BW. At 23 weeks of age, male offspring had increased femur

lengths compared to control offspring, but no differences in biomechanical strength; at 13 weeks of age, the female offspring showed a decrease in energy to failure, which could not be explained by any morphological differences in the bone [63]. In contrast, another study involving mice showed that neither morphological nor biomechanical outcomes were impacted by BPA exposure, regardless of dose, in female offspring, but male offspring showed decreased cortical thickness and biomechanical strength at a higher dose of exposure (10 mg/kg BW). Interestingly, the male offspring exposed to a lower dose (10 µg/kg BW) also had impairments in biomechanical strength, without any morphological changes [64]. Taken together, these data indicate that BPA exposure during gestation can have significant impacts on both bone mass and strength, especially in male offspring. Importantly, these impairments were seen at doses lower than the current safe exposure levels in humans.

Cell culture models

In vivo studies have focused primarily on bone morphology and overall biomechanical strength, rather than measures of bone remodeling, even though ultimately both of those properties are under the control of bone remodeling. However, BPA has been shown to have significant impacts on osteoblast and osteoclast differentiation and activity *in vitro*. BPA enhanced adipogenesis from MSCs and blocked osteoblastic differentiation [201]. BPA exposure blocks both osteoblastic and osteoclastic differentiation and increases markers of apoptosis in a dose-dependent manner in progenitor cells [65]. In human osteosarcoma cells, long-term exposure to BPA and BPS downregulated the expression of several genes involved in bone morphogenesis, such as

Lrp5 and Wnt5A, both of which are involved in the Wnt signaling pathway. In addition, long-term exposure of BPA and BPS downregulated several osteoblastogenic gene markers, such as *Runx2* and osteoprotegerin [66]. Overall, these data suggest that BPA and BPS exposure can have significant effects on bone cell activity, especially osteoblast activity. Measuring the impact of BPA and BPS exposure on osteoblast activity in an *in vivo* model is vital, because osteoblast activity and bone remodeling directly control morphological and biomechanical outcomes.

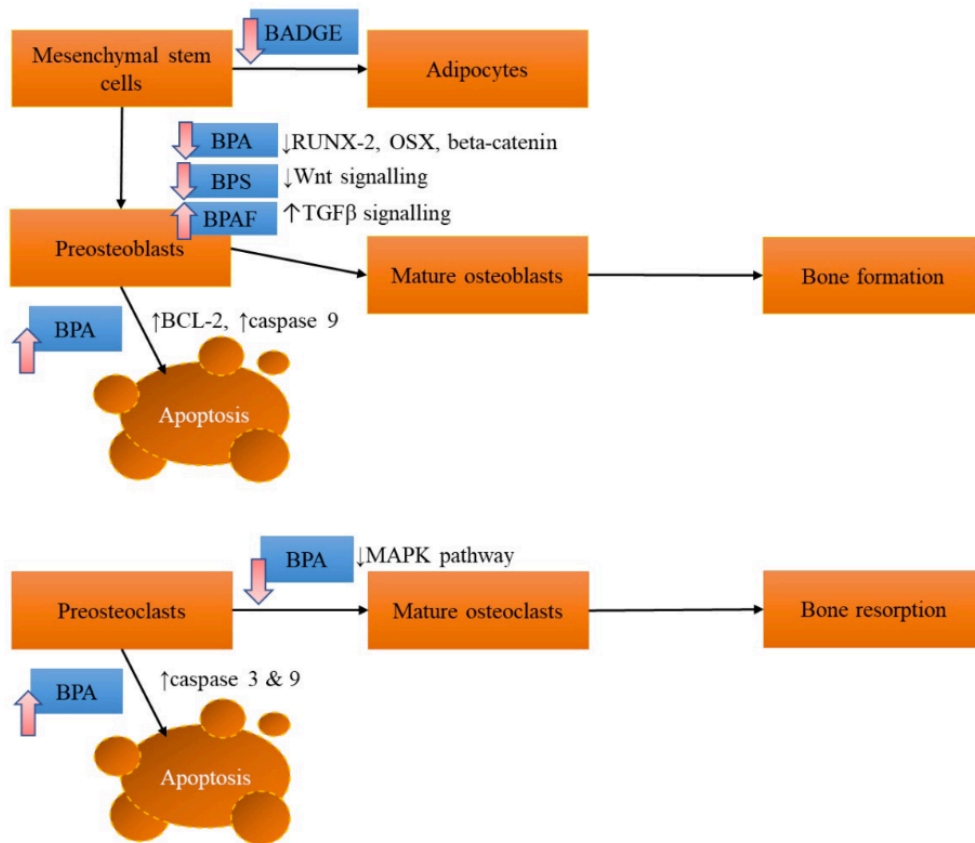


Figure 2.7 Overview of the actions of BPA and other bisphenol analogs on bone cells [275]

CHAPTER 3

Global estrogen receptor- α knockout has differential effects on cortical and cancellous bone in aged male mice [202]

Introduction

Epidemiological evidence supports a strong positive relationship between bioavailable estrogen and bone mass in both women and men [1,203]. Estrogen actions are mediated in part by estrogen binding to the estrogen receptor (ER), which is found in two isoforms, ER α and ER β . Both ER α and ER β are found in bone; however, ER α is more prevalent in cortical bone, whereas ER β is more widely distributed in cancellous bone [15]. ER α and ER β knockout mouse models have been used to determine the significance of this differential expression in the growth and maintenance of bone mass. Male ER α knockout (ERKO) mice generally show increased cancellous bone but decreased cortical bone mass, whereas male ER β knockout (BERKO) mice show equivalent bone mass when compared with wild-type (WT) mice [23]. However, total bone mass is only one determinant of bone strength [82,83], and reduction in estrogen signaling can affect all levels of bone's hierarchical structure [3,4], which collectively determine fracture resistance.

Male ERKO mice have decreased absolute longitudinal bone growth [16–18] relative to their WT counterparts. Young male ERKO mice have decreased cortical bone area, cortical thickness [18,21], and biomechanical bending strength [18], but increased cancellous bone mineral density (BMD) and trabecular number compared to WT mice [21,22]. Aged male ERKO mice have a similar phenotype, with decreased cortical bone area [16,17] compared to WT. And, although cancellous BMD is greater in male ERKO

mice, trabecular microarchitecture has not been examined in an aged male ERKO mouse model. Considering the significant role that trabecular microarchitecture plays in biomechanical bone strength [204], analysis of the trabecular microarchitecture of aged male ERKO animals is important.

Ultimately, the three-dimensional structure of bone is controlled via activity of osteoblasts, osteoclasts, and osteocytes. Osteocytes express sclerostin, a protein which down-regulates bone formation by inhibition of Wnt signaling [33] through paracrine actions on local osteoblasts and osteoclasts [159,162]. Sclerostin expression is regulated by several external factors, such as age and mechanical loading, as well as endogenous hormones such as IGF-I, parathyroid hormone, androgens, and estrogens [33]. In women and female rodent models, estrogen status is inversely related to sclerostin expression, whether measured via serum sclerostin concentrations [189,205,206], or sclerostin mRNA or protein expression in the bone [35,37,38]. In men, circulating sclerostin is negatively correlated with testosterone concentrations [207], though correlation does not prove direct regulation. In fact, estrogen treatment of elderly men decreased circulating sclerostin, whereas testosterone treatment did not [34]. This implies that estrogen directly regulates circulating sclerostin in men, though the direct impact on bony sclerostin and whether this regulatory role requires ER α is still unknown. Thus, further studies looking at the effect of estrogen on bone sclerostin expression in males are warranted.

In addition to direct ER α -mediated effects, estrogen affects bone indirectly by impacting metabolic health. Reduction in ER α activity is associated with increased body weight [21], as well as metabolic dysfunction, including insulin resistance [208] and type 2 diabetes [209], all of which are associated with decreased bone quality [210] and an

increased risk of fracture [211–213]. However, the relative contributions of these indirect metabolic effects to the overall skeletal phenotype of male ERKO mice has yet to be evaluated.

In this study, we compare aged male ERKO mice to their age-matched WT counterparts. We hypothesized that aged male ERKO mice would have improved trabecular microarchitecture in both the femur and the lumbar vertebrae, as well as decreased femoral length, mineral content, and cortical bone area compared to WT mice. Additionally, we hypothesized that, versus WT, male ERKO mice would have a higher percentage of sclerostin-positive osteocytes in cortical bone.

Methods

Experimental design

This study is part of a larger study investigating the effects of ERKO on glycemic control, inflammation, and hepatic steatosis in aged, male mice [214]. Heterozygote ER α +/+ mice on a C57BL/6J background were bred at our facility to produce male homozygote (ER α -/-) and littermate wild-type mice, as previously described [215,216]. Briefly, development of the ER α -/- mouse was accomplished by homologous recombination and insertion of a neomycin sequence containing premature stop codons and polyadenylation sequences into a NotI site in exon 2 of the mouse estrogen receptor gene, resulting in an interruption of gene transcription, but not full removal of the gene [215–217]. Knockout was verified via western blot [214]. After weaning, mice were fed standard rodent chow [(3.3 kcal/g of food), 13% kcal fat, 57% kcal carbohydrate, and 30% kcal protein, 5001, LabDiet, St. Louis, MO, USA] *ad libitum* until 14 months of age, providing 2 experimental groups: ER α -/- mice (ERKO) and wild-type (WT) controls (n=6-7/group). All mice were pair-housed (mixed genotypes) in a temperature-controlled environment at 25°C, with a 0700-1900 light, 1900-0700 dark cycle. Body weight and food intake were measured weekly, and body composition was measured by a nuclear magnetic resonance imaging whole-body composition analyzer (EchoMRI 4in1/1100; Echo Medical Systems, Houston, TX) on conscious mice one week prior to sacrifice. At 14 months of age, mice were euthanized following a 5-hour fast. Blood samples were collected via cardiac puncture and centrifuged; plasma was separated, frozen in liquid nitrogen, and stored at -80°C for further analysis. Circulating estradiol and fasting insulin, glucose, and lipids were measured as previously described [214]. Femurs, tibiae,

forelimbs, and lumbar vertebrae were harvested, wrapped in PBS-soaked gauze, frozen in liquid nitrogen, and stored at -80°C for further analysis. All procedures were approved in advance by the University of Missouri Institutional Animal Care and Use Committee.

Cortical Geometry and Trabecular Microarchitecture

Micro-computed tomographic (μ CT) imaging of the right femur and the fourth lumbar vertebrae was performed using a high-resolution imaging system (Xradia 520 Versa, ZEISS, Oberkochen, Germany). The methods used were in accordance with guidelines for the use of μ CT in rodents put forth by the American Society of Bone and Mineral Research [85]. Scans were acquired using an isotropic voxel size of 0.012 mm, a peak X-ray tube potential of 50 kV, and a 4-sec exposure time. Trabecular bone microarchitecture was evaluated in a 0.5-mm region of interest directly above the growth plate of the distal femur, representing the distal metaphysis, and in a 0.5-mm region of interest of the lumbar vertebral body above the intervertebral disc. Cortical bone cross-sectional geometry was evaluated at a 1-mm region of interest beginning at the end of the third trochanter, representing the diaphysis. The optimize threshold function was used to delineate mineralized bone from soft tissue. Scans were analyzed using BoneJ software [218] (NIH public domain), and measures of cortical geometry and trabecular microarchitecture were collected. Outcomes for cortical geometry included: femur length (Le), total cross-sectional area inside the periosteal envelope (Tt.Ar), marrow area (Ma.Ar), cortical bone area (Ct.Ar), cortical area fraction (Ct.Ar/Tt.Ar), mean cortical thickness (Ct.Th), and robustness (R, total bone area over length calculated as $R = Tt.Ar/Le$). Outcomes for trabecular microarchitecture included: total volume (TV,

volume of region of interest), bone volume (BV, volume of region segmented as bone), bone volume fraction (BV/TV), connectivity density (Conn.D, degree of trabeculae connectivity normalized to TV), mean trabecular thickness (Tb.Th), trabecular separation (Tb.Sp, distance between trabeculae), trabecular number (Tb.N, average number of trabeculae per unit length calculated as $1/(Tb.Th + Tb.Sp)$ [219]), structural model index (SMI), and degree of anisotropy (DA).

Cortical Collagen and AGE Content

Left femur diaphyses were flushed of marrow, acid-hydrolyzed with 6N HCL, dried overnight and reconstituted in 0.001 N HCL. The hydrolysate used to measure collagen and advanced glycated end-product (AGE) content. Collagen content was estimated by determination of hydroxyproline via colorimetric assay using Chloramine T and Erlich's reagents (Sigma-Aldrich, St. Louis, MO, USA) compared to a hydroxyproline standard (Sigma-Aldrich, St. Louis MO, USA). Total AGEs were quantified by fluorescence with excitation at 360 nm and an emission of 460 nm using quinine as a standard (Thermo Fisher Scientific, Waltham, MA, USA) [220].

Ash and Mineral Content

Right forelimbs (humerii, ulnae, and radii) were cleaned of all soft tissue, weighed, and defatted in hexane and diethyl ether each for 24 hours. Following lipid extraction, forelimbs were dried to a constant weight at 60° C. Forelimbs were then placed in a muffle furnace (800° C) overnight to collect ash. Final weight of ash content was recorded, and the ashed forelimbs were analyzed for calcium and phosphorus content

via inductive coupled plasma-optical emission spectroscopy (Agricultural Chem Station, University of Missouri). Results are expressed as gram of calcium or phosphorus per 100 grams of ash (g/100g).

Osteocyte Sclerostin Expression

Right femurs and lumbar vertebrae were fixed in 10% formalin for 48 hours at 4° C, and then decalcified in 14% EDTA at 4° C. Decalcified femurs were embedded in paraffin wax blocks, and 5- μ m sections were taken longitudinally down the midline of the femur. Lumbar vertebrae were embedded in paraffin wax and 5- μ m sections were taken transversely through the vertebral body. The sections were dried and deparaffinized, and then underwent enzymatic antigen retrieval using a 1x solution (20 μ g/ml) of protease K (Fisher Scientific, Hampton, NH) in TE buffer (Fisher Scientific, Hampton, NH), followed by blocking of endogenous peroxidase activity (3% H₂O₂, Ricca Chemical, Arlington, TX) and avidin and biotin expression (Avidin Biotin Blocking Solution, Thermo Scientific, Waltham, MA). Sections were then incubated in anti-sclerostin primary antibodies (Abcam, Cambridge, UK) overnight at 4° C. Secondary antibody binding and detection were accomplished using the Vectastain Elite ABC kit (Vector Laboratories, Burlingame, CA), with diaminobenzidine (ImmPACT DAB, Vector Laboratories, Burlingame, CA) as the chromogen. Sections were counterstained with hematoxylin (Fisher Scientific, Hampton, NH), dried, and mounted. Sections were analyzed at 20x for sclerostin expression. Sclerostin positive (Sost⁺) osteocytes were defined as osteocytes exhibiting brown staining, and sclerostin negative (Sost⁻) osteocytes were defined as osteocytes exhibiting blue (hematoxylin) staining. Data are

reported as percent Sost⁺ osteocytes. In addition to Sost⁺ and Sost⁻ osteocytes, empty osteocytic lacunae revealed by hematoxylin staining were counted, and data are reported as percent empty lacunae, as previously described [221]. For cortical bone, percent Sost⁺ osteocytes were counted in a 1-mm region directly below the third trochanter, and for trabecular bone, percent Sost⁺ osteocytes were counted in the region directly above the growth plate, in order to correlate with the uCT data.

Statistical Analysis

Student's t-tests were used to test for significant differences between groups (ERKO vs WT) for metabolic outcomes, material properties, trabecular microarchitecture, and percentage of sclerostin⁺ osteocytes. Body weight is a strong predictor of cortical bone mass, so cortical geometry was assessed by one-way ANCOVA with final body weight included as a covariate. Pearson correlations between metabolic outcomes (body weight, body fat percentage, and serum insulin and glucose) and circulating estradiol concentrations from the parent study [214] and bone outcomes (trabecular microarchitecture, cortical geometry, sclerostin expression) were performed to determine direct effects of genotype versus indirect effects of metabolic health on bone outcomes. Data are presented as means \pm SEM or adjusted means \pm SEM. Statistical significance was set at $p < 0.05$. All analyses were performed using SPSS software (SPSS/25.0, SPSS, Chicago, IL, USA).

Results

Metabolic Characteristics

The metabolic characteristics for these animals have been previously published as part of a larger study [214] and the results have been summarized in **Table 3.1**. Briefly, ERKO mice had higher body fat percentage ($p=0.026$), fasting glucose ($p=0.024$) and triglycerides ($p=0.013$) compared to WT mice. No differences were detected between groups in body weight, absolute food intake, circulating estradiol, or fasting levels of insulin, total cholesterol, HDL, LDL, or NEFA.

Outcome	WT	ERKO	P-value
Body Mass (g)	33.6 ± 1.0	39.0 ± 3.1	0.148
Body Fat Percentage	16.81 ± 0.46	24.80 ± 2.83	0.034*
Average Food Intake (g/day)	5.10 ± 0.48	4.10 ± 0.25	0.188
Blood Glucose (mg/dL)	227 ± 20	321 ± 29	0.024*
Insulin (uU/L)	36.4 ± 9.6	36.8 ± 8.8	0.974
Cholesterol (mg/dL)	62 ± 4	79 ± 8	0.099
HDL (mg/dL)	32 ± 3	38 ± 2	0.103
LDL (mg/dL)	5 ± 0.6	6 ± 1	0.591
Triglycerides (mg/dL)	122 ± 6	147 ± 6	0.013*
NEFAs (mmol/L)	0.49 ± 0.11	0.52 ± 0.05	0.763
Circulating Estradiol (pg/mL)	7.1 ± 2.0	8.5 ± 1.3	0.567

Table 3.1. Metabolic characteristics of male ER α ^{-/-} mice (ERKO) and wild-type (WT) mice. Data are means ± SEM, n=6 per group. Significance between groups ($p<0.05$) is indicated by asterisk (*). Adapted from [214].

Femoral Cortical Geometry

Femur length was not different between WT and ERKO animals (WT: 15.80 ± 0.17 mm and ERKO: 15.73 ± 0.17 mm; $p=0.788$), though there was a trend toward an increase in robustness in the WT group over the ERKO animals (WT: 0.143 ± 0.003 mm and ERKO: 0.134 ± 0.003 mm; $p=0.075$). ERKO mice showed significantly lower Tt.Ar (ERKO: 2.096 ± 0.052 mm² and WT: 2.277 ± 0.052 mm²; $p=0.042$), Ct.Ar (ERKO: 0.865 ± 0.023 mm² and WT: 0.961 ± 0.023 mm²; $p=0.018$), and Ct.Th (ERKO: 0.198 ± 0.004 mm and WT: 0.212 ± 0.004 mm; $p=0.047$) compared to WT animals. There were no differences between groups in Ma.Ar (WT: 1.315 ± 0.042 mm² and ERKO: 1.232 ± 0.042 mm²; $p=0.205$) or Ct.Ar/Tt.Ar (WT: 0.418 ± 0.009 and ERKO: 0.411 ± 0.009 ; $p=0.629$). No differences were seen in the I_{max}/I_{min} ratio, a measure of the circularity of the diaphysis [222], between groups (WT: 2.287 ± 0.113 and ERKO: 2.364 ± 0.113 ; $p=0.655$). **(Figure 3.1)**

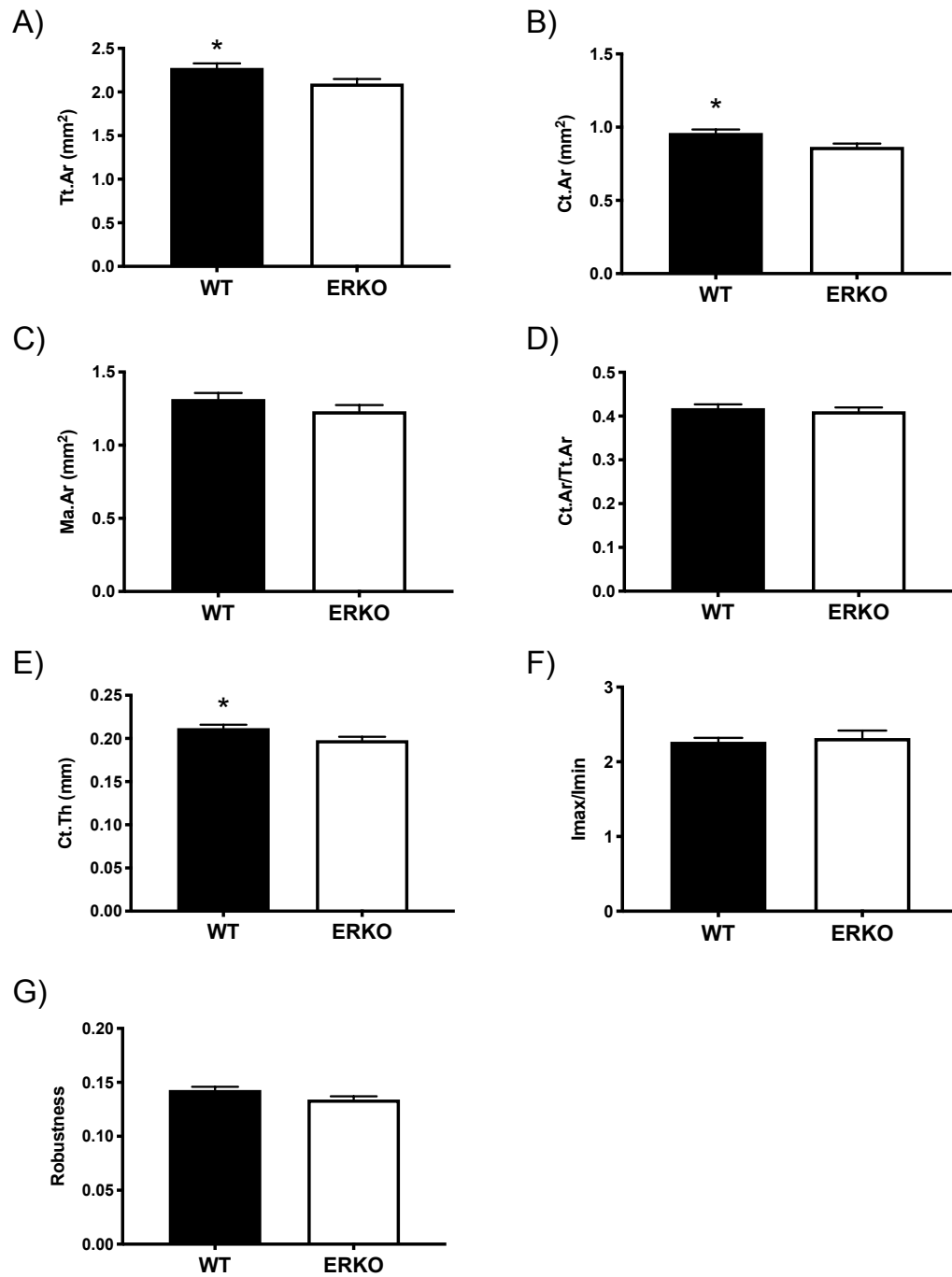


Figure 3.1. Cortical geometry of the femur in male $ER\alpha^{-/-}$ mice (ERKO) compared to wild-type (WT) counterparts. (A) total area, (B) cortical area, (C) marrow area, (D) cortical-to-total area ratio, (E) cortical thickness, (F) I_{max}/I_{min} , (G) robustness. Data are adjusted mean \pm SEM, $n=6$ per group. Significance between groups ($p < 0.05$) is indicated by asterisk (*).

Femoral Trabecular Microarchitecture

ERKO mice had significantly higher BV/TV (ERKO: 0.149 ± 0.011 and WT: 0.090 ± 0.011 ; $p=0.002$), Tb.N (ERKO: $3.192 \pm 0.128 \text{ mm}^{-1}$ and WT: $2.360 \pm 0.128 \text{ mm}^{-1}$; $p=0.001$), and Conn.D (ERKO: $145.69 \pm 16.76 \text{ mm}^{-3}$ and WT: $59.76 \pm 16.76 \text{ mm}^{-3}$; $p=0.005$), compared to WT animals. ERKO mice had significantly lower Tb.Sp (ERKO: $0.245 \pm 0.015 \text{ mm}$ and WT: $0.354 \pm 0.015 \text{ mm}$; $p=0.001$) and DA (ERKO: 0.263 ± 0.029 and WT: 0.373 ± 0.027 ; $p=0.021$) compared to WT animals. Tb.Th (ERKO: $0.073 \pm 0.001 \text{ mm}$ and WT: $0.072 \pm 0.001 \text{ mm}$; $p=0.875$) and SMI (ERKO: 8.927 ± 1.120 and WT: 8.548 ± 1.120 ; $p=0.816$) were not different between groups. **(Figure 3.2)**

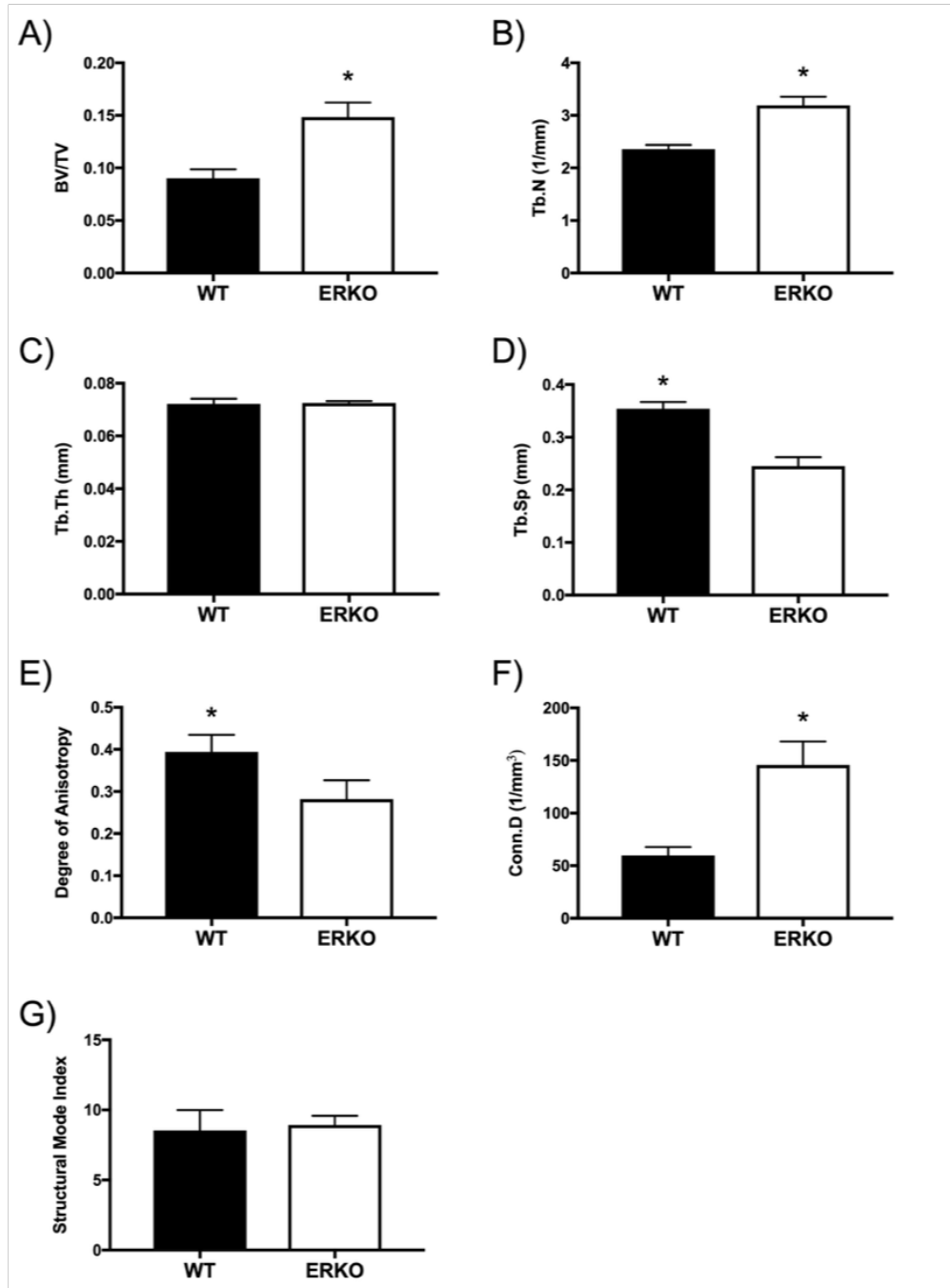


Figure 3.2. Trabecular microarchitecture of the distal femur in male $ER\alpha^{-/-}$ mice (ERKO) compared to wild-type (WT) counterparts. (A) trabecular bone volume, (B) trabecular number, (C) trabecular thickness, (D) trabecular separation, (E) degree of anisotropy, (F) connectivity density, (G) structural mode index. Data are mean \pm SEM, $n=6$ per group. Significance between groups ($p<0.05$) is indicated by asterisk (*).

Vertebral Trabecular Microarchitecture

ERKO mice had significantly higher BV/TV (ERKO: 0.334 ± 0.013 and WT: 0.245 ± 0.013 ; $p=0.001$), Tb.N. (ERKO: $5.616 \pm 0.137 \text{ mm}^{-1}$ and WT: $3.891 \pm 0.137 \text{ mm}^{-1}$; $p=0.001$), and Conn.D (ERKO: $435.42 \pm 24.28 \text{ mm}^{-3}$ and KO: $133.36 \pm 24.28 \text{ mm}^{-3}$; $p=0.001$) compared to WT mice. ERKO mice had significantly lower Tb.Th (ERKO: $0.055 \pm 0.001 \text{ mm}$ and WT: $0.061 \pm 0.001 \text{ mm}$; $p=0.008$), Tb.Sp. (ERKO: $0.124 \pm 0.005 \text{ mm}$ and WT: 0.197 ± 0.005 ; $p=0.001$), and DA (ERKO: 0.713 ± 0.021 and WT: 0.812 ± 0.021 ; $p=0.007$) compared to WT mice. There was no significant difference in SMI (ERKO: 3.946 ± 0.146 and WT: 3.656 ± 0.146 ; $p=0.187$) between groups. **(Figure 3.3)**

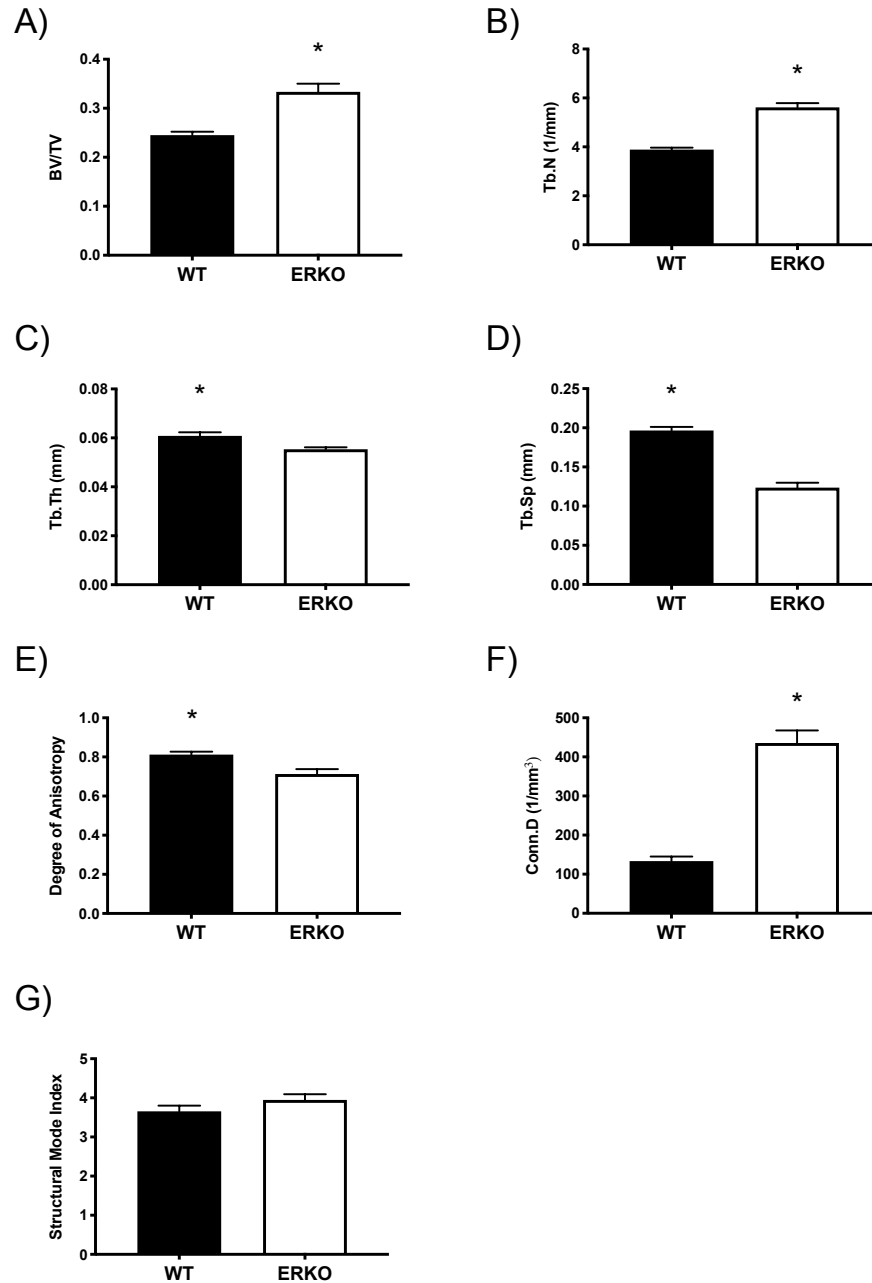


Figure 3.3. Trabecular microarchitecture of the lumbar vertebrae in male $ER\alpha^{-/-}$ mice (ERKO) compared to wild-type (WT) counterparts. (A) trabecular bone volume, (B) trabecular number, (C) trabecular thickness, (D) trabecular separation, (E) degree of anisotropy, (F) connectivity density, (G) structural mode index. Data are mean \pm SEM, $n=6$ per group. Significance between groups ($p<0.05$) is indicated by asterisk (*).

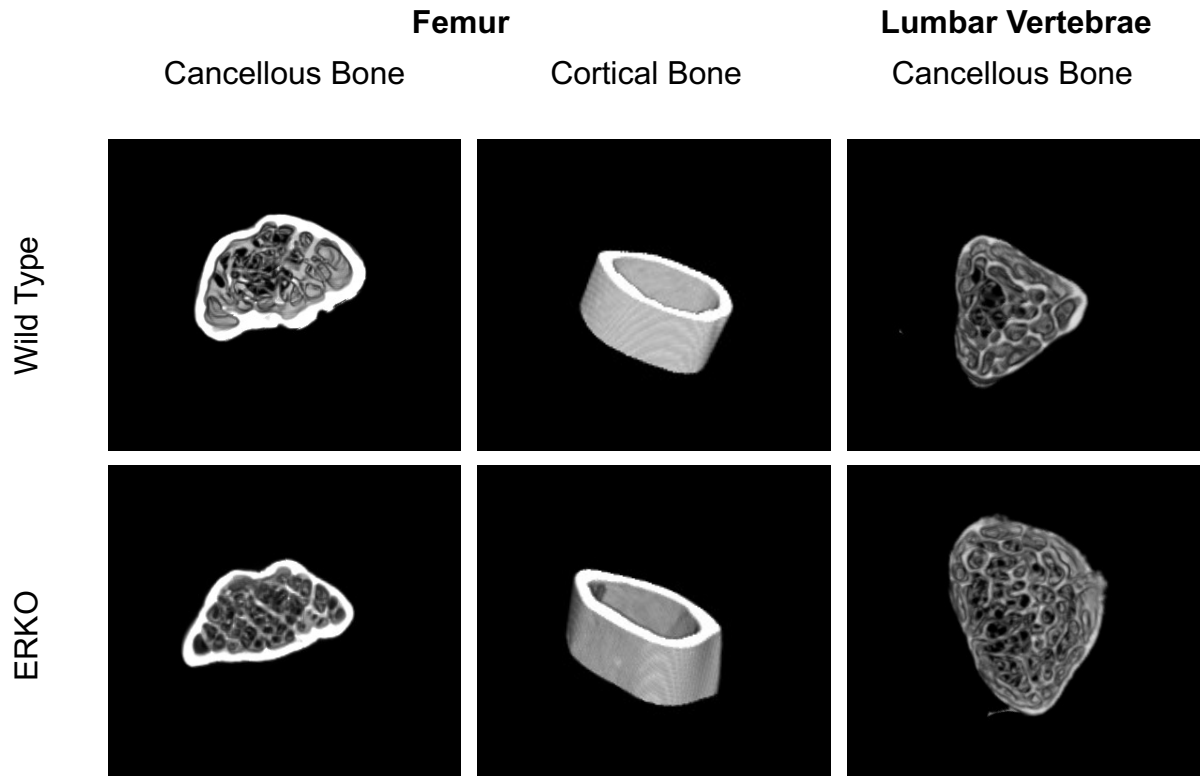


Figure 3.4. 3D reconstructions of regions of interest in cortical and cancellous bone in $ER\alpha^{-/-}$ mice (ERKO) compared to wild-type (WT) counterparts.

Femoral Cortical Collagen and AGE Content

No differences were seen in total femoral collagen content (mg hydroxyproline/g bone) between groups (WT: 15.05 ± 1.32 and ERKO: 15.39 ± 1.34 ; $p=0.654$). There were no differences in total femoral AGE content (ng quinine/mg bone) between groups (WT: 25.53 ± 5.93 and ERKO: 26.92 ± 6.49 ; $p=0.697$). Relative to total collagen content, there also were no differences in AGE content (ng quinine/mg hydroxyproline) between groups (WT: 1718.1 ± 477.6 and ERKO: 1739.0 ± 332.3 ; $p=0.928$). (**Figure 3.5**)

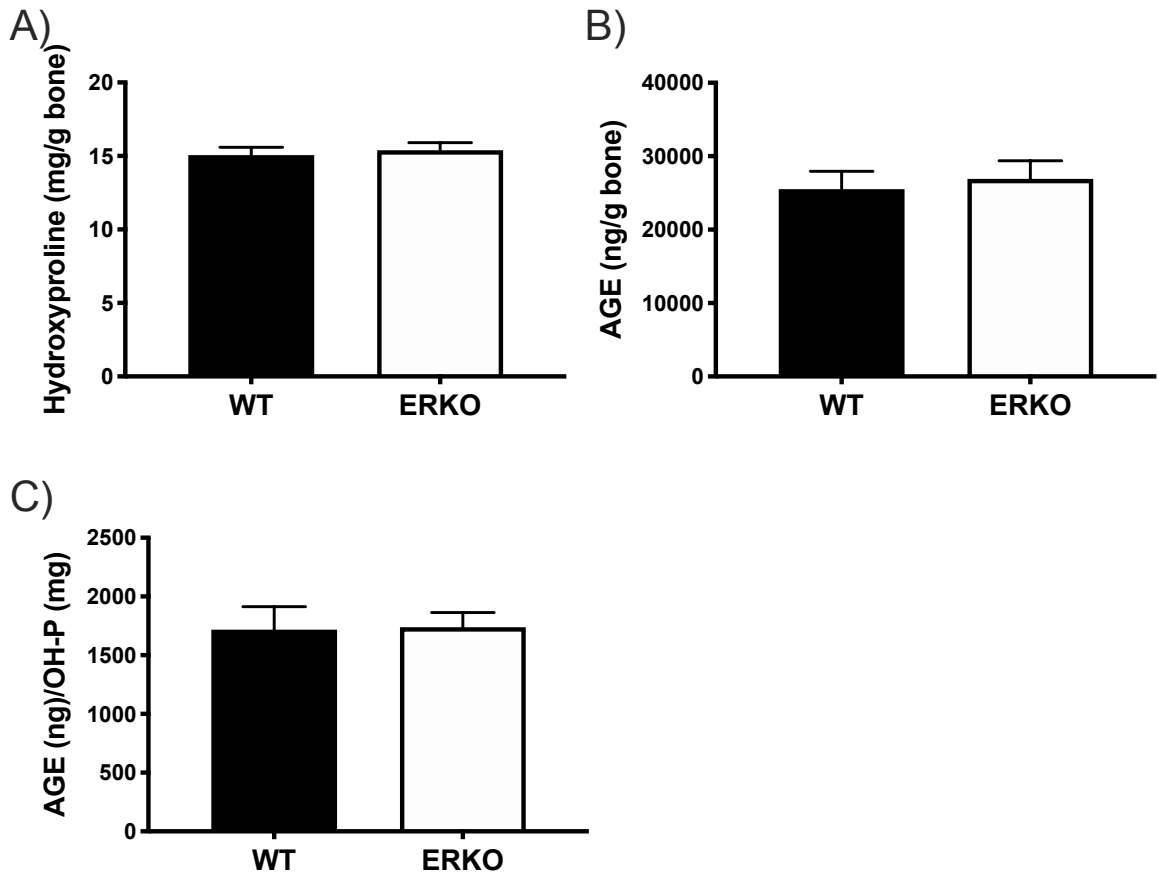


Figure 3.5. Femoral cortical collagen and advanced glycated end-products in male ER α -/- mice (ERKO) compared to wild-type (WT) counterparts. (A) hydroxyproline, (B) advanced glycated end-products (AGE), (C) AGE normalized to hydroxyproline content. Data are mean \pm SEM, n=6 per group. Significance between groups ($p < 0.05$) is indicated by asterisk (*).

Ash and Mineral Content

There were no differences in total ash weight between groups (WT: 26.42 ± 0.55 mg and ERKO 24.97 ± 0.55 mg; $p=0.092$). No differences in calcium content (g Ca/100 g ash) were detected between groups (WT: 38.83 ± 0.45 and ERKO: 39.11 ± 0.42 ; $p=0.286$). There were no differences in phosphorus content (g P/100 g ash; WT: $18.26 \pm$

0.14 and ERKO: $18.46 \pm .26$; $p=.181$) or the calcium to phosphorus ratio between groups (WT: $2.12 \pm .03$ and ERKO: $2.12 \pm .03$; $p=0.834$). (Figure 3.6)

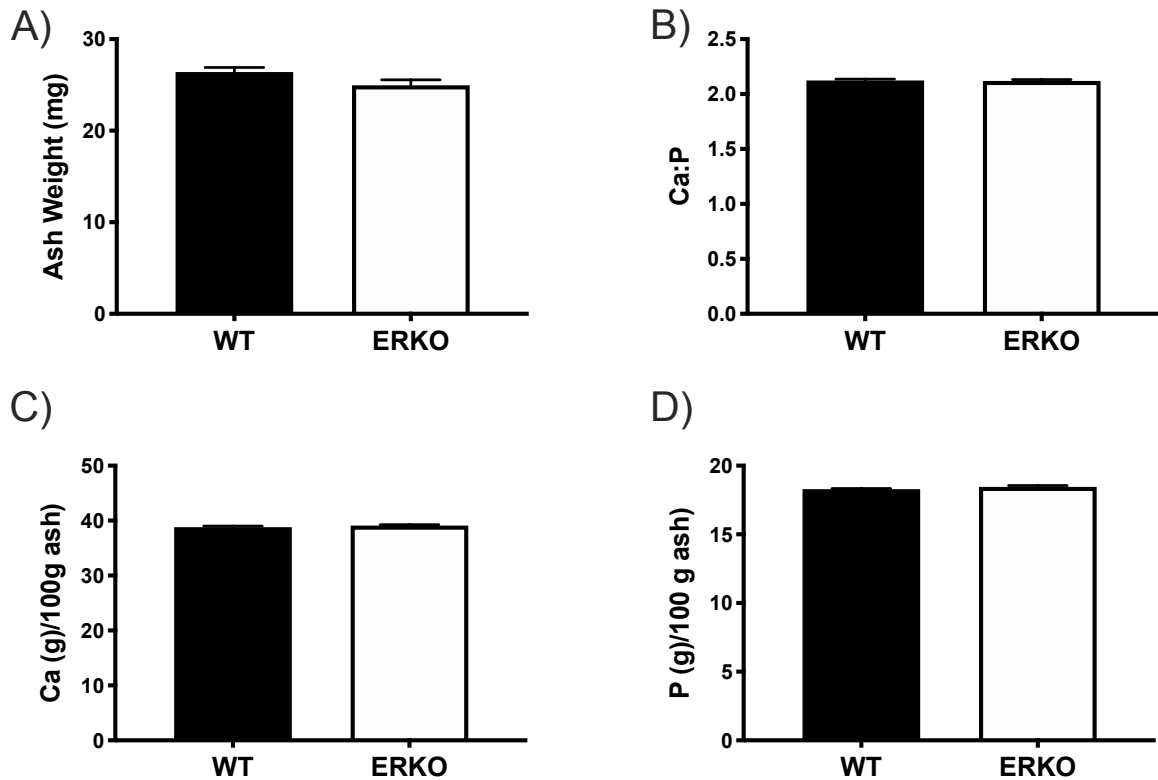


Figure 3.6. Femoral mineral content in male $ER\alpha^{-/-}$ mice (ERKO) compared to wild-type (WT) counterparts. (A) ash weight, (B) calcium-to-phosphorus ratio, (C) grams calcium per 100g ash, (D) grams phosphorus per 100g ash. Data are mean \pm SEM, $n=6$ per group. Significance between groups ($p<0.05$) is indicated by asterisk (*).

Osteocyte Sclerostin Expression

There was a trend towards an increase in percentage of sclerostin-positive osteocytes in ERKO animals compared to WT (WT: 59.35 ± 4.69 % and ERKO: 75.30 ± 5.25 %; $p=0.058$) in the cortical bone of the femoral diaphysis, but no differences in cancellous bone of the femoral metaphysis (WT: 54.61 ± 7.93 % and ERKO: $51.39 \pm$

9.15 %; $p=0.801$) or the lumbar vertebrae (WT: 6.75 ± 0.94 % and ERKO: 5.75 ± 1.03 %; $p=0.491$). No differences were detected in percentage of empty lacunae between WT and ERKO animals in cortical bone of the femoral diaphysis (WT: 24.82 ± 6.32 % and ERKO: 29.79 ± 7.07 %; $p=0.617$) or cancellous bone of the femoral metaphysis (WT: 20.01 ± 4.35 % and ERKO: 14.07 ± 5.03 %; $p=0.413$) or the lumbar vertebrae (WT: 13.31 ± 2.85 % and ERKO: 20.55 ± 3.12 %; $p=0.119$). **(Figure 3.7 and 3.8).**

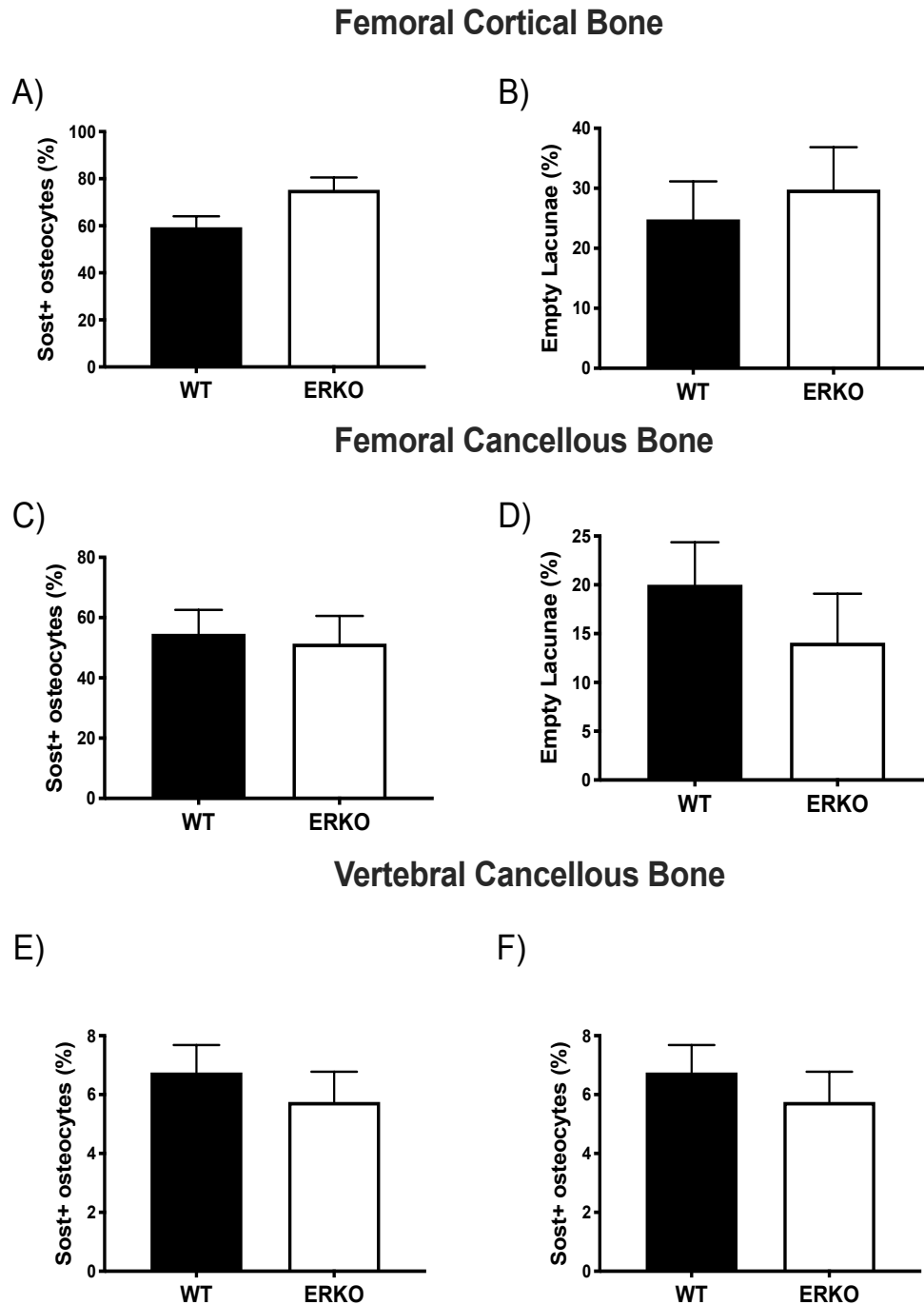


Figure 3.7. Osteocyte sclerostin expression and empty lacunae in male ER α ^{-/-} mice (ERKO) compared to wild-type (WT) counterparts. (A) percent sclerostin positive osteocytes in cortical bone, (B) percent empty lacunae in cortical bone, (C) percent sclerostin positive osteocytes in cancellous bone of the femur, (D) percent empty lacunae in cancellous bone of the femur, (E) percent sclerostin positive osteocytes in cancellous bone of the vertebrae, (F) percent empty lacunae in cancellous bone of vertebrae. Data are mean \pm SEM, n=6 per group. Significance between groups (p<0.05) is indicated by asterisk (*).

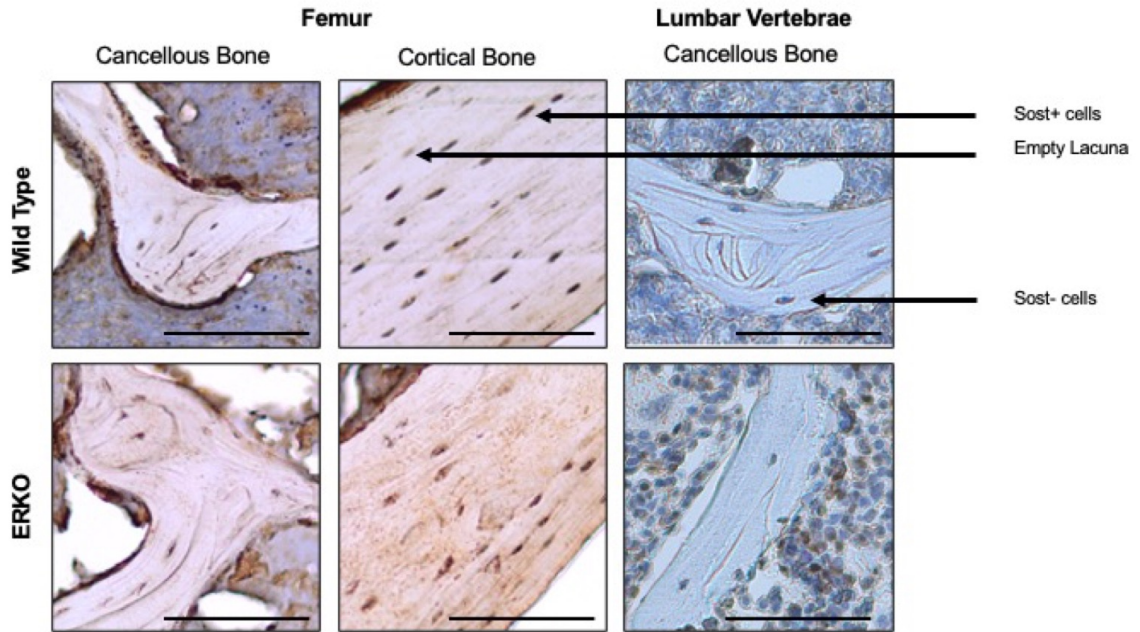


Figure 3.8. Representative photos of sclerostin staining in cortical and cancellous bone in male ER α ^{-/-} mice (ERKO) and wild-type (WT) counterparts. Scale bar represents 100 μ m.

Metabolic influences on skeletal outcomes

Since ERKO can alter metabolic function, and metabolic health can have significant impact on the skeletal phenotype, we determined whether impaired metabolic health was associated with any skeletal outcomes. There were significant positive correlations between circulating fasting glucose and BV/TV of the femoral distal metaphysis ($r=0.666$, $p=0.018$), Tb.N ($r=0.670$, $p=0.017$), and Conn.D ($r=0.623$, $p=0.031$). There were significant negative correlations between circulating fasting glucose and Tb.Sp ($r=-0.668$, $p=0.018$) and DA ($r=-0.634$, $p=0.036$) of the femoral distal metaphysis. In the lumbar vertebrae, there were significant positive correlations between fasting glucose and BV/TV ($r=0.672$, $p=0.017$) and Tb.N ($r=0.594$, $p=0.042$), and a significant negative correlation between fasting glucose and Tb.Sp. ($r=-0.622$, $p=0.031$).

We tested trabecular outcomes with fasting glucose as a covariate to assess the influence of circulating glucose on the group differences seen. In the femoral distal metaphysis, significant differences between groups remained in Tb.N (without glucose: ERKO: $3.192 \pm 0.128 \text{ mm}^{-1}$ and WT: $2.360 \pm 0.128 \text{ mm}^{-1}$, $p=0.001$; with glucose: ERKO: $3.111 \pm 0.143 \text{ mm}^{-1}$ and WT $2.441 \pm 0.143 \text{ mm}^{-1}$, $p=0.015$) and Tb.Sp (without glucose: ERKO: $0.245 \pm 0.015 \text{ mm}$ and WT: $0.354 \pm 0.015 \text{ mm}$, $p=0.001$; with glucose: ERKO: 0.254 ± 0.017 and WT: 0.345 ± 0.017 , $p=0.008$) when glucose was included as a covariate. Significant group differences (KO vs WT) changed to trending group differences in BV/TV (without glucose: ERKO: 0.149 ± 0.011 and WT: 0.090 ± 0.011 , $p=0.002$; with glucose: ERKO: 0.142 ± 0.013 and WT: 0.097 ± 0.013 , $p=0.056$) and Conn.D (without glucose: ERKO: $145.69 \pm 16.76 \text{ mm}^{-3}$ and WT: $59.76 \pm 16.76 \text{ mm}^{-3}$, $p=0.005$; with glucose: ERKO: $136.72 \pm 19.21 \text{ mm}^{-3}$ and WT: $68.73 \pm 19.21 \text{ mm}^{-3}$, $p=0.051$). Significant group differences in DA were abolished when circulating fasting glucose was included as a covariate (without glucose: ERKO: 0.263 ± 0.029 and WT: 0.373 ± 0.027 , $p=0.021$; with glucose: ERKO: 0.282 ± 0.034 and WT: 0.358 ± 0.030 , $p=0.172$). In the lumbar vertebrae, significant group differences remained in BV/TV (without glucose: ERKO: 0.334 ± 0.013 and WT: 0.245 ± 0.013 , $p=0.001$; with glucose: ERKO: $0.325 \pm .014$ and WT: 0.253 ± 0.014 , $p=0.011$), Tb.N (without glucose: ERKO: $5.616 \pm 0.137 \text{ mm}^{-1}$ and WT: $3.891 \pm 0.137 \text{ mm}^{-1}$, $p=0.001$; with glucose: ERKO: $5.603 \pm 0.165 \text{ mm}^{-1}$ and WT: $3.904 \pm 0.165 \text{ mm}^{-1}$, $p=0.001$), and Tb.Sp (without glucose: ERKO: $0.124 \pm 0.005 \text{ mm}$ and WT: 0.197 ± 0.005 , $p=0.001$; with glucose: ERKO: $0.125 \pm 0.006 \text{ mm}$ and WT: 0.195 ± 0.006 , $p=0.001$). There were no significant relationships

between circulating estradiol concentrations, fasting insulin concentrations, or percentage sclerostin+ osteocytes and other outcomes.

Discussion

In this study, we showed that ERKO had differential effects on cancellous and cortical bone in aged male mice. ERKO animals showed changes in cancellous bone microarchitecture of the femoral distal metaphysis and lumbar vertebrae, which others have shown to be associated with increased fracture resistance [223,224]. By contrast, ERKO resulted in detrimental changes in cortical bone geometry of the femoral diaphysis compared to WT counterparts. This is the first study to assess sclerostin expression in a male ERKO model. ERKO did not increase sclerostin expression in cancellous bone of the distal femoral metaphysis or the lumbar vertebrae; however, sclerostin expression trended towards an increase in cortical bone of the femoral diaphysis. Furthermore, the skeletal effects of ERKO were not attributable to differences in overall metabolic health between ERKO and WT, implying that the skeletal phenotype is primarily attributed to the ERKO.

The morphological changes seen in the cortical bone in this study are supported by previous studies [18,21,22]. Estrogen and the estrogen receptors have significant, cell-specific roles in the development and maintenance of bone mass (reviewed in [3,4]), which directly influence bone remodeling. Estrogen blocks osteocyte and osteoblast apoptosis, induces osteoblast differentiation, increases osteoclast apoptosis, and reduces osteoclast differentiation through a direct suppression of receptor activator of NF κ B ligand (RANKL) expression [3,9]. Estrogen indirectly reduces osteoclast differentiation through increased expression of osteoprotegerin (OPG), a decoy receptor for RANKL [10,11]. ER α specifically is required for the maintenance of cortical bone mass, as we can see in cell-specific ER α knockouts. When ER α was deleted from osteoblast

precursors, femoral BMD and cortical thickness were reduced compared to wild-type animals, indicating that ER α controls cortical bone formation through actions on progenitor cells [174]. This agrees with our results, since we only saw detrimental changes in cortical geometry, and not in trabecular microarchitecture of the femur or vertebrae. However, when ER α was deleted from mature osteocytes only, trabecular bone volume of the lumbar vertebrae decreased, which is in contrast with our results [175]. This is most likely due to the difference in cell-type; possibly the deletion of ER α in just the osteocyte produces a small enough effect on estrogen signaling that ER β is not required to compensate as it often does in a whole-body model, though further studies in this area are needed.

As expected in a global knockout model, the improvements in vertebral trabecular microarchitecture were consistent with those observed in the femur and support our original hypothesis. The improvements we saw in trabecular microarchitecture of the femur are also consistent with previous studies done in younger male ERKO mice [21,22]. These improvements can be explained by the greater presence of ER β in cancellous bone. In cancellous bone, ER β and ER α appear to have similar actions, and both play a role in maintaining total bone mass [4]. However, one characteristic in our study that did not match previous studies is the lack of differences in femoral length. This could be in part due to the age of our animals compared to other studies, as mice do not fully close their epiphyseal plates and slowly continue longitudinal growth after sexual maturity [225,226].

Another possible cellular action of estrogen is the downregulation of sclerostin [227], which would also directly affect bone remodeling. In women, estrogen treatment

decreased sclerostin mRNA concentrations in bone biopsy samples [35], but here we were the first to explore how a decrease in ER α could affect sclerostin expression in a male model. We hypothesized that, similar to previous female rodent models [37,38], the reduction in estrogen signaling would increase osteocyte sclerostin expression in male ERKO mice, as measured by immunohistochemistry. We observed increased osteocyte sclerostin expression in cortical bone in the ERKO animals that approached statistical significance ($p=0.058$), supporting the hypothesis that ER α plays role in the control of sclerostin expression. Interestingly, we only saw this change in the cortical bone, which directly correlated with the morphological effects also seen in the cortical bone.

Therefore, we propose that downregulation of sclerostin is an important cellular action of estrogen in the overall control of bone remodeling and bone mass maintenance in cortical bone, and further studies are warranted.

Bone mass declines with aging, due to an imbalance in bone formation and resorption that favors increased bone loss [228,229]. In addition, serum concentrations of sclerostin increase with age in humans [228,230,231], although serum concentrations of sclerostin are not always reflective of sclerostin expression in the bone [33]. For instance, bone needle biopsies of the iliac crest showed no difference in bone levels of sclerostin mRNA between young and old women, despite an increase in circulating sclerostin with age [231]. However, in rodent models, there is a distinct increase in sclerostin as the animals age, whether measured by immunohistochemistry [232] or protein and gene expression [233]. Since the present study used an aged rodent model, it is possible that differences caused by ER α knockout were obscured by age-related increases in sclerostin

[232,233]. Further studies are warranted to fully explore the importance of ER α in osteocyte sclerostin expression throughout the lifespan.

In addition to direct ER α -mediated effects on the bone, decreased ER α expression is associated with increased body weight [21] and metabolic dysfunction, including insulin resistance [208] and type 2 diabetes [209]. These metabolic health concerns are associated with decreased bone quality [210] and an increased risk of fracture [211–213]. In this study, ERKO mice were metabolically unhealthy, characterized by increased body fat percentage, glucose intolerance, liver steatosis, and increased fasting glucose and triglyceride concentrations [214]. We observed significant correlations between fasting glucose concentrations and trabecular microarchitecture outcomes, such as Tb.Sp, Tb.N, Tb.Th, BV/TV, DA, and Conn.D in both the femoral metaphysis and the lumbar vertebrae. Thus, to determine if the improvements in trabecular microarchitecture seen in the ERKO animals could be partly due to differences in glucose levels, we tested group differences with fasting glucose as a covariate. After accounting for differences in fasting glucose, the effect of ERKO on Tb.Sp, Tb.N, and Tb.Th remained, implying a direct effect of the loss of ER α activity on trabecular microarchitecture in the femur and vertebrae.

It is important to note that ERKO does not exactly mimic estrogen deficiency, given that estrogen signaling may occur via ER β and there are ligand-independent effects of the ER α receptor [170]. In addition, female ERKO mice tend to have higher circulating estrogen levels [23], which could overemphasize the role of ER β . However, in our study there were no differences in circulating estradiol between groups, which corroborates other studies done with male ERKO animals [214,234]. Another important

note is that the knockout model used in this study is not a complete gene knockout, as it is achieved by splicing the neo cassette rather than removal of the full gene. In this and previous studies, this method has shown to be an effective knockout model, in that the interruption of the gene reduces estrogen receptor expression to levels undetectable by western blot [215,235]. In addition, previous studies have shown that this knockout model has significantly reduced estrogen receptor activity, which manifests as significant phenotypic differences that can be attributed to the difference in the estrogen receptor gene [215,236,237].

One limitation of this study was that these mice were global ERKO mice, which did not allow for the distinction between osteocyte-, osteoblast-, or osteoclast-specific actions. Other studies have aimed to elucidate these cell-specific actions (reviewed in [4]), but none of them have looked at sclerostin expression, which makes this study novel. Another limitation was the lack of biomechanical strength data. While detrimental effects on cortical strength can be inferred, based on previous literature correlating a loss of cortical mass and thickness with a loss of biomechanical strength [83], we did not have the ability to test to biomechanical strength due to previous cracks and fractures that were revealed in the μ CT analysis. Biomechanical strength can also be effected by the material properties of the bone, such as mineral composition and heterogeneity, collagen composition and amount of crosslinking, and crystallinity of the material [69,238]. While we saw no differences in mineral or collagen composition, the effects of ER α on other material properties are worth exploring.

In conclusion, ERKO had differential effects on cortical and cancellous bone in aged male mice. Specifically, ERKO significantly improved trabecular microarchitecture

of both the femur and lumbar vertebrae, but negatively altered cortical geometry of the femur, which supports a significant role for ER α in the maintenance of cortical bone mass. We also found a trend towards an increase in the percentage of sclerostin positive osteocytes in the cortical bone of the femoral diaphysis, suggesting a possible mechanism for the altered cortical geometry, and thus a regulatory role for ER α in osteocyte sclerostin expression in cortical bone. Taken together, these data warrant further studies to explore the effect of ERKO on osteocyte sclerostin expression.

CHAPTER 4

Voluntary wheel running partially compensates for the effects of global estrogen receptor- α knockout on cortical bone in young male mice

Introduction

Estrogen is one of the most influential hormones in growth and maintenance of the skeleton across the entire lifespan in both males and females [1,2,165,167,168]. Estrogen actions are mediated primarily by estrogen binding with the nuclear estrogen receptor (ER), which is found in two isoforms, ER α and ER β . Bone expresses both ER α and ER β ; however, ER α tends to be more prevalent in cortical bone, whereas ER β is more widely distributed in cancellous bone [15]. Global ER α knock out (ERKO) decreased longitudinal bone growth in both male and female mice [16–18]. Male ERKO mice show reduced bone turnover compared to wild-type (WT) controls [21], resulting in alterations in cortical bone geometry associated with decreased bending strength, such as decreased cortical bone area and cortical thickness [18,21]. However, cancellous BMD and total cancellous bone are increased in male ERKO mice, due to increased trabecular number [21,22]. These differential responses to the loss of ER α in cortical versus cancellous bone are most likely due to the variable distribution of the estrogen receptors [15].

Estrogen and the estrogen receptors in bone play an important role in the skeletal response to mechanical loading [13,14]. ER α is directly involved in the osteoblast response to strain [25,26,184], and ER α is upregulated and activated after application of mechanical strain. *In vitro*, osteoblasts taken from male and female ERKO mice do not proliferate and respond to strain like osteoblast cultures from WT controls [7], and female

ERKO mice had an impaired osteogenic response to exercise [239]. However, male ERKO mice had either no differences or increased osteogenic response to mechanical loading compared to WT controls [28,29]. This implies some type of compensatory mechanism that allows for an osteogenic response to mechanical loading in the ERKO males, possibly through ER β or the androgen receptors in bone [30].

Another recently hypothesized role of estrogen in the skeletal response to mechanical loading is the downregulation of the protein sclerostin. Osteocytes express sclerostin, which is a competitive inhibitor of the canonical Wnt signaling pathway. Canonical Wnt signaling plays a key role in bone formation, as it increases transcription of several osteogenic genes (reviewed in [31,32]). Briefly, association of the Wnt molecule with its receptor, co-receptor lipoprotein receptor-related protein 5 or 6 (LRP 5/6) leads to the release of a transcription factor, β -catenin into the cytosol. β -catenin is then free to translocate into the nucleus, where it activates the transcription of several osteogenic genes, especially those related to osteoblast differentiation, such as osteoprotegerin. Inhibition of the Wnt signaling pathway via sclerostin is associated with decreased bone growth [33]. Animal and cell culture models show that sclerostin expression in osteocytes is regulated by several external factors, including insulin-like growth factor-I, parathyroid hormone, androgens and estrogens, and mechanical loading [33]. In healthy animals, mechanical loading downregulates sclerostin expression and leads to osteogenesis [33,160]. However, the specific role of estrogen in the control of sclerostin expression, and the effects of estrogen status on the sclerostin-mediated skeletal response to mechanical loading is still unknown.

In women and female rodent models, estrogen status is inversely related to sclerostin expression, whether measured via serum sclerostin levels [189,205,206] or by sclerostin mRNA [35] or protein in the bone [37,38]. In osteoblasts derived from female mice, sclerostin expression was downregulated after the application of exogenous estrogen, and ER β appeared to play a greater role in the regulation of sclerostin than ER α [184]. In older men, estrogen treatment lowered circulating levels of sclerostin [34], implying that the inverse relationship between estrogen and sclerostin is also present in males. However, because circulating levels of sclerostin may not reflect bone sclerostin expression [36], further studies looking at the effect of estrogen on bone sclerostin expression in males are warranted.

The essential role of estrogen in bone health throughout the life cycle has been well established in both males and females. However, questions still remain regarding the relative importance of specific estrogen receptors, especially ER α , in osteocyte sclerostin expression and the osteogenic response to exercise in males. Here, we look at the effects of global ER α knock out and voluntary wheel running exercise on cortical geometry, trabecular microarchitecture, biomechanical strength, and osteocyte sclerostin expression in male mice. We hypothesized that ERKO animals would have impaired cortical geometry and biomechanical strength compared to WT animals, but that exercise could lead to partial improvements in cortical geometry and biomechanical strength in ERKO animals, and significant improvements in the WT animals. We also hypothesized that ERKO animals would have increased trabecular bone volume compared to WT animals. Finally, we hypothesized that ERKO animals would have higher sclerostin expression

than WT animals, and that exercise would downregulate sclerostin only in the WT groups.

Methods

Experimental design

This study is part of a larger study investigating the effects of global ERKO on glycemic control, inflammation, and hepatic steatosis in male mice, and whether exercise could be an effective treatment to reverse the negative impacts of ERKO [214]. Heterozygote ER α ^{-/+} mice on a C57BL/6J background were bred at our facility to produce male homozygote (ER α ^{-/-}) and littermate wild-type mice, as previously described [215,216]. Briefly, development of the ER α ^{-/-} mouse was accomplished by homologous recombination and insertion of a neomycin sequence containing premature stop codons and polyadenylation sequences into a NotI site in exon 2 of the mouse estrogen receptor gene [215–217]. After weaning, mice were fed standard rodent chow [(3.3 kcal/g of food), 13% kcal fat, 57% kcal carbohydrate, and 30% kcal protein, 5001, LabDiet, St. Louis, MO, USA] *ad libitum* until 12 weeks of age. At 12 weeks of age, all mice were given *ad libitum* access to a high fat diet [4.65 kcal/g of food; 46.0% kcals from fat, 36.0% kcals from carbohydrate with sucrose content (per weight) of 17.5% and high-fructose corn syrup content of 17.5% (Test Diet modified 58Y1; 5APC)], and both ER α ^{-/-} (ERKO) and wild-type (WT) animals were randomized into two groups - an exercising (EX) group given access to running wheels, and a sedentary (SED) control group with no running wheels - resulting in 4 experimental groups: ERKO-EX, ERKO-SED, WT-EX, and WT-SED (n=6-8/group). All mice were pair-housed (mixed genotypes) in a temperature-controlled environment at 25°C, with a 0700-1900 light, 1900-0700 dark cycle. Body weight and food intake were measured weekly, and body composition was measured by a nuclear magnetic resonance imaging whole-body

composition analyzer (EchoMRI 4in1/1100; Echo Medical Systems, Houston, TX) on conscious mice one week prior to sacrifice. At 22 weeks of age, mice were euthanized following a 5-hour fast. Blood samples were collected via cardiac puncture and centrifuged; plasma was separated, frozen in liquid nitrogen and stored at -80°C for further analysis. Circulating estradiol and fasting insulin, glucose, and lipids were measured as previously described [214]. Hindlimbs were harvested, wrapped in PBS-soaked gauze, frozen in liquid nitrogen, and stored at -80°C for further analysis. All procedures were approved in advance by the University of Missouri Institutional Animal Care and Use Committee.

Tibial Cortical Geometry and Trabecular Microarchitecture

Micro-computed tomographic (μ CT) imaging of the right tibia was performed using a high-resolution imaging system (Xradia 520 Versa, ZEISS, Oberkochen, Germany). The methods used were in accordance with guidelines for the use of μ CT in rodents [85]. Scans were acquired using an isotropic voxel size of 0.012 mm, a peak X-ray tube potential of 60 kV, and a 2-sec exposure time. Trabecular bone microarchitecture was evaluated in a 0.5-mm region of interest directly below the growth plate of the proximal tibia, as previously described [240,241]. Cortical bone cross-sectional geometry was evaluated at a 1-mm region of interest at the mid-diaphysis of the tibia, or the midway point between the tibial crest and the tibiofibular joint, as previously described [240,241]. The optimized threshold function was used to delineate mineralized bone from soft tissue. Scans were analyzed using BoneJ software [218] (NIH public domain), and measures of cortical geometry and trabecular microarchitecture were

collected. Outcomes for cortical geometry included: tibia length (Le), total cross-sectional area inside the periosteal envelope (Tt.Ar), marrow area (Ma.Ar), cortical bone area (Ct.Ar), cortical area fraction (Ct.Ar/Tt.Ar), mean cortical thickness (Ct.Th), and robustness (R, total bone area over length calculated as $R = Tt.Ar/Le$). Outcomes for trabecular microarchitecture included: bone volume fraction (BV/TV), connectivity density (Conn.D, degree of trabeculae connectivity normalized to total bone volume), mean trabecular thickness (Tb.Th), trabecular separation (Tb.Sp, distance between trabeculae), trabecular number (Tb.N, average number of trabeculae per unit length calculated as $1/(Tb.Th + Tb.Sp)$ [219]), structural model index (SMI), and degree of anisotropy (DA).

Tibial Biomechanical Strength

Biomechanical strength of the right tibia was performed using three-point bending [86]. Briefly, tibias were cleaned of all soft tissue and placed in the three-point bending apparatus with a span of 6-mm. Tibiae were loaded via a materials testing machine (Instron 5942; Instron, Inc., Norwood, MA) at a rate of 10 mm/minute at the midpoint of the tibia until fracture. Outputs from the Instron machine were used to produce a load-displacement curve. The slope of the load-displacement curve was used to estimate material stiffness, and the area under the load-displacement curve was used to estimate work-to-fracture [91]. Maximal load was measured as the highest force applied to the bone before fracture [91]. Load-displacement data were converted into stress and strain to produce a stress-strain curve using the geometric measurements of the bone and following the equations of Turner and Burr [91]. The slope of the stress-strain curve was

used to estimate Young's modulus of elasticity, and the area under the curve was used to estimate the modulus of toughness [91].

Femoral Osteocyte Sclerostin Expression

Right femurs were fixed in 10% formalin for 48 hours at 4° C, and then decalcified in 14% EDTA at 4° C. Decalcified femurs were embedded in paraffin wax blocks, and 5- μ m sections were taken transversely at the mid-diaphysis and the proximal metaphysis above the growth place of the femur, for measures of cortical and cancellous bone, respectively. The sections were deparaffinized and underwent heat-induced epitope retrieval overnight at 60 °C using a 10 mM sodium citrate buffer, followed by blocking of endogenous avidin and biotin expression (Avidin Biotin Blocking Solution, Thermo Scientific, Waltham, MA). Sections were then incubated in anti-sclerostin primary antibodies (Abcam, Cambridge, UK) overnight at 4 °C, followed by blocking of endogenous peroxidase activity (3% H₂O₂, Ricca Chemical, Arlington, TX) and secondary antibody application. Secondary antibody binding and detection were accomplished using the Vectastain Elite ABC kit (Vector Laboratories, Burlingame, CA), with diaminobenzidine (ImmPACT DAB, Vector Laboratories, Burlingame, CA) as the chromogen. Sections were counterstained with hematoxylin (Fisher Scientific, Hampton, NH), dried, and mounted. Sections were analyzed at 20x for sclerostin expression. Sclerostin positive (Sost+) osteocytes were defined as osteocytes exhibiting brown staining, and sclerostin negative (Sost-) osteocytes were defined as osteocytes exhibiting blue (hematoxylin) staining. Data are reported as percent Sost+ osteocytes. In addition to Sost+ and Sost- osteocytes, empty osteocytic lacunae revealed by hematoxylin staining

were counted, and data are reported as percent empty lacunae, as previously described [221].

Statistical Analysis

A two-way ANOVA was used to assess the main and interactive effects of genotype and exercise on metabolic outcomes, trabecular microarchitecture, and percentage of sclerostin+ osteocytes. Body weight is a strong predictor of cortical bone size and strength, so cortical geometry and biomechanical strength outcomes were assessed by two-way ANCOVA with final body weight included as a covariate [86]. If an interaction was present, one-way ANOVA or ANCOVA was used as necessary to determine the location of the interaction. Data are presented as means \pm SEM or adjusted means \pm SEM. Statistical significance was set at $p < 0.05$. All analyses were performed using SPSS software (SPSS/25.0, SPSS, Chicago, IL, USA).

Results

Animal Characteristics

The metabolic characteristics of these animals have been previously published as part of a larger study [214], and the results have been summarized in Table 1. Briefly, exercise significantly decreased body mass ($p=0.001$) and body fat percentage ($p=0.004$) and increased average weekly food intake ($p=0.001$), regardless of genotype (**Table 4.1**). Exercise also significantly decreased LDL cholesterol, triglycerides, and leptin [214]. There was no difference in running distance between groups provided with running wheels (**Figure 4.1**, [214]). ERKO animals had significantly higher LDL and total cholesterol compared to WT animals [214]. There was no effect of ERKO or exercise status on fasting blood glucose or insulin levels or HOMA-IR [214].

Outcome	WT		ERKO		P-value
	SED	EX	SED	EX	
Body Mass (g)	39.63 ± 1.70	33.06 ± 1.77*	41.52 ± 1.70	36.39 ± 1.58*	G: 0.129 E: 0.001 G*E: 0.670
Body Fat (%)	32.28 ± 2.33	22.96 ± 2.64*	33.22 ± 2.33	27.56 ± 2.21*	G: 0.254 E: 0.004 G*E: 0.450
Average Food Intake (kcal/d)	6.04 ± 0.14	6.77 ± 0.16*	5.87 ± 0.14	6.38 ± 0.13*	G: 0.054 E: 0.001 G*E: 0.432

Table 4.1. Metabolic Characteristics. Data are means ± SEM, n=6-8 per group. ERKO: ER α knock out; WT: wild type; EX: voluntary wheel running; SED: sedentary. G: genotype; E: exercise status; G*E: genotype by exercise interaction. * $p \leq 0.05$ vs SED. There was a significant main effect of EX on body mass [(g): EX = 34.73 ± 1.19; SED = 40.58 ± 1.18; $p=0.001$], body fat [(%): EX = 25.26 ± 1.72; SED = 32.75 ± 1.65; $p=0.004$], and average food intake [(g/wk): EX = 9.89 ± 0.15; SED = 8.96 ± 0.15; $p=0.001$].

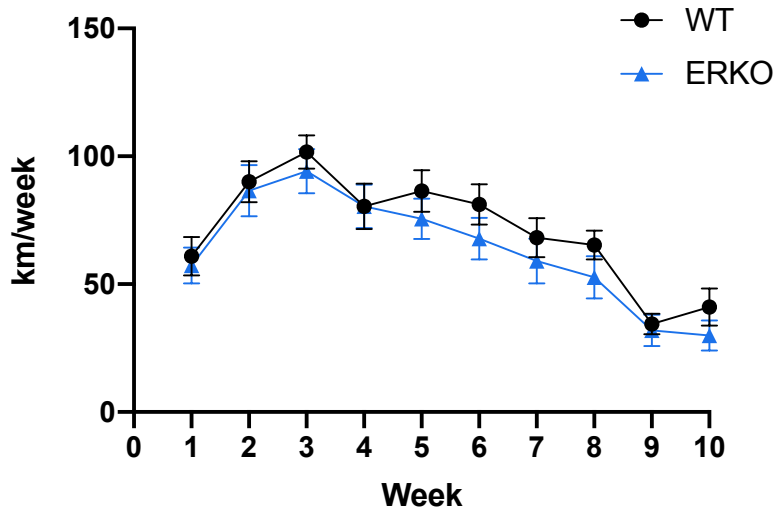


Figure 4.1 Average running distance. ERKO: ER α knock out; WT: wild type.

Tibial Cortical Geometry

Tibial length was not different between groups. There was a main effect of genotype ($p=0.007$) on Tt.Ar, with the ERKO animals having significantly lower Tt.Ar compared to the WT animals. There was a significant interaction ($p=0.05$) between genotype and exercise, in that EX increased Tt.Ar only in the ERKO animals. ERKO animals had significantly lower robustness (Tt.Ar/Le) than WT counterparts ($p=0.01$), but there was a significant interaction ($p=0.01$) between genotype and exercise, in that EX increased robustness only in the ERKO animals. ERKO animals also had significantly lower Ma.Ar. than WT animals ($p=0.05$). There was a main effect of genotype ($p=0.003$) and exercise ($p=0.02$) on Ct.Ar, with ERKO animals having lower Ct.Ar compared to WT and EX animals having higher Ct.Ar than SED animals. There was a significant interaction ($p=0.05$) between genotype and exercise on Ct.Ar, in that EX increased Ct.Ar significantly more in the ERKO animals than the WT animals. There were main effects of genotype ($p=0.02$) and exercise ($p=0.03$) on Ct.Th, with ERKO animals having lower

Ct.Th than WT animals, and EX animals having higher Ct.Th than SED animals. There were no differences in Ct.Ar/Tt.Ar or I_{max}/I_{min} ratios between groups. **(Figure 4.2)**

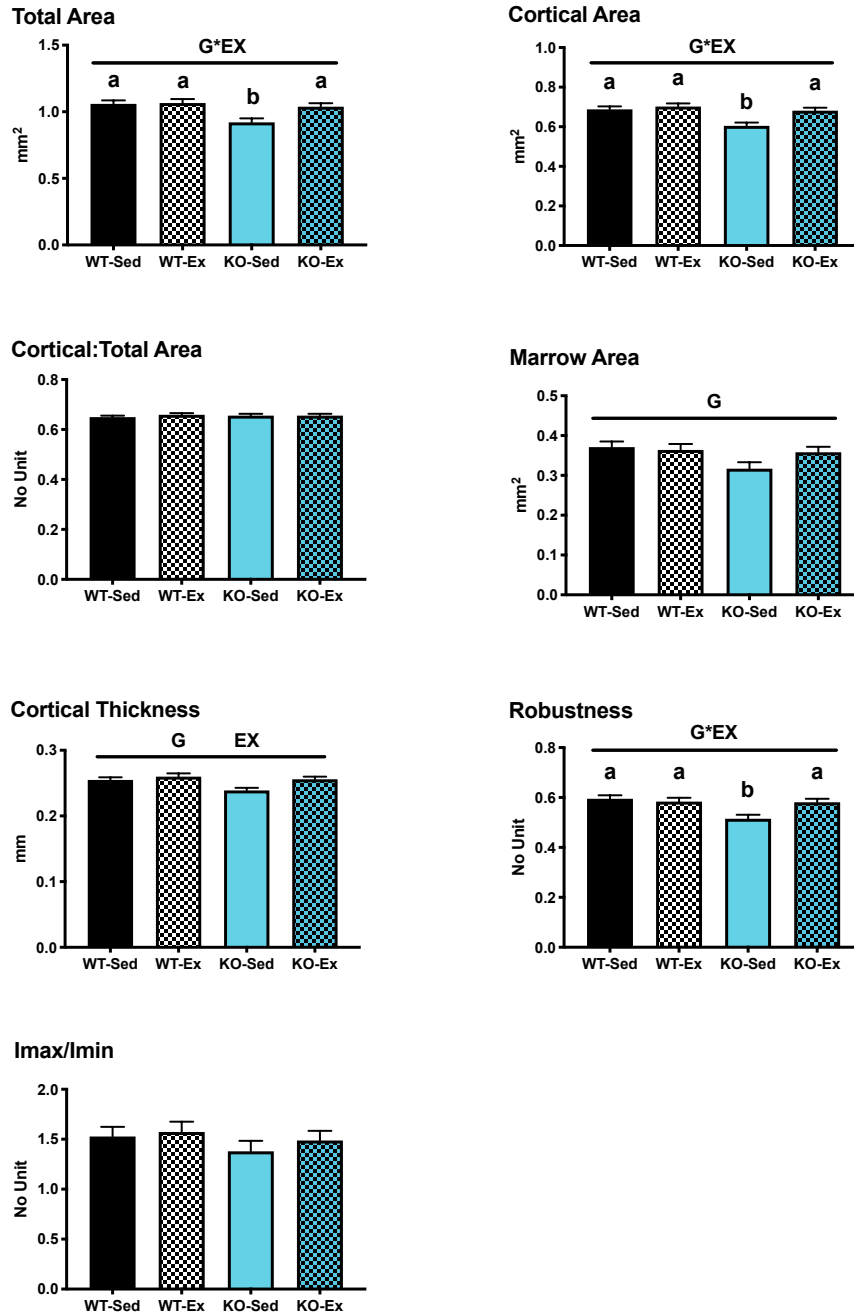


Figure 4.2. Cortical Geometry of the Tibia. Data are adjusted means \pm SEM, n=6-8 per group ERKO: ER α knock out; WT: wild type; Ex: voluntary wheel running; Sed: sedentary. G: main effect of genotype ($p \leq 0.05$); EX: main effect of exercise status ($p \leq 0.05$); different letters denote significance ($p \leq 0.05$) if G*EX interaction is present. There was a significant main effect of G on Tt.Ar [(mm²): ERKO = 0.980 ± 0.019 ; WT = 1.063 ± 0.019 ; $p=0.007$], Ct.Ar [(mm²): ERKO = 0.643 ± 0.011 ; WT = 0.695 ± 0.011 ; $p=0.003$], Ma.Ar [(mm²): ERKO = 0.337 ± 0.010 ; WT = 0.368 ± 0.010 ; $p=0.05$], Ct.Th [(mm): ERKO = 0.247 ± 0.003 ; WT = 0.257 ± 0.003 ; $p=0.02$], and robustness [(no unit): ERKO = 0.55 ± 0.01 ; WT = 0.59 ± 0.01 ; $p=0.01$]. There was a significant main effect of EX on Ct.Ar [(mm²): Ex = 0.691 ± 0.011 ; Sed = 0.646 ± 0.011 ; $p=0.02$] and Ct.Th [(mm): Ex = 0.258 ± 0.003 ; Sed = 0.247 ± 0.003 ; $p=0.03$].

Tibial Biomechanical Strength

Exercising animals had significantly lower Young's modulus of elasticity than their sedentary counterparts ($p=0.04$), regardless of genotype. There were no differences between groups in max force, stiffness, work-to-fracture, or modulus of toughness.

(Figure 4.3)

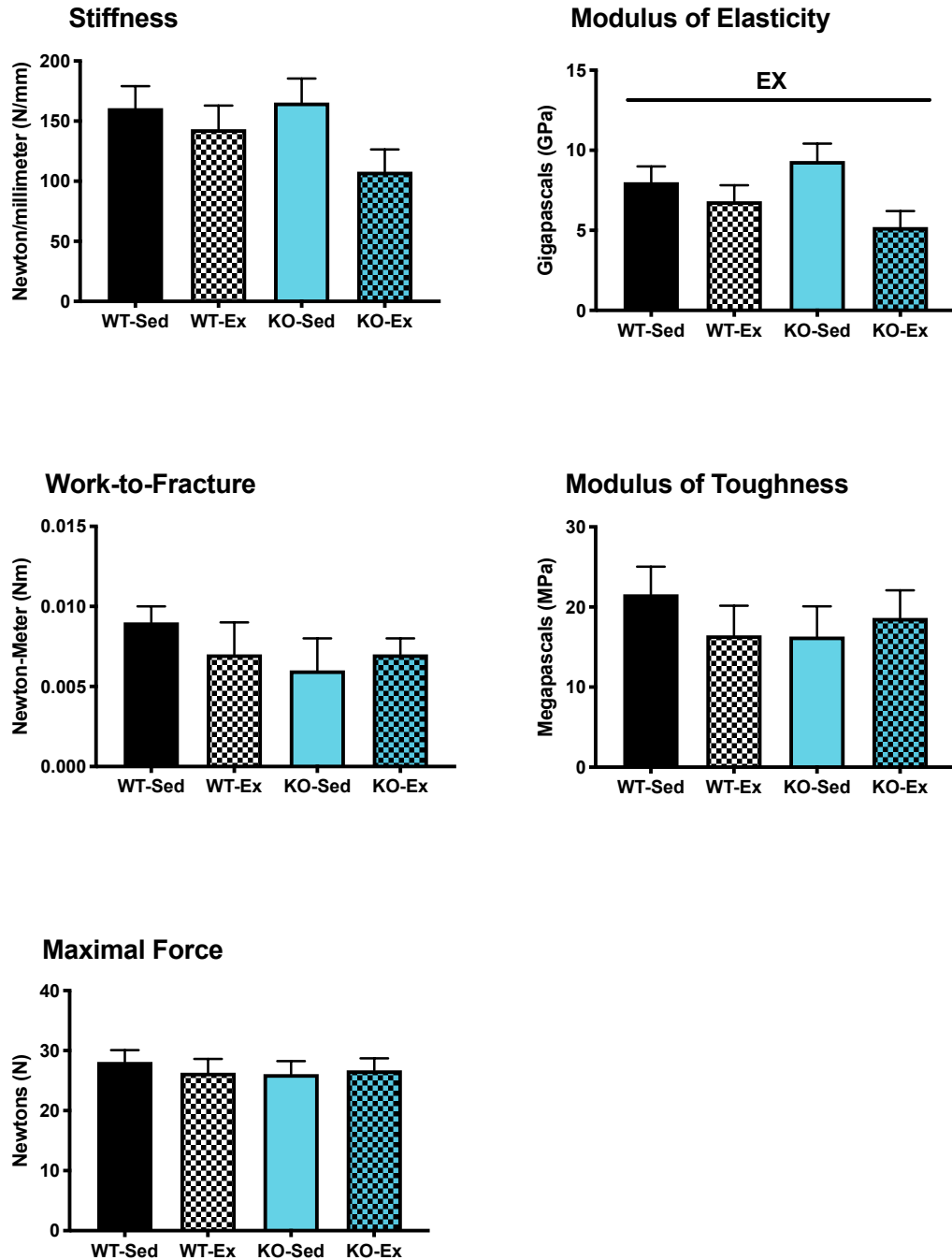


Figure 4.3. Biomechanical Strength of the Tibia. Data are adjusted means \pm SEM, n=6-8 per group ERKO: ER α knock out; WT: wild type; Ex: voluntary wheel running; Sed: sedentary. G: main effect of genotype ($p \leq 0.05$); EX: main effect of exercise status ($p \leq 0.05$). There was a significant main effect of EX on Young's modulus of elasticity [(GPa): Ex = 6.012 ± 0.762 ; Sed = 8.665 ± 0.762 ; $p = 0.04$].

Tibial Trabecular Microarchitecture

There was a main effect of genotype on BV/TV ($p=0.034$), Tb.N ($p=0.001$), Conn.D ($p=0.001$), and SMI ($p=0.04$) with ERKO animals having higher values than WT animals in these outcomes. There was a main effect of genotype on Tb.Th ($p=0.006$) and Tb.Sp ($p=0.001$) with ERKO animals having lower values than WT animals. Exercising animals had significantly higher DA than their sedentary counterparts ($p=0.01$), regardless of genotype. **(Figure 4.4)**

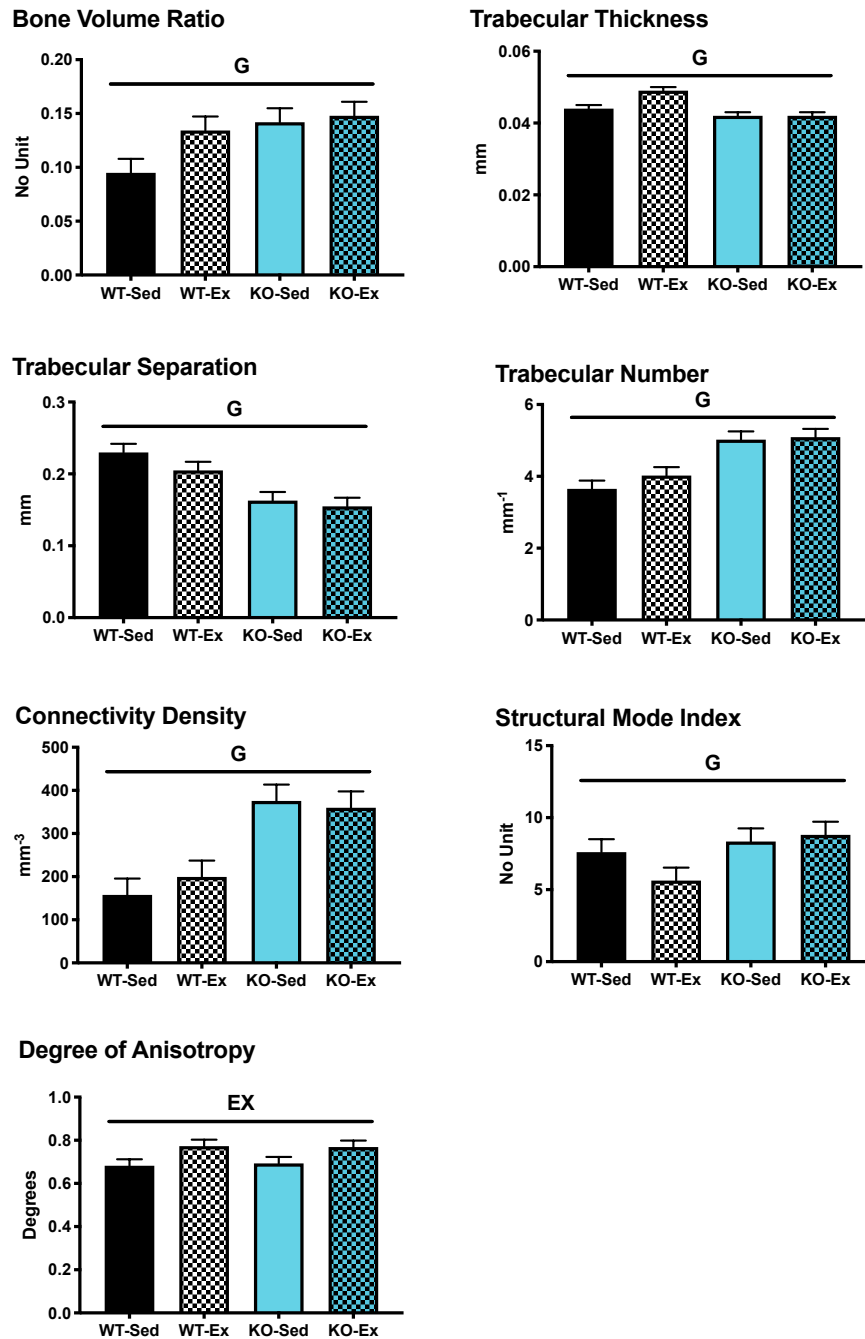


Figure 4.4 Trabecular Microarchitecture of the Tibia. Data are means \pm SEM, n=6-8 per group ERKO: ER α knock out; WT: wild type; Ex: voluntary wheel running; Sed: sedentary. G: main effect of genotype ($p \leq 0.05$); EX: main effect of exercise status ($p \leq 0.05$). There was a significant main effect of G on BV/TV [(no unit): ERKO = 0.145 ± 0.01 ; WT = 0.114 ± 0.01 ; $p=0.03$], Tb.Th [(mm): ERKO = 0.042 ± 0.001 ; WT = 0.047 ± 0.001 ; $p=0.006$], Tb.Sp [(mm): ERKO = 0.159 ± 0.01 ; WT = 0.218 ± 0.01 ; $p=0.001$], Tb.N [(mm⁻¹): ERKO = 5.06 ± 0.163 ; WT = 3.84 ± 0.16 ; $p=0.001$], Conn.D [(mm³): ERKO = 367.7 ± 26.9 ; WT = 178.5 ± 26.9 ; $p=0.001$], and SMI [(no unit): ERKO = 8.58 ± 0.64 ; WT = 6.62 ± 0.64 ; $p=0.04$]. There was a significant main effect of EX on DA [(degree): Ex = 0.771 ± 0.021 ; Sed = 0.688 ± 0.021 ; $p=0.01$].

Femoral Osteocyte Sclerostin Expression

There were no differences in percent empty lacunae or percent sclerostin positive osteocytes between groups in samples of either cortical or cancellous bone. (**Figure 4.5**)

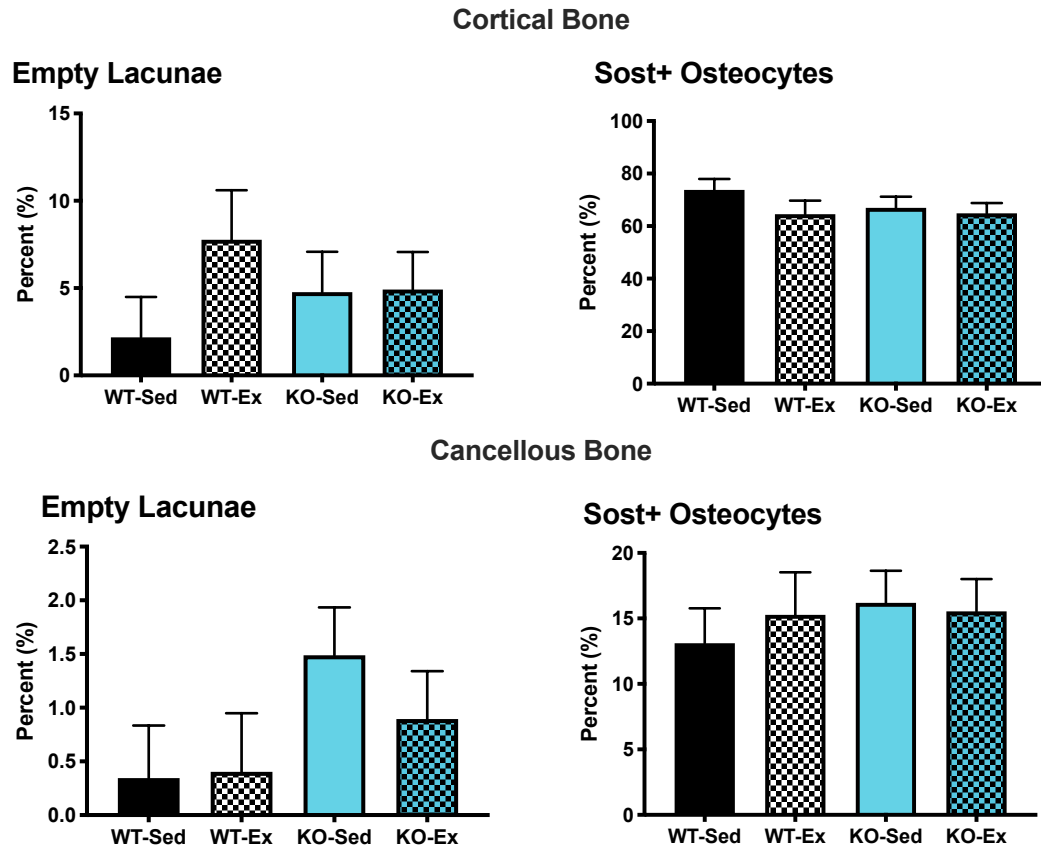


Figure 4.5. Sclerostin Expression in Cortical and Cancellous Bone of the Femur. Data are means \pm SEM, n=6-8 per group ERKO: ER α knock out; WT: wild type; Ex: voluntary wheel running; Sed: sedentary.

Discussion

Here we showed that ERKO had differential effects on cortical and cancellous bone in young, male mice compared to their WT counterparts. More specifically, ERKO animals, regardless of exercise status, had improved measures of trabecular microarchitecture, such as bone volume and trabecular number; however sedentary ERKO animals had significant negative alterations in cortical bone geometry, such as reduced cortical thickness and area relative to controls. We also found that exercise begun after skeletal maturity could reverse some of these negative alterations in cortical bone of ERKO mice. Exercising male ERKO animals had significantly improved measures of cortical geometry than their sedentary counterparts, implying that ER α is not necessary for males to grow bone in response to exercise. Exercise, regardless of genotype, decreased young's modulus of elasticity in the tibia, but there was no effect of exercise or genotype on any other measures of biomechanical strength or sclerostin expression in cortical or cancellous bone of the femur.

The negative morphological changes seen in the cortical bone of male, global ERKO animals in this study are supported by previous studies by both ourselves [202] and others [18,21,22]. Estrogen and the estrogen receptors have significant, cell-specific roles in the development and maintenance of bone mass - estrogen blocks osteocyte and osteoblast apoptosis, induces osteoblast differentiation, increases osteoclast apoptosis, and reduces osteoclast differentiation [3,4,9–11]. ER α is particularly important in the maintenance of cortical bone mass due to its higher prevalence compared to ER β [15] and its actions in certain cell types. When ER α was deleted from osteoblast precursors, femoral BMD and cortical thickness were reduced compared to wild-type animals [174],

whereas there were no alterations in cortical bone when ER α was deleted from mature osteocytes only [175]. This indicates that ER α controls cortical bone formation through actions on progenitor cells and supports our findings in this global knockout model.

Previous studies have shown that both global [28] and osteoblast-specific [29] male ERKO models can respond to exercise despite the loss of ER α , which is in contrast to females, for which ER α is required for the osteogenic response to exercise [239]. However, we were the first to further explore one cellular mechanism of the exercise response by analyzing sclerostin expression in male ERKO animals. We have previously shown that aged, sedentary male ERKO animals have higher sclerostin expression than aged, sedentary male WT animals [202]. Considering exercise downregulates sclerostin [33], we wanted to explore whether ERKO animals would also have higher sclerostin expression under exercise conditions. While exercise decreased sclerostin expression in both groups, it was not statistically significant. There were no differences between ERKO and WT in sclerostin expression, which implies that there is no effect of ERKO on sclerostin expression in younger males. The differences between this study and our previous study could be partially explained by age or metabolic status. In our previous study ERKO animals had higher fasting blood glucose levels than their WT counterparts, and high blood glucose is associated with increased sclerostin expression [33]. In this study, there were no difference in blood glucose, which could partially explain the lack of differences in sclerostin expression. In addition, sclerostin naturally increases with age [33], and this higher expression overall could exacerbate differences triggered by metabolic changes over time. However, more studies are needed to fully understand the interacting effects of ER α , age, and exercise on sclerostin expression.

Exercise had minimal effects in the cortical bone of WT animals. Exercise increased both total area and cortical thickness but did not have a significant effect on marrow or cortical area or robustness. We attribute this to the initiation of exercise after skeletal maturity – exercise began at 12 weeks of age, which is around skeletal maturity [242]. Previous studies have shown that bone cells are less responsive to exercise after skeletal maturity, and it thus takes higher mechanical forces to induce osteogenesis [243]. However, in the ERKO animals, which had significant impairments in cortical bone geometry, exercise induced enough strain for an osteogenic response. Exercising ERKO animals had significantly higher cortical and total area, cortical thickness, and robustness than their sedentary counterparts, which equalized their cortical geometry to that of the WT animals. The difference in magnitude of osteogenic response between the WT and ERKO animals could also be partially attributed to body weight. Higher body weight in the exercising ERKO animals would lead to increased load during exercise, which could lead to increases in bone accrual [151]. Interestingly, exercising animals, regardless of genotype, had lower Young's modulus of elasticity and stiffness, although stiffness was not quite at a significant level ($p=0.10$). Both are measures of the elasticity of the bone, or the ability of the bone to resist deformation before fracture, but stiffness is a measure of the elasticity of the bone material whereas Young's modulus is a measure of the elasticity of the bone as a whole structure. However, there was no effect of exercise or genotype on maximal load sustained, so these alterations in stiffness and elasticity did not appear to have a negative impact on overall strength of the bone.

The positive morphological changes in the trabecular bone of the ERKO animals have also been supported in previous studies by both ourselves [202] and others [21,22].

These improvements can be explained by the greater presence of ER β in cancellous bone. In cancellous bone, ER β and ER α appear to have similar actions, and both play a role in maintaining total bone mass [4]. Thus, the loss of ER α does not lead to a loss of bone mass as it does in cortical bone. However, we were one of the first to explore the effects of exercise on trabecular microarchitecture in ERKO mice, as well as further explore the cellular mechanisms by measuring sclerostin expression. Exercise begun after skeletal maturity increased the degree of anisotropy, which is a strong indicator of trabecular bone strength [83]. Thus, it is possible that exercise increased the strength of the trabecular bone in conjunction with the morphological changes; however, we did not have the capacity to measure trabecular bone strength. We saw no effect of ERKO or exercise on sclerostin expression in cancellous bone, consistent with previous studies [202].

In conclusion, we found that ERKO has differential effects on cortical and cancellous bone in young, male mice. Specifically, ERKO significantly improved trabecular microarchitecture, implying ER α is not required for the maintenance of trabecular bone. However, ERKO negatively impacted cortical geometry, which supports a significant role for ER α in the maintenance of cortical bone in sedentary animals. We also found that exercise started after skeletal maturity was able to reverse the negative alterations in cortical geometry in the ERKO animals. This would indicate that ER α is not necessary for an osteogenic response to mechanical loading in male mice, which is in direct contrast with females. There were no effects of ERKO or exercise on sclerostin expression, and thus further studies are warranted to explore additional cellular mechanisms which allow this osteogenic response to exercise in male ERKO animals and if these mechanisms can translate to humans. This would allow for further understandings

of potential targets to improve the efficacy of exercise treatments for osteoporosis and other diseases of low bone mass in both men and women.

CHAPTER 5

Gestational exposure to BPA, but not BPS, significantly impairs trabecular microarchitecture and cortical geometry in male adult offspring

Introduction

Estrogen is one of the most influential hormones in growth and maintenance of the skeleton across the entire lifespan in both males and females [1,2,165,167,168]. Estrogen actions are mediated primarily by estrogen binding with the nuclear estrogen receptor (ER), which is found in two isoforms, ER α and ER β . Bone expresses both ER α and ER β ; however, ER α tends to be more prevalent in cortical bone, whereas ER β is more widely distributed in cancellous bone [15]. Bisphenols are endocrine disruptors and selective estrogen receptor modulators (SERMs) found in plastics that significantly impact human health [39,40]. The most common bisphenol analog is bisphenol-A (BPA), though bisphenol-S (BPS) and bisphenol-F (BPF) are also found in similar products [244]. BPA and its analogs have structural features that allow them to bind to ERs, although BPA displays a 1000- to 2000-fold lower affinity for binding than estradiol, the most active form of estrogen [199]. Binding of BPA or its analogs to the ERs modifies gene expression in a pattern that differs from that resulting from classic estrogen binding [41–43]. However, different analogs appear to have different binding capabilities and anti-estrogenic effects. BPA and BPF can bind with both ER α and ER β , but there is conflicting on whether BPS can bind with both ER α and ER β or just ER α [44,245,246]. There is also evidence that BPA can act as an agonist for ER α , but an antagonist for ER β , depending on how it interacts with the ligand-binding domain [199]. Despite the possible differences in receptor binding, there is evidence that both BPA and BPS can block

estrogen binding in competitive assays [245], and that both BPA and BPS can stimulate cellular activity, although BPS binding usually leads to a weaker response than BPA binding [40,245–247]. In addition to direct actions on ERs, BPA affects epigenetic programming via DNA methylation or histone modification [46–48], particularly when exposure occurs during gestation [49].

Human studies have associated BPA exposure with several endocrine issues, from low circulating sex hormones and decreased birth weight to metabolic diseases, such as obesity and cardiovascular disease [39]. The most common route of BPA or BPS exposure in humans is food contamination, usually from epoxy resins used to line metal cans [53,197] or from BPA leaching into food from plastic storage containers [198]. While less impactful to human exposure, BPA and its analogues can also be found in thermal paper, dust, and certain dental and medical equipment [53,197]. BPA exposure is essentially ubiquitous in humans, with BPA being detectable in almost 100% of the blood or urine samples tested [39]. Many industrialized countries, such as the United States, China, Germany, and Australia have exposure rates above the current tolerable daily intake (TDI) [54]. In addition, the majority of epidemiological studies show that BPA exposure is associated with adverse health effects even at intakes below the current TDI [39]. However, despite the known anti-estrogenic effects of BPA and its ubiquitous exposure, little is known about the effects that exposure to BPA or its analogs can have on the skeleton. This is surprising given the key role of estrogen in skeletal health.

In humans, few studies have looked at relationships between BPA exposure and skeletal health, and only two of those studies included male subjects. In school-aged boys, there was a significant negative correlation between urinary BPA levels and height,

which remained when adjusted for pubertal status and at a follow-up visit 19 months later [58]. In addition, there was a significant negative correlation between maternal urinary BPA levels in the first trimester and BMD at age 10, regardless of sex [248]. The impact of BPA exposure on BMD or fracture incidence in adult males has not been investigated. Nor have any studies looked at skeletal effects of bisphenols other than BPA. The majority of animal studies involving males have examined gestational, rather than adult, exposure. When BPA is given during gestation, male offspring had decreased cortical cross-sectional area and lower trabecular bone volume compared to control offspring [61,62,64]. However, rarely did these morphological changes result in differences in biomechanical strength [62,63]; one study showed impairments in biomechanical strength but they were dose-dependent [64]. *In vitro*, BPA blocked osteoblastic and osteoclastic differentiation and increased markers of apoptosis [65,66,201]. However, no studies have analyzed osteoblast or osteoclast activity *in vivo*, despite bone remodeling directly controlling morphological and biomechanical outcomes. Overall, these data suggest that BPA exposure can have significant effects on bone cell activity and that gestational exposure might have significant impacts on bone mass and strength in male offspring. However, little is known about the effects of other bisphenol analogs, such as BPS, and there are still many unanswered questions about the mechanisms behind the morphological impairments seen in response to BPA exposure.

In this study, we explored the effects of gestational and lactational BPA or BPS exposure on skeletal outcomes in adult male offspring. Based on previous literature, we hypothesized that the male offspring exposed to BPA during gestation would have decreases in cortical thickness and trabecular bone volume relative to controls, and that

these morphological differences could coincide with impairments in biomechanical strength. We also hypothesized that these changes would be associated with slower skeletal growth from decreased osteoblast activity. Based on the often-weaker anti-estrogenic activity of BPS, we hypothesize that BPS exposure will lead to smaller impairments in morphological and biomechanical outcomes than BPA exposure.

Methods

Experimental Design

Female, sexually mature, C57B6/J mice were randomly assigned to three treatment groups: BPA exposure (BPA), BPS exposure (BPS), or control (CON). Within those treatment groups, they were further randomized into two groups – an exercising treatment (EX) that had an unlocked running wheel in the cage, or a sedentary control (SED) that had a locked running wheel in the cage. This resulted in six treatment groups. All animals were given one small vanilla cookie every day. The animals in the BPA group had the equivalent of 200 µg BPA/kg body weight dissolved in ethanol injected into their cookie daily. The animals in the BPS group had the equivalent of 200 µg BPS/kg body weight dissolved in ethanol injected into their cookie daily. The control animals had unaltered ethanol injected into their cookie. Two weeks after treatment started, all mice were mated to C57B6/J male mice which had not been exposed to BPA or BPS. BPA/BPS/CON and EX/SED treatment continued during gestation and lactation. Once weaned, one male and one female offspring were randomly kept from each dam. Dams were singly housed and kept on a 12-hour light-dark cycle in a temperature-controlled room.

After weaning, the male and female offspring were placed on a high-fat diet (18.6% protein, 37.7% carbohydrate, and 43.8% fat by kcal) and aged to skeletal maturity. Mice were pair-housed by sex and kept on a 12-hour light-dark cycle in a temperature-controlled room. Because of aggressive behavioral issues that began after puberty, male animals were moved to singly housed cages and sacrificed earlier, i.e., at a younger age, than the females to prevent loss of experimental animals. Male animals

were sacrificed at 16 weeks of age, and female offspring were sacrificed at 17 weeks of age. Because of the differences in ages, statistical comparisons based on sex would not be valid and were not performed. Thus, males and female offspring will be treated as separate studies, although the experimental design and overall methods were the same for both sexes. **Female results will be reported in chapter 6.** At sacrifice, body weight was measured, and hind limbs were collected, flash frozen, and stored at -80 °C for further analysis. All procedures were approved in advance by the University of Missouri Institutional Animal Care and Use Committee.

Femoral Cortical Geometry and Trabecular Microarchitecture

Micro-computed tomographic (μ CT) imaging of the right femur was performed using a high-resolution imaging system (Xradia 520 Versa, ZEISS, Oberkochen, Germany), as previously described [202]. The methods used were in accordance with guidelines for the use of μ CT in rodents [85]. Scans were acquired using an isotropic voxel size of 0.012 mm, a peak X-ray tube potential of 60 kV, and a 2-sec exposure time. Trabecular bone microarchitecture was evaluated in a 0.5-mm region of interest directly above the growth plate of the distal femur, as previously described [240,241]. Cortical bone cross-sectional geometry was evaluated at a 1-mm region of interest at the mid-diaphysis of the femur as previously described [240,241]. The optimized threshold function was used to delineate mineralized bone from soft tissue. Scans were analyzed using BoneJ software [218] (NIH public domain), and measures of cortical geometry and trabecular microarchitecture were collected. Outcomes for cortical geometry included: tibia length (Le), total cross-sectional area inside the periosteal envelope (Tt.Ar), marrow

area (Ma.Ar), cortical bone area (Ct.Ar), cortical area fraction (Ct.Ar/Tt.Ar), mean cortical thickness (Ct.Th), and robustness (R, total bone area over length calculated as $R = Tt.Ar/Le$). Outcomes for trabecular microarchitecture included: bone volume fraction (BV/TV), connectivity density (Conn.D, degree of trabeculae connectivity normalized to total bone volume), mean trabecular thickness (Tb.Th), trabecular separation (Tb.Sp, distance between trabeculae), trabecular number (Tb.N, average number of trabeculae per unit length calculated as $1/(Tb.Th + Tb.Sp)$ [219]), structural model index (SMI), and degree of anisotropy (DA).

Femoral Biomechanical Strength

Biomechanical strength of the right femur was performed using three-point bending [86]. Briefly, femurs were cleaned of all soft tissue and placed in the three-point bending apparatus with a span of 6-mm. Tibiae were loaded via a materials testing machine (Instron 5942; Instron, Inc., Norwood, MA) at a rate of 10 mm/minute at the midpoint of the tibia until fracture. Outputs from the Instron machine were used to produce a load-displacement curve. The slope of the load-displacement curve was used to estimate material stiffness, and the area under the load-displacement curve was used to estimate work-to-fracture [91]. Maximal load was measured as the highest force applied to the bone before fracture [91]. Load-displacement data were converted into stress and strain to produce a stress-strain curve using the geometric measurements of the bone and following the equations of Turner and Burr [91]. The slope of the stress-strain curve was used to estimate Young's modulus of elasticity, and the area under the curve was used to estimate the modulus of toughness [91].

Tibial Osteocyte Sclerostin Expression

Sclerostin expression was evaluated using immunohistochemistry as previously described [202]. Briefly, Right tibiae were fixed in 10% formalin for 48 hours at 4 °C, and then decalcified in 14% EDTA at 4 °C. Decalcified tibiae were embedded in paraffin wax blocks, and 5- μ m sections were taken transversely at the mid-diaphysis of the tibia for measures of cortical bone. The sections were deparaffinized and underwent heat-induced epitope retrieval overnight at 60 °C using a 10 mM sodium citrate buffer, followed by blocking of endogenous avidin and biotin expression (Avidin Biotin Blocking Solution, Thermo Scientific, Waltham, MA). Sections were then incubated in anti-sclerostin primary antibodies (Abcam, Cambridge, UK) overnight at 4 °C, followed by blocking of endogenous peroxidase activity (3% H₂O₂, Ricca Chemical, Arlington, TX) and secondary antibody application. Secondary antibody binding and detection were accomplished using the Vectastain Elite ABC kit (Vector Laboratories, Burlingame, CA), with diaminobenzidine (ImmPACT DAB, Vector Laboratories, Burlingame, CA) as the chromogen. Sections were counterstained with hematoxylin (Fisher Scientific, Hampton, NH), dried, and mounted. Sections were analyzed at 20x for sclerostin expression. Sclerostin positive (Sost+) osteocytes were defined as osteocytes exhibiting brown staining, and sclerostin negative (Sost-) osteocytes were defined as osteocytes exhibiting blue (hematoxylin) staining. Data are reported as percent Sost+ osteocytes. In addition to Sost+ and Sost- osteocytes, empty osteocytic lacunae revealed by hematoxylin staining were counted, and data are reported as percent empty lacunae, as previously described [221].

Dynamic Histomorphometry of the Femur

Dynamic histomorphometry of the left femur was analyzed using calcein and alizarin fluorescent labeling. Calcein (15 mg/kg BW) and alizarin (20 mg/kg BW) were administered via intraperitoneal injection 7 and 3 days before sacrifice, respectively. Femora were cleaned of all soft tissue, fixed in 10% formalin overnight at 4 °C, dehydrated in graded alcohols, and dried overnight. Samples were then embedded in low-viscosity epoxy (Epo-Thin, Beuhler Ltd., Lake Bluff, IL) under a vacuum and allowed to cure overnight. A 1-mm slice was taken from the mid-diaphysis using a low-speed saw. Sections were mounted on slides and polished to smooth the bone surface. Slides were imaged using a fluorescent confocal microscope (Leica GSD 3D, Leica Biosystems, Buffalo Grove, IL) with excitations at 560 nm and 642 nm for calcein and alizarin, respectively. Images were analyzed in ImageJ. Mineral apposition rate (MAR) was calculated as the distance between the corresponding edges of the two consecutive labels divided by the time between injections (um/day), as recommended by ASBMR [108].

Statistical Analysis

Two-way ANOVA was used to assess the main and interactive effects of gestational BPA or BPS exposure and exercise status of the dam on metabolic outcomes, trabecular microarchitecture, and percentage of sclerostin+ osteocytes. Body weight is a strong predictor of cortical bone size and strength, so cortical geometry and biomechanical strength outcomes were assessed by two-way ANCOVA with final body weight included as a covariate [86]. If an interaction was present, one-way ANOVA or ANCOVA based on dam group was used as necessary to determine the location of the

interaction. Data are presented as means \pm SEM or adjusted means \pm SEM. Statistical significance was set at $p < 0.05$. All analyses were performed using SPSS software (SPSS/25.0, SPSS, Chicago, IL, USA).

Results

Animal Characteristics

There were no main or interactive effects of gestational exposure or exercise status on final body weight. There was a main effect of exercise status on body fat percentage ($p=0.017$), with offspring of exercising dams having lower body fat percentage than those from sedentary dams, regardless of gestational exposure. (**Figure 5.1**)

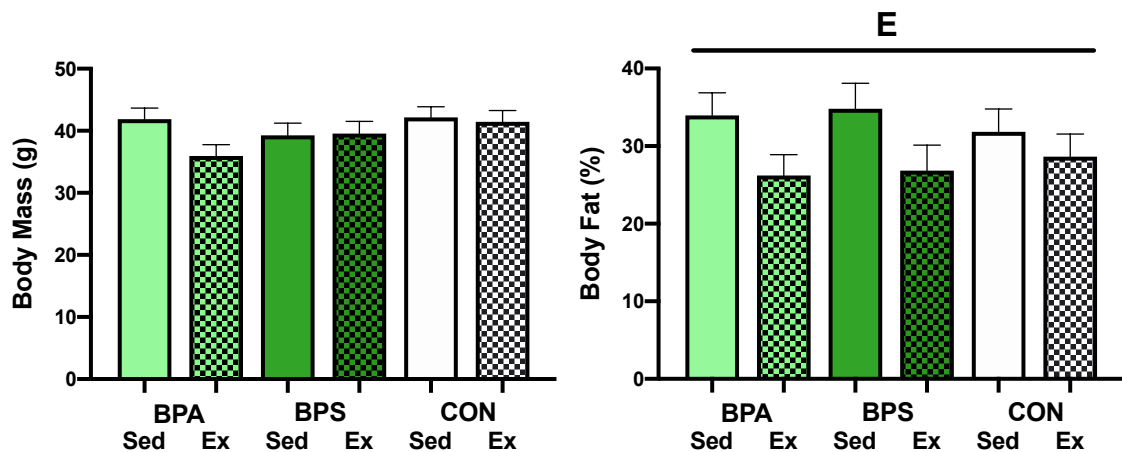


Figure 5.1 Animal Characteristics. Data are means \pm SEM. BPA: gestational bisphenol-A exposure; BPS: gestational bisphenol-S exposure; CON: control group; Ex: dam had access to unlocked running wheel; Sed: dam had locked running wheel. E: main effect of exercise status ($p<0.05$). There was a main effect of exercise on body fat percentage [(%) Ex: 27.23 ± 1.72 ; Sed: 33.53 ± 1.76 ; $p=0.017$].

Femoral Cortical Geometry

There were no main effects of gestational exposure or exercise status on Tt.Ar, Ma.Ar, Ct.Ar, cortical area fraction, or I_{max}/I_{min} ratio. There was a significant interaction ($p=0.022$) between gestational exposure and exercise status on cortical area fraction, in that exercise decreased cortical area fraction in BPA and BPS exposed offspring but increased it in the CON offspring. There was a main effect of gestational

exposure on Ct.Th ($p=0.025$), with BPA offspring having significantly lower Ct.Th than BPS or CON offspring. **(Figure 5.2)**

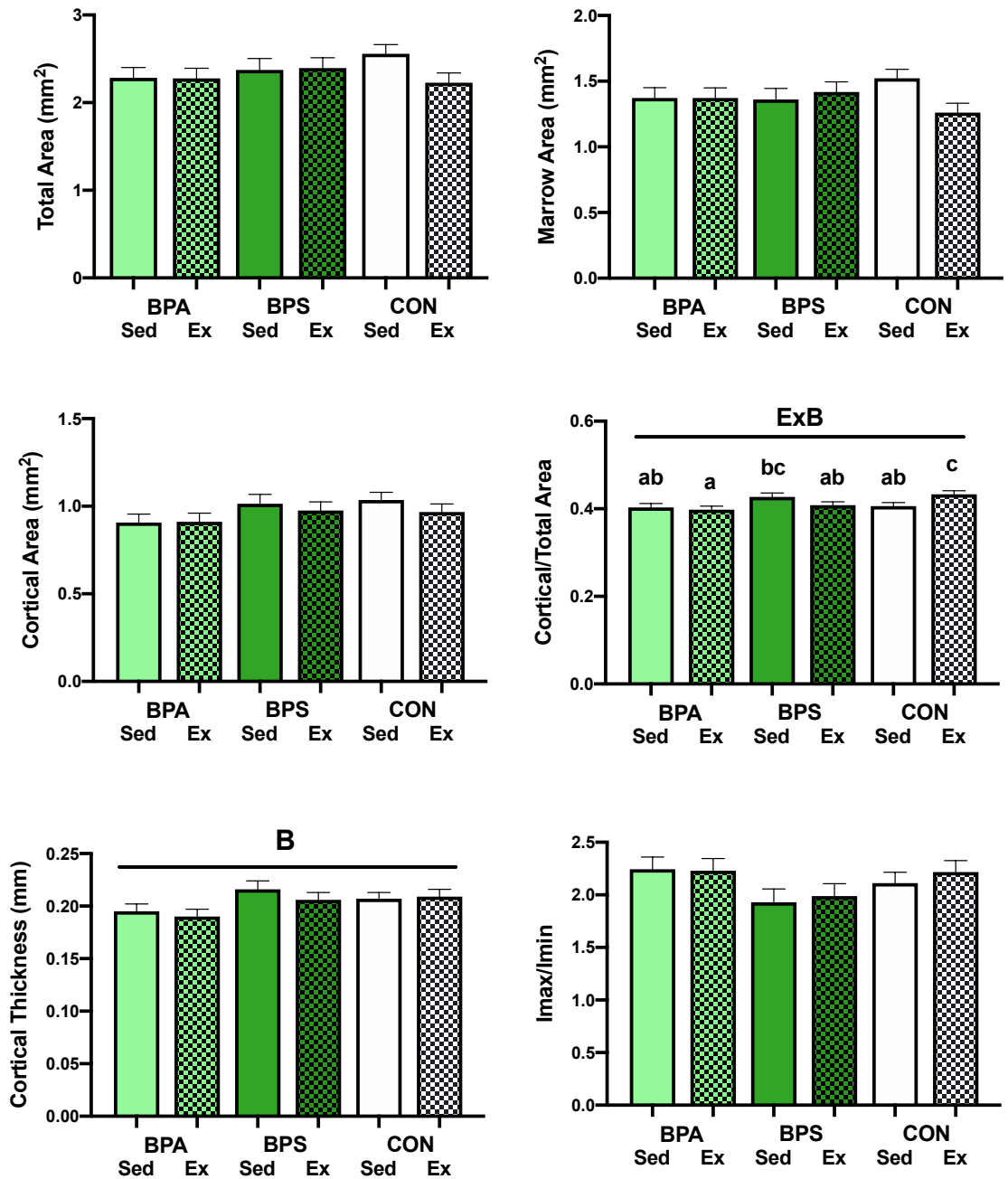


Figure 5.2 Cortical Geometry of the Femur. Data are adjusted means \pm adjusted SEM. BPA: gestational bisphenol-A exposure; BPS: gestational bisphenol-S exposure; CON: control; Ex: dam had access to unlocked running wheel; Sed: dam had locked running wheel. B: main effect of gestational bisphenol exposure ($p < 0.05$); E: main effect of exercise status ($p < 0.05$). Different letters denote significance if a B*E interaction was present. There was a main effect of gestational exposure on cortical thickness [(mm): BPA: 0.193 ± 0.005 ; BPS: 0.211 ± 0.005 ; CON: 0.208 ± 0.004 ; $p = 0.025$].

Femoral Biomechanical Strength

There were no main effects of gestational exposure or exercise status on maximal force, young's modulus of elasticity, work-to-fracture, or modulus of toughness. There was a main effect of exercise status on stiffness ($p=0.031$), with offspring from exercising dams having significantly higher stiffness than offspring from sedentary dams. There was a significant interaction between gestational exposure and exercise status on work-to-fracture ($p=0.044$) and modulus of toughness ($p=0.018$), in that exercise increased both work-to fracture and modulus of toughness in BPS and CON offspring, but not BPA offspring. **(Figure 5.3)**

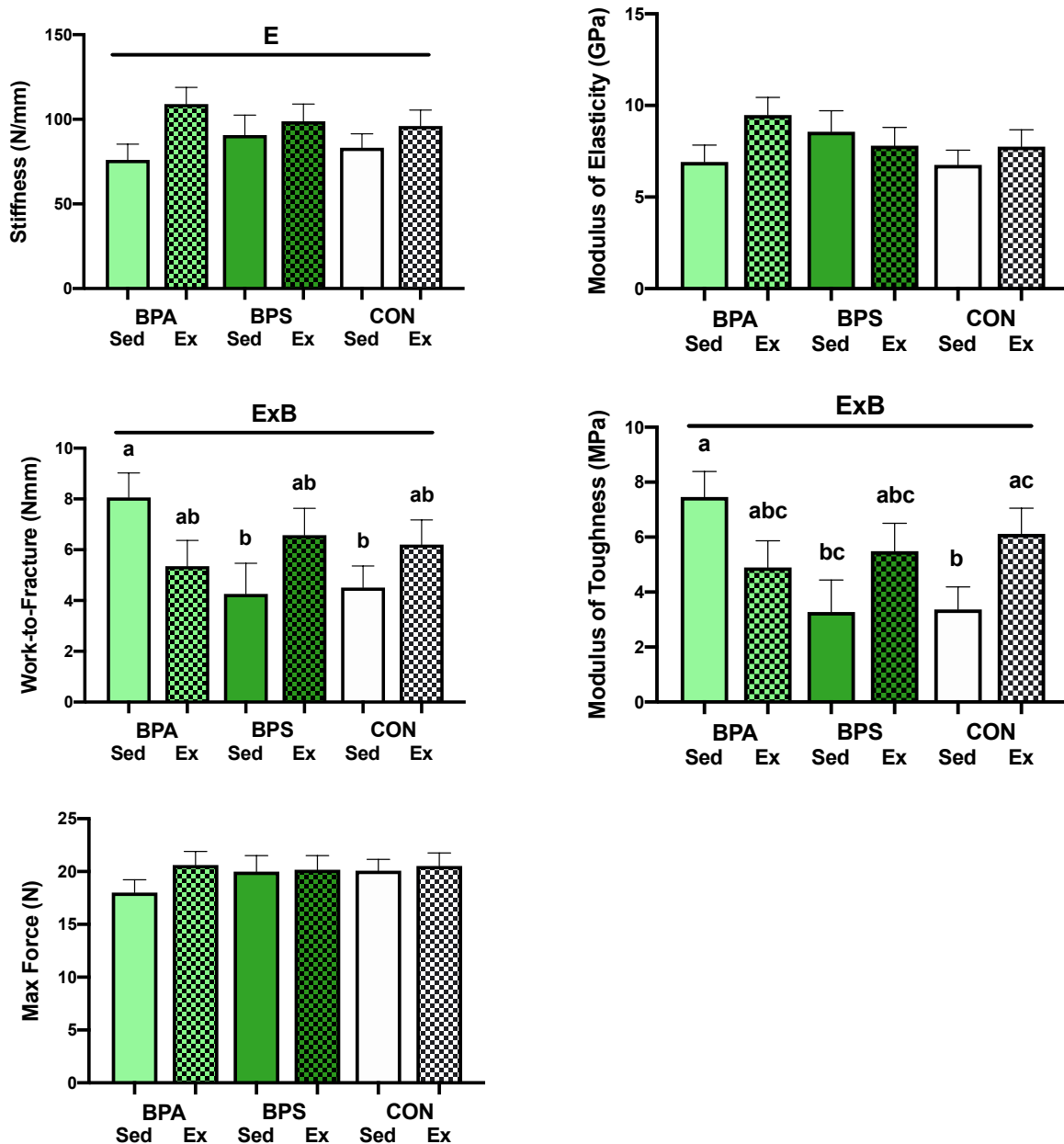


Figure 5.3 Biomechanical Strength of Cortical Bone of the Femur. Data are adjusted means \pm adjusted SEM. BPA: gestational bisphenol-A exposure; BPS: gestational bisphenol-S exposure; CON: control; Ex: dam had access to unlocked running wheel; Sed: dam had locked running wheel. B: main effect of gestational bisphenol exposure ($p < 0.05$); E: main effect of exercise status ($p < 0.05$). Different letters denote significance if a B*E interaction was present. There was a main effect of exercise on stiffness [(N/mm): Ex: 101.29 ± 5.58 ; Sed: 83.33 ± 5.61 ; $p = 0.031$].

Femoral Trabecular Microarchitecture

There was a main effect of gestational exposure on BV/TV ($p=0.001$), Tb.Sp ($p=0.001$), Tb.N ($p=0.001$), Conn.D ($p=0.001$). BPA exposure significantly decreased BV/TV, Tb.N, and Conn.D compared to BPS and CON offspring. BPA exposure significantly increased Tb.Sp compared to BPS and CON offspring. There was a significant interaction between gestational exposure and exercise status on Conn.D ($p=0.036$), with offspring from BPA-Sed dams having significantly lower Conn.D than all other groups except BPA-Ex. There was a significant interaction between gestational exposure and exercise status on SMI ($p=0.001$), in that exercise decreased SMI in BPA and BPS exposed offspring but increased it in the CON offspring. There were no main or interactive effects of gestational exposure or exercise status on Tb.Th, DA, or ellipsoid factor. **(Figure 5.4)**

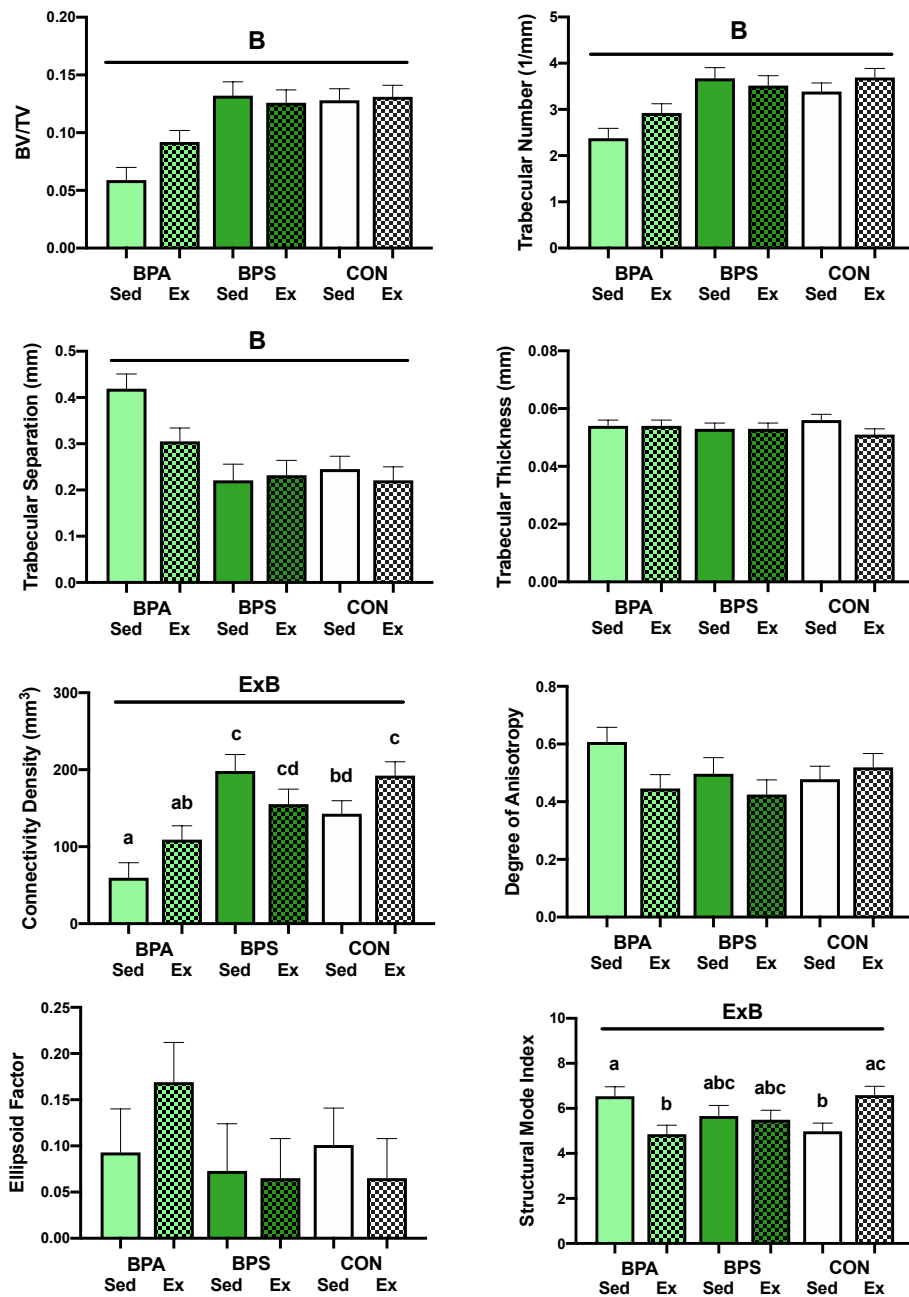


Figure 5.4 Trabecular Microarchitecture of the Femur. Data are means \pm SEM. BPA: gestational bisphenol-A exposure; BPS: gestational bisphenol-S exposure; CON: control; Ex: dam had access to unlocked running wheel; Sed: dam had locked running wheel. B: main effect of gestational bisphenol exposure ($p < 0.05$); E: main effect of exercise status ($p < 0.05$). Different letters denote significance if a B*E interaction was present. There was a main effect of gestational exposure on bone volume fraction [(no unit): BPA: 0.076 ± 0.008 ; BPS: 0.129 ± 0.008 ; CON: 0.129 ± 0.007 ; $p = 0.001$], trabecular number [(1/mm): BPA: 2.65 ± 0.15 ; BPS: 3.60 ± 0.16 ; CON: 3.54 ± 0.14 ; $p = 0.001$], trabecular separation [(mm): BPA: 0.362 ± 0.022 ; BPS: 0.226 ± 0.024 ; CON: 0.233 ± 0.020 ; $p = 0.001$], and connectivity density [(mm³): BPA: 84.43 ± 13.27 ; BPS: 176.86 ± 14.45 ; CON: 167.58 ± 12.35 ; $p = 0.001$].

Cortical Osteocyte Sclerostin Expression of the Tibia

There were no main or interactive effects of gestational exposure or exercise status on percent empty lacunae or percent sclerostin positive osteocytes in the mid-diaphysis of the tibia. (Figure 5.5)

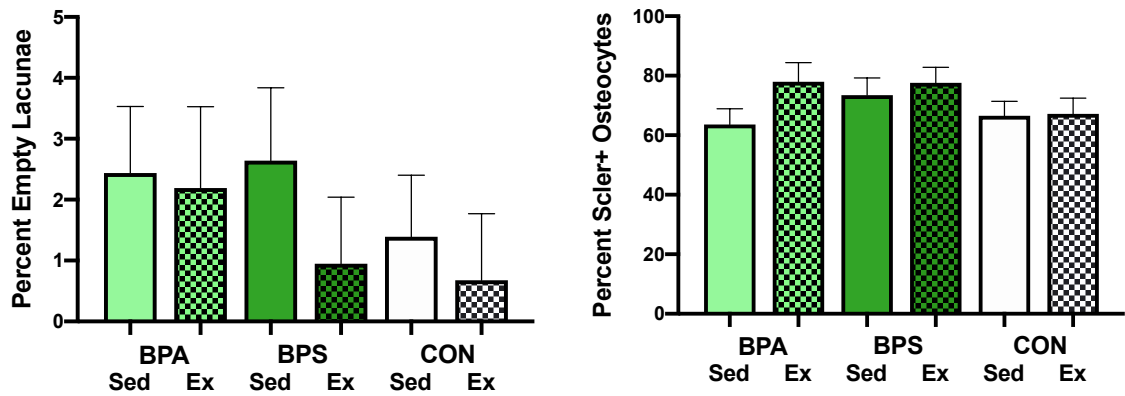


Figure 5.5 Sclerostin Expression of the Tibia. Data are means \pm SEM. BPA: gestational bisphenol-A exposure; BPS: gestational bisphenol-S exposure; CON: control; Ex: dam had access to unlocked running wheel; Sed: dam had locked running wheel.

Dynamic Histomorphometry of the Femur

There were no main or interactive effects of gestational exposure or exercise status on mineral apposition rate of the mid-diaphysis of the femur. (Figure 5.6)

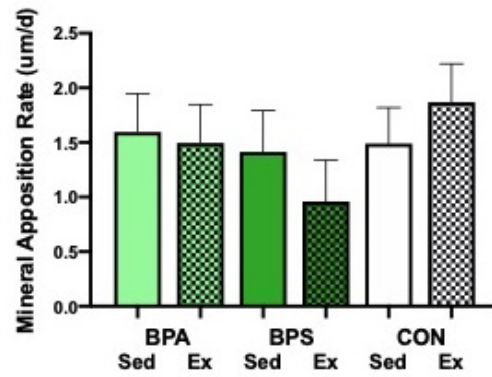
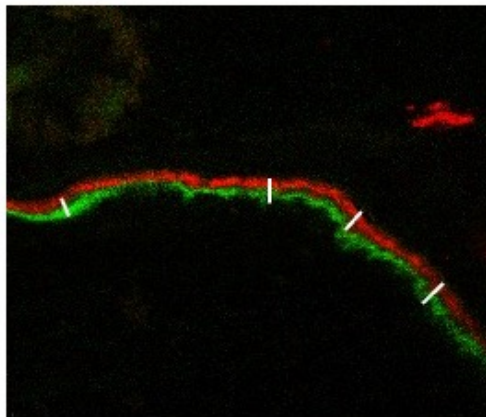


Figure 5.6 Mineral Apposition Rate of the Femur. Data are means \pm SEM. BPA: gestational bisphenol-A exposure; BPS: gestational bisphenol-S exposure; CON: control; Ex: dam had access to unlocked running wheel; Sed: dam had locked running wheel.

Discussion

Here, we showed that gestational and lactational exposure to bisphenol-A (BPA), but not bisphenol-S (BPS), can lead to significant impairments in the skeleton of adult male offspring. We also showed that maternal exercise during gestation and lactation can impact both body composition and bone material properties of adult male offspring. More specifically, offspring of animals exposed to BPA during gestation and lactation had significantly lower measures of cancellous and cortical bone quantity. Interestingly, these decreases in bone quantity did not correlated with decreases in biomechanical strength, although there were interactions with maternal exercise that effected biomechanical strength. Maternal exercise also decreased the stiffness of cortical bone material. Finally, we showed that neither gestational exposure to bisphenols nor maternal exercise impacted sclerostin expression or mineral apposition rate of the adult offspring.

In the current study, gestational BPA exposure decreased cortical thickness in adult male offspring. Previous studies showed that responses in cortical thickness are dose-dependent, with cortical thickness increasing at 25 $\mu\text{g}/\text{kg}$ bw/day, but decreasing at 250 $\mu\text{g}/\text{kg}$ bw/day [61]. The exposure rate in our study was 200 $\mu\text{g}/\text{kg}$ bw/day, which provides more evidence that higher doses lead to decreases in cortical thickness. These alterations in cortical thickness seen in our study and others is most likely due to interrupted estrogen signaling through $\text{ER}\alpha$, which plays a significant role in periosteal expansion in male mice [174]. In addition, a recent study showed that morphological alterations seen at 13 weeks in the male offspring exposed to BPA during gestation and lactation only were no longer present at 52 weeks [249], implying that the changes could

be reversible with time. This encourages further exploration into the mechanisms behind the morphological alterations seen in younger animals.

In addition to BPA, we were the first to explore the effects of other bisphenol analogs by including BPS exposure. Surprisingly, we found that the negative alterations associated with BPA exposure were not seen in the BPS exposure animals, indicating a significant difference in the effects of these two analogs. This could partially be explained by differences in binding kinetics, recruitment of coregulators, or post-binding gene expression modifications between BPA and BPS when bound to ER α [44]. For example, when BPA bound to ER α it had the capability of recruiting 7 of the 32 coregulators that binding with estradiol could recruit, whereas BPS could recruit 14, implying post-binding gene modification of BPS is more similar to that of estradiol [44]. BPS is also not as strong of a competitor for estrogen binding as BPA [245], and these two key molecular differences together could explain the null effects in BPS exposed offspring.

While gestational exposure to BPA led to significant morphological impairments, they did not correlate with any alterations in material properties or biomechanical strength. While surprising that decreases in quantity do not correlate with decreases in strength, two other studies also showed morphological changes without differences in biomechanical strength after gestational BPA exposure [62,63]. This could partially be due to the way that strength was tested. There are limitations to *in vitro* tests, since they do not exactly recreate the load that a bone would experience *in vivo*. Additionally, the equations used to estimate material properties from bending tests are based off engineering beam theory, which assumes that the beam has standardized geometry.

Because the bone does not have a uniform shape, this can lead to overestimations of certain material properties [86]. We also had the added factor of maternal exercise, which could have confounded the effects of BPA or BPS exposure. There was a significant interaction between maternal exercise and BPA or BPS exposure on work-to-fracture and modulus of toughness, which are both measures of the ability of the bone to absorb energy before deformation or fracture. Maternal exercise increased toughness in BPS and CON animals, but not BPA animals, implying that the presence of BPA could interrupt alterations caused by maternal exercise. Maternal exercise also increased stiffness, but this was regardless of BPA or BPS exposure. The difference in these two measures is most likely because stiffness and toughness of the bone material are controlled by different material properties of the bone [69,88]. Also, the stiffness, or elasticity, and toughness of a material work together to determine a structure's ultimate strength [88]. Here, maternal exercise altered both stiffness and toughness, but there was no significant impact on maximal load sustained before fracture.

We were the first to show an impact of maternal exercise on material properties of the bone in male offspring. One other study showed that maternal exercise significantly decreased the OPG/RANKL ratio [250], an indicator of osteoclast formation and activity [105]. Another showed that moderate maternal resistance exercise resulted in lower cortical BMD of the tibia, regardless of the sex of the offspring [251]. This is in contrast with our study, which showed no morphological effects of maternal exercise. These differences could possibly be explained by animal model, or type or intensity of exercise.

Despite the morphological changes in cortical bone in the BPA-exposed animals, we saw no effect of BPA or BPS exposure on mineral apposition rate or sclerostin

expression. While we have previously shown that loss of ER α signaling from genetic knockout could increase sclerostin expression in aged animals [202], these results would indicate that disruption of ER signaling through exogenous estrogens does not impact sclerostin expression. This could be because the estrogen receptor is still present and functioning, and thus signaling from endogenous estrogens or ligand-independent actions are enough to maintain the effects of estrogen and estrogen receptors on sclerostin expression [163]. The lack of effect on cortical mineral apposition rate was most surprising, considering the significant impairments in cortical thickness. However, the fluorescent labels were not given until around 15 weeks of age, and thus the animals were past skeletal maturity and growth rates had significantly slowed [242]. The decreases in cortical thickness were most likely established at a younger age, during a time of quick growth, and then remained into adulthood.

In conclusion, here we found that gestational exposure to BPA, but not BPS, has significant negative impacts on cortical geometry and trabecular microarchitecture in male adult offspring. We also found that maternal exercise can increase the stiffness of cortical bone material, and that BPA exposure and maternal exercise can interact to affect the toughness of cortical bone material. These results warrant further study, especially given the current exposure rates of BPA in industrialized countries. If these results are shown to translate to humans, it could have significant public health impacts on recommendations during pregnancy.

CHAPTER 6

Gestational exposure to BPA or BPS has minimal effects on skeletal outcomes in adult, female mice

Introduction

Estrogen is one of the most influential hormones in growth and maintenance of the skeleton across the entire lifespan in both males and females [1,2,165,167,168]. Estrogen actions are mediated primarily by estrogen binding with the nuclear estrogen receptor (ER), which is found in two isoforms, ER α and ER β . Bone expresses both ER α and ER β ; however, ER α tends to be more prevalent in cortical bone, whereas ER β is more widely distributed in cancellous bone [15]. Bisphenol-A (BPA) and its analogs, bisphenol-S (BPS) and bisphenol-F (BPF) are endocrine disruptors and selective estrogen receptor modulators (SERMs) found in plastics that can have significant impacts on human health [39,40]. Bisphenols have structural features that allow them to bind with ERs and modify gene expression in a pattern that differs from that resulting from classic estrogen binding [41–43]. However, different analogs appear to have different binding capabilities and anti-estrogenic effects. BPA and BPF can bind with both ER α and ER β , but there is conflicting on whether BPS can bind with both ER α and ER β or just ER α [44,245,246]. There is also evidence that BPA can act as an agonist for ER α , but an antagonist for ER β , depending on how it interacts with the ligand-binding domain [199]. Despite the possible differences in receptor binding, there is evidence that both BPA and BPS can block estrogen binding in competitive assays [245], and that both BPA and BPS can stimulate cellular activity, although BPS binding usually leads to a weaker response than BPA binding [40,245–247]. In addition to direct actions on ERs that interrupt

estrogenic activity, BPA can affect epigenetic programming via DNA methylation or histone modification [46–48] particularly when exposure occurs during gestation [49].

Human studies have associated BPA exposure with several endocrine issues, from low circulating sex hormones and decreased birth weight to metabolic diseases, such as obesity and cardiovascular disease [39]. The most common route of exposure of BPA and BPS in humans is food contamination [53,197,198], but they can also be found in thermal paper, dust, and certain dental and medical equipment [53,197]. BPA exposure is essentially ubiquitous in humans, with BPA being detectable in almost 100% of the blood or urine samples tested [39]. Many industrialized countries, such as the United States, China, Germany, and Australia have high exposure rates, often times above the current tolerable daily intake (TDI) [54]. In addition, the majority of epidemiological studies show that BPA exposure is associated with adverse effects on human health even at intakes below the current TDI [39]. However, despite the known anti-estrogenic effects of BPA and its ubiquitous exposure, little is known about the possible effects that exposure to BPA and its analogs can have on the skeleton.

In humans, few studies have looked at possible relationships between BPA exposure and skeletal health. In adult women, serum or urinary BPA levels are not associated with bone mineral density (BMD) [55–57]. Similarly, in school-aged girls, there was no correlation between urinary BPA levels and height [58]. However, there was a significant negative correlation between maternal urinary BPA levels in the first trimester and offspring BMD at age 10, regardless of sex [248]. No studies have looked at possible links between BPA exposure and fracture incidence. In addition, all of these studies have focused on BPA, so very little is known about other bisphenol analogs. In

animal models, the impact of BPA seems to be dependent on timing of exposure. For example, BPA exposure after ovariectomy (OVX) decreased cancellous BMD more than just OVX alone [59]; however, when given during gestation, almost no studies show any positive or negative effects of BPA [61,62,64]. In one study, female offspring had decreased energy-to-failure at 13 weeks of age, which could not be explained by any morphological differences in the bone [63]. In another, female offspring at 52 weeks of age had decreased whole-bone stiffness, which also could not be explained by morphological changes [249].

Here, we explored the effects of gestational BPA or BPS exposure on skeletal outcomes in adult female offspring. Based on previous literature, we hypothesized that gestational exposure to BPA would minimally impact morphological or biomechanical outcomes in the female offspring. Considering that BPS often has weaker effects than BPA, we also hypothesized that gestational BPS exposure would minimally impact morphological or biomechanical outcomes in female offspring.

Results

For experimental design and methods, see chapter 5. Male animals were sacrificed at 16 weeks of age, and female offspring were sacrificed at 17 weeks of age. Because of the differences in ages, statistical comparisons based on sex would not be valid and were not performed. Thus, males and female offspring will be treated as separate studies, although the experimental design and overall methods were the same for both sexes.

Animal Characteristics

There were no main effects of gestational BPA or BPS exposure or exercise status of the dam on final body weight or body fat percentage between groups. There was a significant interaction between gestational exposure and exercise status on offspring body fat percentage ($p=0.018$), in that exercise decreased body fat percentage only in the BPA exposure group. (Figure 6.1)

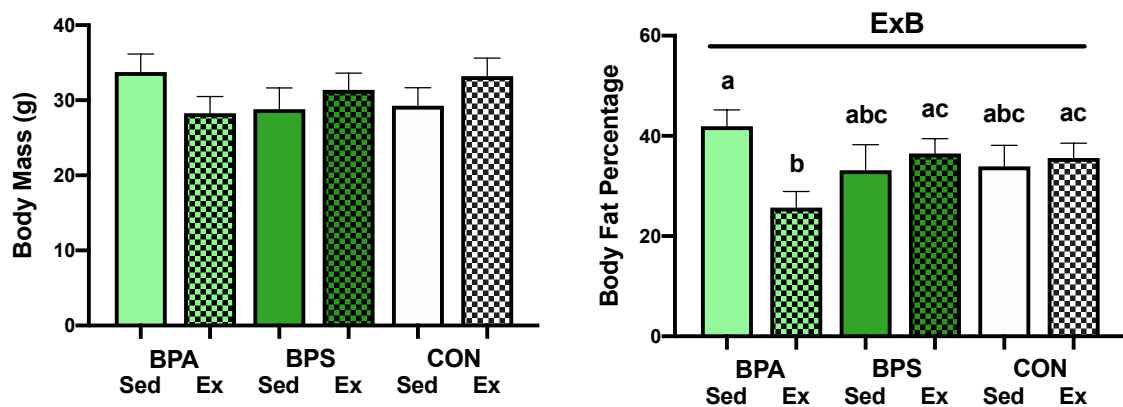


Figure 6.1 Animal Characteristics. Data are means \pm SEM. BPA: gestational bisphenol-A exposure; BPS: gestational bisphenol-S exposure; CON: control; Ex: dam had access to unlocked running wheel; Sed: dam had locked running wheel. B: main effect of gestational bisphenol exposure ($p<0.05$); E: main effect of exercise status ($p<0.05$). Different letters denote significance if a B*E interaction was present.

Femoral Cortical Geometry

There were no main or interactive effects of gestational exposure or exercise status on femur length, total area, marrow area, cortical area, cortical area fraction, cortical thickness, or I_{max}/I_{min} ratio. (**Figure 6.2**)

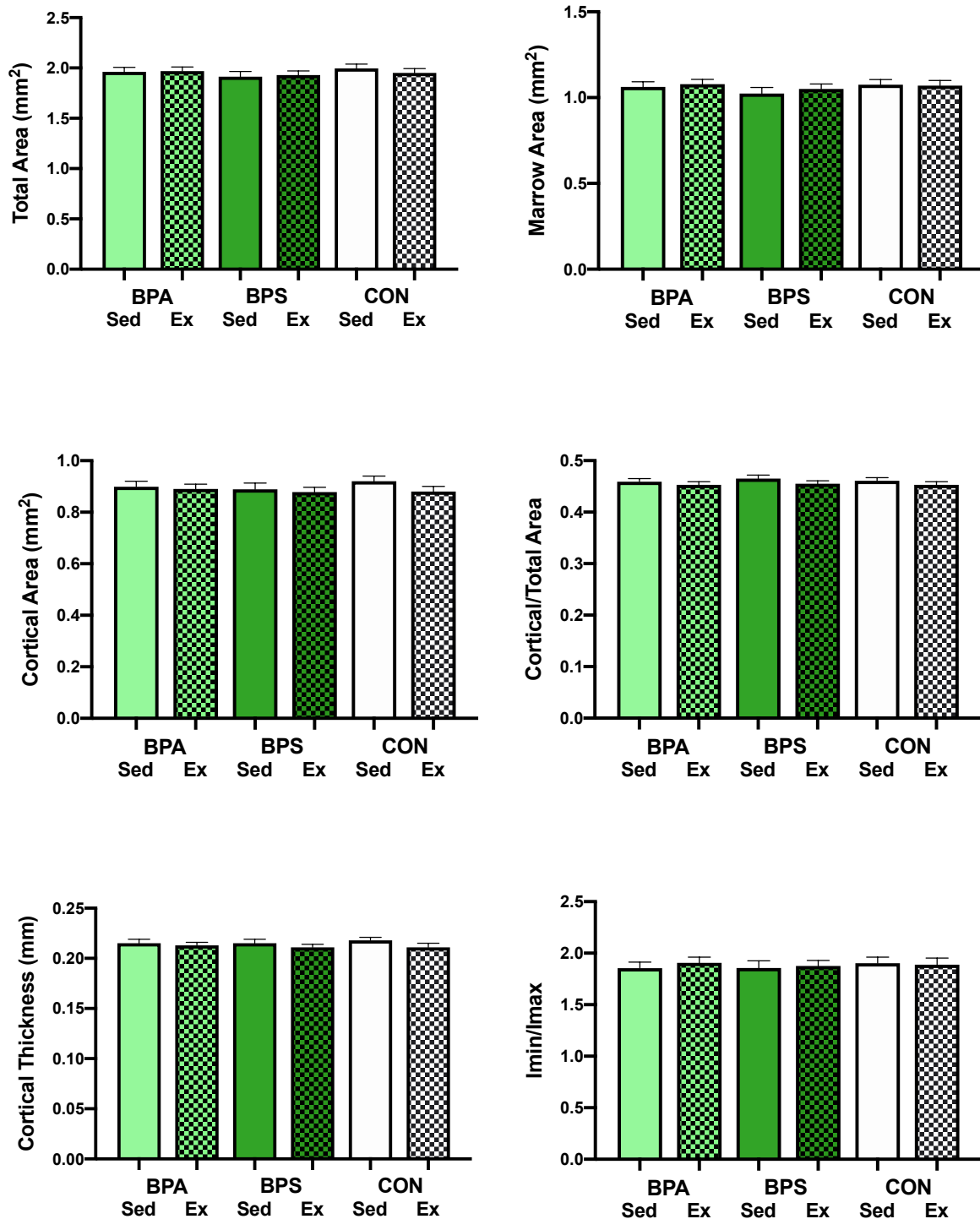


Figure 6.2 Cortical Geometry of the Femur. Data are adjusted means \pm adjusted SEM. BPA: gestational bisphenol-A exposure; BPS: gestational bisphenol-S exposure; CON: control; Ex: dam had access to unlocked running wheel; Sed: dam had locked running

Femoral Biomechanical Strength

There were no main or interactive effects of gestational exposure or exercise status on maximum force, stiffness, young's modulus of elasticity, work-to-fracture, or modulus of toughness. (Figure 6.3)

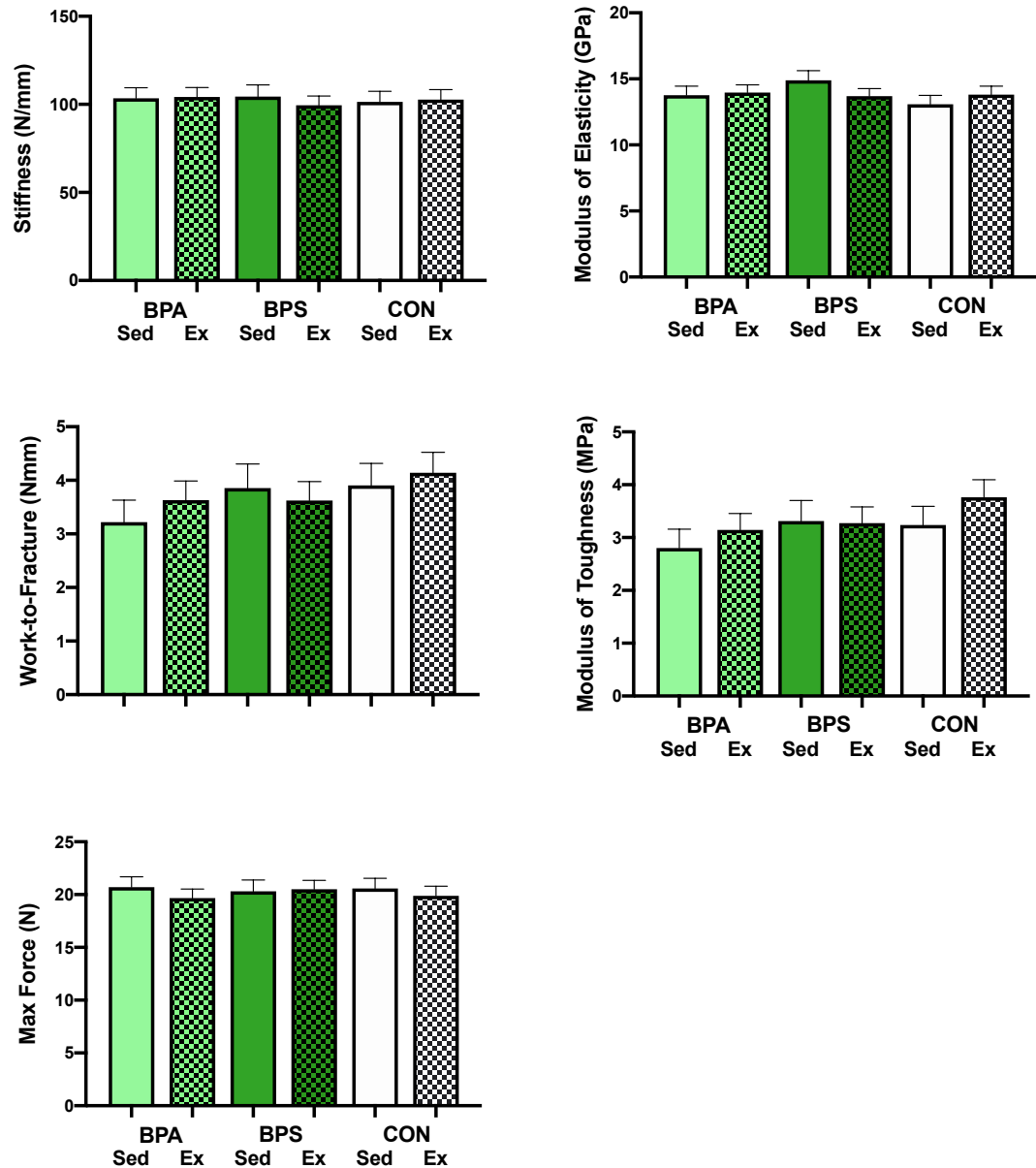


Figure 6.3 Biomechanical Strength of the Femur. Data are adjusted means \pm adjusted SEM. BPA: gestational bisphenol-A exposure; BPS: gestational bisphenol-S exposure; CON: control; Ex: dam had access to unlocked running wheel; Sed: dam had locked running wheel.

Femoral Trabecular Microarchitecture

There were no main effects of gestational exposure or exercise status on bone volume ratio, trabecular thickness, trabecular separation, trabecular number, connectivity density, structural mode index, degree of anisotropy, or ellipsoid factor. There was a significant interaction ($p=0.037$) between gestational exposure and exercise status on ellipsoid factor in that exercise increased ellipsoid factor in the BPA and CON groups, but not the BPS group. **(Figure 6.4)**

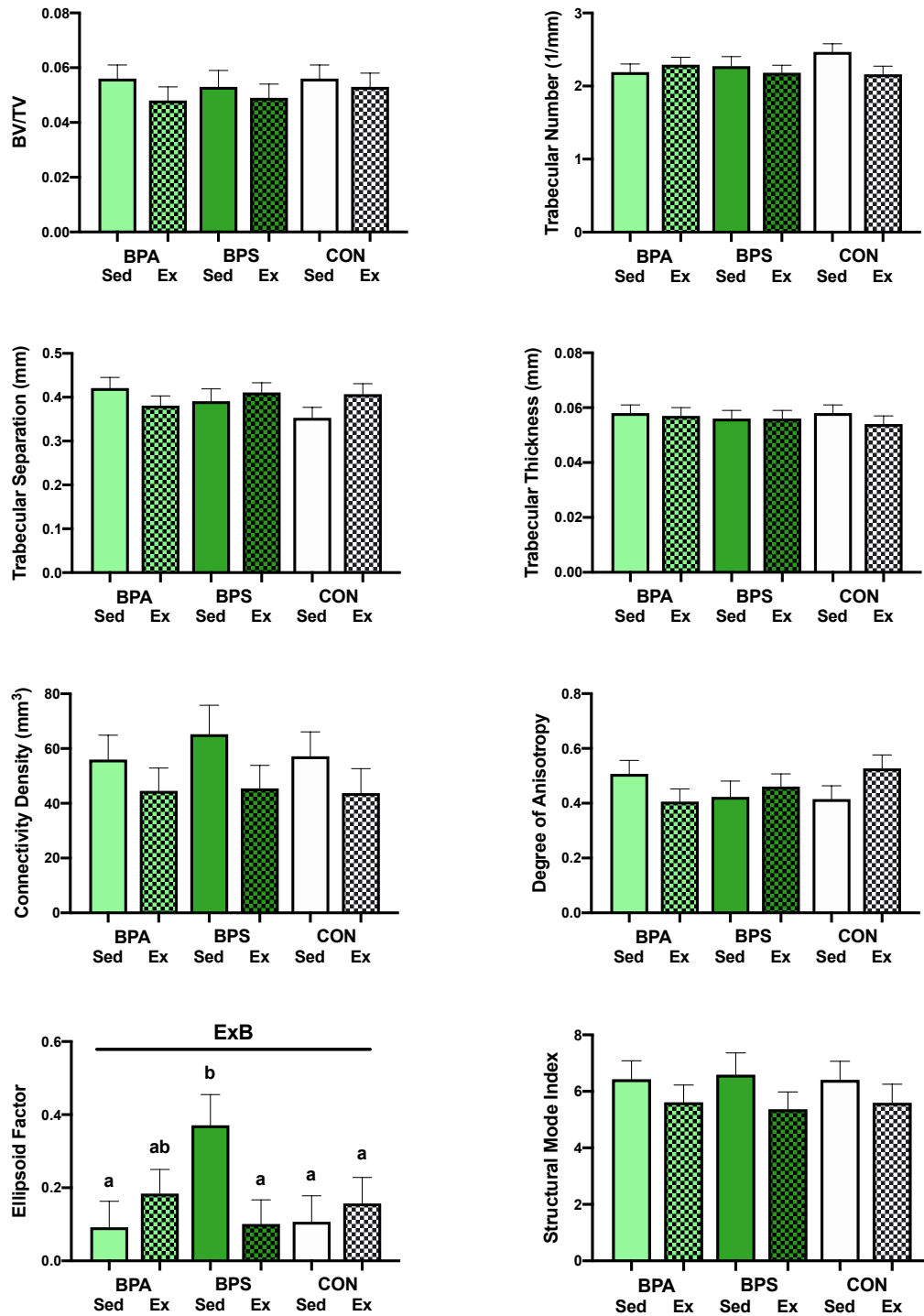


Figure 6.4 Trabecular Microarchitecture of the Femur. Data are means \pm SEM. BPA: gestational bisphenol-A exposure; BPS: gestational bisphenol-S exposure; CON: control; Ex: dam had access to unlocked running wheel; Sed: dam had locked running wheel. B: main effect of gestational bisphenol exposure ($p < 0.05$); E: main effect of exercise status ($p < 0.05$). Different letters denote significance if a B*E interaction was present.

Cortical Osteocyte Sclerostin Expression of the Tibia

There were no main or interactive effects of gestational exposure or exercise status on percent empty lacunae or present sclerostin positive osteocytes of the mid-diaphysis of the tibia. (Figure 6.5)

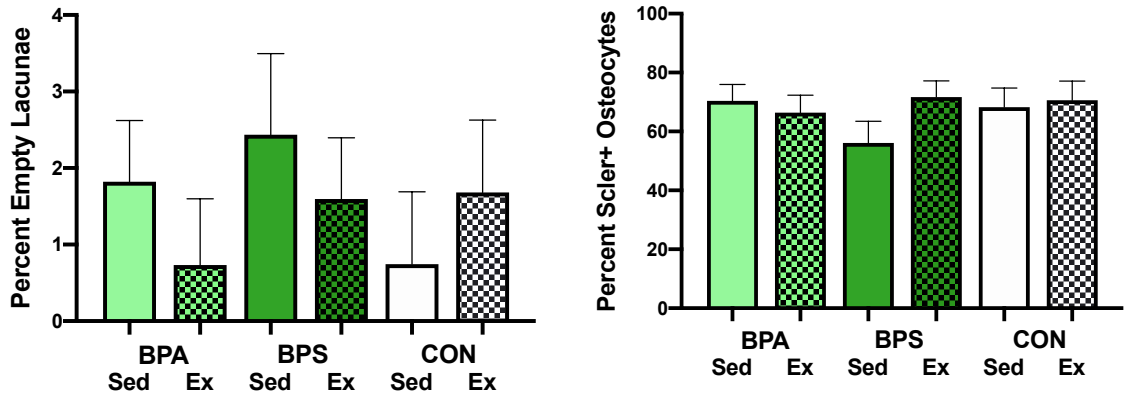


Figure 6.5 Sclerostin Expression of the Tibia. Data are means \pm SEM. BPA: gestational bisphenol-A exposure; BPS: gestational bisphenol-S exposure; CON: control; Ex: dam had access to unlocked running wheel; Sed: dam had locked running wheel.

Dynamic Histomorphometry of the Femur

There were no main or interactive effects of gestational exposure or exercise status on marrow apposition rate of the mid-diaphysis of the femur. (Figure 6.6)

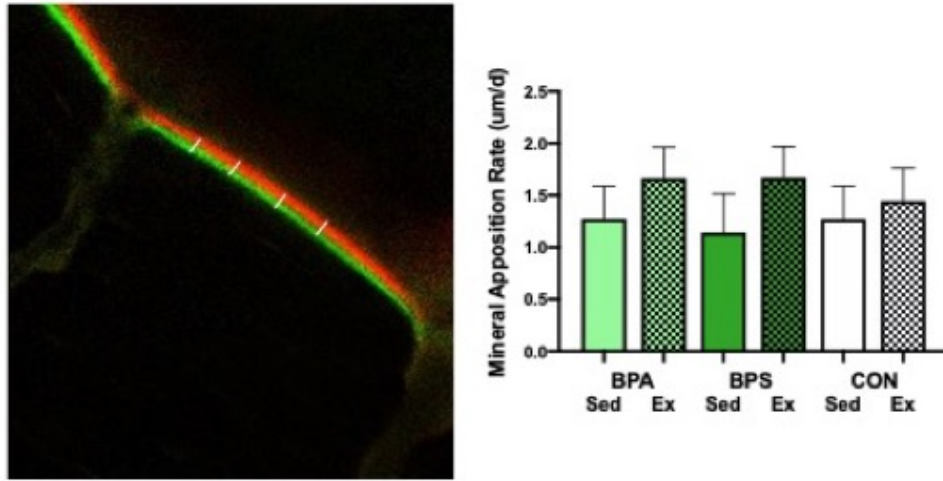


Figure 6.6 Mineral Apposition Rate of the Femur. Data are means \pm SEM. BPA: gestational bisphenol-A exposure; BPS: gestational bisphenol-S exposure; CON: control; Ex: dam had access to unlocked running wheel; Sed: dam had locked running wheel.

Discussion

Here, we showed that gestational exposure to bisphenol-A (BPA) or -S (BPS) had minimal impacts on the skeleton of adult female offspring independent of maternal exercise. There were interactions between gestational exposure and maternal exercise on final body fat percentage and ellipsoid factor of cancellous bone, but no main effects of either experimental treatment on any outcomes.

These minimal impacts of gestational BPA exposure in adult female offspring are supported by previous studies [61–64,249]. However, we were the first to examine gestational exposure to BPS and compare its effects to that of BPA. Considering the often weaker activity of BPS compared to BPA [40,245–247], we hypothesized that BPS would also have minimal effects on the skeleton of the adult female offspring, and that hypothesis was supported by the results of this study. There are a few possible explanations as to why BPA and other bisphenol analogs are not disruptive to the skeleton in female animals, but they remain speculative. For one, alpha-fetoprotein plays a significant role in the female fetal brain to regulate endogenous estrogen exposure during neural development [252]; however, whether that role extends to exogenous estrogens or skeletal development is unknown. In addition, placentas associated with female offspring appear to be more resilient and adaptable to adverse maternal environments than placentas associated with male offspring [253], implying that there could be alterations in gene or protein expression that would protect the female offspring from BPA exposure. Finally, because BPA has a significantly lower binding affinity for the ERs than estradiol [199], it is a possibility that it was out-competed by the high circulating levels of estradiol seen in females. While we saw no main effects of BPA or

BPS exposure on skeletal outcomes, there were some interesting interactions between BPA or BPS and maternal exercise.

Maternal exercise increased ellipsoid factor of the cancellous bone in BPA and CON animals but decreased ellipsoid factor in BPS animals. Ellipsoid factor is a measure of the plate- or rod-like nature of the 3D structure of individual trabeculae [254], which can have direct effects on the material properties of cancellous bone [255,256]. Ellipsoid factor ranges from -1 (purely plate-like) to +1 (purely rod-like). More plate-like trabeculae increases the elasticity of trabecular bone compared to more rod-like structures [256], so results would indicate that exercise decreases the elasticity of the individual trabeculae, except in the presence of BPS. However, we did not have the capacity to measure material properties of cancellous bone, and thus further studies are warranted to explore these possible effects of maternal exercise and the interaction with BPS exposure.

Few other studies have explored the possible impact of maternal exercise on skeletal development in the offspring. One study compared the effects of maternal exercise before pregnancy, during pregnancy, or both on osteogenic gene expression of the femur. In animals that exercised both before and during pregnancy, osteoprotegerin (OPG) increased and receptor activator of nuclear factor- κ B ligand (RANKL) decreased, which significantly decreased the OPG/RANKL ratio [250], an indicator of osteoclast formation and activity [105]. This would indicate a decrease in bone resorption; however, this study only looked at gene expression, and thus it is unknown whether this decrease in bone resorption resulted in more bone mass. Another study showed that moderate maternal resistance exercise during pregnancy resulted in lower cortical, but not cancellous, BMD of the tibia, independent of offspring sex [251]. This is in contrast with

our study, which showed no morphological effects of maternal exercise. These differences could possibly be explained by animal model, since this study was done in rats, or type or intensity of exercise. In conclusion, we showed that skeletal outcomes in adult, female offspring were minimally impacted by gestational BPA or BPS exposure or by maternal exercise, but more studies are warranted to further explore the impact that maternal exercise could have on skeletal outcomes in offspring.

CHAPTER 7

Discussion

The series of studies in this dissertation investigated several unanswered questions related to the effects of estrogen, estrogen receptors, and xenoestrogens on skeletal outcomes. Specifically, we strove to explore the role of estrogen receptor-alpha ($ER\alpha$) on skeletal outcomes in male mice using a global $ER\alpha$ knockout (ERKO) model. We also explored the effects of gestational exposure to the endocrine disruptors bisphenol-A (BPA) and bisphenol-S (BPS) on skeletal outcomes in adult offspring. By focusing on the impact of loss or disruption of estrogen signaling, we furthered our understanding of the importance of estrogen to the skeleton.

We found that loss of $ER\alpha$ led to significant negative impairments in cortical bone mass in both young and aged male animal models, which supports the importance of estrogen and the estrogen receptors in maintaining cortical bone. However, we found that young male mice without $ER\alpha$ could add bone mass after the introduction of voluntary wheel running, implying that $ER\alpha$ is not required for an osteogenic response to exercise in male animal models. In addition, we found that $ER\alpha$ does not appear to be regulate sclerostin expression in the osteocyte in young male mice, regardless of exercise status, but it can regulate sclerostin expression in aged, sedentary male mice. Finally, we found that interruption of estrogen signaling through gestational BPA, but not BPS, exposure negatively impacted both cortical geometry and trabecular microarchitecture in male, but not female, mice. Most surprisingly, we also found that maternal exercise could alter certain material properties of both cortical and trabecular bone in adult offspring.

(Figure 7.1)

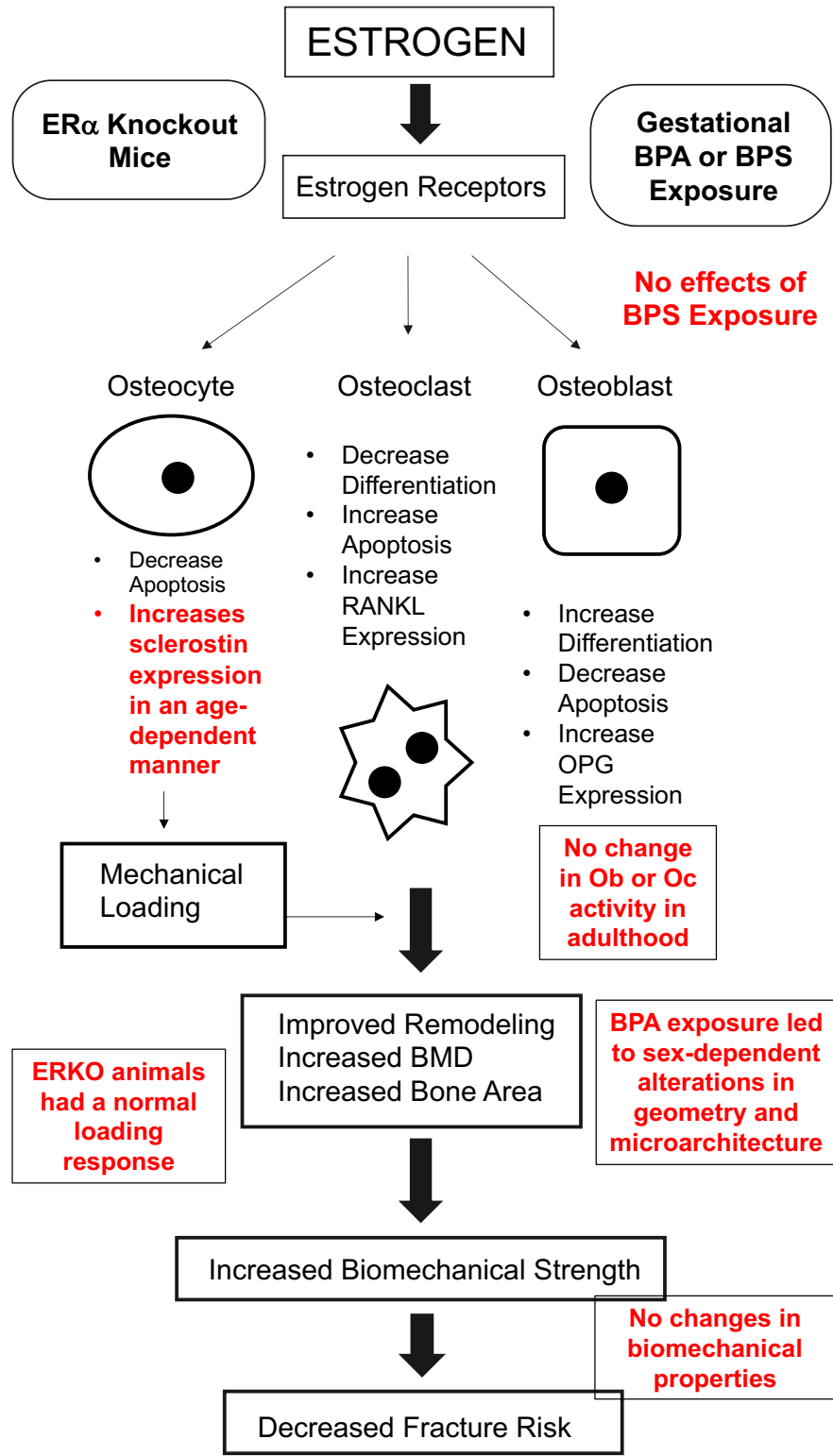


Figure 7.1 Overview of Findings

Novel understandings of ER α

ER α has a regulatory role for sclerostin expression in aged mice

In chapter 3, we focused on aged, sedentary male mice and the effects of global ER α knockout (ERKO). We found that ERKO negatively impacted femoral cortical geometry, specifically decreasing cortical area and cortical thickness. We also found that ERKO improved both femoral and vertebral trabecular microarchitecture, specifically increasing bone volume fraction, trabecular number, and connectivity density, and decreasing trabecular separation. These morphological changes are supported by previous studies, and can be partially attributed to the many actions of estrogen and the estrogen receptors on bone cells [4,18,21,22]. However, we were the first to explore in this model another possible cellular action of estrogen – regulation of sclerostin expression in the osteocyte. We found that aged, sedentary ERKO animals had higher sclerostin expression in cortical bone of the femur but could not detect sclerostin in the vertebrae. Finally, we found that ERKO had no effect on the mineral composition of the bone.

Estrogen is one of the most influential hormones on bone mass in both men and women across the entire lifespan, but until recently the majority of the research focused on women and postmenopausal bone loss [1–3]. Recent studies show that males also lose bone mass over time due to estrogen loss, and that many of estrogen's actions on bone cells are conserved across sexes [1,4,124]. However, some of the cellular actions of estrogen are still unknown in men and have not yet been investigated in male animal models. Here, we showed that ER α has a regulatory role in the expression of sclerostin, a known inhibitor of bone growth [33], in cortical bone in aged male rodent models. This could help explain some of the age-related bone loss in male animal models and

encourages further study to evaluate the role of estrogen and sclerostin expression in this age-related decline of bone mass in older individuals. Understanding the full relationship between sclerostin, estrogen, and bone mass in aging would allow us to explore anti-sclerostin pharmaceuticals as a treatment for age-related bone loss in both men and women. Future studies should further investigate this relationship through more mechanistic studies, such as cell-specific knockout models or cell culture experiments.

ER α is not required for exercise adaptations in male mice

We were one of the first to indicate a possible role for ER α in the control of sclerostin expression in aged, male mice. Since exercise downregulates sclerostin expression [159], we wanted to further explore possible interactions between the presence of ER α and exercise. Thus, in chapter 4, we focused on younger ERKO mice, and introduced exercise as a treatment. Consistent with chapter 3 and other previous studies [18,21,22], we found that ERKO negatively altered cortical geometry but improved measures of trabecular microarchitecture. We also found that exercise begun after skeletal maturity improved cortical geometry in both the WT and the ERKO animals, implying that ER α is not required for an osteogenic response in male mice. In most cortical bone outcomes, such as cortical area and cortical thickness, the exercising ERKO animals had equivalent values as the sedentary WT, implying that exercise, even begun after skeletal maturity, could reverse the negative alterations associated with the loss of ER α . This is in contrast to female mouse models, which require ER α for the osteogenic response to exercise [28,239], and thus further studies are warranted to understand the sexual dimorphism of the osteogenic response. In addition to these findings, we found

that sclerostin expression of the tibia was not altered by ERKO, implying that in younger animals, ER α does not play a regulatory role in sclerostin expression. These age-dependent differences could partially be explained by metabolic differences, as the older ERKO animals had higher blood glucose levels, and there is a positive association between blood glucose and circulating sclerostin in humans [33]. But more research is needed to fully understand the possible interactions between ER α , exercise, age, and sclerostin expression.

Regular exercise and physical activity are essential for improving and maintaining bone health, especially as individuals age [128]. However, there is significant evidence that the osteogenic response to exercise is significantly blunted with aging, and that this could partially be associated with decreasing estrogen levels, as well as other cellular dysfunctions associated with aging [257,258]. Several studies show larger improvements in BMD in response to exercise in postmenopausal women undergoing estrogen treatment compared with untreated women [180–182], but this has not been tested in men. We have shown that ER α is not required for the osteogenic response in male mice, which could indicate that estrogen status is less of a factor in the loss of the mechanoadaptive capabilities of bone than in females. Thus, pharmaceutical treatments for women should not be assumed to work in men, and more sex-specific research into pharmaceuticals and other treatments of low bone mass is needed. Understanding the mechanisms behind this sexual dimorphism would allow for better pharmaceutical and lifestyle treatments of low bone mass in men.

Novel understandings of Xenoestrogens

Genetic knockout models are useful for exploring specific mechanisms, but rarely in nature does one find an individual with a full genetic knockout. To explore a more translatable model, we wanted to use a common environmental molecule that could interrupt endocrine signaling. This allows us to study both endocrine mechanisms and the effect that a commonly exposed molecule could have on skeletal health, which could have significant public health implications. Thus, in chapters 5 and 6 we focused on xenoestrogens, or chemicals that possess estrogenic or antiestrogenic abilities that may interfere with endocrine systems [259]. Specifically, we focused on gestational and lactational exposure to bisphenol-A (BPA) and bisphenol-S (BPS). BPA and BPS are known endocrine disruptors and selective estrogen receptor modulators found in plastics and plastic products [39,40]. Individuals are most commonly exposed to BPA and BPS through epoxy resins in canned food or from the molecules leaching into food out of plastic packaging [53,197,198]. We found that gestational exposure to BPA, but not BPS, negatively impacted both cortical geometry and trabecular microarchitecture, but only in the male offspring. There was very minimal impact of BPA or BPS exposure on skeletal outcomes in the female offspring. We also found no impact of BPA or BPS exposure on biomechanical properties of either sex, in spite of the lower measures of cortical and cancellous bone mass. We also found no impact of BPA or BPS exposure on mineral apposition rate or sclerostin expression in the adult offspring of either sex.

The male and female offspring were different ages at sacrifice, so we could not run direct sex comparisons. However, it is worth noting that we only saw negative impacts of BPA exposure in the male animals. There are a few physiological differences that could contribute to this sexual dimorphism in skeletal outcomes, but they remain

speculative. For one, there could be a protective factor produced by the fetus or placenta during female development [64]. Studies have shown that female fetuses and placentas are more adaptable to adverse maternal environments, such as pre-eclampsia or intrauterine growth restriction, than male fetuses, and often have better pregnancy outcomes such as higher gestational age, in these conditions [253]. However, whether this protection applies to other maternal conditions, such as xenoestrogen exposure, is unknown. Male and female fetuses also have distinct epigenetic patterning during development [260], and it is possible that male epigenetic programming is more susceptible to the epigenetic alterations of BPA. Finally, because BPA has a significantly lower binding affinity for the ERs than estradiol [199], it could be out-competed by endogenous estrogens. Since females have higher endogenous estrogen levels in general, there would be more opportunity for competition. **(Figure 7.2)**

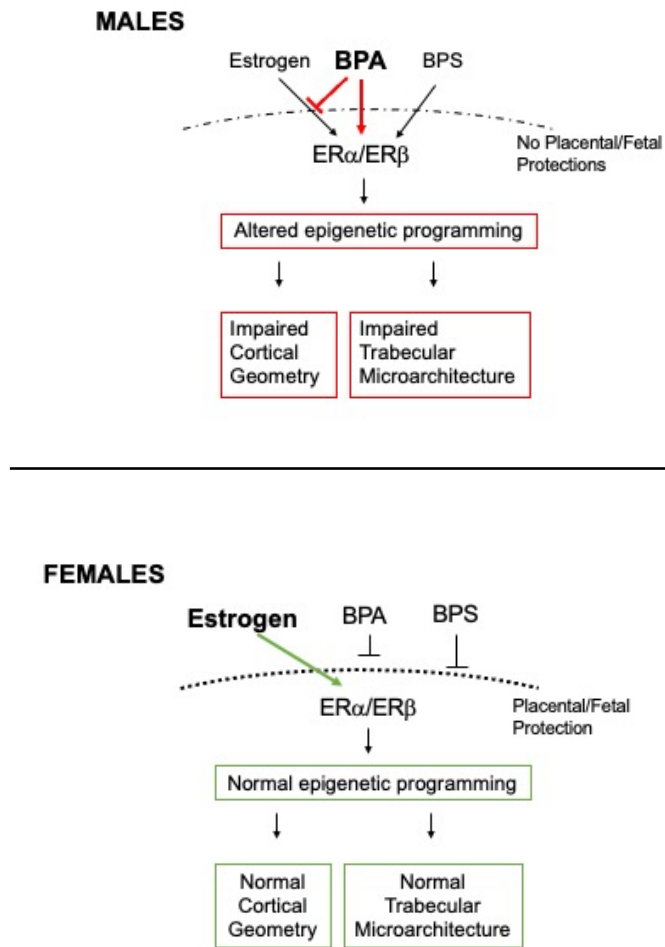


Figure 7.2 Sexual dimorphism in gestational BPA and BPS exposure

Interestingly, we only saw negative effects of BPA exposure and not BPS, which would imply different mechanisms of action between these two analogs in the skeleton based on differing chemical structures (**Figure 7.3**). Results from cell culture models vary based on model used – in MELN cells, BPA and BPS showed similar binding affinity and estrogenic activities [261], but in yeast cells and MCF-7 BPS had significantly lower estrogenic activity than BPA [245,262]. In another cell culture study using MCF-7 breast cancer cell lines, BPA and BPS were shown to have differential gene

modifications after binding with ER α , and BPS gene modification was more similar to standard gene modification seen after binding with estradiol [44]. In another study using competition assays in MCF-7 cells, BPA was shown to be a stronger competitive blocker of estradiol than BPS [245]. Taken together, this could indicate that BPS leads to a weaker, but more estrogenic, response than BPA after ER binding, and this could explain the differential skeletal outcomes between BPA and BPS exposure in our study. However, more research on the molecular kinetics of various bisphenol analogs, particularly in bone cell lines, would help elucidate the mechanisms behind these differences.

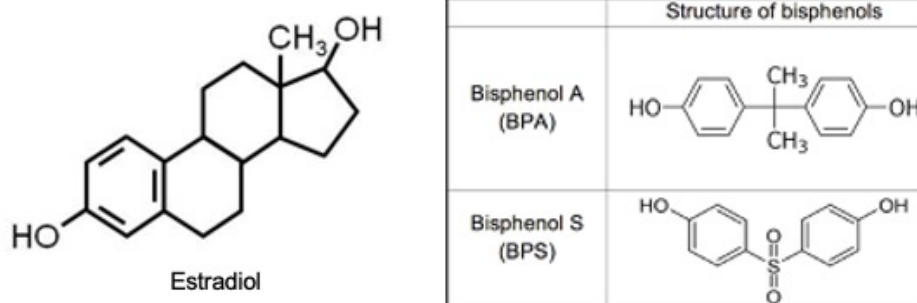


Figure 7.3 Chemical structures of estradiol and bisphenol analogs

While the skeletal differences between the animals exposed to BPA and BPS during gestation have significant implications on the cellular actions of differing bisphenol molecules, the differences between BPA and control animals have significant implications on the actions of estrogen in the skeleton, particularly in males. For one, this supports the importance of estrogen actions in uterine bone development, as BPA was given during gestation. Since BPA exposure continued during lactation, it also supports the importance of estrogen actions in early skeletal development. After weaning, there

was no more exposure to BPA in the offspring, and thus this study also supports the long-term effects of disrupted uterine and early childhood skeletal development, as we saw impairments in adult, skeletally mature mice. Further studies using just gestational or just lactational BPA exposure are warranted to fully understand the specific timing of these significant disruptions.

Maternal exercise can alter bone material properties

Our most surprising finding was the impact of maternal exercise on skeletal outcomes, particularly material properties of the bone in the male offspring. Originally, maternal exercise was introduced to explore metabolic effects on body weight and composition in the offspring. Previous studies indicate that maternal exercise can alter body composition by lowering fat mass in infants [263–265], but the long-term impacts on adult offspring are less known. Here, we found that maternal exercise led to significant decreases in body fat percentage, but not body weight, in adult male offspring. In the female offspring there was an interaction between maternal exercise and gestational BPA or BPS exposure, in that exercise decreased body fat percentage in BPA exposed animals but not BPS or CON animals. This shows that maternal exercise can have long-term impacts on body composition, at least in male offspring, which encourages further study into the mechanisms of these effects. However, we were most surprised by the impacts of maternal exercise on material properties of the bone, specifically stiffness and toughness, in the male offspring. Maternal exercise, regardless of BPA or BPS exposure, increased the stiffness of the bone, and there was an interaction between exercise and BPA or BPS exposure on the toughness of the bone. Interestingly,

although stiffness and toughness were both altered, there was no effect of exercise on maximal load sustained before fracture. Different material properties work together to determine a structure's ultimate strength [88], and in this case the alterations to stiffness and toughness may have compensated for each other in order to maintain bone strength. Much more research is needed to fully understand the impacts of maternal exercise on material properties of the bone.

Few other studies have looked at maternal exercise and skeletal outcomes. In one, maternal exercise significantly decreased the OPG/RANKL ratio in 8 week old offspring [250], an indicator of osteoclast formation and activity [105]. This could lead to higher bone mass through a decrease in bone resorption, but BMD was not measured. Another showed that moderate maternal resistance exercise in rats resulted in lower cortical BMD of the tibia, regardless of the sex of the offspring, and this was associated with higher circulating osteocalcin [251]. We saw no effects of maternal exercise on cortical geometry or trabecular microarchitecture, though the differences could partly be related to type of exercise, running versus resistance training, or animal model used. There is also little research into mechanisms behind these skeletal alterations, although one study in rats showed that maternal exercise increased fetal IGF-1 expression [266]. In addition, exercise is known to alter epigenetic programming of skeletal muscle [267], and there is a possibility that maternal exercise could alter fetal epigenetic programming as well [268], although whether this skeletal outcomes is unknown.

Considering the conflicting results of studies performed to this date and the lack of research into underlying mechanisms, more research into the effects of BPA or BPS exposure and maternal exercise on the skeleton of adult offspring. If these results are

translatable to humans, this would have particular impacts on recommendations during pregnancy. Current guidelines from the American College of Obstetrics and Gynecology (ACOG) recommend 30-60 minutes of moderate physical activity 3-5 days per week for pregnant women [269], but that is primarily based off recommendations for maternal health, such as appropriate weight gain, decreased risk of gestational diabetes, and shorter post-partum recovery time. There is some evidence that exercise during pregnancy can promote appropriate birth weight in the offspring, but research is still ongoing on long-term benefits of maternal exercise on offspring health [270]. In nutrition and food safety recommendations, the ACOG briefly mentions bisphenol A, but not other bisphenol analogs, as something to be avoided, but this is primarily due to an increased risk of miscarriage [271,272]. Again, no recommendations are based on fetal health outcomes. Further research into fetal or offspring health outcomes could expand our knowledge base and lead to more specific recommendations for a healthy mother and child.

Overall, we have significantly added to the scientific literature covering the interactions of estrogen, exercise, and bone health. We found that ER α plays a significant role in the growth and maintenance of cortical bone mass in both young and aged male animal models, which supports the importance of estrogen and the estrogen receptors in male bone. However, we also found that ER α is not required for an osteogenic response to exercise in male animal models, which is in direct contrast to female models, and that exercise could alter the material properties of the bone. However, this does not appear to be related to sclerostin expression in the osteocyte. Finally, we found that exposure to BPA, but not BPS, during gestation and lactation negatively impacted both cortical geometry and trabecular microarchitecture. We also found that maternal exercise could

alter certain material properties of both cortical and trabecular bone, as well as impact body composition, but not body weight, in adult offspring. These studies have significantly contributed to the scientific literature, specifically related to the importance of estrogen and the estrogen receptors to the skeleton and the role of environmental estrogens in skeletal development. They also open up many avenues for further exploration, especially if these results translate to humans, because that could have significant public health impacts on recommendations during pregnancy.

REFERENCES

- [1] S. Khosla, L.J. Melton, B.L. Riggs, Estrogens and Bone Health in Men, *Calcif. Tissue Int.* 69 (2001) 189–192. doi:10.1007/s00223-001-1044-8.
- [2] J.A. Cauley, Estrogen and bone health in men and women, *Steroids.* 99 (2015) 11–15. doi:10.1016/j.steroids.2014.12.010.
- [3] S. Khosla, M.J. Oursler, D.G. Monroe, Estrogen and the skeleton, *Trends Endocrinol. Metab.* 23 (2012) 576–581. doi:10.1016/j.tem.2012.03.008.
- [4] A.B. Khalid, S.A. Krum, Estrogen receptors alpha and beta in bone, *Bone.* 87 (2016) 130–135. doi:10.1016/j.bone.2016.03.016.
- [5] Y.-H. Yang, K. Chen, B. Li, J.-W. Chen, X.-F. Zheng, Y.-R. Wang, S.-D. Jiang, L.-S. Jiang, Estradiol inhibits osteoblast apoptosis via promotion of autophagy through the ER–ERK–mTOR pathway, *Apoptosis.* 18 (2013) 1363–1375. doi:10.1007/s10495-013-0867-x.
- [6] G. Gu, T.A. Hentunen, M. Nars, P.L. Härkönen, H.K. Väänänen, Estrogen protects primary osteocytes against glucocorticoid-induced apoptosis, *Apoptosis.* 10 (2005) 583–595. doi:10.1007/s10495-005-1893-0.
- [7] R. Okazaki, D. Inoue, M. Shibata, M. Saika, S. Kido, H. Ooka, H. Tomiyama, Y. Sakamoto, T. Matsumoto, Estrogen Promotes Early Osteoblast Differentiation and Inhibits Adipocyte Differentiation in Mouse Bone Marrow Stromal Cell Lines that Express Estrogen Receptor (ER) α or β , *Endocrinology.* 143 (2002) 2349–2356. doi:10.1210/endo.143.6.8854.
- [8] T. Kameda, H. Mano, T. Yuasa, Y. Mori, K. Miyazawa, M. Shiokawa, Y. Nakamaru, E. Hiroi, K. Hiura, A. Kameda, N.N. Yang, Y. Hakeda, M. Kumegawa, Estrogen Inhibits Bone Resorption by Directly Inducing Apoptosis of the Bone-resorbing Osteoclasts, *J. Exp. Med.* 186 (1997).
- [9] F. Syed, S. Khosla, Mechanisms of sex steroid effects on bone, *Biochem. Biophys. Res. Commun.* 328 (2005) 688–696. doi:10.1016/j.bbrc.2004.11.097.
- [10] N.K. Shevde, A.C. Bendixen, K.M. Dienger, J.W. Pike, H.F. Deluca, Estrogens suppress RANK ligand-induced osteoclast differentiation via a stromal cell independent mechanism involving c-Jun repression, *PNAS.* 97 (2000) 7829–7834.
- [11] S. Bord, D.. Ireland, S.. Beavan, J.. Compston, The effects of estrogen on osteoprotegerin, RANKL, and estrogen receptor expression in human osteoblasts, *Bone.* 32 (2003) 136–141. doi:10.1016/S8756-3282(02)00953-5.
- [12] B.F. Boyce, L. Xing, Functions of RANKL/RANK/OPG in bone modeling and

remodeling, *Arch. Biochem. Biophys.* 473 (2008) 139–146.
doi:10.1016/J.ABB.2008.03.018.


- [13] G.L. Galea, J.S. Price, L.E. Lanyon, Estrogen receptors' roles in the control of mechanically adaptive bone (re)modeling, *Bonekey Rep.* 2 (2013).
doi:10.1038/bonekey.2013.147.
- [14] J. Klein-Nulend, R.F.M. Van Oers, A.D. Bakker, R.G. Bacabac, Bone cell mechanosensitivity, estrogen deficiency, and osteoporosis, *J. Biomech.* 48 (2015) 855–865. doi:10.1016/j.jbiomech.2014.12.007.
- [15] Y. Onoe, C. Miyaura, H. Ohta, S. Nozawa, T. Suda, Expression of Estrogen Receptor β in Rat Bone, *Endocrinology.* 138 (1997) 4509–4512.
doi:10.1210/endo.138.10.5575.
- [16] V. Parikka, Z. Peng, T. Hentunen, J. Risteli, T. Elo, H.K. Väänänen, P. Härkönen, Estrogen responsiveness of bone formation in vitro and altered bone phenotype in aged estrogen receptor- α -deficient male and female mice, *Eur. J. Endocrinol.* 152 (2005) 301–314. doi:10.1530/eje.1.01832.
- [17] L. Vandenput, A.G.H. Ederveen, R.G. Erben, K. Stahr, J. V. Swinnen, E. Van Herck, A. Verstuyf, S. Boonen, R. Bouillon, D. Vanderschueren, Testosterone Prevents Orchidectomy-Induced Bone Loss in Estrogen Receptor- α Knockout Mice, *Biochem. Biophys. Res. Commun.* 285 (2001) 70–76.
doi:10.1006/bbrc.2001.5101.
- [18] O. Vidal, M.K. Lindberg, K. Hollberg, D.J. Baylink, G. Andersson, D.B. Lubahn, S. Mohan, J.A. Gustafsson, C. Ohlsson, Estrogen receptor specificity in the regulation of skeletal growth and maturation in male mice., *Proc. Natl. Acad. Sci. U. S. A.* 97 (2000) 5474–9. doi:10.1073/PNAS.97.10.5474.
- [19] S.H. Windahl, G. Andersson, J.-Å. Gustafsson, Elucidation of estrogen receptor function in bone with the use of mouse models, *Trends Endocrinol. Metab.* 13 (2002) 195–200. doi:10.1016/S1043-2760(02)00594-5.
- [20] N.. Sims, S. Dupont, A. Krust, P. Clement-Lacroix, D. Minet, M. Resche-Rigon, M. Gaillard-Kelly, R. Baron, Deletion of estrogen receptors reveals a regulatory role for estrogen receptors- β in bone remodeling in females but not in males, *Bone.* 30 (2002) 18–25. doi:10.1016/S8756-3282(01)00643-3.
- [21] F. Callewaert, K. Venken, J. Ophoff, K. De Gendt, A. Torcasio, G.H. van Lenthe, H. Van Oosterwyck, S. Boonen, R. Bouillon, G. Verhoeven, D. Vanderschueren, Differential regulation of bone and body composition in male mice with combined inactivation of androgen and estrogen receptor- α ., *FASEB J.* 23 (2009) 232–40. doi:10.1096/fj.08-113456.

- [22] M.K. Lindberg, M. Erlandsson, S.L. Alatalo, S. Windahl, G. Andersson, J.M. Halleen, H. Carlsten, J.A. Gustafsson, C. Ohlsson, Estrogen receptor alpha, but not estrogen receptor beta, is involved in the regulation of the OPG/RANKL (osteoprotegerin/receptor activator of NF-kappa B ligand) ratio and serum interleukin-6 in male mice., *J. Endocrinol.* 171 (2001) 425–33. doi:10.1677/JOE.0.1710425.
- [23] L. Vico, J.-M. Vanacker, Sex hormones and their receptors in bone homeostasis: insights from genetically modified mouse models, *Osteoporos. Int.* 21 (2010) 365–372. doi:10.1007/s00198-009-0963-5.
- [24] G.L. Galea, L.B. Meakin, T. Sugiyama, N. Zebda, A. Sunters, H. Taipaleenmaki, G.S. Stein, A.J. Van Wijnen, L.E. Lanyon, J.S. Price, Estrogen Receptor-alpha Mediates Proliferation of Osteoblastic Cells Stimulated by Estrogen and Mechanical Strain, but Their Acute Down-regulation of the Wnt Antagonist Sost Is Mediated by Estrogen Receptor -Beta, *J. Biol. Chem.* 288 (2013) 9035–9048. doi:10.1074/jbc.M112.405456.
- [25] V.J. Armstrong, M. Muzylak, A. Sunters, G. Zaman, L.K. Saxon, J.S. Price, L.E. Lanyon, Wnt/Beta-Catenin Signaling Is a Component of Osteoblastic Bone Cell Early Responses to Load-bearing and Requires Estrogen Receptor-alpha, *J. Biol. Chem.* 282 (2007) 20715–20727. doi:10.1074/jbc.M703224200.
- [26] H.L. Jessop, M. Sjöberg, M.Z. Cheng, G. Zaman, C.P.D. Wheeler-Jones, L.E. Lanyon, Mechanical Strain and Estrogen Activate Estrogen Receptor α in Bone Cells, *J. Bone Miner. Res.* 16 (2001) 1045–1055. doi:10.1359/jbmr.2001.16.6.1045.
- [27] K.C.L. Lee, H. Jessop, R. Suswillo, G. Zaman, L.E. Lanyon, The adaptive response of bone to mechanical loading in female transgenic mice is deficient in the absence of oestrogen receptor-a and -B, *J. Endocrinol.* 182 (2004) 193–201. <http://www.endocrinology.org> (accessed May 28, 2020).
- [28] L.K. Saxon, G. Galea, L. Meakin, J. Price, L.E. Lanyon, Estrogen Receptors Alpha and Beta Have Different Gender-Dependent Effects on the Adaptive Responses to Load Bearing in Cancellous and Cortical Bone, *Endocrinology.* 153 (2012) 2254–2266. doi:10.1210/en.2011-1977.
- [29] K.M. Melville, N.H. Kelly, G. Surita, D.B. Buchalter, J.C. Schimenti, R.P. Main, F.P. Ross, M.C. van der Meulen, Effects of Deletion of ER α in Osteoblast-Lineage Cells on Bone Mass and Adaptation to Mechanical Loading Differ in Female and Male Mice, *J. Bone Miner. Res.* 30 (2015) 1468–1480. doi:10.1002/jbmr.2488.
- [30] F. Callewaert, M. Sinnesael, E. Gielen, S. Boonen, D. Vanderschueren, Skeletal sexual dimorphism: Relative contribution of sex steroids, GH-IGF1, and mechanical loading, *J. Endocrinol.* 207 (2010) 127–134. doi:10.1677/JOE-10-

0209.

- [31] U.H. Lerner, C. Ohlsson, The WNT system : background and its role in bone, *J. Intern. Med.* 277 (2015) 630–649. doi:10.1111/joim.12368.
- [32] T.A. Burgers, B.O. Williams, L.F. Bonewald, M.E. Johnson, M. Kneissel, Regulation of Wnt/ β -catenin signaling within and from osteocytes, *Bone*. 54 (2013) 244–249. doi:10.1016/j.bone.2013.02.022.
- [33] J. Delgado-Calle, A.Y. Sato, T. Bellido, Role and mechanism of action of sclerostin in bone, *Bone*. 96 (2017) 29–37. doi:10.1016/j.bone.2016.10.007.
- [34] U. IL Mödder, J.A. Clowes, K. Hoey, J.M. Peterson, L. McCready, M.J. Oursler, B.L. Riggs, S. Khosla, Regulation of circulating sclerostin levels by sex steroids in women and in men, *J. Bone Miner. Res.* 26 (2011) 27–34. doi:10.1002/jbmr.128.
- [35] K. Fujita, M.M. Roforth, S. Demaray, U. Mcgregor, S. Kirmani, L.K. Mccready, J.M. Peterson, M.T. Drake, D.G. Monroe, S. Khosla, Effects of Estrogen on Bone mRNA Levels of Sclerostin and Other Genes Relevant to Bone Metabolism in Postmenopausal Women, *J. Clin. Endocrinol. Metab.* 99 (2014) E81–E88. doi:10.1210/jc.2013-3249.
- [36] J. Delgado-Calle, C. Sañudo, A. Bolado, A.F. Fernández, J. Arozamena, M.A. Pascual-Carra, J.C. Rodriguez-Rey, M.F. Fraga, L. Bonewald, J.A. Riancho, DNA methylation contributes to the regulation of sclerostin expression in human osteocytes, *J. Bone Miner. Res.* 27 (2012) 926–937. doi:10.1002/jbmr.1491.
- [37] B.-J. Kim, S.J. Bae, S.-Y. Lee, Y.-S. Lee, J.-E. Baek, S.-Y. Park, S.H. Lee, J.-M. Koh, G.S. Kim, TNF-alpha mediates the stimulation of sclerostin expression in an estrogen-deficient condition, *Biochem. Biophys. Res. Commun.* 424 (2012) 170–175. doi:10.1016/j.bbrc.2012.06.100.
- [38] H.B. Jia, J.X. Ma, X.L. Ma, J.T. Yu, R. Feng, L.Y. Xu, J. Wang, D. Xing, S.W. Zhu, Y. Wang, Estrogen alone or in combination with parathyroid hormone can decrease vertebral MEF2 and sclerostin expression and increase vertebral bone mass in ovariectomized rats, *Osteoporos. Int.* 25 (2014) 2743–2754. doi:10.1007/s00198-014-2818-y.
- [39] J.R. Rochester, Bisphenol A and human health: A review of the literature, *Reprod. Toxicol.* 42 (2013) 132–155. doi:10.1016/J.REPROTOX.2013.08.008.
- [40] J.R. Rochester, A.L. Bolden, Bisphenol S and F: A systematic review and comparison of the hormonal activity of bisphenol a substitutes, *Environ. Health Perspect.* 123 (2015) 643–650. doi:10.1289/ehp.1408989.
- [41] Y.B. Wetherill, B.T. Akingbemi, J. Kanno, J.A. McLachlan, A. Nadal, C.

- Sonnenschein, C.S. Watson, R.T. Zoeller, S.M. Belcher, In vitro molecular mechanisms of bisphenol A action, *Reprod. Toxicol.* 24 (2007) 178–198. doi:10.1016/J.REPROTOX.2007.05.010.
- [42] E.J. Routledge, R. White, M.G. Parker, J.P. Sumpter, Differential effects of xenoestrogens on coactivator recruitment by estrogen receptor (ER) alpha and ERbeta., *J. Biol. Chem.* 275 (2000) 35986–93. doi:10.1074/jbc.M006777200.
- [43] P. Diel, T. Schulz, K. Smolnikar, E. Strunck, G. Vollmer, H. Michna, Ability of xeno- and phytoestrogens to modulate expression of estrogen-sensitive genes in rat uterus: estrogenicity profiles and uterotrophic activity, *J. Steroid Biochem. Mol. Biol.* 73 (2000) 1–10. doi:10.1016/S0960-0760(00)00051-0.
- [44] Y. Li, L. Perera, L.A. Coons, K.A. Burns, J.T. Ramsey, K.E. Pelch, R. Houtman, R. Van Beuningen, C.T. Teng, K.S. Korach, Differential in Vitro Biological Action, Coregulator Interactions, and Molecular Dynamic Analysis of Bisphenol A (BPA), BPAF, and BPS Ligand-ERα Complexes, *Environ. Health Perspect.* (2018) 1–16. doi:10.1289/EHP2505.
- [45] H.D. Morgan, H.G.E. Sutherland, D.I.K. Martin, E. Whitelaw, Epigenetic inheritance at the agouti locus in the mouse, *Nat. Genet.* 23 (1999) 314–318. doi:10.1038/15490.
- [46] D.C. Dolinoy, D. Huang, R.L. Jirtle, Maternal nutrient supplementation counteracts bisphenol A-induced DNA hypomethylation in early development, *PNAS.* 104 (2007) 13056–13061. www.pnas.orgcgidoi10.1073pnas.0703739104 (accessed November 26, 2018).
- [47] T. Yaoi, K. Itoh, K. Nakamura, H. Ogi, Y. Fujiwara, S. Fushiki, Genome-wide analysis of epigenomic alterations in fetal mouse forebrain after exposure to low doses of bisphenol A, *Biochem. Biophys. Res. Commun.* 376 (2008) 563–567. doi:10.1016/J.BBRC.2008.09.028.
- [48] L.F. Doherty, J.G. Bromer, Y. Zhou, T.S. Aldad, H.S. Taylor, In Utero Exposure to Diethylstilbestrol (DES) or Bisphenol-A (BPA) Increases EZH2 Expression in the Mammary Gland: An Epigenetic Mechanism Linking Endocrine Disruptors to Breast Cancer, *Horm. Cancer.* 1 (2010) 146–155. doi:10.1007/s12672-010-0015-9.
- [49] M. Kundakovic, F.A. Champagne, Epigenetic perspective on the developmental effects of bisphenol A, *Brain Behav. Immun.* 25 (2011) 1084–1093. doi:10.1016/j.bbi.2011.02.005.
- [50] T. Corbel, V. Gayrard, S. Puel, M.Z. Lacroix, A. Berrebi, S. Gil, C. Viguié, P.-L. Toutain, N. Picard-Hagen, Bidirectional placental transfer of Bisphenol A and its main metabolite, Bisphenol A-Glucuronide, in the isolated perfused human placenta, *Reprod. Toxicol.* 47 (2014) 51–58. doi:10.1016/j.reprotox.2014.06.001.

- [51] T.J. Mørck, G. Sorda, N. Bechi, B.S. Rasmussen, J.B. Nielsen, F. Ietta, E. Rytting, L. Mathiesen, L. Paulesu, L.E. Knudsen, Placental transport and in vitro effects of Bisphenol A, *Reprod. Toxicol.* 30 (2010) 131–137. doi:10.1016/j.reprotox.2010.02.007.
- [52] B. Balakrishnan, K. Henare, E.B. Thorstensen, A.P. Ponnampalam, M.D. Mitchell, Transfer of bisphenol A across the human placenta, *Am. J. Obstet. Gynecol.* 202 (2010) 393.e1-393.e7. doi:10.1016/j.ajog.2010.01.025.
- [53] T. Geens, D. Aerts, C. Berthot, J.-P. Bourguignon, L. Goeyens, P. Lecomte, G. Maghuin-Rogister, A.-M. Pironnet, L. Pussemier, M.-L. Scippo, J. Van Loco, A. Covaci, A review of dietary and non-dietary exposure to bisphenol-A, *Food Chem. Toxicol.* 50 (2012) 3725–3740. doi:10.1016/J.FCT.2012.07.059.
- [54] R. Huang, Z. Liu, S. Yuan, H. Yin, Z. Dang, P. Wu, Worldwide human daily intakes of bisphenol A (BPA) estimated from global urinary concentration data (2000–2016) and its risk analysis, *Environ. Pollut.* 230 (2017) 143–152. doi:10.1016/j.envpol.2017.06.026.
- [55] D.H. Kim, C.H. Oh, Y.-C. Hwang, I.-K. Jeong, K.J. Ahn, H.-Y. Chung, J.-S. Chang, Serum Bisphenol A Concentration in Postmenopausal Women with Osteoporosis  DH Kim, et al Serum Bisphenol A Concentration in Postmenopausal Women with Osteoporosis, *J. Bone Metab.* 19 (2012) 87–93. doi:10.11005/jbm.2012.19.2.87.
- [56] H.-Y. Zhao, Y.-F. Bi, L.-Y. Ma, L. Zhao, T.-G. Wang, L.-Z. Zhang, B. Tao, L.-H. Sun, Y.-J. Zhao, W.-Q. Wang, X.-Y. Li, M.-Y. Xu, J.-L. Chen, G. Ning, J.-M. Liu, The effects of bisphenol A (BPA) exposure on fat mass and serum leptin concentrations have no impact on bone mineral densities in non-obese premenopausal women, *Clin. Biochem.* 45 (2012) 1602–1606. doi:10.1016/j.clinbiochem.2012.08.024.
- [57] J. Vitku, L. Kolatorova, L. Franekova, J. Blahos, M. Simkova, M. Duskova, T. Skodova, L. Starka, J. Vitku-Kubatova, Endocrine Disruptors of the Bisphenol and Paraben Families and Bone Metabolism, *Physiol. Res.* 67 (2018) 455–464. doi:10.33549/physiolres.934005.
- [58] Z. Wang, H. Liang, X. Tu, W. Yuan, Z. Zhou, L. Jin, M. Miao, D.-K. Li, Bisphenol A and pubertal height growth in school-aged children, *J. Expo. Sci. Environ. Epidemiol.* (2018). doi:10.1038/s41370-018-0063-8.
- [59] D. Seidlová-Wuttke, H. Jarry, W. Wuttke, Pure estrogenic effect of benzophenone-2 (BP2) but not of bisphenol A (BPA) and dibutylphtalate (DBP) in uterus, vagina and bone, *Toxicology.* 205 (2004) 103–112. doi:10.1016/J.TOX.2004.06.042.
- [60] K. Toda, C. Miyaura, T. Okada, Y. Shizuta, Dietary bisphenol A prevents ovarian

- degeneration and bone loss in female mice lacking the aromatase gene (*Cyp19*), Eur. J. Biochem. 269 (2002) 2214–2222. doi:10.1046/j.1432-1033.2002.02879.x.
- [61] M.H. Lejonklou, S. Christiansen, J. Örberg, L. Shen, S. Larsson, J. Boberg, U. Hass, P.M. Lind, Low-dose developmental exposure to bisphenol A alters the femoral bone geometry in wistar rats, Chemosphere. 164 (2016) 339–346. doi:10.1016/J.CHEMOSPHERE.2016.08.114.
- [62] T. Lind, M.H. Lejonklou, L. Dunder, A. Rasmusson, S. Larsson, H. Melhus, P.M. Lind, Low-dose developmental exposure to bisphenol A induces sex-specific effects in bone of Fischer 344 rat offspring, Environ. Res. 159 (2017) 61–68. doi:10.1016/J.ENVRES.2017.07.020.
- [63] K.E. Pelch, S.M. Carleton, C.L. Phillips, S.C. Nagel, Developmental Exposure to Xenoestrogens at Low Doses Alters Femur Length and Tensile Strength in Adult Mice, Biol. Reprod. 86 (2012) 1–9. doi:10.1095/biolreprod.111.096545.
- [64] F. Xin, L.M. Smith, M. Susiarjo, M.S. Bartolomei, K.J. Jepsen, Endocrine-disrupting chemicals, epigenetics, and skeletal system dysfunction: exploration of links using bisphenol A as a model system, Environ. Epigenetics. 4 (2018) 1–12. doi:10.1093/eep/dvy002.
- [65] J.K. Hwang, K.H. Min, K.H. Choi, Y.C. Hwang, I.-K. Jeong, K.J. Ahn, H.-Y. Chung, J.S. Chang, Bisphenol A reduces differentiation and stimulates apoptosis of osteoclasts and osteoblasts, Life Sci. 93 (2013) 367–372. doi:10.1016/J.LFS.2013.07.020.
- [66] A. Fic, S. Jurkovic Mlakar, P. Juvan, V. Mlakar, J. Marc, M. Sollner Dolenc, K. Broberg, L. Peterlin Mašič, Genome-wide gene expression profiling of low-dose, long-term exposure of human osteosarcoma cells to bisphenol A and its analogs bisphenols AF and S, Toxicol. Vit. 29 (2015) 1060–1069. doi:10.1016/j.tiv.2015.03.014.
- [67] B. Clarke, Normal bone anatomy and physiology., Clin. J. Am. Soc. Nephrol. 3 Suppl 3 (2008) S131–S139. doi:10.2215/CJN.04151206.
- [68] E.F. Morgan, G.L. Barnes, T.A. Einhorn, The Bone Organ System: Form and Function, in: Osteoporosis, 2013: pp. 3–20. https://books.google.com/books?hl=en&lr=&id=dNrY--qA9d0C&oi=fnd&pg=PA1&dq=The+Bone+Organ+System:+Form+and+Function+Morgan+EF&ots=5MHpTFic2n&sig=3l-Wr2RVlmq0DeYQ_7Zr6qcCe0M#v=onepage&q&f=false (accessed January 3, 2017).
- [69] Y. Bala, • E Seeman, Bone’s Material Constituents and their Contribution to Bone Strength in Health, Disease, and Treatment, Calcif. Tissue Int. 97 (2015) 308–326.

doi:10.1007/s00223-015-9971-y.

- [70] R. Florencio-Silva, G.R.D.S. Sasso, E. Sasso-Cerri, M.J. Simões, P.S. Cerri, G. Rodrigues Da, S. Sasso, E. Sasso-Cerri, M.J. Simões, P.S. Cerri, *Biology of Bone Tissue: Structure, Function, and Factors That Influence Bone Cells*, *Biomed Res. Int.* 2015 (2015) 1–17. doi:10.1155/2015/421746.
- [71] B. Langdahl, S. Ferrari, D.W. Dempster, *Bone modeling and remodeling: potential as therapeutic targets for the treatment of osteoporosis*, *Ther. Adv. Musculoskelet. Dis.* 8 (2016) 225–235. doi:10.1177/1759720X16670154.
- [72] R.D. Prisby, *Mechanical, hormonal, and metabolic influences on blood vessels, blood flow and bone*, *J. Endocrinol.* 235 (2017) R77–R100. doi:10.1530/JOE-16-0666.
- [73] R.E. Tomlinson, M.J. Silva, *Skeletal Blood Flow in Bone Repair and Maintenance*, *Bone Res.* 1 (2013) 311–322. doi:10.4248/BR201304002.
- [74] R.A. Nissenson, *Parathyroid Hormone and Parathyroid Hormone-Related Protein*, in: *Osteoporosis*, 2013: pp. 259–281. doi:10.1016/B978-0-12-415853-5.00012-1.
- [75] M. Zaidi, A.. Inzerillo, B.. Moonga, P.J.. Bevis, C.L.-H. Huang, *Forty years of calcitonin—where are we now? A tribute to the work of Iain Macintyre, FRS*, *Bone.* 30 (2002) 655–663. doi:10.1016/S8756-3282(02)00688-9.
- [76] E. Mrak, F. Guidobono, G. Moro, G. Fraschini, A. Rubinacci, I. Villa, *Calcitonin gene-related peptide (CGRP) inhibits apoptosis in human osteoblasts by β -catenin stabilization*, *J. Cell. Physiol.* 225 (2010) 701–708. doi:10.1002/jcp.22266.
- [77] F.J.A. de Paula, C.J. Rosen, *Bone Remodeling and Energy Metabolism: New Perspectives*, *Bone Res.* 1 (2013) 72–84. doi:10.4248/BR201301005.
- [78] A. Afghani, E. Barrett-Connor, *Resting Energy Expenditure: A Stronger Marker Than Body Weight for BMD in Caucasian Women But Not Men? The Rancho Bernardo Study*, *Clin J Sport Med.* 19 (2009) 39–45. doi:10.1097/JSM.0b013e318193105f.
- [79] A. Afghani, E. Barrett-Connor, W.J. Wooten, *Resting Energy Expenditure: A Better Marker than BMI for BMD in African-American Women*, *Med. Sci. Sport. Exerc.* 37 (2005) 1203–1210. doi:10.1249/01.mss.0000170080.87526.85.
- [80] R.C. Riddle, T.T.L. Clemens, M. Okabe, A. Graham, D. DiGirolamo, T.T.L. Clemens, S. Kousteni, M. Tatar, A. Bartke, A. Antebi, R. Denver, R. Bonett, G. Boorse, J. Pritchard, A. Martin, V. David, L. Quarles, P. Ducy, E. Hinoi, K. Fulzele, M. Ferron, N. Lee, M. Ferron, M. McKee, R. Levine, P. Ducy, G. Karsenty, J. Wei, R. Farese, G. Karsenty, F. Oury, T. Hahn, S. Westbrook, T.

- Sullivan, W. Goodman, L. Halstead, E. Zoidis, C. Ghirlanda-Keller, C. Schmid, E. Esen, J. Chen, C. Karner, A. Okunade, B. Patterson, F. Long, Insulin, osteoblasts, and energy metabolism: why bone counts calories, *J. Clin. Invest.* 124 (2014) 1465–1467. doi:10.1172/JCI75554.Bone.
- [81] M.L. Zoch, T.L. Clemens, R.C. Riddle, New insights into the biology of osteocalcin, *Bone*. 82 (2016) 42–49. doi:10.1016/j.bone.2015.05.046.
- [82] H. Fonseca, D. Moreira-Goncalves, H.-J.A. Coriolano, J.A. Duarte, Bone quality: The determinants of bone strength and fragility, *Sport. Med.* 44 (2014) 37–53. doi:10.1007/s40279-013-0100-7.
- [83] P. Ammann, A.R. Rizzoli, Bone strength and its determinants, (2003). doi:10.1007/s00198-002-1345-4.
- [84] K.K. Nishiyama, E. Shane, Clinical Imaging of Bone Microarchitecture with HR-pQCT, *Curr. Osteoporos. Rep.* 11 (2013) 147–155. doi:10.1007/s11914-013-0142-7.
- [85] M.L. Bouxsein, S.K. Boyd, B.A. Christiansen, R.E. Guldborg, K.J. Jepsen, R. Müller, Guidelines for assessment of bone microstructure in rodents using micro-computed tomography, *J. Bone Miner. Res.* 25 (2010) 1468–1486. doi:10.1002/jbmr.141.
- [86] K.J. Jepsen, M.J. Silva, D. Vashishth, X.E. Guo, M.C.H. Van Der Meulen, Establishing biomechanical mechanisms in mouse models: Practical guidelines for systematically evaluating phenotypic changes in the diaphyses of long bones, *J. Bone Miner. Res.* 30 (2015) 951–966. doi:10.1002/jbmr.2539.
- [87] A.D.P. Bankoff, Biomechanical Characteristics of the Bone, in: *Hum. Musculoskelet. Biomech.*, 2012. doi:10.5772/19690.
- [88] P. Zioupos, J. Currey, Changes in the Stiffness, Strength, and Toughness of Human Cortical Bone With Age, *Bone*. 22 (1998) 57–66. doi:10.1016/S8756-3282(97)00228-7.
- [89] L. Karim, M.L. Bouxsein, Effect of type 2 diabetes-related non-enzymatic glycation on bone biomechanical properties, *Bone*. 82 (2016) 21–27. doi:10.1016/j.bone.2015.07.028.
- [90] P.J. Thurner, C.G. Chen, S. Ionova-Martin, L. Sun, A. Harman, A. Porter, J.W. Ager, R.O. Ritchie, T. Alliston, Osteopontin deficiency increases bone fragility but preserves bone mass, *Bone*. 46 (2010) 1564–1573. doi:10.1016/J.BONE.2010.02.014.
- [91] C.H. Turner, D.B. Burr, Experimental Techniques for Bone Mechanics, in: *Bone*

Mech., 2001: pp. 7.1-7.35. <https://doc-04-24-docs.googleusercontent.com/docs/securesc/5bsd23h7nijs0o191tafmm7te1qj95pc/qkrv573nk7i06ql51smbun5sj4uhp211/1560981600000/03597488174621737607/07265225710666323276/1wa2m7nwhy2gB7Vo0uVu7SAArC8F6NO1E?nonce=e9c26ime80ukc&user=072652257106663> (accessed June 19, 2019).

- [92] R.M. Radasch, BIOMECHANICS OF BONE AND FRACTURES, *Fract. Manag. Bone Heal.* 29 (1999) 1045–1082. doi:10.1016/S0195-5616(99)50102-2.
- [93] F. Xu, S.L. Teitelbaum, Osteoclasts: New Insights, *Bone Res.* 1 (2013) 11–26. doi:10.4248/BR201301003.
- [94] K. Henriksen, J. Bollerslev, V. Everts, M.A. Karsdal, Osteoclast Activity and Subtypes as a Function of Physiology and Pathology—Implications for Future Treatments of Osteoporosis, *Endocr. Rev.* 32 (2011) 31–63. doi:10.1210/er.2010-0006.
- [95] N.S. Soysa, N. Alles, Osteoclast function and bone-resorbing activity: An overview, *Biochem. Biophys. Res. Commun.* 476 (2016) 115–120. doi:10.1016/J.BBRC.2016.05.019.
- [96] A. Neve, A. Corrado, F.P. Cantatore, Osteoblast physiology in normal and pathological conditions, *Cell Tissue Res.* 343 (2011) 289–302. doi:10.1007/s00441-010-1086-1.
- [97] M. Fakhry, E. Hamade, B. Badran, R. Buchet, D. Magne, Molecular mechanisms of mesenchymal stem cell differentiation towards osteoblasts, *World J. Stem Cells.* 5 (2013) 136–148. doi:10.4252/wjsc.v5.i4.136.
- [98] J.P. van Leeuwen, B. van der Eerden, J. van de Peppel, G.S. Stein, J. Lian, Osteoblast Biology, in: *Osteoporosis, 2013*: pp. 161–207. doi:10.1016/B978-0-12-415853-5.00009-1.
- [99] L.F. Bonewald, Osteocyte Biology, in: *Osteoporosis, 2013*: pp. 209–234. doi:10.1016/B978-0-12-415853-5.00010-8.
- [100] L.F. Bonewald, The amazing osteocyte, *J. Bone Miner. Res.* 26 (2011) 229–238. doi:10.1002/jbmr.320.
- [101] I. Matic, B.G. Matthews, X. Wang, N.A. Dymant, D.L. Worthley, D.W. Rowe, D. Grevic, I. Kalajzic, Quiescent Bone Lining Cells Are a Major Source of Osteoblasts During Adulthood, *Stem Cells.* 34 (2016) 2930–2942. doi:10.1002/stem.2474.
- [102] D.J. Hadjidakis, I.I. Androulakis, Bone remodeling., *Ann. N. Y. Acad. Sci.* 1092 (2006) 385–96. doi:10.1196/annals.1365.035.

- [103] L.G. Raisz, Physiology and Pathophysiology of Bone Remodeling, *Clin. Chem.* 45 (1999) 1353–1358.
<http://clinchem.aaccjnls.org/content/clinchem/45/8/1353.full.pdf> (accessed April 30, 2017).
- [104] J.C. Crockett, M.J. Rogers, F.P. Coxon, L.J. Hocking, M.H. Helfrich, Bone remodelling at a glance, *J. Cell Sci.* 124 (2011) 991–998. doi:10.1242/jcs.063032.
- [105] X. Chen, Z. Wang, N. Duan, G. Zhu, E.M. Schwarz, C. Xie, Osteoblast-Osteoclast Interactions, *Connect Tissue Res.* 59 (2018) 99–107.
doi:10.1080/03008207.2017.1290085.
- [106] K.K. Naylor, R. Eastell, Bone turnover markers: use in osteoporosis, *Nat. Rev. Rheumatol.* 8 (2012) 379–389. doi:10.1038/nrrheum.2012.86.
- [107] K. Jung, M. Lein, Bone turnover markers in serum and urine as diagnostic, prognostic and monitoring biomarkers of bone metastasis, *Biochim. Biophys. Acta.* 1846 (2014) 425–438. doi:10.1016/j.bbcan.2014.09.001.
- [108] D.W. Dempster, J.E. Compston, M.K. Drezner, F.H. Glorieux, J.A. Kanis, H. Malluche, P.J. Meunier, S.M. Ott, R.R. Recker, A.M. Parfitt, Standardized nomenclature, symbols, and units for bone histomorphometry: a 2012 update of the report of the ASBMR Histomorphometry Nomenclature Committee., *J. Bone Miner. Res.* 28 (2013) 2–17. doi:10.1002/jbmr.1805.
- [109] E.J. Mackie, Y.A. Ahmed, L. Tatarczuch, K.-S. Chen, M. Mirams, Endochondral ossification: How cartilage is converted into bone in the developing skeleton, *Int. J. Biochem. Cell Biol.* 40 (2008) 46–62. doi:10.1016/j.biocel.2007.06.009.
- [110] S.H. Ralston, Bone mass through the lifespan, *Women's Heal. Med.* 3 (2006) 145–148. doi:10.1383/WOHM.2006.3.4.145.
- [111] A.D. Berendsen, B.R. Olsen, Bone development, *Bone.* 80 (2015) 14–18.
doi:10.1016/j.bone.2015.04.035.
- [112] M.A. Hill, Musculoskeletal System - Bone Development Timeline, *Embryology.* (2020).
- [113] J. Baron, L. Savendahl, F. De Luca, A. Dauber, M. Phillip, J.M. Wit, O. Nilsson, Short and tall stature: a new paradigm emerges, *Nat. Rev. Endocrinol.* 11 (2015) 735–746. doi:10.1038/nrendo.2015.165.
- [114] K.S. Shim, Pubertal growth and epiphyseal fusion, *Ann Pediatr Endocrinol Metab.* 20 (2015) 8–12. doi:10.6065/apem.2015.20.1.8.
- [115] J.N. Farr, S. Khosla, Skeletal changes through the lifespan-from growth to

senescence, *Nat. Rev. Endocrinol.* 11 (2015) 513–521.
doi:10.1038/nrendo.2015.89.

- [116] O. Nilsson, R. Marino, F. De Luca, M. Phillip, J. Baron, Endocrine Regulation of the Growth Plate, *Horm Res.* 64 (2005) 157–165. doi:10.1159/000088791.
- [117] A. Giustina, G. Mazziotti, E. Canalis, Growth Hormone, Insulin-Like Growth Factors, and the Skeleton, *Endocr. Rev.* 29 (2008) 535–559. doi:10.1210/er.2007-0036.
- [118] M. Weise, S. De-Levi, K.M. Barnes, R.I. Gafni, V. Abad, J. Baron, Effects of estrogen on growth plate senescence and epiphyseal fusion, *Proc. Natl. Acad. Sci. U. S. A.* 98 (2001) 6871–6871. doi:10.1073/pnas.79.24.7734.
- [119] S.E. McCormack, D.L. Cousminer, A. Chesi, J.A. Mitchell, S.M. Roy, H.J. Kalkwarf, J.M. Lappe, Association Between Linear Growth and Bone Accrual in a Diverse Cohort of Children and Adolescents, *JAMA Pediatr.* 171 (2017) 171769. doi:10.1001/jamapediatrics.2017.1769.
- [120] S. Khosla, L.J. Melton III, M.B. Dekutoski, S.J. Achenbach, A.L. Oberg, B.L. Riggs, Incidence of Childhood Distal Forearm Fractures Over 30 Years, *JAMA.* 290 (2003) 1479. doi:10.1001/jama.290.11.1479.
- [121] A.D. Baxter-Jones, R.A. Faulkner, M.R. Forwood, R.L. Mirwald, D.A. Bailey, Bone mineral accrual from 8 to 30 years of age: An estimation of peak bone mass, *J. Bone Miner. Res.* 26 (2011) 1729–1739. doi:10.1002/jbmr.412.
- [122] J. Lu, Y. Shin, M.-S. Yen, S.S. Sun, Peak bone mass and patterns of change in total bone mineral density and bone mineral contents from childhood into young adulthood, *J Clin Densitom.* 19 (2016) 180–191. doi:10.1016/j.jocd.2014.08.001.
- [123] F. Rauch, Bone Growth in Length and Width: The Yin and Yang of Bone Stability, *J Musculoskelet Neuronal Interact.* 3 (2005) 194–201.
[http://publicationslist.org/data/frauch/ref-221/Rauch 2005 growth JMNI.pdf](http://publicationslist.org/data/frauch/ref-221/Rauch%2005%20growth%20JMNI.pdf)
(accessed April 20, 2020).
- [124] D. Vanderschueren, M.R. Laurent, F. Claessens, E. Gielen, M.K. Lagerquist, L. Vandendput, A.E. Börjesson, C. Ohlsson, Sex Steroid Actions in Male Bone, *Endocr. Rev.* 35 (2014) 906–960. doi:10.1210/er.2014-1024.
- [125] L. Gabel, H.M. Macdonald, H.A. McKay, H. McKay, Sex differences and growth-related adaptations in bone microarchitecture, geometry, density and strength from childhood to early adulthood: a mixed longitudinal HR-pQCT study, *J Bone Min. Res.* 32 (2017) 250–263. doi:10.1002/jbmr.2982.
- [126] B.L. Riggs, L.J. Melton, R.A. Robb, J.J. Camp, E.J. Atkinson, J.M. Peterson, P.A.

- Rouleau, C.H. McCollough, M.L. Bouxsein, S. Khosla, Population-Based Study of Age and Sex Differences in Bone Volumetric Density, Size, Geometry, and Structure at Different Skeletal Sites, *J. Bone Miner. Res.* 19 (2004) 1945–1954. doi:10.1359/jbmr.040916.
- [127] R. Bouillon, M. Bex, D. Vanderschueren, S. Boonen, Estrogens Are Essential for Male Pubertal Periosteal Bone Expansion, *J. Clin. Endocrinol. Metab.* 89 (2004) 6025–6029. doi:10.1210/jc.2004-0602.
- [128] C.M. Weaver, C.M. Gordon, K.F. Janz, H.J. Kalkwarf, J.M. Lappe, R. Lewis, M. O’Karma, T.C. Wallace, B.S. Zemel, The National Osteoporosis Foundation’s position statement on peak bone mass development and lifestyle factors: a systematic review and implementation recommendations, *Osteoporos. Int.* 27 (2016) 1281–1386. doi:10.1007/s00198-015-3440-3.
- [129] C. Morcov, C. Vulpoi, D. Brănișteanu, Relationship between bone mineral density, weight, and estrogen levels in pre and postmenopausal women., *Intern. Med. - Pediatr.* 116 (2012) 946–950.
- [130] V.B. Papat, K.A. Calis, V.H. Vanderhoof, G. Cizza, J.C. Reynolds, N. Sebring, J.F. Troendle, L.M. Nelson, Bone Mineral Density in Estrogen-Deficient Young Women, *J. Clin. Endocrinol. Metab.* 94 (2009) 2277–2283. doi:10.1210/jc.2008-1878.
- [131] J. V. Zborowski, J.A. Cauley, E.O. Talbott, D.S. Guzick, S.J. Winters, Bone Mineral Density, Androgens, and the Polycystic Ovary: The Complex and Controversial Issue of Androgenic Influence in Female Bone, *J. Clin. Endocrinol. Metab.* 85 (2000) 3496–3506. doi:10.1210/jcem.85.10.6902.
- [132] D. Dempster, R. Lindsay, A. Dempster, B. Lindsay, B. Larijani, S.M. Kimiagar, C. Barrett, D. Dempster, R. Lindsay, D. Scharbo, F. Groeneveld, F. Bareman, r Barenzen, M. Glazier, M. Bowman, P. Ross, H. Norimatsu, J. Davis, K. Yano, R. Wasnich, H. Adlercreutz, W. Mazur, F. Simoon, M. Kurzer, X. Xu, L. Coward, N. Barnes, E. Setchell, S. Barnes, K. Wangen, A. Duncan, B. Merz-Demlow, G. Kuiper, B. Carisson, K. Grandien, N. Watts, B. Arjmandi, L. Alekel, B. Hollis, D. Amin, Y. Chang, M. Nair, X. Xu, K. Harris, H. Wang, P. Murphy, S. Hendrich, N. Sathyamoorthy, T. Wang, K. Setchell, H. Adlercreutz, T. Register, M. Jayo, M. Anthony, T. Clarkson, M. Anthony, T. Morgan, K. Setchell, N. Brown, E. Lydeking-Olsen, B. Arjmandi, D. Khalil, B. Smith, Y. Yamori, E. Moriguchi, T. Teramoto, A. Miura, C. Picherit, C. Pelissero, B. Chanteranne, P. Lebecque, T. Uesugi, Y. Fukui, Y. Yamori, P. Fanti, M. Monier-Faugere, Z. Geng, D. Agnusdei, G. Crepaldi, G. Isaia, C. Gennari, D. Agnusdei, G. Crepaldi, S. Potter, J. Baum, H. Teng, R. Stillman, D. Alekel, A. Germain, C. Peterson, K. Hanson, S. Barnes, Pathogenesis of osteoporosis, *Lancet.* 341 (1993) 797–801. doi:10.1016/0140-6736(93)90570-7.

- [133] C.M. Nielson, L.M. Marshall, A.L. Adams, E.S. LeBlanc, P.M. Cawthon, K. Ensrud, M.L. Stefanick, E. Barrett-Connor, E.S. Orwoll, BMI and fracture risk in older men: The osteoporotic fractures in men study (MrOS), *J. Bone Miner. Res.* 26 (2011) 496–502. doi:10.1002/jbmr.235.
- [134] B.L. Clarke, S. Khosla, C.B. Edu, B.L. Clarke, K.S. Edu, (S Khosla, Female reproductive system and bone, *Arch. Biochem. Biophys.* 503 (2010) 118–128. doi:10.1016/j.abb.2010.07.006.
- [135] P. Salari, M. Abdollahi, The influence of pregnancy and lactation on maternal bone health: a systematic review., *J. Fam. Reprod. Heal.* 8 (2014) 135–48. <http://www.ncbi.nlm.nih.gov/pubmed/25530765> (accessed April 23, 2020).
- [136] T.J. De Villiers, J.C. Stevenson, The WHI: The effect of hormone replacement therapy on fracture prevention, *Climacteric.* 15 (2012) 263–266. doi:10.3109/13697137.2012.659975.
- [137] K. PJ, E. JA, S. PN, Interaction of Genetic and Environmental Influences on Peak Bone Density, *Osteoporos. Int.* 1 (1990). doi:10.1007/BF01880417.
- [138] J. Dequeker, J. Nijs, A. Verstraeten, P. Geusens, G. Gevers, Genetic determinants of bone mineral content at the spine and radius: a twin study., *Bone.* 8 (1987) 207–9. doi:10.1016/8756-3282(87)90166-9.
- [139] J.E. Compston, Sex Steroids and Bone, *Physiol. Rev.* 81 (2001) 419–447. doi:10.1152/physrev.2001.81.1.419.
- [140] J.-G. Zhao, X.-T. Zeng, J. Wang, L. Liu, Association Between Calcium or Vitamin D Supplementation and Fracture Incidence in Community-Dwelling Older Adults: A Systematic Review and Meta-analysis., *JAMA.* 318 (2017) 2466–2482. doi:10.1001/jama.2017.19344.
- [141] I.R. Reid, M.J. Bolland, A. Grey, Effects of vitamin D supplements on bone mineral density: a systematic review and meta-analysis, *Lancet.* 383 (2014) 146–155. doi:10.1016/S0140-6736(13)61647-5.
- [142] A. Heinonen, H. Sievänen, P. Kannus, P. Oja, M. Pasanen, I. Vuori, High-Impact Exercise and Bones of Growing Girls: A 9-Month Controlled Trial, *Osteoporos. Int.* 11 (2001) 1010–1017. doi:10.1007/s001980070021.
- [143] D.A. Bailey, H.A. Mckay, R.L. Mirwald, P.R.E. Crocker, R.A. Faulkner, A Six-Year Longitudinal Study of the Relationship of Physical Activity to Bone Mineral Accrual in Growing Children: The University of Saskatchewan Bone Mineral Accrual Study, *J. Bone Miner. Res.* 14 (1999) 1672–1679. doi:10.1359/jbmr.1999.14.10.1672.

- [144] K.A. Bolam, J.G.Z. van Uffelen, D.R. Taaffe, The effect of physical exercise on bone density in middle-aged and older men: A systematic review, *Osteoporos. Int.* 24 (2013) 2749–2762. doi:10.1007/s00198-013-2346-1.
- [145] J. Xu, G. Lombardi, W. Jiao, G. Banfi, Effects of Exercise on Bone Status in Female Subjects, from Young Girls to Postmenopausal Women: An Overview of Systematic Reviews and Meta-Analyses, *Sport. Med.* 46 (2016) 1165–1182. doi:10.1007/s40279-016-0494-0.
- [146] R. Nikander, H. Sievänen, A. Heinonen, R.M. Daly, K. Uusi-Rasi, P. Kannus, Targeted exercise against osteoporosis: A systematic review and meta-analysis for optimising bone strength throughout life, *BMC Med.* 8 (2010) 47. doi:10.1186/1741-7015-8-47.
- [147] J.M. Muir, C. Ye, M. Bhandari, J.D. Adachi, L. Thabane, The effect of regular physical activity on bone mineral density in post-menopausal women aged 75 and over: a retrospective analysis from the Canadian multicentre osteoporosis study, *BMC Musculoskelet. Disord.* 14 (2013) 253. doi:10.1186/1471-2474-14-253.
- [148] K.-Z. Kim, A. Shin, J. Lee, S.-K. Myung, J. Kim, The Beneficial Effect of Leisure-Time Physical Activity on Bone Mineral Density in Pre- and Postmenopausal Women, *Calcif. Tissue Int.* 91 (2012) 178–185. doi:10.1007/s00223-012-9624-3.
- [149] L. Langsetmo, C.L. Hitchcock, E.J. Kingwell, K.S. Davison, C. Berger, S. Forsmo, W. Zhou, N. Kreiger, J.C. Prior, Physical activity, body mass index and bone mineral density—associations in a prospective population-based cohort of women and men: The Canadian Multicentre Osteoporosis Study (CaMos), *Bone.* 50 (2012) 401–408. doi:10.1016/J.BONE.2011.11.009.
- [150] S. Bass, P. Eser, R. Daly, The effect of exercise and nutrition on the mechanostat, *J. Musculoskelet. Neuronal Interact.* 5 (2005) 239–254.
- [151] J.M. Hughes, M.A. Petit, Biological underpinnings of frost’s mechanostat thresholds: The important role of osteocytes, *J. Musculoskelet. Neuronal Interact.* 10 (2010) 128–135.
- [152] Y. Uda, E. Azab, N. Sun, C. Shi, P.D. Pajevic, Osteocyte Mechanobiology., *Curr. Osteoporos. Rep.* 15 (2017) 318–325. doi:10.1007/s11914-017-0373-0.
- [153] M.L. Knothe Tate, P. Niederer, U. Knothe, In Vivo Tracer Transport Through the Lacunocanalicular System of Rat Bone in an Environment Devoid of Mechanical Loading, *Bone.* 22 (1998) 107–117. doi:10.1016/S8756-3282(97)00234-2.
- [154] R. Baron, G. Rawadi, Wnt Signaling and the Regulation of Bone Mass, *Curr. Osteoporos. Reports Curr. Med. Gr. LLC ISSN.* 5 (2007) 73–80. <https://link.springer.com/content/pdf/10.1007%2Fs11914-007-0006-0.pdf>

(accessed January 18, 2018).

- [155] L.F. Bonewald, M.L. Johnson, Osteocytes, mechanosensing and Wnt signaling, *Bone*. 42 (2008) 606–615. doi:10.1016/j.bone.2007.12.224.
- [156] Y. Huybrechts, G. Mortier, E. Boudin, W. Van Hul, WNT Signaling and Bone: Lessons From Skeletal Dysplasias and Disorders, *Front. Endocrinol. (Lausanne)*. 11 (2020) 1–18. doi:10.3389/fendo.2020.00165.
- [157] R.L. Van Bezooijen, P. Ten Dijke, S.E. Papapoulos, C.W.G.M. Löwik, SOST/sclerostin, an osteocyte-derived negative regulator of bone formation, *Cytokine Growth Factor Rev.* 16 (2005) 319–327. doi:10.1016/j.cytogfr.2005.02.005.
- [158] G.L. Galea, A. Sunters, L.B. Meakin, G. Zaman, T. Sugiyama, L.E. Lanyon, J.S. Price, *Sost* down-regulation by mechanical strain in human osteoblastic cells involves PGE2 signaling via EP4, *FEBS Lett.* 585 (2011) 2450–2454. doi:10.1016/j.febslet.2011.06.019.
- [159] A.G. Robling, P.J. Niziolek, L.A. Baldrige, K.W. Condon, M.R. Allen, I. Alam, S.M. Mantila, J. Gluhak-Heinrich, T.M. Bellido, S.E. Harris, C.H. Turner, Mechanical stimulation of bone in vivo reduces osteocyte expression of *Sost/sclerostin*, *J. Biol. Chem.* 283 (2008) 5866–5875. doi:10.1074/jbc.M705092200.
- [160] G.L. Galea, L.E. Lanyon, J.S. Price, Sclerostin's role in bone's adaptive response to mechanical loading, *Bone*. 96 (2017). doi:10.1016/j.bone.2016.10.008.
- [161] G. Holdsworth, S.J. Roberts, H.Z. Ke, Novel actions of sclerostin on bone, *J. Mol. Endocrinol.* 62 (2019) R167–R185. doi:10.1530/JME-18-0176.
- [162] A. Moustafa, T. Sugiyama, J. Prasad, G. Zaman, T.S. Gross, L.E. Lanyon, J.S. Price, Mechanical loading-related changes in osteocyte sclerostin expression in mice are more closely associated with the subsequent osteogenic response than the peak strains engendered, *Osteoporos. Int.* 23 (2012) 1225–1234. doi:10.1007/s00198-011-1656-4.
- [163] M.T. Drake, S. Khosla, Hormonal and systemic regulation of sclerostin, *Bone*. 96 (2017) 8–17. doi:10.1016/j.bone.2016.12.004.
- [164] J.N. Farr, M.M. Roforth, K. Fujita, K.M. Nicks, J.M. Cunningham, E.J. Atkinson, T.M. Therneau, L.K. McCready, J.M. Peterson, M.T. Drake, D.G. Monroe, S. Khosla, Effects of Age and Estrogen on Skeletal Gene Expression in Humans as Assessed by RNA Sequencing, *PLoS One*. 10 (2015) e0138347. doi:10.1371/journal.pone.0138347.

- [165] G.B. Cutler, The Role of Estrogen in Bone Growth and Maturation During Childhood and Adolescence, *J. Steroid Biochem. Mol. Biol.* 616 (1997) 141–144.
- [166] H.A. McKay, D.A. Bailey, R.L. Mirwald, K.S. Davison, R.A. Faulkner, Peak bone mineral accrual and age at menarche in adolescent girls: A 6- year longitudinal study, *J. Pediatr.* 133 (1998) 682–687. doi:10.1016/S0022-3476(98)70112-X.
- [167] C.M.T. Fortes, T.B.L. Goldberg, C.S. Kurokawa, C.C. Silva, M.R. Moretto, T.P. Biazon, A.S. Teixeira, H.R. De Carvalho Nunes, Relationship between chronological and bone ages and pubertal stage of breasts with bone biomarkers and bone mineral density in adolescents, *J. Pediatr. (Rio. J.)* 90 (2014) 624–631. doi:10.1016/j.jped.2014.04.008.
- [168] D. Yilmaz, B. Ersoy, E. Bilgin, G. Gümüşer, E. Onur, E.D. Pinar, Bone mineral density in girls and boys at different pubertal stages: Relation with gonadal steroids, bone formation markers, and growth parameters, *J. Bone Miner. Metab.* 23 (2005) 476–482. doi:10.1007/s00774-005-0631-6.
- [169] M. Almeida, M.R. Laurent, V. Dubois, F. Claessens, C.A. O'brien, R. Bouillon, D. Vanderschueren, S.C. Manolagas, Estrogens and Androgens in Skeletal Physiology and Patho-physiology, *Physiol Rev.* 97 (2017) 135–187. doi:10.1152/physrev.00033.2015.-Estrogens.
- [170] S.C. Manolagas, S.C. Manolagas, C.A. O 'brien, M. Almeida, The role of estrogen and androgen receptors in bone health and disease, *Nat. Rev. Endocrinol.* 9 (2013) 699–712. doi:10.1038/nrendo.2013.179.
- [171] S.H. Windahl, K. Hollberg, O. Vidal, J.-Å. Gustafsson, C. Ohlsson, G. Andersson, Female Estrogen Receptor β -/- Mice Are Partially Protected Against Age-Related Trabecular Bone Loss, *J. Bone Miner. Res.* 16 (2001) 1388–1398. doi:10.1359/jbmr.2001.16.8.1388.
- [172] S.H. Windahl, G. Andersson, J.-Å. Gustafsson, Elucidation of estrogen receptor function in bone with the use of mouse models, *Trends Endocrinol. Metab.* 13 (2002) 195–200. doi:10.1016/S1043-2760(02)00594-5.
- [173] M. Martin-Millan, M. Almeida, E. Ambrogini, L. Han, H. Zhao, R.S. Weinstein, R.L. Jilka, C.A. O'Brien, S.C. Manolagas, The Estrogen Receptor-in Osteoclasts Mediates the Protective Effects of Estrogens on Cancellous But Not Cortical Bone, *Mol. Endocrinol.* 24 (2010) 323–334. doi:10.1210/me.2009-0354.
- [174] M. Almeida, S. Iyer, M. Martin-Millan, S.M. Bartell, L. Han, E. Ambrogini, M. Onal, J. Xiong, R.S. Weinstein, R.L. Jilka, C.A. O'Brien, S.C. Manolagas, Estrogen receptor- α signaling in osteoblast progenitors stimulates cortical bone accrual., *J. Clin. Invest.* 123 (2013) 394–404. doi:10.1172/JCI65910.

- [175] S.H. Windahl, A.E. Börjesson, H.H. Farman, C. Engdahl, S. Movérare-Skrtic, K. Sjögren, M.K. Lagerquist, J.M. Kindblom, A. Koskela, J. Tuukkanen, P.D. Pajevic, J.Q. Feng, K. Dahlman-Wright, P. Antonson, J.-Å. Gustafsson, C. Ohlsson, Estrogen receptor- α in osteocytes is important for trabecular bone formation in male mice, *PNAS*. 110 (2013) 2294–2299. doi:10.1073/pnas.1220811110.
- [176] S. Kondoh, K. Inoue, K. Igarashi, H. Sugizaki, Y. Shiode-Fukuda, E. Inoue, T. Yu, J.K. Takeuchi, J. Kanno, L.F. Bonewald, Y. Imai, Estrogen receptor α in osteocytes regulates trabecular bone formation in female mice, *Bone*. 60 (2014) 68–77. doi:10.1016/J.BONE.2013.12.005.
- [177] F.L. Morris, W.R. Payne, J.D. Wark, The Impact of Intense Training on Endogenous Estrogen and Progesterone Concentrations and Bone Mineral Acquisition in Adolescent Rowers, *Osteoporos. Int.* 10 (1999) 361–368. doi:10.1007/s001980050241.
- [178] B.A. Wallace, R.G. Cumming, Systematic Review of Randomized Trials of the Effect of Exercise on Bone Mass in Pre- and Postmenopausal Women, *Calcif. Tissue Int.* 67 (2000) 10–18. doi:10.1007/s00223001089.
- [179] E. Marín-Cascales, P.E. Alcaraz, D.J. Ramos-Campo, A. Martínez-Rodríguez, L.H. Chung, J.Á. Rubio-Arias, Whole-body vibration training and bone health in postmenopausal women: A systematic review and meta-analysis., *Medicine (Baltimore)*. 97 (2018) e11918. doi:10.1097/MD.00000000000011918.
- [180] R. Zhao, Z. Xu, M. Zhao, Effects of Oestrogen Treatment on Skeletal Response to Exercise in the Hips and Spine in Postmenopausal Women: A Meta-Analysis, *Sport. Med.* 45 (2015) 1163–1173. doi:10.1007/s40279-015-0338-3.
- [181] L.A. Milliken, S.B. Going, L.B. Houtkooper, H.G. Flint-Wagner, A. Figueroa, L.L. Metcalfe, R.M. Blew, S.C. Sharp, T.G. Lohman, Effects of Exercise Training on Bone Remodeling, Insulin-Like Growth Factors, and Bone Mineral Density in Postmenopausal Women With and Without Hormone Replacement Therapy, *Calcif. Tissue Int.* 72 (2003) 478–484. doi:10.1007/s00223-001-1128-5.
- [182] S. Going, T. Lohman, L. Houtkooper, V. Stanford, E. Cussler, J. Martin, P. Teixeira, M. Harris, L. Milliken, A. Figueroa-Galvez, J. Weber, L. Metcalfe, H. Flint-Wagner, R. Blew, Effects of exercise on bone mineral density in calcium-replete postmenopausal women with and without hormone replacement therapy, *Osteoporos. Int.* 14 (2003) 637–643. doi:10.1007/s00198-003-1436-x.
- [183] T. Remes, S.B. Väisänen, A. Mahonen, J. Huuskonen, H. Kröger, J.S. Jurvelin, I.M. Penttilä, R. Rauramaa, Aerobic exercise and bone mineral density in middle-aged Finnish men: a controlled randomized trial with reference to androgen receptor, aromatase, and estrogen receptor gene polymorphisms, *Bone*. 32 (2003)

412–420. doi:10.1016/S8756-3282(03)00032-2.

- [184] G.L. Galea, L.B. Meakin, T. Sugiyama, N. Zebda, A. Sunters, H. Taipaleenmaki, G.S. Stein, A.J. Van Wijnen, L.E. Lanyon, J.S. Price, Estrogen receptor α mediates proliferation of osteoblastic cells stimulated by estrogen and mechanical strain, but their acute down-regulation of the Wnt antagonist Sost is mediated by estrogen receptor β ., *J. Biol. Chem.* 288 (2013) 9035–48. doi:10.1074/jbc.M112.405456.
- [185] E. Damien, J.S. Price, L.E. Lanyon, Mechanical Strain Stimulates Osteoblast Proliferation Through the Estrogen Receptor in Males as Well as Females, *J. Bone Miner. Res.* 15 (2000) 2169–2177. doi:10.1359/jbmr.2000.15.11.2169.
- [186] H.L. Jessop, R.F. Suswillo, S.C. Rawlinson, G. Zaman, K. Lee, V. Das-Gupta, A.A. Pitsillides, L.E. Lanyon, Osteoblast-Like Cells From Estrogen Receptor α Knockout Mice Have Deficient Responses to Mechanical Strain, *J. Bone Miner. Res.* 19 (2004) 938–946. doi:10.1359/jbmr.2004.19.6.938.
- [187] K.C.L. Lee, L.E. Lanyon, Mechanical Loading Influences Bone Mass Through Estrogen Receptor ??, *Exerc. Sport Sci. Rev.* 32 (2004) 64–68. doi:10.1097/00003677-200404000-00005.
- [188] E. Damien, J.S. Price, L.E. Lanyon, The Estrogen Receptor's Involvement in Osteoblasts' Adaptive Response to Mechanical Strain, *J. Bone Miner. Res.* 13 (1998) 1275–1282. doi:10.1359/jbmr.1998.13.8.1275.
- [189] W. Kim, Y. Chung, S.H. Kim, S. Park, J.H. Bae, G. Kim, S.J. Lee, J.E. Kim, B.-W. Park, S.-K. Lim, Y. Rhee, Increased Sclerostin Levels after Further Ablation of Remnant Estrogen by Aromatase Inhibitors, *Org Endocrinol Metab.* 30 (2015) 58–64. doi:10.3803/EnM.2015.30.1.58.
- [190] E. Diamanti-Kandarakis, J.-P. Bourguignon, L.C. Giudice, R. Hauser, G.S. Prins, A.M. Soto, R.T. Zoeller, A.C. Gore, Endocrine-Disrupting Chemicals: An Endocrine Society Scientific Statement, *Endocr. Rev.* 30 (2009) 293–342. doi:10.1210/er.2009-0002.
- [191] K.-C. An, Selective Estrogen Receptor Modulators., *Asian Spine J.* 10 (2016) 787–91. doi:10.4184/asj.2016.10.4.787.
- [192] S.K. Wong, N.V. Mohamad, P.A. Jayusman, A.N. Shuid, S. Ima-Nirwana, K.Y. Chin, The use of selective estrogen receptor modulators on bone health in men, *Aging Male.* 22 (2019) 89–101. doi:10.1080/13685538.2018.1448058.
- [193] K.D.R. Setchell, Soy Isoflavones—Benefits and Risks from Nature's Selective Estrogen Receptor Modulators (SERMs), *J. Am. Coll. Nutr.* 20 (2001) 354S-362S. doi:10.1080/07315724.2001.10719168.

- [194] B.S. Rubin, Bisphenol A: An endocrine disruptor with widespread exposure and multiple effects, *J. Steroid Biochem. Mol. Biol.* 127 (2011) 27–34. doi:10.1016/J.JSBMB.2011.05.002.
- [195] J. Yang, L. Wen, Y. Jiang, B. Yang, Natural Estrogen Receptor Modulators and Their Heterologous Biosynthesis, *Trends Endocrinol. Metab.* 30 (2019). doi:10.1016/j.tem.2018.11.002.
- [196] M. Akhlaghi, M. Ghasemi Nasab, M. Riasatian, F. Sadeghi, Soy isoflavones prevent bone resorption and loss, a systematic review and meta-analysis of randomized controlled trials, *Crit. Rev. Food Sci. Nutr.* 8398 (2019) 1–15. doi:10.1080/10408398.2019.1635078.
- [197] W. Qiu, H. Zhan, J. Hu, T. Zhang, H. Xu, M. Wong, B. Xu, C. Zheng, The occurrence, potential toxicity, and toxicity mechanism of bisphenol S, a substitute of bisphenol A: A critical review of recent progress, *Ecotoxicol. Environ. Saf.* 173 (2019) 192–202. doi:10.1016/j.ecoenv.2019.01.114.
- [198] R.U. Halden, Plastics and Health Risks, *Annu. Rev. Public Heal.* 31 (2010) 179–194. doi:10.1146/annurev.publhealth.012809.103714.
- [199] F. Acconcia, V. Pallottini, M. Marino, Molecular Mechanisms of Action of BPA, Dose-Response An Int. J. (2015) 1–9. doi:10.1177/1559325815610582.
- [200] A. Bolli, P. Bulzomi, P. Galluzzo, F. Acconcia, M. Marino, Bisphenol A impairs estradiol-induced protective effects against DLD-1 colon cancer cell growth, *IUBMB Life.* 62 (2010) 684–687. doi:10.1002/iub.370.
- [201] A.L. Strong, D.F.B. Miller, A.M. Buechlein, F. Fang, J. Glowacki, J.A. McLachlan, K.P. Nephew, M.E. Burow, B.A. Bunnell, Bisphenol A alters the self-renewal and differentiation capacity of human bone-marrow-derived mesenchymal stem cells, *Endocr. Disruptors.* 4 (2016) e1200344. doi:10.1080/23273747.2016.1200344.
- [202] R.K. Dirkes, N.C. Winn, T.J. Jurrissen, D.B. Lubahn, V.J. Vieira-Potter, J. Padilla, P.S. Hinton, Global estrogen receptor- α knockout has differential effects on cortical and cancellous bone in aged male mice, *FACETS.* 5 (2020) 328–348. doi:10.1139/facets-2019-0043.
- [203] A. Piot, R.D. Chapurlat, B. Claustrat, P. Szulc, Relationship between sex steroids and deterioration of bone microarchitecture in older men: the prospective STRAMBO Study, *J. Bone Miner. Res.* (2019) jbmr.3746. doi:10.1002/jbmr.3746.
- [204] R. Oftadeh, M. Perez-Viloria, J.C. Villa-Camacho, A. Vaziri, A. Nazarian, Biomechanics and Mechanobiology of Trabecular Bone: A Review, *J. Biomech. Eng.* 137 (2015) 010802. doi:10.1115/1.4029176.

- [205] U.I. Mödder, K.A. Hoey, S. Amin, L.K. McCready, S.J. Achenbach, B.L. Riggs, L.J. Melton, S. Khosla, Relation of age, gender, and bone mass to circulating sclerostin levels in women and men, *J. Bone Miner. Res.* 26 (2011) 373–379. doi:10.1002/jbmr.217.
- [206] F.S. Mirza, I.D. Padhi, L.G. Raisz, J.A. Lorenzo, Serum Sclerostin Levels Negatively Correlate with Parathyroid Hormone Levels and Free Estrogen Index in Postmenopausal Women, *J. Clin. Endocrinol. Metab.* 95 (2010) 1991–1997. doi:10.1210/jc.2009-2283.
- [207] A. Di Nisio, L. De Toni, E. Speltra, M. Santa Rocca, G. Tagliavero, A. Ferlin, C. Foresta, Regulation of Sclerostin Production in Human Male Osteocytes by Androgens: Experimental and Clinical Evidence, *Endocrinology.* 156 (2015) 4534–4544. doi:10.1210/en.2015-1244.
- [208] M.H. Faulds, C. Zhao, K. Dahlman-Wright, J.-Å. Ke Gustafsson, The diversity of sex steroid action: regulation of metabolism by estrogen signaling, *J. Endocrinol.* 212 (2012) 3–12. doi:10.1530/JOE-11-0044.
- [209] G. Bryzgalova, H. Gao, B. Ahren, J.R. Zierath, D. Galuska, T.L. Steiler, K. Dahlman-Wright, S. Nilsson, J.-A. Gustafsson, S. Efendic, A. Khan, Evidence that oestrogen receptor- α plays an important role in the regulation of glucose homeostasis in mice: insulin sensitivity in the liver, *Diabetologia.* 49 (2006) 588–597. doi:10.1007/s00125-005-0105-3.
- [210] J. Starup-Linde, P. Vestergaard, Biochemical bone turnover markers in diabetes mellitus — A systematic review, *Bone.* 82 (2016) 69–78. doi:10.1016/j.bone.2015.02.019.
- [211] M. Janghorbani, R.M. Van Dam, W.C. Willett, F.B. Hu, Systematic review of type 1 and type 2 diabetes mellitus and risk of fracture, *Am. J. Epidemiol.* 166 (2007) 495–505. doi:10.1093/aje/kwm106.
- [212] D. Merlotti, L. Gennari, F. Dotta, D. Lauro, R. Nuti, Mechanisms of impaired bone strength in type 1 and 2 diabetes, *Nutr. Metab. Cardiovasc. Dis.* 20 (2010) 683–690. doi:10.1016/j.numecd.2010.07.008.
- [213] J. Compston, Obesity and Bone, *Curr. Osteoporos. Rep.* 11 (2013) 30–35. doi:10.1007/s11914-012-0127-y.
- [214] N.C. Winn, T.J. Jurrissen, Z.I. Grunewald, R.P. Cunningham, M.L. Woodford, J.A. Kanaley, D.B. Lubahn, C. Manrique-Acevedo, R.S. Rector, V.J. Vieira-Potter, J. Padilla, Estrogen receptor alpha signaling maintains immunometabolic function in males and is obligatory for exercise-induced amelioration of nonalcoholic fatty liver, *Am. J. Physiol. Metab.* (2018) ajpendo.00259.2018. doi:10.1152/ajpendo.00259.2018.

- [215] D.B. Lubahn, J.S. Moyer, T.S. Golding, J.F. Couse, K.S. KoRACH, O. Smithies, Alteration of reproductive function but not prenatal sexual development after insertional disruption of the mouse estrogen receptor gene, *Genetics*. 90 (1993) 11162–11166. <http://www.pnas.org/content/90/23/11162.full.pdf> (accessed August 2, 2017).
- [216] E.M. Eddy, T.F. Washburn, D.O. Bunch, E.H. Goulding, B.C. Gladen, D.B. Lubahn, K.S. Korach, Targeted disruption of the estrogen receptor gene in male mice causes alteration of spermatogenesis and infertility., *Endocrinology*. 137 (1996) 4796–4805. doi:10.1210/endo.137.11.8895349.
- [217] G.M. Rubanyi, A.D. Freay, K. Kauser, D. Sukovich, G. Burton, D.B. Lubahn, J.F. Couse, S.W. Curtis, K.S. Korach, Vascular estrogen receptors and endothelium-derived nitric oxide production in the mouse aorta. Gender difference and effect of estrogen receptor gene disruption., *J. Clin. Invest.* 99 (1997) 2429–37. doi:10.1172/JCI119426.
- [218] M. Doube, M.M. Kłosowski, I. Arganda-Carreras, F.P. Cordelières, R.P. Dougherty, J.S. Jackson, B. Schmid, J.R. Hutchinson, S.J. Shefelbine, *BoneJ: Free and extensible bone image analysis in ImageJ*, 2010. doi:10.1016/j.bone.2010.08.023.
- [219] Bruker-microCT, Morphometric parameters measured by Skyscan™ CT - analyser software ., Ref. Man. (2012) 1–49. <http://bruker-microct.com/next/CTAn03.pdf>.
- [220] S.Y. Tang, U. Zeenath, D. Vashishth, Effects of non-enzymatic glycation on cancellous bone fragility, *Bone*. 40 (2007) 1144–1151. doi:10.1016/j.bone.2006.12.056.
- [221] M. Pereira, S. Gohin, N. Lund, A. Hvid, P.J. Smitham, M.J. Oddy, I. Reichert, D. Farlay, J.P. Roux, M.E. Cleasby, C. Chenu, Sclerostin does not play a major role in the pathogenesis of skeletal complications in type 2 diabetes mellitus, *Osteoporos. Int.* 28 (2017) 309–320. doi:10.1007/s00198-016-3718-0.
- [222] C.N. Shaw, J.T. Stock, Intensity, repetitiveness, and directionality of habitual adolescent mobility patterns influence the tibial diaphysis morphology of athletes, *Am. J. Phys. Anthropol.* 140 (2009) 149–159. doi:10.1002/ajpa.21064.
- [223] E.N. Ebbesen, J.S. Thomsen, H. Beck-Nielsen, H.J. Nepper-Rasmussen, L. Mosekilde, Age- and gender-related differences in vertebral bone mass, density, and strength, *J. Bone Miner. Res.* 14 (1999) 1394–1403. doi:10.1359/jbmr.1999.14.8.1394.
- [224] H. Oxlund, M. Dalstra, T.T. Andreassen, Statin Given Perorally to Adult Rats Increases Cancellous Bone Mass and Compressive Strength, *Calcif. Tissue Int.* 69

(2001) 299–304. doi:10.1007/s00223-001-2027-5.

- [225] R.L. Jilka, The Relevance of Mouse Models for Investigating Age-Related Bone Loss in Humans, *J Gerontol A Biol Sci Med Sci.* 68 (2013) 1209–1217. doi:10.1093/gerona/glt046.
- [226] S.H. Kilborn, G. Trudel, H. Uthoff, Review of Growth Plate Closure Compared with Age at Sexual Maturity and Lifespan in Laboratory Animals, *J. Am. Assoc. Anim. Lab. Sci.* 41 (2002) 21–26. <https://www.ingentaconnect.com/content/aalas/jaalas/2002/00000041/00000005/art00005#> (accessed July 12, 2019).
- [227] R.Y. Kim, H.J. Yang, Y.M. Song, I.S. Kim, S.J. Hwang, Estrogen Modulates Bone Morphogenetic Protein-Induced Sclerostin Expression Through the Wnt Signaling Pathway, *Tissue Eng. Part A.* 21 (2015) 2076–2088. doi:10.1089/ten.tea.2014.0585.
- [228] S. Khosla, Pathogenesis of Age-Related Bone Loss in Humans, *Med. Sci. Cite J. as J Gerontol A Biol Sci Med Sci.* 68 (2013) 1226–1235. doi:10.1093/gerona/gls163.
- [229] G.K. Chan, G. Duque, Age-Related Bone Loss: Old Bone, New Facts, 2002. www.karger.com/journals/ger (accessed August 30, 2018).
- [230] E. Hay, W. Bouaziz, T. Funck-Brentano, M. Cohen-Solal, Sclerostin and Bone Aging: A Mini-Review, *Gerontology.* 62 (2016) 618–623. doi:10.1159/000446278.
- [231] M.M. Roforth, K. Fujita, U.I. Mcgregor, S. Kirmani, L.K. Mccready, J.M. Peterson, M.T. Drake, D.G. Monroe, S. Khosla, Effects of Age on Bone mRNA Levels of Sclerostin and Other Genes Relevant to Bone Metabolism in Humans, *Bone.* 59 (2014). doi:10.1016/j.bone.2013.10.019.
- [232] M.L. Thompson, J.M. Jimenez-Andrade, P.W. Mantyh, Sclerostin Immunoreactivity Increases in Cortical Bone Osteocytes and Decreases in Articular Cartilage Chondrocytes in Aging Mice, *J. Histochem. Cytochem.* 64 (2016) 179–189. doi:10.1369/0022155415626499.
- [233] K. Ota, P. Quint, M. Ruan, L. Pederson, J.J. Westendorf, S. Khosla, M. Jo Oursler, Sclerostin Is Expressed in Osteoclasts From Aged Mice and Reduces Osteoclast-Mediated Stimulation of Mineralization, *J Cell Biochem.* 114 (2013) 1901–1907. doi:10.1002/jcb.24537.
- [234] M.K. Nanjappa, A.M. Mesa, S.G. Tevosian, L. de Armas, R.A. Hess, I.C. Bagchi, P.S. Cooke, Membrane Estrogen Receptor 1 is Required for Normal Reproduction in Male and Female Mice, *J. Endocrinol. Reprod.* 21 (2018) 1–14.

doi:10.18311/JER/2017/21013.

- [235] M.D. Iafrazi, R.H. Karas, M. Aronovitz, S. Kim, T.R. Sullivan, D.B. Lubahn, T.F. O'donnell, K.S. Korach, M.E. Mendelsohn', Estrogen inhibits the vascular injury response in estrogen receptor α -deficient mice, *Nature*. 3 (1997) 545–548. <http://www.nature.com/naturemedicine> (accessed July 25, 2019).
- [236] E.M. Eddy, T.F. Washburn, D. O Bunch, E.H. Goulding, B.C. Gladen, D.B. Lubahn, K.S. Korach, G. Biology, R.B. Section, Targeted Disruption of the Estrogen Receptor Gene in Male Mice Causes Alteration of Spermatogenesis and Infertility, *Endocrinology*. 137 (1996) 4796–4805. <https://academic.oup.com/endo/article-abstract/137/11/4796/3037471> (accessed July 12, 2019).
- [237] P.A. Heine, J.A. Taylor, G.A. Iwamoto, D.B. Lubahn, P.S. Cooke, Increased adipose tissue in male and female estrogen receptor-knockout mice, *PNAS*. 97 (2000) 12729–12734. www.pnas.org (accessed July 12, 2019).
- [238] M. Unal, A. Creecy, J.S. Nyman, The Role of Matrix Composition in the Mechanical Behavior of Bone HHS Public Access, *Curr Osteoporos Rep*. 16 (2018) 205–215. doi:10.1007/s11914-018-0433-0.
- [239] S.H. Windahl, L. Saxon, A.E. Börjesson, M.K. Lagerquist, B. Frenkel, P. Henning, U.H. Lerner, G.L. Galea, L.B. Meakin, C. Engdahl, K. Sjögren, M.C. Antal, A. Krust, P. Chambon, L.E. Lanyon, J.S. Price, C. Ohlsson, Estrogen receptor- α is required for the osteogenic response to mechanical loading in a ligand-independent manner involving its activation function 1 but not 2, *J. Bone Miner. Res*. 28 (2013) 291–301. doi:10.1002/jbmr.1754.
- [240] L.C. Ortinau, M.A. Linden, R.K. Dirkes, R.S. Rector, P.S. Hinton, Exercise initiated after the onset of insulin resistance improves trabecular microarchitecture and cortical bone biomechanics of the tibia in hyperphagic Otsuka Long Evans Tokushima Fatty rats, *Bone*. 103 (2017) 188–199. doi:10.1016/j.bone.2017.07.010.
- [241] L.C. Ortinau, M.A. Linden, R. Dirkes, R.S. Rector, P.S. Hinton, Obesity and type 2 diabetes, not a diet high in fat, sucrose, and cholesterol, negatively impacts bone outcomes in the hyperphagic Otsuka Long Evans Tokushima Fatty rat, *Bone*. 105 (2017) 200–211. doi:10.1016/j.bone.2017.09.003.
- [242] J.M. Somerville, R.M. Aspden, K.E. Armour, K.J. Armour, D.M. Reid, Growth of C57Bl/6 Mice and the Material and Mechanical Properties of Cortical Bone from the Tibia, *Calcif. Tissue Int*. 74 (2004) 469–475. doi:10.1007/s00223-003-0101-x.
- [243] C.H. Turner, Y. Takano, I. Owan, Aging changes mechanical loading thresholds for bone formation in rats, *J. Bone Miner. Res*. 10 (2009) 1544–1549. doi:10.1002/jbmr.5650101016.

- [244] A. Usman, M. Ahmad, From BPA to its analogues: Is it a safe journey?, *Chemosphere*. 158 (2016) 131–142. doi:10.1016/j.chemosphere.2016.05.070.
- [245] J.-M. Molina-Molina, E. Amaya, M. Grimaldi, J.-M. Sáenz, M. Real, M.F. Fernández, P. Balaguer, N. Olea, In vitro study on the agonistic and antagonistic activities of bisphenol-S and other bisphenol-A congeners and derivatives via nuclear receptors, (2013). doi:10.1016/j.taap.2013.05.015.
- [246] V. Le Fol, S. Aït-Aïssa, M. Sonavane, J.-M. Porcher, P. Balaguer, J.-P. Cravedi, D. Zalko, F. Brion, In vitro and in vivo estrogenic activity of BPA, BPF and BPS in zebrafish-specific assays, *Ecotoxicol. Environ. Saf.* 142 (2017) 150–156. doi:10.1016/J.ECOENV.2017.04.009.
- [247] A. Maćczak, M. Cyrkler, B. Bukowska, J. Michałowicz, Bisphenol A, bisphenol S, bisphenol F and bisphenol AF induce different oxidative stress and damage in human red blood cells (in vitro study), *Toxicol. Vitro*. 41 (2017) 143–149. doi:10.1016/J.TIV.2017.02.018.
- [248] C. van Zwol - Janssens, L. Trasande, A.G. Asimakopoulos, M.P. Martinez-Moral, K. Kannan, E.M. Philips, F. Rivadeneira, V.W.V. Jaddoe, S. Santos, Fetal exposure to bisphenols and phthalates and childhood bone mass: a population-based prospective cohort study., *Environ. Res.* 186 (2020) 109602. doi:10.1016/j.envres.2020.109602.
- [249] T. Lind, M.H. Lejonklou, L. Dunder, M.M. Kushnir, C. Öhman-Mägi, S. Larsson, H. Melhus, P.M. Lind, Developmental low-dose exposure to bisphenol A induces chronic inflammation, bone marrow fibrosis and reduces bone stiffness in female rat offspring only, *Environ. Res.* 177 (2019) 108584. doi:10.1016/j.envres.2019.108584.
- [250] A. Gaeini, M.B. Eslaminejad, S. Choobineh, N. Mousavi, S. Satarifard, L. Shafieineek, Effects of exercise prior or during pregnancy in high fat diet fed mice alter bone gene expression of female offspring: An experimental study, *Int. J. Reprod. Biomed.* 15 (2017) 93–100. doi:10.29252/ijrm.15.2.93.
- [251] B. V. Rosa, H.T. Blair, M.H. Vickers, K.E. Dittmer, P.C.H. Morel, C.G. Knight, E.C. Firth, Moderate Exercise during Pregnancy in Wistar Rats Alters Bone and Body Composition of the Adult Offspring in a Sex-Dependent Manner, *PLoS One*. 8 (2013) e82378. doi:10.1371/journal.pone.0082378.
- [252] J. McHenry, N. Carrier, E. Hull, M. Kabbaj, Sex differences in anxiety and depression: Role of testosterone, *Front. Neuroendocrinol.* 35 (2014) 42–57. doi:10.1016/J.YFRNE.2013.09.001.
- [253] V.L. Clifton, Review: Sex and the Human Placenta: Mediating Differential Strategies of Fetal Growth and Survival, *Placenta*. 31 (2010) S33–S39.

doi:10.1016/J.PLACENTA.2009.11.010.

- [254] M. Doube, The Ellipsoid Factor for Quantification of Rods, Plates, and Intermediate Forms in 3D Geometries, *Front. Endocrinol. (Lausanne)*. 6 (2015) 15. doi:10.3389/fendo.2015.00015.
- [255] M. Stauber, L. Rapillard, G.H. van Lenthe, P. Zysset, R. Müller, Importance of Individual Rods and Plates in the Assessment of Bone Quality and Their Contribution to Bone Stiffness, *J. Bone Miner. Res.* 21 (2006) 586–595. doi:10.1359/jbmr.060102.
- [256] X.S. Liu, P. Sajda, P.K. Saha, F.W. Wehrli, X.E. Guo, Quantification of the roles of trabecular microarchitecture and trabecular type in determining the elastic modulus of human trabecular bone, *J. Bone Miner. Res.* 21 (2006) 1608–1617. doi:10.1359/jbmr.060716.
- [257] V. Carina, E. Della Bella, V. Costa, D. Bellavia, F. Veronesi, S. Cepollaro, M. Fini, G. Giavaresi, Bone's Response to Mechanical Loading in Aging and Osteoporosis: Molecular Mechanisms, *Calcif. Tissue Int.* 107 (2020) 301–318. doi:10.1007/s00223-020-00724-0.
- [258] B. Javaheri, A.A. Pitsillides, Aging and Mechanoadaptive Responsiveness of Bone, *Curr. Osteoporos. Rep.* 17 (2019) 560–569. doi:10.1007/s11914-019-00553-7.
- [259] S.O. Mueller, Xenoestrogens: mechanisms of action and detection methods, *Anal. Bioanal. Chem.* 378 (2004) 582–587. doi:10.1007/s00216-003-2238-x.
- [260] V.S. Ratnu, M.R. Emami, T.W. Bredy, Genetic and epigenetic factors underlying sex differences in the regulation of gene expression in the brain, *J. Neurosci. Res.* 95 (2017) 301–310. doi:10.1002/jnr.23886.
- [261] E. Grignard, S. Lapenna, S. Bremer, Weak estrogenic transcriptional activities of Bisphenol A and Bisphenol S, *Toxicol. Vitro.* 26 (2012) 727–731. doi:10.1016/J.TIV.2012.03.013.
- [262] M.-Y. Chen, M. Ike, M. Fujita, Acute toxicity, mutagenicity, and estrogenicity of bisphenol-A and other bisphenols, *Environ. Toxicol.* 17 (2002) 80–86. doi:10.1002/tox.10035.
- [263] M. Bisson, F. Tremblay, O. St-Onge, J. Robitaille, E. Pronovost, D. Simonyan, I. Marc, Influence of maternal physical activity on infant's body composition, *Pediatr. Obes.* 12 (2017) 38–46. doi:10.1111/ijpo.12174.
- [264] C.S. Harrod, L. Chasan-Taber, R.M. Reynolds, T.E. Fingerlin, D.H. Glueck, J.T. Brinton, D. Dabelea, Physical activity in pregnancy and neonatal body

composition: the Healthy Start study., *Obstet. Gynecol.* 124 (2014) 257–64. doi:10.1097/AOG.0000000000000373.

- [265] D.L. Dahly, X. Li, H.A. Smith, A.S. Khashan, D.M. Murray, M.E. Kiely, J. O'b Hourihane, F.P. Mccarthy, L.C. Kenny, P.M. Kearney, Associations between maternal lifestyle factors and neonatal body composition in the Screening for Pregnancy Endpoints (Cork) cohort study, (n.d.). doi:10.1093/ije/dyx221.
- [266] Y.T.M. Mangwiro, J.S.M. Cuffe, J.F. Briffa, D. Mahizir, K. Anevaska, A.J. Jefferies, S. Hosseini, T. Romano, K.M. Moritz, M.E. Wlodek, Maternal exercise in rats upregulates the placental insulin-like growth factor system with diet- and sex-specific responses: minimal effects in mothers born growth restricted, *J. Physiol.* 596 (2018) 5947–5964. doi:10.1113/JP275758.
- [267] S.L. McGee, M. Hargreaves, Epigenetics and Exercise, *Trends Endocrinol. Metab.* 30 (2019) 636–645. doi:10.1016/J.TEM.2019.06.002.
- [268] T.E. Chalk, W. M Brown, Exercise epigenetics and the fetal origins of disease, *Epigenomics.* 6 (2014) 469–472. doi:10.2217/epi.14.38.
- [269] M.L. Birsner, C. Gyamfi-Bannerman, Physical Activity and Exercise During Pregnancy and the Postpartum Period, 2015. <https://www.acog.org/-/media/project/acog/acogorg/clinical/files/committee-opinion/articles/2020/04/physical-activity-and-exercise-during-pregnancy-and-the-postpartum-period.pdf> (accessed November 3, 2020).
- [270] M. Vargas-Terrones, T.S. Nagpal, R. Barakat, Impact of exercise during pregnancy on gestational weight gain and birth weight: an overview., *Brazilian J. Phys. Ther.* 23 (2019) 164–169. doi:10.1016/j.bjpt.2018.11.012.
- [271] T.A.C. of O. and G.C. on H.C. for U.W. ACOG, Exposure to Toxic Environmental Agents Report Companion Piece, 2013.
- [272] T.A.C. of O. and G.C. on H.C. for U.W. ACOG, Exposure to Toxic Environmental Agents Report, 2013. <http://prhe.ucsf>. (accessed November 3, 2020).
- [273] K. Kapinas, A.M. Delany, MicroRNA biogenesis and regulation of bone remodeling, *Arthritis Res. Ther.* 13 (2011) 1–11. doi:10.1186/ar3325.
- [274] C. Karrer, T. Roiss, N. Von Goetz, D. Gramec Skledar, L.P. Maši, K. Hungerbühler, Physiologically Based Pharmacokinetic (PBPK) Modeling of the Bisphenols BPA, BPS, BPF, and BPAF with New Experimental Metabolic Parameters: Comparing the Pharmacokinetic Behavior of BPA with Its Substitutes, *Environ. Health Perspect.* 126 (2018) 1–17. doi:10.1289/EHP2739.
- [275] K.-Y. Chin, K.-L. Pang, W. Fui Mark-Lee, A Review on the Effects of Bisphenol

A and Its Derivatives on Skeletal Health, *Int. J. Med. Sci.* 15 (2018) 1043–1050.
doi:10.7150/ijms.25634.

APPENDIX A – DETAILED METHODS AND PROTOCOLS

μCT Analysis in BoneJ

Tissue Processing and Scanning

1. Clean bone of all soft tissue, wrap in PBS-soaked gauze, flash freeze in liquid nitrogen, and store in the -80 freezer until ready for analysis
 - a. Note: Often the bone used for μCT analysis is also the one used for biomechanical property testing. Too many freeze-thaw cycles can alter material properties, so best if bones are cleaned and processed on day of sacrifice
2. Once samples from all animals are collected, contact the MU X-ray Microanalysis Core (MizzoμX) in the Geology building and schedule a time to drop off samples.
3. Take your samples over to the Geology building on ice so that they remain frozen, and they will store them in their -80
4. Work with the lab manager to get good pictures of the bone at the right resolution and voxel size.
 - a. A voxel size of 12 μm works well for mice, but settings might need to be adjusted based on breed and sample
5. Make sure that you receive the final scans in .TIFF format

Analysis

1. Drag and drop the stack of photos for a bone into Fiji or BoneJ (whichever you are using)
 - a. Note, you will need to drag and drop the whole folder or stack of photos, not individual photo files
 - b. A window will pop up that says “open [file] as a stack?”
 - c. Click YES
 - i. ****NOTE** if you accidentally drag and drop the wrong folder, click CANCEL, not NO. Clicking NO will attempt to open each photo in the folder individually and likely crash your computer, whereas clicking CANCEL will stop the program from opening anything. Learn from my mistakes ☺
 - d. If the program says it cannot open all of the photos or the whole file (Error: not enough memory) it’s okay to delete some of the individual TIFF files from the beginning and the end if they are blank (just show grey, and have no bone info), but try to avoid deleting any photos that contain bone images
2. Once the file is open, make sure that the settings are correct. Sometimes the program can read the voxel size from the files, sometimes you have to hand enter it, so always check
 - a. Go to Image → Properties
 - b. If the voxel size is in pixels, adjust by typing in a new unit and voxel size
 - c. Note that whatever unit you give it will be your output. Usually you want mm or m as an output, not μm, so you will need to type in mm and 0.012 if your voxel size is 12 μm

3. Once the settings are correct, select your region of interest (ROI). Since you will be cropping part of the bone, you will need to select the ROI for cortical or cancellous bone, run the full analysis, and then reopen the full stack and start again for the other type of bone
 - a. For cortical bone, you will need a 1 mm section surrounding the mid-diaphysis
 - i. Find the middle of the diaphysis based on anatomical structures, and then cut 500 μm above and 500 μm below
 - ii. To calculate how many slices are needed to get a 1 mm section, divide 1 mm by the voxel size. For example, if your voxel size is 12 μm , you will need 84 slices ($1/0.012 = 83.33$), or 42 above your midpoint and 42 below
 - b. For trabecular bone, you need a 500 μm ROI of secondary spongiosa, the bone right before the growth plate
 - i. The growth plate should be very distinctive on the scan, so just start your ROI directly after you are through the growth plate
 - ii. To calculate the number of slices, divide 500 μm by the voxel size. If your voxel size is 12 μm , you need 42 slices ($.500/0.012 = 41.67$)
 - c. To cut out a portion of your bone go to Plugins \rightarrow Stacks \rightarrow Delete Slice Range
 - i. Make sure to start at one of the ends of your ROI and not the midpoint, as this is not reversible
 - ii. Also remember the software is asking for the part you want deleted, not the part you want to save
 1. For example, if your cortical midpoint is slice 780, then your ROI is from slice 738 to 822. You want to delete slice ranges of 1-737 and 823-end
 - d. Once you have your ROI, save the stack of images in case you need them for re-analysis
 - i. Go to File \rightarrow Save As \rightarrow Image Sequence
4. Cortical Bone Analysis
 - a. Once you have your ROI, you are ready to analyze your cortical bone. First, you need to get it to a binary (black and white) image, and then you can run analysis
 - b. Go to Plugins \rightarrow BoneJ \rightarrow Optimize Threshold
 - i. Make sure Threshold Only and Apply Threshold are selected
 - ii. Click OK
 - iii. This will give you a binary photo
 - c. To calculate Total Area, select the wand tool from the Fiji tool bar, and click on the cortical region of the bone. A yellow outline should appear around the outer perimeter of the bone
 - i. Press "M" to measure the area
 - ii. Repeat for each slice in the stack

- d. To calculate Marrow Area, repeat step C but click on the marrow region of the bone. A yellow outline should appear around the inner perimeter of the bone
 - i. Press “M” to measure the area
 - ii. Repeat for each slice in the stack
 - e. Save the measurement output as a .csv file by going to File → Save
 - f. Next, go to Plugins → BoneJ → Slice Geometry
 - i. Select the type of bone that is being analyzed
 - ii. Make sure to select “process stack”
 - iii. Click ok
 - iv. This should open a new measurement output with slice geometry data for each slice in the stack, save that by going to File → Save
 - v. Make sure to distinguish the two outputs somehow
5. Trabecular Bone Analysis
- a. Once you have your ROI, you are ready to analyze the trabecular bone. First, you need to get it to a binary (black and white) image, and then you can run analysis
 - b. Go to Plugins → BoneJ → Optimize Threshold
 - i. Make sure Threshold Only and Apply Threshold are selected
 - ii. Click OK
 - iii. This will give you a binary photo
 - b. Trabecular bone analysis is all done using plugins. Go through each of the following:
 - i. Plugins → BoneJ → Volume Fraction
 - ii. Plugins → BoneJ → Thickness
 1. Make sure Trabecular thickness and Trabecular spacing are selected
 2. Uncheck graphic results. Click ok.
 - iii. Plugins → BoneJ → Anisotropy
 - iv. Plugins → BoneJ → Connectivity
 - v. Plugins → BoneJ → SMI
 - vi. Plugins → BoneJ → Ellipsoid Factor
 1. Ellipsoid factor will not be saved to the measurement output, so record EF mean and EF SD in an excel file
 - vii. Save your measurement output by going to File → Save
6. Once you have all of your cortical and trabecular bone measurement outputs, you are ready to build your excel file with all outcomes
- a. Cortical Bone
 - i. Total Area = average of all total area measurements
 - ii. Marrow Area = average of all marrow area measurements
 - iii. Cortical Area = Total Area – Marrow Area
 - iv. Cortical Area Ratio = Cortical Area/Total Area
 - v. Cortical Thickness = average of all Ct.Th measurements from slice geometry
 - vi. Imin = average of all Imin measurements from slice geometry
 - vii. Imax = average of all Imax measurements from slice geometry

- viii. Inertia ratio = I_{max}/I_{min}
- b. Trabecular Bone
 - i. Unlick cortical bone, most trabecular bone measurements are already averaged by the plugin and they can just be copied over directly
 - ii. BV/TV = copied value from output
 - iii. Trabecular Thickness = copied value from output
 - iv. Trabecular Separation = copied value from output
 - v. Trabecular Number = $1/(Tb.Th + Tb.Sp)$
 - vi. Degree of Anisotropy = copied value from output
 - vii. Connectivity Density = copied value (Conn.D) from output
 - viii. SMI = copied value from output
 - ix. Ellipsoid Factor – not in output but should already be saved in the excel file from your analysis

Hydroxyproline Assay

Day 1

Acid Hydrolyzation

1. Check that glass tubes are air-tight: Fill glass tubes with 1 mL dd H₂O and secure the caps. Mark one tube as the control and loosen the cap. Place the tubes in an oven set at 124°C for 30 minutes (typically once the tissues have been weighed is a good point to remove them from the oven and check for leaks)
2. Record the weight of eight empty 2 mL microcentrifuge tubes.
3. Pulverize the samples using the socket and bolt apparatus (find in the supply box in the Gwynn lab). You will need to scrape the bone fragments back to the center of the bolt and repeat the process 2 additional times.
4. Place the crushed bone tissue in respective pre-weighed tubes and the weigh the tubes again to get tissue weights.
 - * 30-50 mg of cortical bone is typically on the curve
5. Add 400 ul dd H₂O to the weighed tubes. Then homogenize the samples, cleaning the homogenizer with dd H₂O after every sample (change wash water after 4 tubes).
6. Label glass tubes that didn't lose water while in the oven and pour the homogenate into its appropriate glass tube.
 - *It's normally helpful to hold the microcentrifuge tube and the glass tube together and tap gently to remove as much tissue from the tube as possible.
7. Add 100 ul dd H₂O to the microcentrifuge tube and vortex. Then transfer this into the glass tube with the rest of the sample (again tap the tubes gently if necessary)
8. Under the hood, add 500 ul of 12M HCl to the microcentrifuge tubes.
9. Vortex the samples and pour the HCL from the microcentrifuge tube into the glass tube (tap the tube if there is still tissue in the tube).
10. Cap the glass tubes tightly, vortex them to assure mixing and place in a glass beaker (250 ml size should fit all 8 samples).

11. Place the beaker in the oven set at 124°C for 3 hours

Acid Neutralization

1. Once glass tubes are removed from the oven, let them cool for 5-10 minutes, remove the caps, and place them back into the beaker.
2. Put enough NaOH pellets to coat, but not fill, the bottom of a desiccator. Put the white disk back into the desiccator and place the desiccator into a water bath set at 85°C.
3. Fill the water bath as full as possible with ddH₂O/tap H₂O (50/50)
4. Place the beaker the glass tubes are in into the desiccator on the white disk.
5. Put the lid on the desiccator, attach the vacuum line with a solvent trap, and turn the vacuum all the way on.
6. Cover the water bath with all-purpose wrap (having it touch the water actually helps prevent more water from evaporating than if you don't).
7. Cover the all-purpose wrap with aluminum foil and place the water bath lid on top of the foil.
8. Leave in water bath under a vacuum until dry (8 samples typically takes overnight and 24 samples typically take 24 hours to dry).

Day 2

Reconstitution

1. Add 1 mL of 0.001 N HCl to the dried neutralized samples and vortex (it's essential that the samples be completely dry before this step).
2. Allow the samples to sit at room temperature for **no less than 30 min**, vortexing occasionally.
3. Pour the solutions into pre-labeled 1.5 mL microcentrifuge tubes and centrifuge at max speed for 15 minutes.
4. Transfer supernatant to new pre-labeled 1.5 or 2 mL tubes.

Colormetric Assay

Reagents & standards to make ahead of time

Stock OH-proline standard (10mg/mL):

Dissolve 1 g of OH-proline into 100 mL of 0.001 N HCL

-use volumetric flask – add some HCl to the bottle of 1 g OH-proline then transfer this to a 100 mL volumetric flask. Rinse the OH-proline container 2 more times with HCL. Then bring the stock solution to volume).

-There should be aliquots of this stock standard in the -20°C

*Standards can/should be made ahead of time and stored in the -20°C (avoid repeated freeze thaw cycles).

To make standard follow the chart below:

Std	Concentration	Dilutions
6	3.0 ug/100 ul	15 µL (10 mg/mL) stock + 4.985 mL of 0.001 N HCl
5	2.0 ug/100 µL	20 µL stock + 9.98 mL of 0.001 N HCl
4	1.0 ug/100 µL	5 mL of Std 5 + 5 mL of 0.001 N HCl
3	0.5 ug/100 µL	5 mL of Std 4 + 5 mL of 0.001 N HCl
2	0.25 ug/100 µL	5 mL of Std 3 + 5 mL of 0.001 N HCl
1	0.125 ug/100 µL	5 mL of Std 2 + 5 mL of 0.001 N HCl
0	0 ug/100 µL	0.001 N HCl

*Aliquot standards (100 µL) into 2 mL microcentrifuge tubes and store at -20°C so they are ready-to-go when you run the assay.

Make OH-proline assay buffer ahead of time

11.4 g Na Acetate (anhydrous)
 7.5 g Na Citrate
 40 mL H₂O
 Acetic acid (for adjusting pH)
 77 mL isopropanol
 dd H₂O

- Add 11.4 g Na acetate and 7.5 g Na citrate to 40 mL dd H₂O in a 200 mL beaker with a stir bar. Place on a hot-plate to stir until the Na acetate and Na citrate are dissolved (this step takes a couple of minutes-use a little heat if necessary).
- Once dissolved check the pH of the solution and adjust to a pH of 6.0 using glacial acetic acid
- Pour this mixture into a 200 mL volumetric flask and add 77 mL of isopropanol (there will be 2 solvent layers, don't worry adding H₂O in the next step removes this solvent gradient).
- Bring to volume with dd H₂O.

Assay procedure

1. Label two 2 mL microcentrifuge tubes per sample and one blank (zero).
2. Add 100 uL of 0.001 N HCl to the blank tube
3. Add 98.5 uL of 0.001 N HCl to each sample tube. Then add 1.5 uL of sample to the respective tubes.
4. Make Chloramine T solution *This needs to be made fresh every time
For 8 samples (in duplicate with standards):

0.07 g	Chloramine T
1 mL	ddH ₂ O
4 mL	OH-proline buffer
5. Add 100 uL of Chloramine T reagent to each sample plus blank/standards. Vortex and let stand at room temperature for 9-10 minutes.
6. While samples are incubating, make the Erlich's reagent *This needs to be made fresh every time

For 8 samples (in duplicate with standards):

2 g p-dimethylaminobenzaldehyde
6 mL 60%
26 mL OH-proline buffer

7. Add 1.3 mL of Erlich's reagent to each sample, blank, and standards and then vortex.
8. Turn on the spectrometer
9. Place the tubes in a 55°C water bath for 20 minutes.
10. After incubation, invert each tube to mix again. Look at the color closely, if there is a gradient from yellow to pink, keep inverting until it is completely mixed.
11. Allow the samples to sit at room temperature for 5 minutes.
12. Take absorbance readings at 558 nm using disposable cuvettes. Read the standards from lowest to highest concentration, and then read the samples.
13. Record absorbance values and use the OH-proline excel template to calculate results.

AGEs Assay (Quinine)

Materials:

Sulfuric Acid (H₂SO₄)
Quinine
96-well plates
Fluorescent plate reader

Methods:

0.1 N H₂SO₄

Add 200 mL of dd h₂O to a 1 L volumetric flask
Add 2.77 mL 36M H₂SO₄ to the 1 L flask and swirl gently to mix
Fill the flask to volume with dd H₂O

Preparation of Stock Quinine Solution (10ug/mL in 0.1 N H₂SO₄)

1. Weight out 0.025 g quinine and place in a 50 mL volumetric flask
2. Fill the flask to volume with 0.1 N H₂SO₄. This will create a concentration of 500 ug/mL
3. Mix the solution well
4. Transfer 1mL of the 500 ug/mL quinine solution to a new 50 mL volumetric flask
5. Bring the solution to volume with 0.1 N H₂SO₄. The concentration of the stock quinine solution will now be 10 ug/mL.

Preparation of Quinine Standards for Assay

To make standards follow the chart below:

Std	Quinine Standard Concentration (ng/mL)	Dilutions
7	500	50 µL (10 ug/mL) stock + 950 mL 0.1 N H ₂ SO ₄
6	250	500 µL Std 7 + 500 µL 0.1 N H ₂ SO ₄
5	125	500 µL Std 6 + 500 µL 0.1 N H ₂ SO ₄
4	62.5	500 µL Std 5 + 500 µL 0.1 N H ₂ SO ₄
3	31.25	500 µL Std 5 + 500 µL 0.1 N H ₂ SO ₄
2	15.625	500 µL Std 5 + 500 µL 0.1 N H ₂ SO ₄
1	7.8125	500 µL Std 5 + 500 µL 0.1 N H ₂ SO ₄
0	0	0.1 N H ₂ SO ₄

*This will make enough standard for 1 plate. Scale up or down as necessary for the number of plates to be used so that the same standards are used for all the samples

Sample dilution/Running the Assay

1. Create a solution with a concentration of 1 mg of bone in 200 µL of solution per well.

-Use the Excel file on the network for these calculations (Protocols → Hydroxyproline & Age → Making Samples Concentrations Template.xlsx)

2. Load 200 μL of the standards and the 1 mg/ 200 μL solution for each sample in duplicate on a 96-well plate
3. Take a fluorescence reading with the plate reader set for 360 nm excitation and 460 nm emission.

Save the output, then calculate the standard curve and sample concentrations for the standard curve.

Ashing for Mineral Analysis

1. Clean bone of interest of as much muscle and connective tissues as possible
 - a. Measure wet weight
2. Immerse bone in hexane overnight, or up to 24 hours, to extract lipids
 - a. Use disposable glass tubes, as the diethyl ether will dissolve plastic tubes
 - b. Work under the fume hood
 - c. Label tubes
3. Immerse bone in diethyl ether overnight, or up to 24 hours, to dissolve organic material
 - a. Use a new set of disposable glass tubes
 - b. Work under fume hood
 - c. Label tubes
4. Dry bones at room temperature to make sure that all organic solvents are gone
5. Dry bone for 24 hours
 - a. Place in incubator at 60 °C
 - b. Remove from incubator and place in desiccator. Allow to cool to room temperature in desiccator. Measure dry weight and return to desiccator.
6. After dry weight has been taken, place back in the incubator for 8-12 hours and check that dry weight is stable. If dry weight after 8 hours is less than original dry weight, place back in the incubator for another 8-12 hours. Continue until two consecutive readings of dry weight match.
7. Prepare porcelain crucibles
 - a. Acid wash and rinse with deionized water 20x; dry in oven
 - b. Measure dry weight of crucibles
 - c. WEAR PPE DURING ANY STEPS USING STRONG ACIDS
8. Ash bone overnight in a muffle furnace
 - a. Set the furnace to 800 °C
 - b. Place the bones in prepared crucibles
 - c. Label the crucibles.
 - i. Most markers will burn off in the ashing process. Thus, make sure to also make a map of how the bones went into the furnace. Also can try etching the number into the crucible.
 - d. Confirm the furnace turned on
 - e. Leave the bones in the furnace overnight or up to 24 hours. Turn the furnace off, and allow to cool before opening.
9. Get the dry weight of the ash
 - a. Needs to be measured at room temperature
 - b. Take care to ensure that no water or other material gets into the ash
 - c. Leave sample in desiccator while cooling to ensure no contamination
 - d. After weighing, place the ashed bone in a new glass tube and save for mineral analysis
 - i. Glass tubes used to store ashed bones need to be acid washed prior to use
10. Take labeled glass tubes with ash to the Ag Experiment Station for mineral (Ca and P) analysis

Histology/Immunohistochemistry Sample Prep Protocol

- 1) Prepare bone samples
 - a) Clean bone of as much soft tissue as possible
 - b) Place each bone in clearly labeled, individual 15 mL glass vials

- 2) Fix
 - a) Fix in 10% Formalin for 24-48 hours
 - i) Keep in refrigerator at 4 °C
 - ii) Formalin can destroy certain antigens and fluorochromes, check your IHC protocol for fixation time
 - (1) Calcein/alizarin stains should not spend more than 24 hours in formalin
 - b) After 24-48 hours, remove the 10% formalin and wash with PBS 2x30 minutes
 - i) Can store/wash in PBS for up to 24 hours if necessary, before continuing to next step
 - c) Make sure to dispose of the formalin in an approved, labeled disposal container. Store used formalin in the flammable cabinet until scheduled pickup by EHS

- 3) Decalcify
 - a) After wash, replace PBS with 14% EDTA
 - b) Keep vials in refrigerator at 4 °C, changing the 14% EDTA solution every 3-4 days until fully decalcified
 - i) Mouse bones: 10-14 days
 - ii) Rat bones: 4+ weeks
 - c) Make sure to dispose of the EDTA into an approved, labeled disposal container. Store used EDTA in the flammable cabinet until scheduled pickup by EHS
 - d) After decalcification, wash with PBS 2x30 minutes
 - i) Can store/wash in PBS for up to 24 hours if necessary, before continuing to next step

- 4) Store in 70% ethanol until bones can be taken to the VMDL for embedding and slicing
 - a) Prolonged storage in 70% ethanol can damage certain antigens, check your IHC protocol but also try to get samples to the VMDL as quickly as possible

14% EDTA solution

- b) To make 14% EDTA solution (under the fume hood)
 - i) Measure 140 g EDTA into a 1 L glass container
 - ii) Add 700 mL diH₂O and stir vigorously with stir bar
 - iii) Add ammonium hydroxide 30 mL at a time until solution is clear (usually needs around 90 mL)
 - iv) Adjust pH to 7.2-7.4 using more ammonium hydroxide or glacial acetic acid
 - v) Add diH₂O to get 1 L total volume
 - vi) Store in refrigerator at 4 °C

Immunohistochemistry Protocol

Deparaffinize slides – 3 minutes in each solution

1. Xylene
2. Xylene
3. 1:1 Xylene:EtOH
4. 100% EtOH
5. 100% EtOH
6. 95% EtOH
7. 70% EtOH
8. 50% EtOH
9. Water

Make sure to not let your samples dry out between each step

Washes should be done gently on the western shaker. Esp. important for PBST washes

Antigen Retrieval – 2 methods, but I prefer heat, it seems to give a better picture

If using method 1, establish hydrophobic barriers before beginning. If using method 2, establish barriers after this step, before starting permeabilization

Method 1 – enzymatic

1. 1x Protease K solution for 15 minutes
2. Wash with PBS 3x5 min

Method 2 – heat

1. Pour 50 mL of 10 mM sodium citrate buffer into a Coplin jar
2. Place the Coplin jar into a water bath set to 60 °C (best to do this before deparaffinization so that it has time to warm up before you put the slides in)
3. Once the citrate buffer has warmed up, place slides into the Coplin jar and leave overnight
4. In the morning, remove Coplin jars with slides from the water bath and allow to cool to room temperature
5. Wash slides with PBS 3x5 min

Permeabilization

1. 0.02% Triton-X100 (diluted in PBS) for 15 minutes
2. Wash with PBS 3x5 min

Blocking

1. Block with dilute normal goat serum for 30 min
2. Wash with PBS 3x5 min
3. Block with avidin blocking solution for 20 min
 - a. Store avidin blocking solution at 4° C
4. Wash with PBS 3x5 minutes
5. Block with biotin blocking solution for 20 min
 - a. Store biotin blocking solution at 4° C

6. Wash with PBS 3x5 minutes
7. Apply primary antibody overnight at 4° C in humidified chamber
 - a. Dilute in 1% BSA
 - i. Dilution is dependent on antibody
 - ii. Sclerostin (abcam) is 1:1000 for rats, 1:100 for mice
 - b. Make sure to leave a negative control that is blocked with 1% BSA with no primary

Activation

1. Wash with PBST 3X10 min
2. Quench endogenous peroxidase activity
 - a. 3% H₂O₂ for 15 min
3. Wash with PBS 3x5 min
4. Apply dilute secondary antibody solution for 30 min
 - a. Make ABC solution and let it sit for 30 minutes at room temperature while secondary antibody is blocking
5. Wash with PBST 3x10 minutes
6. Incubate with ABC solution for 30 minutes
7. Wash with PBST 3x10 minutes
8. Apply substrate-chromogen solution (DAB)
 - a. Time is dependent on what you are binding to, but for mouse sclerostin (at 1:100), usually takes about 5 minutes to get a good color
9. Wash with water 3x3 min

Counter-Staining

10. Stain with Mayer's hematoxylin for 5 seconds
11. Wash with water 3x3 minutes
12. Dip 10X in 0.037M ammonia
13. Wash with water 2x2 min

Fixing/Mounting – 3 minutes in each solution

14. 50% EtOH
15. 70% EtOH
16. 95% EtOH
17. 100% EtOH
18. 100% EtOH
19. 1:1 Xylene:EtOH
20. Xylene
21. Xylene
22. Let slides air dry
23. Mount the slide cover with Faramount
 - a. Seal edges of slide cover to the slide with nail polish and let dry overnight

Stock Solutions

Protease K (20x)

Protease K (30 units/mg)	8 mg
TE buffer (pH 8.0)	10 mL
Glycerol	10 mL

Dissolve protease K into TE buffer, then add glycerol and mix. Aliquot out in 1 mL portions and store at -20° C.

To make 1x working solution, combine 1ml of 20x stock solution with 19 ml of TE buffer (pH 8.0). 1x solution can be stored in refrigerator (4° C) for up to 6 months

10 mM Sodium Citrate Buffer

Tri-sodium citrate (dihydrate)	2.94 g
Distilled water	1000 mL

Mix to dissolve. Adjust pH to 6.0 with 1N HCl and then add 0.5 mL of Tween-20 and mix well. Store at room temperature for up to 3 months or in the refrigerator (4 °C) for up to 6 months.

BSA (1%)

Bovine Serum Albumin	1 g
TBS or PBS	100 mL

Fully dissolve BSA into TBS/PBS. Aliquot out in 1-2 mL portions and store at -20° C. Thaw as needed.

ABC Kit Solutions

Dilute Normal Goat Serum

1. Mix 10 mL PBS with 3 drops of the normal goat serum from ABC kit
2. Premade dilute goat serum is stable at 4° C for 30 days

Dilute Secondary Antibodies

1. Mix 10 mL PBS with 3 drops of the normal goat serum and 1 drop of the secondary concentrate from ABC kit
2. Premade dilute secondary solution is stable at 4° C for 30 days

ABC Solution

1. Mix 10 mL of PBS with 4 drops of substrate A, shake, and then add 4 drops of substrate B from ABC kit
2. Premade ABC solution is stable at 4° C for 30 days

PBST = 0.1% tween

Fluorescent Label Injections

1. Make calcein (15 mg/kg body weight) and alizarin (30 mg/kg body weight) solutions according to recipe on the P-drive (see calcein and alizarin doses Excel file).
 - a. Using measurements provided in the excel file, combine all ingredients in a small glass beaker and heat on the hot plate until dissolved. Filter into an injection vial.
2. Wrap vials containing completed solution with foil to block light, and store in the refrigerator until needed (but no longer than 1 week)
3. On injection day, weigh the animal getting the injection. Using the information in the calcein and alizarin doses Excel file, measure out the mL of solution needed based on animal body weight
4. Administer solution through IP injection to each animal that needs it
 - a. Give calcein first, and then give alizarin 4 days later
5. Monitor animals for 5-10 minutes after injection to check for negative impacts

Epoxy Embedding of Calcified Bone

Sample Preparation

1. Clean bones of as much soft and connective tissue as possible
2. Fix bones in formalin for <24 hours (usually just overnight)
3. Dehydrate bones in graded alcohols in glass test tubes. Allow the solution in each step to reach full saturation before changing solutions
 - a. 1-2 hours 70% ethanol
 - b. 1-2 hours 70% ethanol
 - c. 1-2 hours 95% ethanol
 - d. 1-2 hours 95% ethanol
 - e. 1-2 hours 100% ethanol
 - f. 1-2 hours 100% ethanol
4. Leave bones to dry in the hood until completely dry (24-48 hours)
 - a. Make sure to keep them protected from the light as much as possible during this time
5. Place each bone in a centrifuge tube and leave in the dark until ready for embedding

Embedding Process

Day 1

1. If applicable, remove the resin and resin hardener from the refrigerator so that it can come to room temperature. If you will be using the resin for a few days, there is no need to put it back in the refrigerator after each use, you can just put it back when you are completely done with it.
2. Cut squares of foil (about 1.5"x1.5"), one for each bone (plus a few extras in case of tears)
3. Using the plexiglass guide (square of plexiglass with a screw in the top, can be found in the Middleton lab), fold each square of foil into a rectangular "boat"
4. Glue the boats to a paper plate with a glue stick (can usually get 12-15 per plate), spaced out so that you have room to label each boat with sample numbers
5. Take the plate under the hood, and gather a paper cup, wooden popsicle stick, and transfer pipette. Cut the thinnest end of the transfer pipette off.
6. Place the paper cup on the scale and then zero it. Pour resin into the paper cup until you reach desired weight
7. Use the calculator attached to the outside of the hood to calculate the amount of resin hardener needed
 - a. $\text{Weight of resin} \times 1.45 = \text{total weight of resin} + \text{hardener}$
8. Using the transfer pipette, slowly add the correct weight of hardener to the resin in the cup
 - a. DO NOT mix the resin and the hardener in the bottles
9. Stir the resin and hardener together gently with the wooden popsicle stick for 1-2 minutes until mixed, trying to avoid developing any air bubbles
10. Gently pour a small amount of epoxy into each boat to cover the bottom, ending when the epoxy is about ¼" thick

11. Place the paper plate with the filled boats into the vacuum, place the top on the vacuum and seal using the pump. This will allow any air bubbles that did form to be pulled to the top of the epoxy so they will pop. Leave the paper plate in the vacuum sealer overnight.

Day 2

1. Remove the paper plate from the vacuum sealer and carry it over to your work surface
2. Label the boats with sample numbers by writing on the paper plate above or below each individual boat
3. For each bone, you will need to repeat the following steps:
 - a. Remove the bone from the centrifuge tube
 - b. Mark with colored pencil where you want to cut the bone
 - i. For example, if you want to take a slice of cortical bone, make a mark in the center of the diaphysis
 - c. Place 1 or 2 small drops of super glue on the epoxy layer in the foil boat
 - d. Place the bone on these drops of super glue and hold until the glue hardens, and the bone is secured in place
 - i. Make sure that you are placing the bones uniformly on the epoxy – all should be facing the same direction, same side up, etc.
4. Once all of the bones are secured in their boats, take the paper plate over to the hood and stir together more epoxy like you did on day 1. You will need a larger volume of epoxy on day 2.
5. Once the epoxy is mixed, gently pour it over each bone until the bone is covered and there is about ¼” of epoxy above the bone
6. Place the paper plate in the vacuum, remove the air and leave the bones in the vacuum for 2 days
 - a. If you are doing several bones (more than can fit on one plate), you can pull the first set out of the vacuum seal and start another set of empty boats. However, you then need to let the first set sit for another day before you try slicing them, to fully allow the epoxy to harden. The vacuum seal is just to help draw out air bubbles, once those are removed the epoxy can harden anywhere.
7. Once the epoxy is fully hardened, remove the foil from the block. Place the epoxy block with the bone in a small, labeled, resealable bag (usually use the little jewelry bags from Walmart) and store in the dark until you are ready to slice samples.

**fluorescent labels can be destroyed by light, so when leaving samples for long periods of time (particularly in the vacuum sealer or between drying and embedding) make sure to cover them with something opaque or store them in the dark

Calcified Tissue Slicing

1. Assemble and turn on the IsoMet saw and MetaServ grinder/polisher (ask Kevin Middleton for initial instructions). Make sure that water is flowing through the polisher and that water is in the tray of the saw
2. Line up and label weigh boats for each individual bone that needs to be cut.
3. Place the block with the bone in the holder and tighten the screws with the Allen wrench to keep it in place. Make sure that the bone (not block) is straight to get an even cut
4. Screw the block holder onto the arm of the saw and line up the blade with the colored pencil mark on the bone. **NOTE: you do not want to cut directly on the colored pencil mark. The colored pencil mark should be the location of the bone you want to analyze, and you will need to make a cut on either side of that mark to get a slice that includes your ROI
5. Once the blade is lined up correctly, turn it on and slice through the bone and block completely.
6. Remove the portion that was cut off and place into the respective weigh boat
7. Remove the block holder from the saw arm and polish the cut end of the block until smooth (5-10 seconds). Dry the cut end of the block with air or a towel and mark it with a sharpie. When it comes time to mount the slice, this side will be “down”.
8. Turn the knob on the saw arm twice to move it in by 1 mm
9. Double check the alignment of the blade – it should be just past the colored pencil mark
10. Once the blade is lined up correctly, turn it on and slice through the bone and block completely
11. Remove the slice and place it on a labeled slide or piece of plexiglass.
12. If you are cutting more than one slice, adjust the placement of the block in the holder and repeat steps 4-11
13. Once you have cut all your bones, mix a small amount of epoxy under the hood (see Embedding Protocol for epoxy mixing instructions)
14. Pour the epoxy out onto a paper plate or folded paper towel
15. With forceps, dip the back- or down-side (side with sharpie mark) of each slice into the puddle of epoxy, and then mount it onto the labeled slide
16. Arrange the labeled slides on a tray or plate and allow them to sit overnight in the dark to harden the epoxy
17. Once all of the slides are dried and the epoxy is hardened, polish the top of the slide on the polisher until smooth (5-10 seconds) for better pictures
 - a. It's easy to polish the ends of your fingers off (ouch!) so try wrapping your fingers first with parafilm, band-aids, rubber thimbles, etc. to protect them
18. Once all slices are polished, allow to dry, then store in a slide box and take to the Molecular Cytology Core for pictures

Three-point Bending Protocol

1. Clean bones of as much soft and connective tissue as possible
2. Freeze in PBS-wrapped gauze to keep the samples moist
 - a. DO NOT fix or allow to dry, as that will influence the outcomes
3. When ready to do strength testing, move the samples over to the freezer in Kevin Middleton's lab (M314 - where the materials testing machine is)

Machine Set Up

4. Turn on the Instron materials testing machine by opening the BlueHill program on the computer
5. Make sure you have the right attachments on the machine and that they are lined up correctly
 - a. The top attachment (attached to the moving arm) should be the central point, with the point facing down, as that is the direction the arm will move
 - b. The bottom attachment should be the one with the two outside points, evenly spaced so that the central arm hits directly between them
 - i. The distance between the two points will vary based on the type of bone, but generally is 6-10 mm (for calculations, this span distance will be L)
 - c. Make sure all attachments are secured tightly so that they WILL NOT MOVE during testing
6. Once the machine is set up correctly, select the correct testing program folder in the BlueHill testing program
 - a. There should be Dirkes_femur and Dirkes_tibia programs already set, but depending on the bone you are testing and your test parameters it might be easier to just start a new one
 - b. Within your testing program, you need to at minimum define the span between the two outside points (L), the force on the arm (I believe the standard is 500 N but double check!), and set the speed of the arm (10 mm/min)
 - c. Make sure you have selected to export your outputs to the correct folder (make yourself a folder on the desktop to temporarily store outputs, but bring an external hard drive so you can take your outputs with you when you leave)
7. Adjust the moveable arm so that the central point is 1-2 cm above the bottom two points. This will allow enough space for you to place samples correctly but not so much space that each test takes too long. Once you have chosen a place for the testing arm DO NOT move it until you are completely done with testing, because some of your calculations are dependent on this distance, and changing it will change your outcomes
8. Once the machine is set up, you are ready to start testing samples

Testing

1. For each sample, take the following steps

- a. Place the sample (in its freezer tube) in a beaker of water on the desk until thawed
 - i. You can have 2-3 samples in the beaker of water at a time, then they will be thawed by the time you are ready to do the test. But you don't want them to dry out or be thawed too long so don't just pull the whole box of samples out
- b. Remove the thawed sample from its cryo/centrifuge tube and wipe excess moisture off with a piece of gauze
 - i. You want the sample to not be dried out, but also not slippery
- c. Place the sample on the bottom two points, making sure that the ROI to be broken is in the center
 - i. For certain bones this is easier said than done, tibiae tend to slip because of their curve. More practice is probably needed with these, maybe there's a cool attachment someone can come up with? Femurs tend to sit pretty well though
- d. Make sure the test program in BlueHill has been labeled with the correct sample number
- e. Zero out the extension (mm) and force (N)
- f. Press Start Test
- g. Stand back and allow the arm to move uniformly and apply force to the sample until breaking
 - i. Take note if the bone breaks weird or moves during the testing process
 - ii. YOU CANNOT REDO A TEST so try to be as consistent as possible. However, if something does go weird, just note it so that it can be removed from analysis if necessary. There's always 1 or 2 that just do their own thing.
- h. Once the test is over (bone has fractured), click Ok on the screen when asked if the arm should be reset
- i. Remove the sample from the machine and clean off any marrow that may have gotten on the points or attachments
 - i. Sometimes the bone pieces will fall in between the two bottom points when you are trying to remove them after the central point is moved. To prevent losing any sample pieces, I usually place a piece of gauze between the two bottom points to catch anything that falls.
 - ii. Sometimes the bone pieces will go flying across the room – try to gather them up off the floor as much as possible, so they don't rot. Also make sure to stand back during the test so you don't get hit with flying bone shards (the mice are very small and probably not a real safety concern, but might want to have some kind of shield in place if you are doing anything larger than a mouse).
- j. The outputs should autosave to the assigned folder, and then there should be a prompt that comes up that says, "do another test with the same parameters?" You can select yes, and then a prompt will come up to

change the sample number, and then you can start a new test without going back to the main home screen

- k. Place the broken pieces of the sample back in the gauze in their cryo/centrifuge tube, replace in the freezer, and pull out a new sample

Three-point Bending Analysis

1. To do the analysis of the 3-point bending outputs from the Instron machine, you will need the following information from your uCT analysis and the instrument
 - a. Diameter and radius of the bone at the breaking axis (ML, AP, etc)
 - i. NOT just the largest and smallest diameter and radius but the actual axis
 - ii. The axis used (AP vs ML) will depend on how the bone is positioned for the breaking test and what axis the force is being applied to
 - b. I (moment of inertia) of the bone around the breaking axis
 - c. Span of distance between two outside points on the machine
 - d. ALL OF THE ABOVE need to be converted to (or acquired in) METERS, not millimeters
 - i. For I and the diameter/radii it's easiest to just rerun your BoneJ analysis with it set to meters as the units. You will most likely be rerunning your analysis anyway to make sure the axes are correct, so while you are doing that, make sure you are getting meters as your output
2. The output from BlueHill will be an excel file with many data pairs of extension (mm) and force (N). The extension data will also need to be converted into meters.
3. Build your excel file. You will need the following information in order to do the further calculations
 - a. RAP or RML: radius of the bone at the breaking axis
 - b. IAP or IML: moment of inertia around the breaking axis
 - c. L: span of length between the two outside points
 - d. Data (extension and force) from TWO points along the linear portion of the force-distance curve generated by the BlueHill output
 - i. You can use whichever two points you want (you will be calculating slope), but double check the two points selected are on the LINEAR portion, or else the slope calculation will be incorrect
 - e. Extension and Force at fracture
4. Pull the MAX FORCE data from the BlueHill output and enter it in your excel sheet. You won't need this for calculations, but it is an outcome you should be interested in
 - a. Max Force is the largest force (N) that was applied to the bone
 - i. Not necessarily the same as point of fracture
5. Begin calculations (see below)
6. Final outcomes you should have for each bone for publication:
 - a. S: Stiffness (N/m)
 - b. M: Max Force (N)
 - c. E: Young's Modulus of Elasticity (N/m²)
 - d. U: Work-to-fracture (Nm)
 - e. u: Modulus of Toughness (N/m²)
 - f. Optional:

- i. Ultimate Stress
- ii. Ultimate Strain

Calculations

S: Stiffness = slope of the linear portion of the force-distance curve (N = force, M = distance in meters)

$$S = \left(\frac{N2 - N1}{M2 - M1} \right)$$

*You then need to convert force and distance into stress and strain, respectively, to make a stress-strain curve. The stress-strain curve should be analogous to the force-distance curve, but it takes into account the size and shape of the bone. Make sure to convert both of your points from the first curve to stress and strain because again you will need to calculate the slope of the stress-strain curve (E).

Stress (o): N = force

$$o = (N) * \left(\frac{L * RAP}{4 * IAP} \right)$$

Ultimate Stress = stress at fracture, calculate it from force at fracture

Strain (e): M = distance in meters

$$e = (M) * \left(\frac{12 * RAP}{L^2} \right)$$

Ultimate Strain = strain at fracture, calculate it using distance at fracture

*Note: the distance measurements start when the arm of the machine begins to move. However, ultimate strain should be calculated based on the distance the bone moved, meaning it needs to be calculated based on when the arm began to physically touch the bone and not just moved through the air. To do this, subtract the distance at 0.01 N from the distance at fracture to get the difference and use that as your M

E: Young's Modulus of Elasticity = slope of the linear portion of the stress-strain curve

$$E = \left(\frac{o2 - o1}{e2 - e1} \right)$$

U: Work-to-fracture = the integral of the force-distance curve

To calculate U, you will need to integrate the portion of the force-distance output when the bone is physically being touched and force is being applied. To do a point-by-point integration, you will need to treat each pair of data sets as if it were a tiny trapezoid. The area of a trapezoid is calculated as follows: $A = \left(\frac{a+b}{2} \right) * h$ with a and b being the bases of the trapezoid and h being the height. In the original output from BlueHill, the distance (m) will be the height of the trapezoid and the force (N) will be the bases. Calculate the area for each tiny trapezoid made by each pair of data points, and then add the areas together. **The integral (U) is the sum of the areas.**

u: Modulus of Toughness = integral of the stress-strain curve

$$u = U * \left(\frac{3 * RAP}{IAP * L} \right)$$

*NOTE: In all of these examples I used RAP and IAP because the AP axis is most likely the axis you are breaking around. However, if you end up breaking around the ML axis, make sure to use RML and IML in the calculations.

Ashing for Mineral Analysis

11. Clean bone of interest of as much muscle and connective tissues as possible
 - a. Measure wet weight
12. Immerse bone in hexane overnight, or up to 24 hours, to extract lipids
 - a. Use disposable glass tubes, as the diethyl ether will dissolve plastic tubes
 - b. Work under the fume hood
 - c. Label tubes
13. Immerse bone in diethyl ether overnight, or up to 24 hours, to dissolve organic material
 - a. Use a new set of disposable glass tubes
 - b. Work under fume hood
 - c. Label tubes
14. Dry bones at room temperature to make sure that all organic solvents are gone
15. Dry bone for 24 hours
 - a. Place in incubator at 60 °C
 - b. Remove from incubator and place in desiccator. Allow to cool to room temperature in desiccator. Measure dry weight and return to desiccator.
16. After dry weight has been taken, place back in the incubator for 8-12 hours and check that dry weight is stable. If dry weight after 8 hours is less than original dry weight, place back in the incubator for another 8-12 hours. Continue until two consecutive readings of dry weight match.
17. Prepare porcelain crucibles
 - a. Acid wash and rinse with deionized water 20x; dry in oven
 - b. Measure dry weight of crucibles
 - c. WEAR PPE DURING ANY STEPS USING STRONG ACIDS
18. Ash bone overnight in a muffle furnace
 - a. Set the furnace to 800 °C
 - b. Place the bones in prepared crucibles
 - c. Label the crucibles.
 - i. Most markers will burn off in the ashing process. Thus, make sure to also make a map of how the bones went into the furnace. Also can try etching the number into the crucible.
 - d. Confirm the furnace turned on
 - e. Leave the bones in the furnace overnight or up to 24 hours. Turn the furnace off, and allow to cool before opening.
19. Get the dry weight of the ash
 - a. Needs to be measured at room temperature
 - b. Take care to ensure that no water or other material gets into the ash
 - c. Leave sample in desiccator while cooling to ensure no contamination
 - d. After weighing, place the ashed bone in a new glass tube and save for mineral analysis
 - i. Glass tubes used to store ashed bones need to be acid washed prior to use
20. Take labeled glass tubes with ash to the Ag Experiment Station for mineral (Ca and P) analysis

VITA

Rebecca (Becca) Dirkes was born on March 8th, 1990 in Turlock, CA, the youngest of 6 children. At 5 months of age, her family moved to Bakersfield, CA, where they remained until 2012. After graduating from Shafter High School in Shafter, CA in 2008, she moved to Bozeman, MT to pursue her undergraduate education. She completed a bachelor's degree in Exercise Science from Montana State University in 2012. However, she had realized during her courses that nutrition and dietetics were her true interests and passions. She decided to stay and pursue another degree in Food and Nutrition and complete the course requirements for a dietetics program. She graduated with that bachelor's degree in 2015, at which point she moved to Columbia, MO to begin her PhD at the University of Missouri in Nutrition Sciences. She is graduating from the University of Missouri in December 2020. After graduation, she is planning on pursuing her dietetics internship to become a registered dietitian. As a RD-PhD she plans on using her combined passions for nutrition, education, and research to pursue a more healthful world.